FACTORS INFLUENCING THE ACCURACY OF REMOTE SENSING CLASSIFICATIONS: A COMPARATIVE STUDY

by

Mahesh Pal

Thesis submitted to the University of Nottingham for the degree of Doctor of Philosophy

May 2002

To

My Mother

and

Daughter Niharika

Acknowledgement

First of all, I would like to express my sincere gratitude and thanks to my supervisor, Professor Paul Mather. I am grateful to Professor Paul Mather for his continuous support, help and guidance throughout the period of this study. Without all his help and suggestions, this work would not have been possible.

I am very grateful to my sponsor, the Association of Commonwealth Universities, for giving me the opportunity and financial support to pursue a PhD degree at the University of Nottingham. I would like to convey my thanks to all the staff members of the School of Geography, Nottingham University, especially to Dr. Dee Omar, Ian Conway, Elaine Watts, Chris Lewis, and John Love for their co-operation and support.

Thanks are also due to Dr. Carlos Vieira in providing help for my programming problem and especially to Dr. Taskin Kavzoglu in allowing me to use his MATLAB toolkit for feature selection. I am also thankful to Dr. Premalatha Balan for helping me in the initial stage of my work and wish to thank Jorge Rubiano for his invaluable assistance and advice as well as his friendship during this work. I would like to acknowledge Prof. J. Gumuzzio, Autonomous University of Madrid for providing the DAIS datasets that enabled me to carry out some part of this study. Thanks are also due to Helmi Shafri for his valuable help during my field visit to La Mancha, Spain.

I wish to extend my thanks to Prof. S. K. Sood, Prof. D. V. S. Verma, Prof. R. K. Bansal, my friends in Regional Engineering College, Kurukshetra, Haryana (INDIA), and Dr. Manoj Arora, IIT, Roorkee (INDIA) for their kind help. Gyan Bhushan deserve special thanks for his help in getting my study leave sanctioned.

Special recognition is due to my family and relatives in India for their continuous encouragement and support. Special thanks is due to my wife Ritu Singh for her endless patience and understanding during all long hours of work that kept me busy in my research.

Table of Contents

List of Figures

List of Tables

Abstract

Within last 20 years, a number of methods have been employed for classifying remote sensing data, including parametric methods (e.g. the maximum likelihood classifier) and non-parametric classifiers (such as neural network classifiers). Each of these classification algorithms has some specific problems which limits its use. This research studies some alternative classification methods for land cover classification and compares their performance with the well established classification methods. The areas selected for this study are located near Littleport (Ely), in East Anglia, UK and in La Mancha region of Spain. Images in the optical bands of the Landsat ETM+ for year 2000 and InSAR data from May to September of 1996 for UK area, DAIS hyperspectral data and Landsat ETM+ for year 2000 for Spain area are used for this study. In addition, field data for the year 1996 were collected from farmers and for year 2000 were collected by field visits to both areas in the UK and Spain to generate the ground reference data set. The research was carried out in three main stages.

The overall aim of this study is to assess the relative performance of four approaches to classification in remote sensing - the maximum likelihood, artificial neural net, decision tree and support vector machine methods and to examine factors which affect their performance in term of overall classification accuracy.

Firstly, this research studies the behaviour of decision tree and support vector machine classifiers for land cover classification using ETM+ (UK) data. This stage discusses some factors affecting classification accuracy of a decision tree classifier, and also compares the performance of the decision tree with that of the maximum likelihood and neural network classifiers. The use of SVM requires the user to set the values of some parameters, such as type of kernel, kernel parameters, and multi-class methods as these parameters can significantly affect the accuracy of the resulting classification. This stage involves studying the effects of varying the various user defined parameters and noting their effect on classification accuracy. It is concluded that SVM perform far better than decision tree, maximum likelihood and neural network classifiers for this type of study.

The second stage involves applying the decision tree, maximum likelihood and neural network classifiers to InSAR coherence and intensity data and evaluating the utility of this type of data for land cover classification studies.

Finally, the last stage involves studying the response of SVMs, decision trees, maximum likelihood and neural classifier to different training data sizes, number of features, sampling plan, and the scale of the data used. The conclusion from the experiments presented in this stage is that the SVMs are unaffected by the Hughes phenomenon, and perform far better than the other classifiers in all cases. The performance of decision tree classifier based feature selection is found to be quite good in comparison with MNF transform. This study indicates that good classification performance depends on various parameters such as data type, scale of data, training sample size and type of classification method employed.

Chapter 1

Introduction

1.1 Introduction

The interpretation of remotely sensed data uses techniques from a number of disciplines including remote sensing, pattern recognition, artificial intelligence, computer vision, image processing and statistical analysis. The move towards automated analysis of remotely sensed data is encouraged by the ever increasing volumes of data as well as by the high cost of ground surveying. The new generation of satellite-borne instruments is providing higher spatial and spectral resolution data, leading to the wider application of remotely sensed products and further emphasising the need for more automated forms of analysis.

The methodology of pattern recognition applied to a particular problem depends on the data, the data model, and the information that one is expecting to find within the data (Bezdek, 1981). A number of methodologies have been developed and employed for image classification from remotely sensed data within the past 20 years. Statistical image classification techniques are ideally suited for data in which the distribution of the data within each of the classes can be assumed to follow a theoretical model. The most commonly used statistical classification methodology is based on maximum likelihood, a pixel-based probabilistic classification method which assumes that spectral classes can be described by a normal probability distribution in multispectral space (Swain and Davis, 1978). This traditional approach to classification is found to have some limitations in resolving interclass confusion if the data used are not normally distributed. As a result, in recent years, and following advances in computer technology, alternative classification strategies have been proposed.

Artificial intelligence and knowledge-based expert systems have been used in image classification. The major contribution of the artificial intelligence and expert system paradigm to pattern analysis has been the study of how domain-specific and heuristic knowledge can be represented and used to control the process of extracting meaningful descriptors and objects from images. The problem with these classifiers is that heuristic knowledge requires a number of experts to solve a single problem. Further details of these knowledge based classifiers can be found in Civco (1989), Estes et al. (1986), Goldberg et al. (1983), Friedl et al. (1988), Nagao and Matsuyama (1980) and Wharton (1987).

In most instances, human beings are good pattern recognisers. This observation led researchers in the field of pattern recognition to consider whether computer systems based on a simplified model of the human brain can be more effective than the standard statistical and knowledge-based classification methods. Research in this field led to the adoption of artificial neural networks (ANN), which have been used in remote sensing over the past ten years, mainly for image classification. Studies carried out using ANN suggest that, due to their nonparametric nature, they generally perform better than statistical classifiers. The performance of a neural network classifier depends to a significant extent on how well it has been trained. During the training phase, the neural network learns about regularities present in the training data and, based on these regularities, constructs rules that can be extended to the unknown data. However, the user must determine a number of properties such as the architecture of network, learning rate, number of iterations and learning algorithms, all of which affect classification accuracy. There is no clear rule to fix the values of these parameters, and only rules of thumb exist to guide users in their choice of network parameters. Kavzoglu (2001) discusses all these issue in detail.

Another type of classifier, called the decision tree (DT) classifier, is now being used for image classification problems in remote sensing because, like ANN, these classifiers are nonparametric. Unlike ANN, they do not need extensive design and training (Friedl and Brodley, 1997, Safavian and Landgrebe, 1991, Hensen et al., 1996). They are trained by iterative selection of individual features or a combination of features at each node of a tree. During classification, only those features are considered that are needed for the test pattern under consideration, so feature selection is implicitly built-in. However, the main advantage of the decision tree classifier as compared to ANN, besides its speed, is the possibility to interpret the decision rule in terms of individual features (Borak and Strahler, 1999). Other studies using decision tree classifiers in image classification can be found in Evans (1998), Friedl et al. (1999), Gahegan and West (1998) and Muchoney et al. (2000).

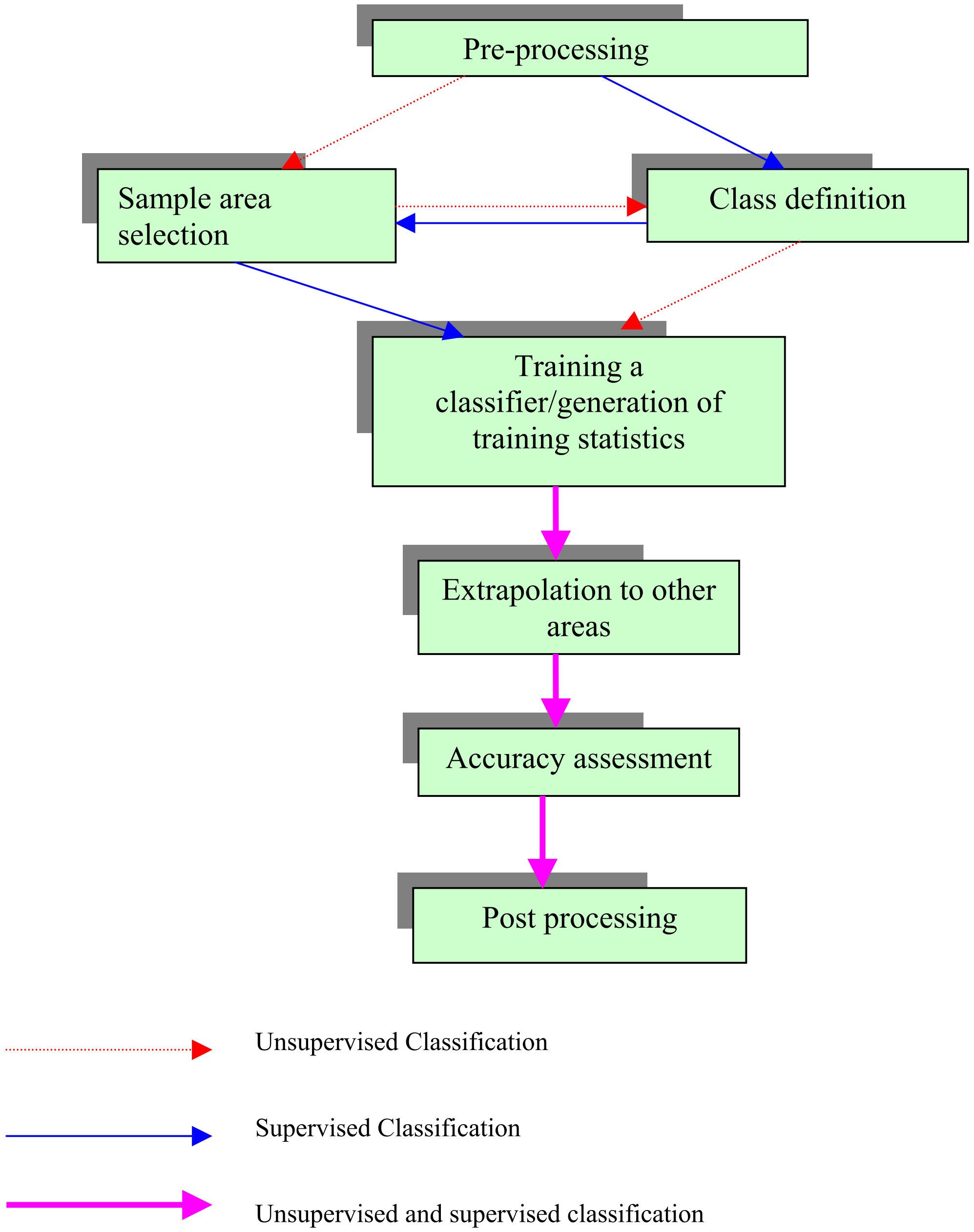
Pre-processing
Sample area selection
Class definition
Training a classifier/generation of training statistics
Extrapolation to other areas
Accuracy assessment
Post processing
Unsupervised Classification
Supervised Classification
Unsupervised and supervised classification

Figure 1. 1. Principal stages in image classification (adapted from Townshend and Justice, 1981).

Recently, a new classification technique based on statistical learning theory, called support vector machines, has been applied to the problem of image classification (Zhu and Blumberg, 2002; Huang et al, 2002; Gualtieri and Cromp, 1998; Chapelle et al., 1999). Support vector machines use optimisation algorithms to find the optimal boundaries between classes, and generalise these boundaries to unseen samples with the least errors among all possible boundaries separating the classes and minimising confusion between classes.

Image classification involves the execution of several stages (Figure 1.1). Moreover, within each of these principal stages there are several substages and hence further decisions need to be made. The performance of a classifier depends on the interrelationship between sample size, number of features, and classifier complexity. One of the important stages in image classification is that of collection of samples for training and testing the classifier. Sample size has an influence on the classification accuracy with which estimates of statistical parameters are obtained for statistical classifiers. Sample selection also depends on a number of factors which finally affect classification accuracy. The factors affecting sample selection are:

1. Number of training sites for sample collection.
2. Sampling method (random or systematic sampling).
3. Data source for labelling training sites (ground data, air photographs etc).
4. Timing of data collection.

With high-dimensional data sets, such as those acquired by an imaging spectrometer, the training set size requirements for the correct application of a classification system may be too high. It is well known that the probability of misclassification of a decision rule does not increase as the number of features increases, as long as number of training samples is arbitrarily large. However, it has been observed in practice that additional features may degrade the performance of a classifier if the number of training samples that are used to design the classifier is small relative to the number of features. This behaviour is referred to as the "peaking phenomenon" (Raudys and Jain, 1991; Jain and Chandrasekaran, 1982). Several authors, including Hord and Brooner (1976), Fitzpatrick-Lins (1981), Congalton (1988, 1991), Mather (1999) and Tso and Mather (2001) study the effect of sample size and sampling plan in detail.

1.2 Objective of this research

The work reported in this thesis focuses on the various factors that influence the accuracy of remote sensing classifications. As reported by a number of studies (Raudys and Pikelis, 1980; Congalton, 1988; Mather, 1999; Swain and Davis, 1978; Markham and Townshend, 1981) several factors, such as type of classifier and data used, sample size and sampling plan, and the scale of the data have a significant effect on the resulting classification accuracy. Although individual studies have highlighted specific problems, no comprehensive research study has attempted to consider all these aspects in the context of the classification of remotely sensed images. This study is designed to evaluate the behaviour of different classifiers with optical and radar data as well as data at different scales. Further, the behaviour of different classification algorithms with changing training data set size and different sampling plans is explored.

The experiments reported in this thesis were undertaken in order to achieve the objectives listed below, while at the same time addressing a variety of other issues that are extremely important for successful applications of any classification algorithm for land cover classification studies.

Decision tree classifiers have been used in land cover classification over the last few years. However, a number of issues related to the performance of these classifiers have not yet been fully discussed in the literature. The main issues that need further clarification are:

1. Determining how different attribute selection measures and pruning methods affect classification accuracy.

2. Determination of optimal number of samples required to train the decision tree classifier.

Other problems relating to the use of the decision tree classifier that have been recognised in the literature and which need further investigation are:

1. Effect of boosting on classifier performance.

2. Type of decision tree classifier (i.e., univariate or a multivariate), and under what conditions each is to be used.

Although a few studies have highlighted specific problems, such as the influence of boosting on the results produced by the decision tree classifiers, or the effect of using univariate and multivariate decision tree classifiers on classification accuracy, no research study to date has attempted to consider all of the factors listed above in the context of the classification of remotely sensed images.

The level of classification accuracy achieved using support vector machines is also affected by several factors. The research reported here discusses the following points:

1. How classification accuracy changes by using various kernels and different multi-class methods of generating support vector machines.

2. The effect of training set size on classification accuracy, and

3. Comparing the performance of this classifier with neural and decision tree classifiers using hyperspectral data with small training data set sizes.

In addition to the above topics, this study involves the comparison of the classification accuracy, training time, ease of use, and various user defined parameters required for training neural, decision tree and support vector classifiers.

Irrespective of the classifier used, the nature of the data (and of derived features such as texture) also influences the accuracy of land cover classification. In view of this, some further objectives that are set for this study are:

1. To study the effect of ETM+ panchromatic band and its texture features for land cover classification in combination with ETM+ multispectral data.

2. To study the use of interferometric SAR data, especially coherence images, for land cover classification in combination with the InSAR intensity images. To improve the classification accuracy, the use of texture features (based on GLCM, the MAR model, and fractals) derived from

coherence and intensity images were also studied, and feature selection techniques were used to reduce the dimensionality of the datasets.

The research reported in this thesis involves a range of other experiments that are carried out to achieve the following objectives:

1. To conduct an extensive study to investigate the effect of number of training data with changes in the number of features, the sampling plan used to select the pixels for training and testing classifiers, and the scale (resolution) of remote sensing data on classification accuracy using DAIS hyperspectral and ETM+ data of the same area.

2. To study the effectiveness of feature extraction methods such as maximum noise fraction (MNF) applied to hyperspectral data for land cover classification accuracy.

3. To study the effectiveness of decision tree classifiers for feature selection with hyperspectral data.

1.3 Thesis structure

The work described in this thesis covers the period October 1999 to mid 2002. Initially, attention was focused on the use of interferometric SAR in agricultural crop classification. This work is reported in chapter 6. It proved more difficult than expected to obtain suitable InSAR data for the study area, and so the scope of the research was broadened to cover factors influencing the accuracy of agricultural crop classification derived from remotely sensed data. The present structure of the thesis reflects this re-orientation of the research. Naturally, new ideas developed over the study period, and research is still progressing in areas such as the use of support vector machines.

This study consists of eight chapters including this introductory chapter describing the details of problem, techniques and methodologies used and analysis of results obtained using different methodologies. The early chapters mainly provide background information about the theory of classification and fundamentals of decision tree and support vector machine classifiers.

- In *chapter 2* the classification process and various classification algorithms including unsupervised and supervised, parametric and non parametric classification techniques, are discussed in detail. A general idea of the incorporation of spatial information including context and texture in classification is also discussed. Finally, the methodologies used to assess classification accuracy, such as the Kappa value and its confidence limits, are described.

- *Chapter 3* consists of a detailed description of the decision tree classifier and support vector machines to be used for image classification problems. Various methods of designing a decision tree are discussed critically. Details of various attribute selections and pruning methods used with different decision tree classifiers are also discussed. A section is devoted to a comparative study of various types of decision tree classifiers. Ways of using continuous attributes in decision tree classifier are described. The second part of this chapter deals with a recently developed nonparametric classification technique, called the support vector machine (SVM) for remote sensing image classification, which includes the theory behind the development of this type of classifier. Finally, a new way to create an ensemble of same base classifiers using boosting and bagging techniques are discussed in detail.

- *Chapter 4* considers the relevance of the type of data on the outcome of a classification. The principles of interferometric SAR, including differential interferometry, are discussed in detail, with details of the derivation of coherence images. Various factors affecting the magnitude of coherence are also discussed. Some details of Landsat 7 ETM+ and DAIS hyperspectral data are also provided. The problems associated with the use of DAIS data are also discussed.

- *Chapter 5* presents the results achieved by decision tree and support vector machine classifiers for a land cover classification problem. The various factors that affect land cover classification accuracy are investigated using both classification systems. A comparison of the results obtained using decision tree classifiers, neural networks, support vector machines and maximum likelihood classifiers is presented. The advantages and disadvantage of using decision tree and support vector machine classifiers are compared to those associated with neural network classifiers. Finally the effect of including the Landsat ETM+ panchromatic band and its internal texture on classification accuracy using a decision tree classifier is discussed. The effects of changing the values of user defined parameters affecting the classification accuracy of SVMs are also considered.

- *Chapter 6* discusses the results obtained using interferometric SAR images for land cover classification studies. The usefulness of texture information derived from coherence as well as intensity images is also discussed. This chapter contains a detailed consideration of the main approaches to texture extraction used in this study (based on GLCM, the MAR model, and fractals) as well as the method used to choose the most appropriate number of features for a specific classification problem.

- *Chapter 7* discuss the effects of factors such as sampling plan, sample size, and scale of data on land cover classification using hyperspectral and ETM+ data. Factors such as feature extraction using orthogonal techniques and decision trees are also discussed. Results obtained using data at different scales, with different number of features with fixed numbers of training patterns as well as changing training patterns with fixed number of features are discussed, so as to examine the relevance of the Hughes phenomenon with four different classification systems.

- In *chapter 8,* overall conclusions drawn from this research are presented. This chapter also summarises the major findings of this research, and provides a number of recommendations for future work using different classifiers.

Chapter 2

Classification

2.1 Introduction

The science of remote sensing consists of interpretation of measurements of electromagnetic energy reflected from or emitted from a target. Sensors mounted on aircraft or satellite platforms records this electromagnetic radiation. The first civilian satellite, known as Television and Infrared Observation Satellite (TIROS), was launched in 1960 for the purposes of meteorological observation, acquiring images of weather patterns for use in forecasting. Landsat-1 was launched in 1972 to monitor the earth’s land surface using a multispectral imaging system. The Landsat series has since proved to be one of the main sources of global environmental information and still continues to provide coverage for the planet between 82^0 N and 82^0 S, making a repeat coverage every 16-18 days (Wilkinson, 2000; Mather, 1999).

According to Wilkinson (2000), "The main advantage of satellite remote sensing over alternative forms of environmental data gathering is that large global surface areas can be monitored without the need for ground level surveys. In addition, satellite observations are less costly than aerial surveys for long term and large-area mapping and monitoring".

Remote sensing satellites record data in digital form, which is then processed by computer. Computer processing applications range from calibration of the data for the effects of factors such as the changing response of sensors over time to the identification of patterns in multi- and hyper-spectral data that relate to features on the ground.

Classification of satellite images is one of the most commonly applied techniques used in remote sensing data processing. "Classification involves performing a transformation from the numerical spectral measurements into a set of meaningful classes or labels, which can describe a landscape. Classification effects a transformation from a physical measurement into a cartographic or thematic description of the earth's surface, for examples into terms such as forest, built-up area, water bodies, etc. As such, classification can be viewed as a signal inversion process" (Wilkinson, 2000). A number of techniques exist in the literature for classification of remotely sensed data (Mather, 1999; Richards, 1993; Swain and Davis, 1978; Schowengerdt, 1997).

Classification is a method by which labels are attached to pixels in view of their character (Richards, 1993). This character is generally their response in different spectral ranges. Labelling is implemented through pattern classification procedures. The term "pattern" refers to the set of radiance measurements obtained in the various wavebands for a given pixel, and spectral pattern classification refers to the family of classification procedures that utilises this pixel-by-pixel spectral information as the basis for land cover classification. In contrast, spatial pattern recognition involves the classification of image pixels on the basis of their spatial relationship with pixels surrounding them. Temporal pattern recognition uses change in spectral reflectance over time as the basis of feature identification.

The classification process has two main stages. In the first stage, the number and nature of the categories are determined, whilst in the second stage every unknown or unseen element is assigned to one of the categories according to its level of resemblance (or similarity) to the basic patterns. These stages are often called classification and identification, respectively. In the context of remote sensing, the categories could be land cover features or cloud types, and the assignment to one of the categories is carried out by allocating numerical labels, corresponding to the classes, to individual pixels. Hence, for a researcher working in the remote sensing field, classification basically means determining the class membership of each pixel in an image by comparing the characteristics of that pixel to those of categories known a priori.

2.2 The classification process

Image classification is the process of creating a meaningful digital thematic map from an image dataset. The classes shown on the map are derived either from known cover types (such as wheat or soil) or by algorithms that search the data for similar pixels. Once data values are known for the distinct cover types in the image, a computer algorithm can be used to divide or segment the image into regions that correspond to each cover type or class. The classified image can be converted to a land use map if the use of each area of land is known. The term land use refers to the purpose for which people use the land (e.g. city, parks, and road), whereas cover type refers to the material that an area is made from (concrete, vegetation). Image classification can be done using a single image dataset, multiple images acquired at different times, or image data with additional information such as elevation measurements, or expert knowledge about the area.

Traditionally, land cover classification based on remotely sensed data involves several steps (Schowengerdt, 1997), as shown in Figure 2.1:

(i) "*Feature extraction*: The term feature refers to a single element of a pattern (such as one of the Landsat ETM+ bands). More generally, a feature can be thought of "…as a distillation of that information contained in the measurements which is useful for deciding on the class to which the pattern belongs" (Swain and Davis, 1978). The original data may contain information relating to atmospheric and topographic conditions. In addition data are often highly correlated between spectral bands, which may not be useful for land cover classification and even may reduce classification accuracy. Thus, feature extraction performs two functions:

(1) separation of useful information from noise or non-information and

(2) reduction of the dimensionality of the data in order to simplify the calculations performed by the classifier, and to increase the efficiency of statistical estimators in a statistical classifier.

These aims can be achieved by applying spatial or spectral transform to the image, such as selection of a subset of bands, or a principal component transformation to reduce the data dimensionality.

This step is optional in classification of remotely sensed images i.e. the images can be used directly, if desired.

(ii) *Training:* The term "training" arose from the fact that many pattern recognition systems were "trainable"; i.e., they learned the discriminant functions in the feature space by adjusting their parameters when applied to a training pattern (pixel vector) whose true class is known. This process of training a classifier is either supervised by the analyst or unsupervised.

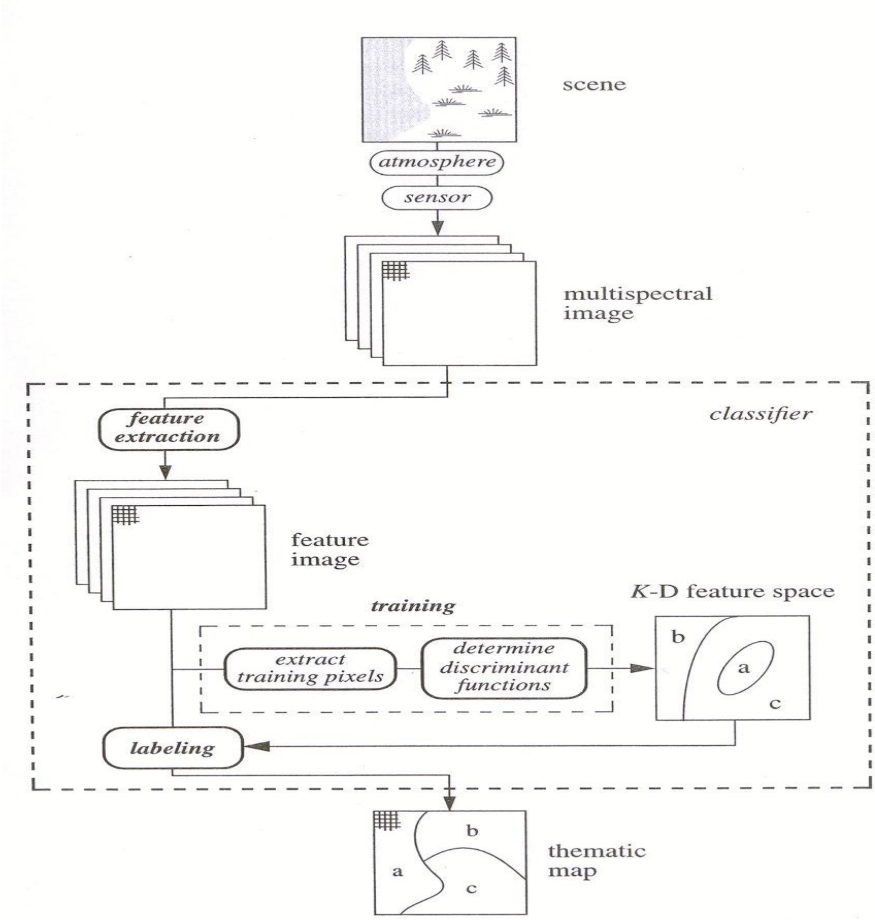

Figure 2. 1. The classification process (Adapted from Schowengerdt, 1997)

(iii) *Labelling*: The process of allocating individual pixels to their most likely class is known as labelling. This process of labelling can be approached in one of two ways. If the analyst knows the number of separable pixels that exist in the area covered by the image, and if it is possible to estimate the statistical properties of the values taken on by the features describing each

> of these pixels (in statistical classifiers), then individual pixels (test pixels) can be labelled as belonging to the classes based on these statistical properties. The other method is where the analyst has no clear idea of the number and character of the land cover classes present in the images. A method of allocating and reallocating the individual pixels to one of an initial set of randomly-chosen pixels is used. At each stage, each pixel in turn is given the label of one of these randomly chosen pixels using some classifier. At the end of first iteration, when every pixel has been labelled, the randomly chosen pixels can be altered in character (either by combining, splitting, and removing some of the pixels) according to the nature of the pixels which have been associated with them. This process of pixel labelling is repeated until the process converges. At this stage the user can relate these pixels to some land cover class" (Schowengerdt, 1997).

2.3 Classification techniques

The methodology of pattern classification applied to a particular problem depends on the data, the model of the data, and the information that one is expecting to find within the data (Bezdek, 1981). The data may be qualitative, quantitative, numerical, pictorial, textual, linguistic, or any combination of the above. Pictorial data carry information about the object in the scene depicted in the image. Image information can be described at many levels of abstraction. A description may range from one expressed in terms of meaningful attributes of the scene depicted in the image to one that describes only the spatial variation of intensity. Any of these descriptions can be expressed with a model that captures only the relevant features of the image at that level of abstraction and leaves others unspecified. The role of a model is to convert information in the image into usable form and, therefore, to enable the user to draw conclusions about the properties of the objects being studied. The model used must be such that it transforms the data and makes them compatible with the search and matching strategies to be used. Each search and matching strategy corresponds to a different pattern classification methodology. This is the reason for the use of different approaches to pattern classification, e.g., mathematical or statistical, heuristic, and structural etc (Tou and Gonzalez, 1974).

Human problem solving is generally an exercise in studying input conditions to predict an outcome based upon previous experience with similar situations. Using a computer program for developing rules based upon a series of these experiences is called ‘‘supervised’’ learning. Supervised learning is used for data sets with cases having known outcomes; this type of learning is the more common form because data are usually collected with some outcome in mind. Unsupervised learning, on the other hand, is not guided - the classes into which data fall are not known a priori. Such might be the case for a new problem for which the user has little experience.

Generally, image classification techniques in remote sensing can be divided into supervised and unsupervised methods based on the involvement of the user during the classification process. Methods can be further sub-divided into parametric and non-parametric techniques, based on whether or not the classifier employs some distributional assumption about the data.

Supervised classification techniques require training areas to be defined by the analyst in order to determine the characteristics of each category. Each pixel in the image is, thus, assigned to one of the categories using the extracted discriminating information. Problems of diagnosis, pattern recognition, identification, assignment and allocation are essentially supervised classification problems, since in each case the aim is to classify an object into one of a pre-specified set of classes. Unsupervised classification, on the other hand, searches for natural groups of pixels, called clusters, present within the data by means of assessing the relative locations of the pixels in the feature space. In these classification systems, an algorithm is used to identify unique clusters of points in feature space, which are then assumed to represent unique categories. These are automated procedures and therefore require minimal user interaction.

Supervised learning is the more useful technique when the data samples have known outcomes that the user wants to predict. On the other hand, unsupervised learning is more appropriate when the user does not know the subdivisions into which the data samples should be divided. Prior categorical division may not be obvious because the problem may be a new one, for which the user has little experience. In such a case, an unsupervised learning procedure can provide insight into groupings that may make physical sense and facilitate future analysis.

Parametric classification procedures use some statistical measures to derive rules from the data, which leads to some assumptions. The most common assumption of this kind is that of the normal (Gaussian) frequency distribution of the data being used. However, non-parametric methods do not make any assumptions about the frequency distribution of the data used, and do not use statistical estimates. The minimum distance and maximum likelihood classifiers are examples of statistical classification methods, whilst the artificial neural network, support vector machine, and decision tree methods can be given as examples of non-parametric classification methods. Detailed information about unsupervised and supervised and parametric and non-parametric classification methods is given in the following sections.

2.3.1 Unsupervised classification

When ground information concerning the characteristics of individual classes is not available in land cover classification problems, an unsupervised classification technique is used to identify a number of distinct or separable categories. In other words, an unsupervised classification method is used to determine the number of spectrally-separable groups or clusters in an image for which there is insufficient ground reference information available. These unsupervised methods can be viewed as techniques of identifying natural groups, or structures, within multispectral image data. While applying an unsupervised method, the analyst generally specifies only the number of classes (or the upper and lower bound on the number of classes) and some statistical measure, depending upon the type of clustering algorithms used. These methods generate the specified number of clusters in feature space, and the user assigns these clusters (spectral classes) to information classes depending on his or her knowledge of the area. Determination of the clusters is performed by estimating the distances or comparison of the variance within and between the clusters. These automated classification methods are expected to delineate (or extract) those land cover features that are desired by the analyst. After the specified number of groups is determined, they are labelled by allocating pixels to land cover features present in the scene. However, some groups may be inappropriate since they represent either irrelevant categories for the purpose of the study or else they are mixed classes. Therefore, the spectral characteristics of the area of interest should be sufficiently well known to the analyst to allow him/her to correctly label the clusters representing actual land cover features. Unsupervised classification techniques generally require user interaction in specifying the number of groups to be recognised and in labelling the correctly identified areas with the individual feature (or class) label. Owing to the minimal amount of user involvement, they are usually considered as automated procedures. Clustering has been used for several decades in various fields for grouping data. There are numerous clustering algorithms that can be used to determine the natural spectral grouping present in the data set, each having its own characteristics. Some procedures iterate to a local minimum for the average distance from each pixel to the nearest cluster means. The most popular clustering algorithms used in remote sensing image classification are ISODATA, a statistical clustering method, and the SOM (self organising feature maps), an unsupervised neural classification method. The details of other clustering algorithms can be found in Jain and Dubes (1988) and Mather (1999).

2.3.1.1 ISODATA method

In the migrating means (or ISODATA, or nearest mean) algorithm (Ball and Hall, 1965), the value of the function to be minimised is the average Euclidean distance between each sample point and the corresponding cluster mean. Intuitively, this is equivalent to generating spherical clusters with small variances or scatter. There is no analytical method for generating clusters that minimises the value of this function. There are a number of different forms of this algorithm, but in all of them at least two parameters must be specified by the user: the number of clusters and the maximum number of iterations. The latter parameter ensures the method will terminate if convergence is not achieved.

2.3.1.2 Self-organising Feature Maps (SOM)

This is an artificial neural network algorithm that has been used for unsupervised data clustering in remote sensing (Schalle and Furrer, 1995; Tso, 1997). The self-organising map neural network algorithms developed by Kohonen (1989) is a unique type of neural network, having only two layers, the input (sensory cortex) and output (mapping cortex) layers. A SOM's learning strategy is based on the competitive learning concept. The training procedures for SOM can be separated into two stages: unsupervised and supervised training. At the learning stage, the SOM is firstly driven by an unsupervised training algorithm. At the end of the learning stage the weights connecting the two layers are adjusted in order to simulate the input data distribution. The patterns in the input space are therefore clustered. However, if a supervised classification task is to be performed, a second stage of supervised training is carried out in order to label the output layer neurones in terms of real-world objects. A SOM models data via a multidimensional array of competing neurones, each of which learns to represent a prototype cluster from a given data set. The learning algorithm for the SOM accomplishes two important things. It starts by clustering the input data and then proceeds to spatial ordering of the neurones in the competitive layer so that similar input patterns tend to produce a response in units that are spatially close to each other. After initialising the competitive layer with normalised random vectors, the input pattern vectors are presented to all competitive units in parallel and the best matching (nearest) unit is chosen as the winner. The topological ordering is achieved by using a spatial neighbourhood relation between the competitive units during training. The array of neurons effectively becomes a map of the natural relationship between the patterns (spectral measurements) given to the networks. SOM have been found to be powerful tools for complex pattern recognition problems. "Their usefulness is not universally agreed upon as it has also been found that they demand excessive computation time in comparison with other methods for data clustering in the remote sensing context" (Wilkinson, 2000).

ISODATA and SOM are the most widely used clustering algorithms in remote sensing image classification. Although the description of these methods as automated procedures seems complicated and powerful, the results of such methods are generally inferior to those achieved by supervised methods. This is partly because most real-world features exhibit complexity in their nature, and therefore may not be easily separable in terms of their spectral characteristics. In addition, the assumption forming the basis of the unsupervised approach, that the pixels belonging to a particular class will have similar spectral values in feature space, and all classes are relatively distinct from each other in feature space, is difficult to satisfy in practice. It also depends upon the user's expertise in defining appropriate parameter values and in correlating the clusters with information classes. Consequently, the accuracy of the results obtained by unsupervised classification methods is limited.

2.3.2 Supervised classification

Supervised classification methods are most commonly used in remote sensing and based on the knowledge of the area to be classified. "These methods are often central to the image analysis process, since these concerns the direct transformation from pixel counts to thematic map" (Wilkinson, 2000). Supervised classification may be defined as the process of identifying unknown objects by using the spectral information derived from training data provided by the analyst. The result of the identification is the assignment of unknown pixels to pre-defined categories. The main difference between the unsupervised and supervised classification approaches is that supervised classification requires training data. The analyst locates specific sites in the remotely sensed image that represent homogeneous examples of known land cover types. These areas are commonly referred to as training sites because the spectral characteristics of these known areas are used to train the classifier. The training data thus extracted is used to find the properties of each individual class. The training data are generally derived from fieldwork, analysis of aerial photographs, from the study of appropriate maps, or from personal experience.

For the purposes of this research, four supervised classifiers: Maximum Likelihood (ML), Artificial Neural Network using backpropagation (ANN), the Decision Tree (DT), and Support Vector Machines (SVMs) are used to label image pixels. These supervised classifiers perform a decision-making function on a data vector by assigning it to one of a given set of possible classes. The data vector can be derived from any set of measurements and, in the case of remotely sensed data, the measurements are generally levels of reflected or emitted electromagnetic energy. The measurements of the spectral bands form an *n* dimensional vector, which is the input to the classifier used.

In the supervised approach (Figure 2.2) the information required from the training data varies from one algorithm to another. The Maximum Likelihood classifier requires estimates of the mean vector and variance-covariance matrix for each class. In contrast, neural network models, support vector machines, and decision tree classifiers do not use any statistical information to identify unknown pixels present in an image, and no assumption is made about the frequency distribution of the data.

Supervised classification is performed in two stages; the first stage is the training of the classifier, and the second stage is testing the performance of the trained classifier on unknown pixels. In the training stage, the analyst defines the regions that will be used to extract training data, from which statistical estimates of the

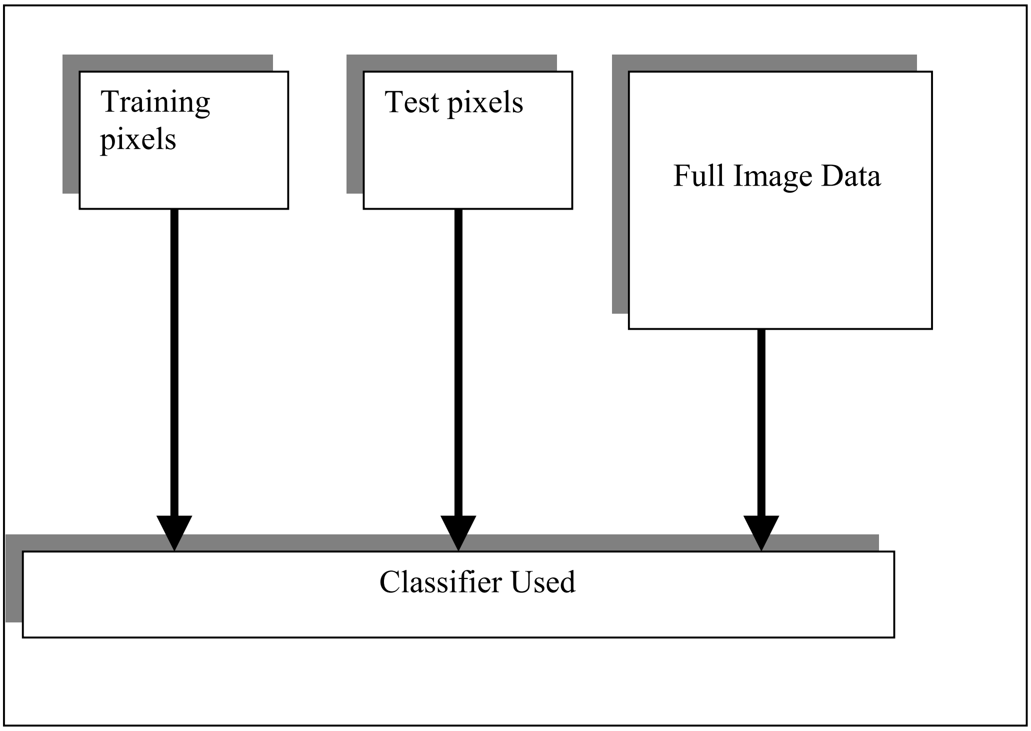

Figure 2.2. Principle of supervised classification.

data properties are computed. At the classification stage, every unknown pixel in the test image is labelled in terms of its spectral similarity to specified land cover features. If a pixel is not spectrally similar to any of the classes, then it can be allocated to an unknown class. As a result, an output image, or thematic map is produced, showing every pixel with a class label. The characteristics of the training data selected by the analyst have a considerable effect on the reliability and the performance of a supervised classification process. The training data must be defined by the analyst in such a way that they accurately represent the characteristics of each individual feature and class used in the analysis. Two features of the training data are of key importance. One is that data must represent the range of variability within class and the other is that the size of the training data set should be sufficient. In order to have a representative set of data, the pixels should be so selected that they correctly represent the spectral diversity of each class. Pixels should be selected from each of the fields to include all spectral classes. The best sampling strategy is to select training pixels randomly from the whole test image. Unfortunately, this is generally not possible in practice, as ground data for the whole area are generally not available.

The size of the training data set is also very important in supervised classification, if statistical estimates are to be reliable. Sample size is mainly related to the number of features whose statistical properties are to be estimated. Typically, it is recommended that the minimum training set size is some 10-30 times the number of wave bands per class being used for classification (Mather, 1999; Piper, 1992). Generally, a large training set is required for mapping from multispectral data sets. Supervised classification methods require more user interaction, especially in the collection of training data. The accuracy of supervised classification is determined partly by the quality of the ground truth data and partly by how well the set of ground truth pixels are representative of the full image. In order to measure the accuracy, it is common practice to use only part of the ground truth data for training the classifier and to use the remaining pixels for testing, that is to see if the classifier output corresponds to reality.

2.3.3 Parametric classifiers

Parametric approaches to classification make use of a parameterised model of the classes in the spectral feature space. These are generally more powerful than non-parametric methods and lead to higher overall classification accuracy if the data used satisfy the requirements of the model. The maximum likelihood method is the most common parametric approach. This procedure models classes according to the frequency distributions of the training pixels. Most often classes are modelled by using the multivariate form of the normal probability density function. Pixels are then classified by assigning them to the class to which they have the highest statistical likelihood of belonging.

2.3.3.1 Maximum Likelihood classifier

In the past thirty years or so, maximum likelihood classification has found wide application in the field of remote sensing. Based on multivariate normal distribution theory, the maximum likelihood classification algorithm has been in use since the late 1940s. Providing a probabilistic method for recognising similarities between individual measurements and pre-defined standards, the algorithm found increasing use in the field of pattern recognition (Nilsson, 1965). In remote sensing, the development of multispectral scanning technology in the 1970s to produce layered multispectral digital images of land areas provided the opportunity to use the maximum likelihood procedure to produce thematic classification maps of large areas for the purpose of land use/land cover determination.

The maximum likelihood method is a well known supervised classification algorithm that is based on the assumption that the probability density function for each class is normal (Gaussian) (Tou and Gonzalez, 1974). The normal distribution describes the probability of a single feature and it is specified by two parameters, the mean and the variance. The mean of the distribution controls the location of the distribution and the variance controls the spread of the data. When more than one feature is involved, then the multivariate generalisation of the normal distribution has to be used, i.e. the multivariate normal distribution. Instead of a single mean controlling the location of the distribution there is now one mean for each feature making up a mean vector. The multivariate equivalent of the variance is the variance-covariance matrix, representing the variability of pixel values for each feature within a particular class and the correlations between the features. These two parameters are computed for each sample, and they are used to describe each class.

The maximum likelihood classifier generates estimates of both the variance-covariance matrix and mean of the category spectral response patterns during the *classifier training* process. These estimates are derived by selecting samples that represent each class to be recognised from the total population to be classified. The assumption of normality is generally reasonable for common spectral response distributions. Under this assumption, the distribution of a class response pattern can be completely described by the mean vector and the covariance matrix. With these parameters, it is possible to compute the statistical probability of a given pixel being a member of a particular land cover class. The pixel is assigned to the class for which the probability of membership is the highest. Although in practice the assumption of "normally distributed" data is not generally met, the classifier generally outputs an acceptable result.

For the multivariate case, statistical theory describes the probability that an observation vector $X, X = (x_1, x_2, ..., x_n)$ belongs to class k_j, j = 1, 2, ….,c, based on the following formula:

$$\mathrm{P}_{\mathrm{k}_\mathrm{j}}(\mathrm{X}) = (2\pi)^{-1/2\rho} \left|\sum{}_{\mathrm{k}_\mathrm{j}}\right|^{-1/2} \times \mathrm{e}^{-1/2\left(\mathrm{X}-\mu_{\mathrm{k}_\mathrm{j}}\right)^{\mathrm{T}} . \sum_{\mathrm{k}_\mathrm{j}}^{-1} \left(\mathrm{X}-\mu_{\mathrm{k}_\mathrm{j}}\right)} \qquad (2.1)$$

where $\mathrm{P}_{\mathrm{k}_\mathrm{j}}(\mathrm{X})$ is the probability density value associated with the observation vector X quantified for class k_j, $\Sigma_{\mathrm{k}_\mathrm{j}}$ is the covariance matrix of the class k_j with dimension $\rho \times \rho$, $\mu_{\mathrm{k}_\mathrm{j}}$ is the mean vector of the class k_j, and $|.|$ represents the determinant of the given matrix. As applied in a maximum likelihood decision rule,, equation 2.1 allows the calculation of the separate probabilities that an observation is a member of each of *k* classes. The individual is then assigned to the class for which the probability value is greatest. In an operational context, the above equation can be reduced to the following expression by taking logarithms to the base *e*.

$$\ln\left[P_{k_j}(X)\right] = -\frac{1}{2}\rho.\ln(2\pi) - \frac{1}{2}\ln\left|D_{k_j}\right| - \frac{1}{2}\left(X - m_{k_j}\right)^T.D_{k_j}^{-1}.\left(X - m_{k_j}\right) \quad (2.2)$$

where D_{k_j} is the estimate of matrix Σ_{k_j} and m_{k_j} is the estimate of μ_{k_j}. These estimates are computed from the training data. From equation 2.2 it is clear that the use of the logarithmic form reduces the computational efforts, while using this classifier. As the term $\rho\ln(2\pi)$ is the same for all classes it can be regarded as a constant and omitted. The remainder of the equation 2.2 can be written in the following way:

$$-2\ln\left[P_{k_j}(X)\right] = \ln\left|D_{k_j}\right| + \left(X - m_{k_j}\right)^T.D_{k_j}^{-1}\left(X - m_{k_j}\right) \quad (2.3)$$

where the expression

$$\left(X - m_{k_j}\right)^T.D_{k_j}^{-1}.\left(X - m_{k_j}\right) \quad (2.4)$$

is the measure of the distance of one observation vector from the class mean m_{k_j}, corrected for the variance and covariance of the class k_j, and is known as the Mahalanobis distance. An observation vector will be assigned to the class for which the value -2 $\ln[P_{k_j}(x)]$ is the smallest.

The reliability of the results obtained with this classifier declines when the frequency distribution of the data departs from normality, especially when the distribution is bimodal. In extreme cases, where the multivariate normal assumption does not properly describe the data distribution in feature space, the results can be misleading. The other drawback of this method is the computational cost required to classify each pixel. This is particularly important in circumstances where data to be classified are measured in a large number of spectral bands, or include many spectral classes to be discriminated. The reliability of the estimates of mean vector and variance-covariance matrix, which are fundamental to the calculation of the likelihood, is affected by the relationship between sample size and the number of features. It should also be noted that all features are used to discriminate between classes, rather than the minimum effective set. It is not possible to use categorical data with this classifier as the classifier assumes that the data forming each class are normally distributed. The maximum likelihood classification method is available in almost all remote sensing and image processing software packages, and it is generally used as the standard supervised classification method.

2.3.4 Non-parametric classifiers

Many types of supervised classification algorithm are used for land cover classification in remote sensing, and most software packages used by satellite image analysis offer alternatives. The objective of training a classifier is to define discrimination surfaces that divide the multidimensional feature space into regions corresponding to different thematic classes. The simplest forms of classifier rely on non-parametric methods, because these algorithms make no assumptions about the probability distribution of the data, and are often considered robust because they may work well for a wide variety of class distributions, as long as the class signatures are reasonably distinct. A wide variety of non-parametric spectral classifiers is available. These consist of statistical methods such as the parallelepiped or box classifier, the minimum distance classifier, and non-statistical methods such as the neural network, support vector machines, and decision tree classifiers.

2.3.4.1 Parallelepiped classifier

This classifier, also known as the box classifier, is perhaps the simplest of all nonparametric classification systems because this requires the least information from the user of the supervised classification methods. In this method, for each of the class specified, the user provides an estimate of minimum and maximum values of each of the features used, from the training data. Another way is to define a range, by adding and subtracting a given number of standard deviations (generally 2-3) on either side of the mean of each feature can be used. This range allows the estimation of the position of the boundaries of each parallelepiped (Figure 2.3). An unknown pixel is classified if it lies inside any of the parallelepipeds. If the pixel does not lie inside any of the regions defined by the parallelepipeds, such pixels are of unknown type.

The problem with the parallelepiped technique occurs when a pixel lies inside two or more overlapping parallelepipeds, which makes the labelling process difficult. Classification of such pixels and allotting these pixels to their correct class is of great importance, as overlapping parallelepipeds are common in remotely sensed data analysis. Several suggestions have been made to overcome this problem. The easiest way for these types of problems is to allocate the pixel to the first or some other arbitrary-selected parallelepiped inside whose boundaries it falls. The problem with this approach is to select the correct parallelepiped and there is no rule that can be used to find out the correct parallelepiped. The second solution is to employ another, generally more complicated, decision rule, such as to calculate

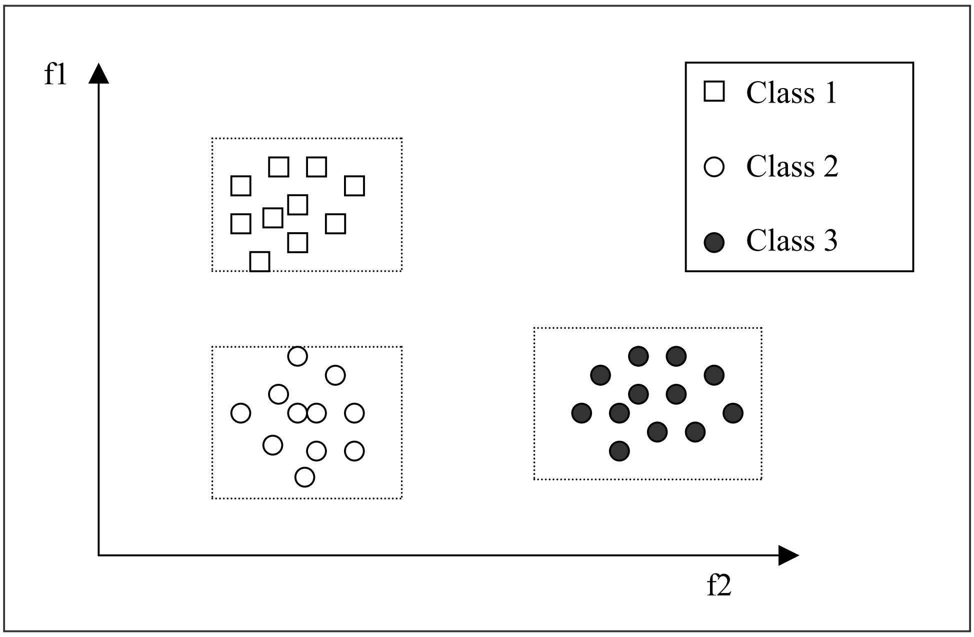

Figure 2. 3. Parallelepiped classification strategy.

the Euclidean distance between the doubtful pixel and the centre point of each parallelepiped and use a minimum distance rule to allocate these pixels to a specified class. To solve these problems, Lillesand and Kiefer (1994) suggested another method of using a series of rectangles with stepped borders in place of the single rectangle.

2.3.4.2 The Minimum Distance classifier

This is another simple non-parametric classification method, which uses the minimum distance between the pixel and the centroid of the training class. This classification method uses the Euclidean distance (or in a little more complicated way by adopting the Mahalanobis distance) in multidimensional feature space to measure the degree of dissimilarity between pixels and class centroids computed from training data. The pixel is assigned to the least dissimilar class centroid. Like the parallelepiped classifier, this algorithm does not take all the training data into consideration. It considers the mean (or average) spectral value in each band for each class. The mean centre of each class is estimated from the training dataset, which results in a mean vector. In order to assign a pixel to a specified class, Euclidean distances are calculated for each mean (or centroid) centre, and then the

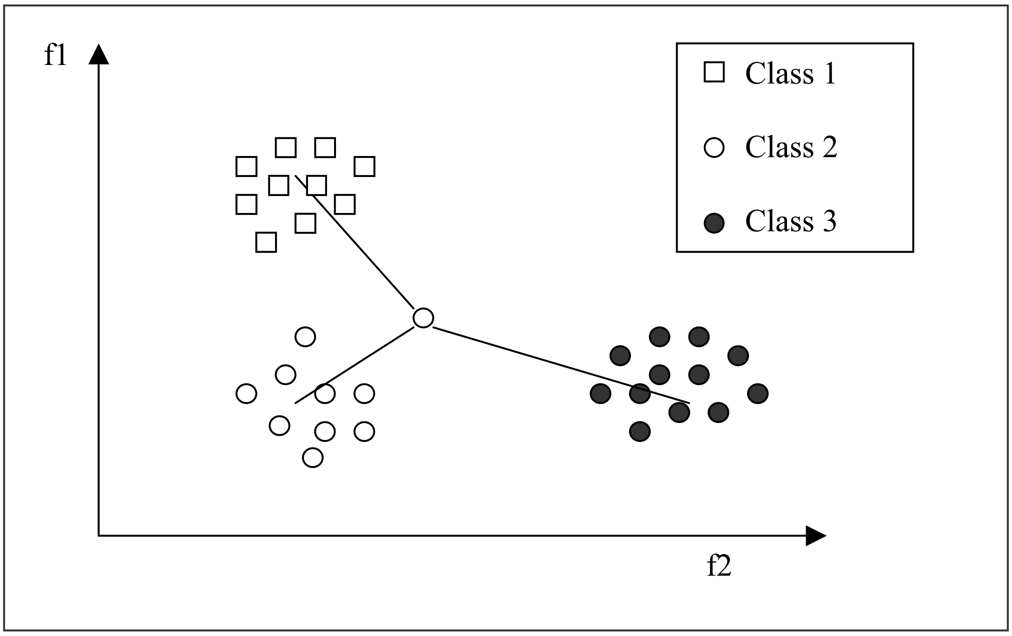

Figure 2. 4. Minimum distance to mean classification strategy

minimum value, i.e. the shortest distance, is determined. As a result, the pixel is allocated to the class that is the closest in terms of the estimated multidimensional Euclidean distance from mean centres (Figure 2.4).

.

This type of classifier is mathematically simple and computationally efficient, but has certain limitations. Most importantly, it is sensitive to different degrees of variance in the spectral response data. Due to these problems, this classifier is not widely used in applications where spectral classes are close to one another in measurement space and have high variance. However, it can give results that are comparable to other statistical classifiers, such as the maximum likelihood classifier in cases where the classes are well defined in feature space.

2.3.4.3 Artificial Neural Network classifiers

Since the late 1980s, supervised classification of satellite image data has also been carried out using neural network classifiers. These classifiers differ significantly from the parallelepiped and minimum distance algorithms in their approach to classification. A neural network is a form of artificial intelligence that imitates some function of the human brain. Neural networks are general-purpose computing tools that can solve complex non-linear problems (Fischer, 1996). The network comprises a large number of simple processing elements linked to each other by weighted connections according to a specified architecture. These networks learn from the training data by adjusting the connection weights (Bishop, 1995). They have been used in remote sensing and image analysis including supervised classification (Benediktsson et al., 1990; Hepner et al., 1990; Heerman and Khazenie, 1992; Foody and Arora, 1997) and unsupervised classification (Baraldi and Parmiggiani, 1995; Schaale and Furrer, 1995; Tso, 1997).

There are a range of artificial neural network architectures designed and used in various fields, including pattern recognition (Bishop, 1995; Aleksander and Morton, 1991). In remote sensing applications the multi-layered feedforward network, also called the multi-layer perceptron, and the Kohonen networks are generally used. These networks differ from each other in their approach to classifying the remotely sensed data. In this study, a feed-forward neural network with back propagation learning algorithm is used, as suggested by various researchers for remote sensing data (Benediktsson, 1990; Zhang and Scofield, 1994; Foody, 1995(a)).

The basic element of a back-propagation neural network is the processing node. Each processing node behaves like a biological neuron and performs two functions. First, it sums the values of its inputs. This sum is then passed through an activation function to generate an output. Any differentiable function can be used as an activation function, *f*.

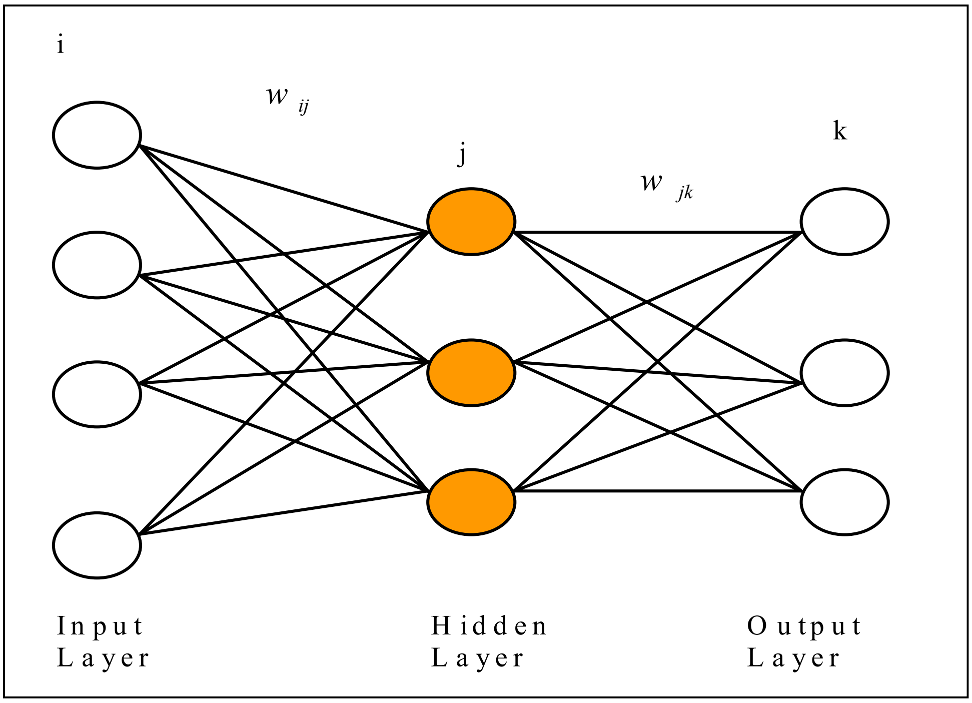

Figure 2.5. A back-propagation neural network, showing the input layer, one hidden layer and the output layer, with interconnecting links being associated with weights.

All the processing nodes are arranged into layers, each fully interconnected to the following layer. There is no interconnection between the nodes of the same layer. In a back propagation neural network, generally, there is an input layer that acts as a distribution structure for the data being presented to the network. This layer is not used for any type of processing. After this layer, one or more processing layers follow, called the hidden layers. The final processing layer is called the output layer. Figure 2.5 show the structure of a commonly used back propagation neural network.

All the interconnections between each node have an associated weight. When a value is passed from the input layer, down these interconnections, these values are multiplied by the associated weight and summed to derive the net input (n_j) to the unit

$$n_j = \sum_i w_{ji} o_i$$

where w_{ji} is the weight of the interconnection to unit j from unit i (called input) and o_i is the output of the unit i. The net input obtained by the above equation is then transformed by the activation function to produce an output (o_j) for the unit j. The sigmoid function is defined as:

$$f(n_j) = \frac{1}{1 + e^{-n_j}}$$

The shape of the sigmoid function can be modified by multiplying n_j by a constant, called the gain parameter, which is often set to the value one (Schalkoff, 1992). The values of the interconnecting weights are not set by the analyst but are determined by the network during the training process, starting with randomly assigned initial weights. There are a number of algorithms that can be used to adjust the interconnecting weights to achieve minimal overall training error in multi-layer networks (Bishop, 1995). The generalised delta rule, or back-propagation (Rumelhart et al., 1996) is one of the most commonly used methods. This method uses an iterative process to minimise an error function over the network output and a set of target outputs, taken from the training data set. The training data consists of a pair of data vectors. The training data vector is the pattern to be learned and the desired output vector is the set of output values that should be produced by the network. The goal of training is to minimise the overall error difference between the desired and the actual outputs of the network. The process of training begins with the entry of the training data to the network. These data flow forward through the network to the output units. At this stage, the network error, which is the difference between the desired and actual network output, is computed. This error is then fed backwards through the network towards the input layer with the weights connecting the units being changed in relation to the magnitude of the error. This process is repeated until the error rate is minimised or reaches an acceptable level, or until a specified number of iterations has been accomplished.

The neural network weights are adjusted either after the entire sum is obtained for all training patterns, called batch or epoch training, or after each training pattern is presented, called sequential training. The sequential training method allows more flexibility with the training data but requires more training time as compared to the batch training, because weights are adjusted with every training pattern instead of at the end of the cycle in batch training.

Training a neural network involves the setting of several initial parameters that strongly influence network performance, especially in terms of speed and accuracy. Even if these parameters are selected judiciously there is no guarantee that the neural network will provide an acceptable solution. The user-selected values influencing the neural classifier are:

- *Learning parameters* - the back-propagation learning algorithm requires that the user provides values of the learning rate and momentum. The value of these parameters significantly influence the performance of a network.
- *Initial weights* - the initial weight settings of the pre-trained network influence the network performances. These settings are generally chosen randomly.
- *Number of training iterations* - this is a very important parameter as it controls the degree of generalisation as opposed to specialisation of the solution: if network is trained using very large number of iterations on training data, it might not function well on the test data and if it is not trained well enough it will not be able to separate the classes.
- *Number of hidden layers and units* - this determines the capacity of the network to learn and generalise.

- *Number of input patterns* - several studies suggested that classification accuracy is affected by the number of training patterns.

In this study, all of the above parameters are set as suggested in an earlier study carried out by Kavzoglu (2001).

2.3.4.4 Decision Tree classifiers

Decision tree induction algorithms have long been popular in machine learning, statistics, and other disciplines for solving classification and related tasks (Morgan and Sondquist, 1963; Hunt et al., 1966; Friedman, 1977; Breiman et al., 1984; Quinlan 1993). A decision tree can be used to classify a query (or test) case as follows.

Given a query q to classify, a tree is traversed along a path from its root to a leaf node, whose class label is assigned to q. Each internal node contains a test that determines which of its subtrees is traversed for q. A test typically evaluates a feature used to describe cases, or a boolean or linear combination of features. A decision tree algorithm has four inputs:

1. a training set, in which each case is defined by a set of features and their respective values, and a class label,
2. a set of candidate tests that partition or split a set of training cases into subsets,
3. a heuristic evaluation function that assesses the quality of a given test and resulting partition, and
4. a stopping criterion function that defines when to terminate tree expansion.

The algorithm outputs a decision tree whose leaves typically bear a single class label. Decision trees are usually induced from the root downwards using a recursive divide-and-conquer algorithm (Quinlan 1993). The task of constructing a tree from the training data is called tree induction. Most existing tree induction systems proceed in a top-down fashion, starting with an empty tree and the entire training set. Decision tree classifiers are discussed in detail in chapter 3.

2.3.4.5 Support Vector Machines

Support vector machines (SVM) are classification and regression methods which have been derived from statistical learning theory (Vapnik, 1995). These classification techniques are based on the principle of *optimal separation*, in which - if the classes are separable - this method selects, from among the infinite number of linear classifiers that separate the data, the one that minimise the generalisation error, or at least an upper bound on this error, derived from structural risk minimisation. Thus, the selected hyperplane will be one that leaves the maximum margin between the two classes, where margin is defined as the sum of the distances of the hyperplane from the closest point of the two classes (Vapnik, 1995).

If the two classes are non-separable, the SVM tries to find the hyperplane that maximises the margin and that, at the same time, minimises a quantity proportional to the number of misclassification errors. The trade off between margin and misclassification error is controlled by a positive constant that has to be chosen beforehand.

This technique of designing a SVM can be extended to allow for non-linear decision surfaces. This can be achieved by projecting the original set of variables into a higher dimensional feature space and formulating a linear classification problem in the feature space. Further details of SVM based classifiers are discussed in chapter 3.

2.4 Incorporation of nonspectral features

Though, spectral information alone provides useful information about the characteristics of land cover features, the addition of a different kind of information may help in the identification of different classes that are not easily distinguished using spectral data alone. Spatial information, such as texture and context, which depends on the neighbourhood of the pixel, has been widely used, while the second kind of information represents external or non-remotely-sensed information such as elevation values or data derived from soil or geology maps.

Spectral, textural, and contextual features are the fundamental pattern elements used in human interpretation of satellite images. Spectral features describe the tonal variations in the various bands of the image, obtained in different bands of the electromagnetic spectrum, whereas textural features contain information about the spatial distribution of tonal variation within a band. Contextual feature contain information derived from blocks of image data surrounding the area being analysed.

A number of textural measures have been proposed in literature, including the grey-level co-occurrence matrix (Haralick et al. (1973), auto-regressive models (Frankot and Chellappa, 1987), fourier transform, and fractal based texture (Keller and Chen, 1989). Recently, wavelet-based texture features (Fukuda and Hirosawa, 1999) have been used in classification of remotely sensed data. A considerable amount of research has been carried out to investigate the effectiveness of texture features for the classification of remotely sensed images. For example, Weszka et al. (1976) perform a comparative study of texture measures including the Fourier power spectrum, second-order grey-level statistics, and first-order statistics of grey-level differences in a study aimed at identifying three geological terrain types. Recently Mather et al. (1998) investigate the effectiveness of spectral and textural information in the identification of surface rock type in an arid region using Landsat TM and SIR-C SAR image data. A number of other studies (Barber and LeDrew, 1991 and Peddle and Franklin, 1991) have shown that classification accuracy can be improved by using the texture features in combination with image.

Generally, contextual information can be used in classification processes for smoothing purposes. The smoothing techniques can be categorised into pre-smoothing and post-smoothing. In pre-smoothing processes, contextual information is incorporated before classification by increasing the dimensionality of the data with additional bands in which contextual information is present, while post-smoothing processes are usually more or less smoothing filters (Townshend, 1986), so they work on previously classified images.

2.5 Accuracy assessment

The results of any classification process applied to remotely sensed data classification must be quantitatively assessed in order to determine their accuracy. As suggested by Lillesand and Kiefer (1994), a classification process is not complete until its accuracy is assessed. There may be different ways to assess the accuracy of a classification process. Accuracy assessment can be qualitative or quantitative, expensive or inexpensive, quick or time consuming, well-designed and efficient. The purpose of quantitative accuracy assessment is the identification and measurement of map errors. Quantitative accuracy assessment involves comparison of an area on a map against reference information of the same area, assuming reference data to correct. There are number of ways to determine the degree of error in the end-product, which is typically a thematic map or image, but for this research accuracy assessment is carried out by measuring overall classification accuracy, and calculation of the Kappa statistics for a given number of test data.

2.5.1 Confusion matrix

The accuracy of classification has traditionally been measured by the overall accuracy by generating a confusion matrix (Table 2.1) and determining accuracy levels by dividing the total number of correctly classified pixels (sum of major diagonal of confusion matrix, also called *actual agreement*) by the total number of reference pixels. However as a single measure of accuracy, the overall accuracy gives no insight into how well the classifier is performing for each of the different classes (Fitzgerald and Lees, 1994). In particular, a classifier might perform well for a single class that accounts for a large proportion of the test data and this will create a bias in overall accuracy, despite low class accuracies for other classes. To avoid such a bias when assessing the accuracy of a classifier, it is important to consider the individual class accuracies. Individual class accuracy can be obtained by dividing the total number of correctly classified pixels in that category by the total number of pixels of that category. Individual class accuracy can be determined by using the reference data (called *producer's accuracy*). The resulting percentage accuracy indicates the probability that a reference pixel will be correctly classified. Story and Congalton (1986) suggested that producer's accuracy is a measure of *error of omission*. However, a misclassification error is not only an omission from the correct class but also a commission into another class. Individual class accuracy obtained from the classified data in that category (*user's accuracy*) is a measure of *error of commission* (Story and Congalton, 1986). Before confusion matrices were the standard accuracy reporting mechanism, it was common to report the overall accuracy and either only the producer's or user's accuracy. Example in Table 2.1 demonstrate the need of the entire confusion matrix so that all three accuracy measures can be computed.

Table 2.1. Confusion matrix

Class	1	2	3	4	5	6	7	8	Total	Users
1	423	0	70	0	0	0	2	14	509	83.1
2	0	500	0	0	0	0	0	0	500	100
3	43	0	287	10	6	0	12	103	461	62.3
4	1	0	15	312	108	6	43	34	519	60.1
5	3	0	12	79	307	9	12	13	435	70.6
6	0	0	6	11	37	449	56	12	571	78.6
7	3	0	18	47	38	31	182	73	392	46.4
8	27	0	92	41	4	5	73	251	493	50.9
Total	500	500	500	500	500	500	380	500	3880	
Produc	84.6	100	57.4	62.4	61.4	89.8	47.9	50.2		

Overall accuracy = 69.9 Kappa value = 0.655

Considering the confusion matrix shown in Table 2.1, there exist considerable differences between the user’s and producer’s accuracies for corresponding classes. The values of user's and producer's accuracies shows significant variation from the overall accuracy (69.9%). If the overall accuracy is solely taken into account, it can be concluded that the classifier has an average accuracy of about 70%, without giving the effectiveness of the classification on a particular class, which could be misleading. If the overall accuracy and one of the individual class accuracy measures are considered, the analyst could again reach some misleading conclusions. For example, a producer’s accuracy of 57.4% is achieved for the class 3, which is quite low when compared to the overall accuracy. The analyst can conclude at this stage that, although the overall accuracy is average, the class 3 can be classified with lower accuracy (57.4%). Drawing such a conclusion could be a mistake because the user’s accuracy of the class 3 is 62.3%. This means that although 57.4% of the class 3 areas have been correctly identified as class 3, 62.3% of the areas called class 3 on the classification map are actually class 3 on the ground. Thus, suggesting that a careful analysis of the confusion matrix is necessary to present the results and conclusions in a meaningful way.

Generally, the confusion matrix is an appropriate tool for assessing the accuracy of land cover classifications. However, Congalton (1991) suggested the use of the Kappa coefficient as a suitable measure of the accuracy of a thematic classification. It is a measure of the randomness of the classification results. It measures the difference between the actual agreement in the confusion matrix (i.e., the agreement between the remotely sensed classification and the reference data as indicated by the major diagonal) and the chance agreement which is indicated by row and column totals. It provides a better measure of the accuracy of a classifier than the overall accuracy, and it takes into account the whole confusion matrix rather than the diagonal elements alone.

The Kappa statistic is calculated from the confusion matrix by using the following formula:

$$K = \frac{n\sum_{i=1}^{p} x_{ii} - \sum_{i=1}^{p} x_{io} x_{oi}}{n^2 - \sum_{i=1}^{p} x_{io} x_{oi}} \qquad (2.5)$$

Where n = total number of pixels used for testing the accuracy of a classifier

p = number of classes

$\sum x_{ii}$ = sum of diagonal elements of confusion matrix

$\sum x_{io}$ = sum of row i

$\sum x_{oi}$ = sum of column i

Kappa value computed for each confusion matrix is a measure of how well the remotely sensed classification agrees with the reference data. The value of the Kappa coefficient vary from +1.0 to –1.0. A positive value of the Kappa coefficient is expected to have a positive correlation between the image and reference data being used for classification. A value of zero indicates no agreement in classification, while a value of 1.0 indicates perfect agreement between the classifier output and the reference data.

Confidence intervals can be calculated for the Kappa value using the approximate large sample variance. The approximate large sample variance of Kappa is calculated as follows (Bishop et al., 1975):

$$\sigma(K)=\frac{1}{n}\left[\frac{\theta_1(1-\theta_1)}{(1-\theta_2)^2}+\frac{2(1-\theta_1)(2\theta_1\theta_2-\theta_3)}{(1-\theta_2)^2}+\frac{(1-\theta_1)^2(\theta_4-4\theta_2)^2}{(1-\theta_2)^4}\right] \quad (2.6)$$

where $\theta_1=\sum_{i=1}\frac{x_{ii}}{n}$, $\theta_2=\sum_{i=1}\frac{x_{io}*x_{oi}}{n^2}$, $\theta_3=\sum_{i=1}\frac{x_{ii}}{n}\left(\frac{x_{io}}{n}+\frac{x_{oi}}{n}\right)$ and

$$\theta_4=\sum_{i=1}\sum_{j=1}\frac{x_{ij}}{n}\left(\frac{x_{jo}}{n}+\frac{x_{oj}}{n}\right)^2$$

A test of significance for the Kappa statistic can be performed for each confusion matrix separately to determine if the agreement between the classification and the reference data is significantly greater than zero. In other words, a test can be performed to see if the classification is significantly better than a random assignment of land cover categories to pixels. The significance of a single confusion matrix can be calculated by

$$Z=\frac{K}{\sqrt{\sigma(K)}} \quad (2.7)$$

where Z is standardised and normally distributed and σ is the large sample variance of the Kappa coefficient.

A pair-wise test of significance can be performed between two independent Kappa values using the normal curve deviate to determine if the two confusion matrices are significantly different (Cohen, 1960). The test statistic for significant difference in large sample is given by

$$Z = \frac{K_1 - K_2}{\sqrt{\sigma(K_1) + \sigma(K_2)}} \tag{2.8}$$

where Z is standardised and normally distributed and K_1 ,K_2 are the two Kappa coefficients being compared. This test between two independent Kappa values allows any two error matrices to be compared in order to determine if they are significantly different. In other words, error matrices generated from several classification algorithms can be compared, two at a time, to determine which classifications are significantly better than the others. The computed value of Z is compared with a critical value $Z_{\alpha/2}$ for some predefined confidence level (i.e., α/2 is the confidence level of the two-tailed *Z* test and the degrees of freedom are assumed to be infinity), and if $Z \geq Z_{\alpha/2}$ the classification is significantly better than a random classification.

2.6 Conclusions

This chapter reviews the philosophy underlying classification procedures used in remote sensing. Classification techniques, categorised using four criteria (supervised and unsupervised, parametric and non-parametric) are discussed in detail. Some of the advantages and disadvantages of the techniques are also discussed. The most appropriate classification system used is dependent upon the characteristics of the data (such as scale and type of data) used and also on the nature of the classifier to be employed (the assumption on which classifier is working). A short discussion is also included about incorporating spatial information, texture and context, as both texture and context are sources of spatial information which are widely used for image classification.

Chapter 3

Advanced Classification Algorithms

3.1 Introduction

Statistical procedures such as the maximum likelihood classifier require that data must be based on some pre-defined model (usually the Gaussian normal distribution). The performance of a statistical classification will thus depend on how well the data match the pre-defined model. If the data are complex in structure then to model them in an appropriate way can become a real problem. These types of classifiers are also called single-stage classifiers because an observation is given the label of one of a predetermined number of classes in a single step. The statistical approach to classification has two significant drawbacks (Swain and Hauska, 1977):

1. Only one of the possible combinations of features is used in the classification.
2. Each sample is tested against all classes, which leads to a relatively high degree of inefficiency.

An inherent weakness of the maximum likelihood procedure is that the subset of features used in classification is not necessarily the optimal choice for all classes. Usually, a set of features is selected by the criterion of maximum average interclass separability, i.e., in a multi-class multi-feature classification the set of features for which the average pair-wise separability is largest is used. The problem of using only one feature subset as the basis of a classification is particularly severe when there is a large number of classes. In principle, one could combine the features that are useful in discriminating between all possible combinations of pairs of classes and use the combination of these features in a single stage classifier.

Much research effort in the past ten years has been devoted to analysis of the performance of artificial neural networks in image classification. The preferred algorithm is feed-forward multi-layer perceptron using back-propagation, due to its ability to handle any kind of numerical data, and to its freedom from distributional assumptions (section 2.3.4.3). A number of studies have reported that users of neural classifiers have problems in setting the choice of various parameters during training. The choice of architecture of the network, the sample size for training, learning algorithms, and number of iterations required for training are some of these problems.

In practice, and especially since the advent of hyperspectral data, the so-called dimensionality problem can be encountered, i.e., with a fixed and relatively small sample size, the classification accuracy may actually decrease as the number of features is increased (Hughes, 1968). Hence, if a large number of features is used, then a corresponding increase in the number of training and testing samples is required in order to ensure that the results obtained are reliable. Furthermore, some patterns may not need all the features in order to arrive at the correct classification, but a one stage classifier uses these features anyway, which results in decreased efficiency.

As progress in new sensor technology for earth observation remote sensing continues, increasingly high spectral resolution multi-spectral imaging sensors are being developed. These sensors give more detailed and complex data for each picture element and greatly increase the dimensionality of the data compared with multispectral systems. As the number of features, number of samples, and classification accuracy are interrelated in a complex fashion, one may need to know how many features should be used to maximise the overall classification accuracy. Where training sample size is limited and the dimensionality of the feature space is high, then the estimate of first and second-order statistics (e.g., as required by maximum likelihood classifier) cannot accurately summarise all information which is contained in the data and results are thus less reliable.

For such problems, it would be preferable to have a classification system which could decompose the multi-class classification problem into several stages, and which finally may simplify the decision-making process by taking partial decisions at successive stages, or alternatively to use a classification system that is independent of the dimensionality of the feature space. The technique of decomposing the multi-class classification problem into several stages is termed multistage classification. It has several attractive features, the most important of which, perhaps, is understandability. In many instances, taking such partial decisions is conceptually simpler, as each involves only that information relevant to the current stage. This also saves the expense of gathering information not required for the current stage. These points have contributed to the increased popularity of multistage decision making in several engineering problems, especially in pattern recognition.

Another classification system, called the support vector machine, is said to be independent of the dimensionality of feature space. The main idea behind this classification technique is to separate the classes with a surface that maximise the margin between them, using boundary pixels to create the decision surface. It has been observed that the optimal hyperplane is determined by only a small fraction of the data points, thus requiring a small number of training data even at high dimensionality.

This chapter discusses various stages for the development of multistage and support vector machine classification algorithms.

3.2 Multistage classifiers

A large number of multistage classification techniques have been proposed for pattern recognition. These techniques can be categorised into three groups.

1. Converting a decision table to an optimal decision tree.
2. Dynamic tree development.
3. Hierarchical classification methods.

The problem of converting a decision table to an optimal decision tree is to design a decision tree to efficiently evaluate the value of a multiple input, multiple output function given the values of independent variables. Each of the independent variables has a finite domain. In pattern recognition, the range of the output is the set of classes. There are a number of table conversion methods available in the literature for pattern recognition problems. The details of these methods can be found in Meisel and Michalopoulos (1973), Stoffel (1974), and Sethi and Chatterjee (1977).

Dynamic tree development methods select a feature and split its region at every stage (node). Later stages handle smaller regions of the feature space and repeat the procedure. These are essentially top-down methods. Swain and Hauska (1977) used an evaluation function to optimise decision trees. Every node in a tree is taken as a classifier and a performance measure is defined for the node. All possible specifications are searched to find the best node configuration. A variety of other techniques use simple dynamic data splitting to design binary trees. For further details readers are referred to Breiman et al. (1984), Casey and Nagy (1984), Friedman (1977), Rounds (1980), and You and Fu (1976).

Hierarchical classifiers are multistage pattern classifiers in which classes are sequentially rejected along a path to a finally accepted class label. The hierarchical subgrouping of classes, the features required at nonterminal nodes of the hierarchy and the decision rules are interdependent. With a class hierarchy, individual nodes themselves acts as a pattern classifiers. However the node classifiers cannot be designed independently of each other. In the analysis process the potential advantages of using hierarchical classification are an increase in the accuracy, speed, and the level of details which can be reached.

Classification trees offer an effective implementation of hierarchical classifiers. Indeed, classification trees have become increasingly popular due to their conceptual simplicity and computational efficiency. A decision tree classifier has a simple form, which can be compactly stored, and it classifies new data efficiently. A decision tree classifier carries out automatic feature selection and complexity reduction, and the tree structure gives easily understandable and interpretable information regarding the predictive or generalisation ability of the data.

Another significant advantage of decision tree classifiers is that they are non-parametric, i.e., capable of handling non-normal and non-homogenous data sets (Quinlan, 1993) and can be very useful for land cover classification in remote sensing due to their simplicity, flexibility, and computational efficiency (Friedl and Brodley, 1997).

3.3 Decision tree classifiers

In general, there are two approaches to the design of decision trees (Swain and Hauska, 1977). These approaches are similar in principle, but differ significantly in the way the tree is designed in practice.

1. Manual design method
2. Heuristic search method

Manual methods use statistics such as the mean vector and covariance matrix, which are calculated for all classes. Then a graph is derived in which the means and variances for all the classes are plotted for each feature. This graph is called a coincident spectral plot. It is often possible to estimate suitable decision boundaries from this graph such that all classes are separated in a number of decision steps. As long as one feature is used in each stage, this is roughly equivalent to estimating a simple distance measure between the classes. This method is not suitable, firstly, when two or more features are to be used in a given stage of the tree, because the graph does not show how the interactions between features can be used, and secondly, if the data are not normally distributed, thus making it difficult to estimate the covariance matrices in an unbiased way.

The coincident spectral plot provides an estimate of interclass separability based on single features. If the difficulty of discriminating the classes requires the use of a combination of several features, the manual design approach based on the spectral plot is severely limited. In general, a more analytical design procedure is desirable when the complexity of the problem in terms of the number of classes or the number of features required for adequate classification accuracy is significant.

To construct a classification tree using the heuristic approach, it is assumed that a training data set consisting of feature vectors and their corresponding class labels is available. The feature set is selected on the basis of problem-specific knowledge. The decision tree is then constructed by recursively partitioning the training data set into purer, more homogenous, subsets on the basis of a set of tests applied to one or more attribute values at each branch or node in the tree. This procedure involves three steps: splitting nodes, determining which nodes are terminal nodes, and assigning class label to terminal nodes. The assignment of class labels to terminal nodes is straightforward: labels are assigned based on a majority vote or a weighted vote when it is assumed that certain classes are more likely than others.

A tree is composed of a root node (containing all the data), a set of internal nodes (splits), and a set of terminal nodes (leaves). Each node in a decision tree has only one parent node and two or more descendent nodes (Figure 3.1). A data set is classified by moving down the tree and sequentially subdividing it according to the decision framework defined by the tree until a leaf is reached.

The method of constructing a decision tree is as follows (Quinlan, 1993):
To construct a decision tree from a set T of training data having m classes denoted by $\{C_1, C_2,\ldots,C_m\}$. There are three probabilities:

- If T contains one or more objects, all belonging to a single class C_i, then the decision is a leaf identifying class C_i.
- If T contains no data, the decision tree is again a leaf determined from information other than T.
- If T contains data that belongs to a mixture of classes then a test is chosen, based on a single attribute or a combination of attributes, that has one or more mutually exclusive outcomes $\{\mathrm{O}_{1,}\mathrm{O}_2.......,\mathrm{O}_\mathrm{k}\}$. T is partitioned into subsets $\mathrm{T}_1, \mathrm{T}_2,........, \mathrm{T}_\mathrm{k}$, where T_i contains all the data in T that have outcome O_i of the chosen test. The decision tree for T consists of a decision node identifying the test, and one branch for each possible

outcome. The same tree building process is applied recursively to each subset of training data.

A typical decision tree for classification is shown in Figure 3.1. The elliptical nodes are decision nodes whose two descendants are determined by a threshold η_i on a specified feature value x_i. The same feature may occur in different parts of the tree associated with a different threshold. The rectangular nodes are terminal nodes and are assigned a class label. Based on the outcome of testing a feature value against a threshold, either a 'yes' or a 'no' branch will be taken. When an unknown feature vector is submitted for classification, the feature vector is assigned the class label of the terminal node that it reaches.

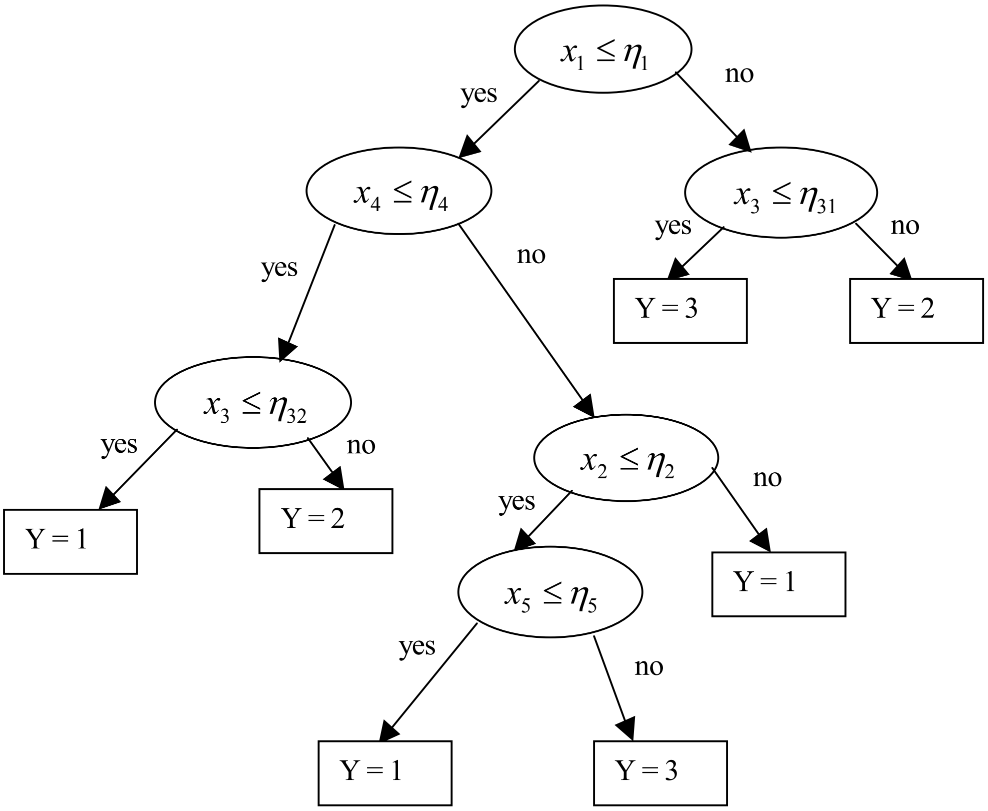

Figure 3. 1. A classification tree for a five dimensional feature space and three classes. The x_i are the feature values, the η_i are the thresholds, and Y is the class label.

3.4 Decision tree design approaches

Numerous tree construction approaches have been developed in the last thirty or so years, but most of the research in decision tree classifier design has concentrated in the area of finding splitting rules, which finally gives the idea of the termination rules. A number of algorithms have been developed to split the training data at each internal node of a decision tree into regions that contain examples from just one class, and this is the most important element of a decision tree classifier. These algorithms either minimise the impurity of the training data or maximise the goodness of split. The approaches to design a decision tree are:

- Bottom-up approach.
- Top-down approach.
- Hybrid approach.
- Growing-pruning approach.

3.4.1 Bottom-up approach

In the bottom-up approach (Landeweered et al., 1983), a binary tree is constructed using the training set and some distance measure, such as the Mahalanobis distance. The pairwise distances between a priori defined classes are computed and in each step the two classes with the smallest distance are merged to form a new group. The mean vector and covariance matrix for each group are computed from training samples of classes in that group, and the process is repeated until one is left with a single group at the root. In a tree constructed this way, the more obvious discriminations are done first, near the root, and more difficult ones at later stages of the tree.

3.4.2 Top-down approach

In top-down approach, the design of a decision tree classifier consists of the following three tasks:

1. Selection of a node splitting rule,
2. Decision as to which nodes are terminal,

3. Assignment of each terminal node to a class label.

The class assignment problem is the easiest of above-mentioned tasks. Terminal nodes are assigned to the classes that have the highest probabilities by using a basic majority rule; i.e., assign to the terminal node the label of the class that has most samples at that terminal node. The basic idea in choosing any splitting criterion at an internal node is to make the data in the descendent nodes purer.

The overall approach adopted by this process is to choose the attribute that best divides the training data into classes and then partition the data according to the value of that attribute. This process is applied recursively to each partitioned subset, with the procedure terminating when all examples in the current subset have the same class. The result is represented as a tree in which each node specifies an attribute and each branch emanating from a node specifies a possible value of that attribute.

Thus, the main task of this process is to select the attribute to be used as criterion because at each node in the development of a decision tree there will be a set of observations and a number of attributes to classify them. One cannot select an individual attribute without first determining the "quality" of all of the attributes, and seeing how well each one separates the data into various classes. The quality of an attribute should reflect the useful information provided by that attribute. There are two major approaches to estimating the quality of an attribute.

In the first approach, the quality of an attribute may be estimated by ignoring the other attributes, therefore assuming, for the purpose of estimation, the independence of attributes. In the second approach, the quality of an attribute may be estimated in the context of other attributes. The first approach is also called the *myopic approach* (Kononenko and Hong, 1997), which has the advantage of computational speed. The latter approach is computationally more demanding but has the potential to discover higher-order dependencies among the attributes.

3.4.2.1 Attribute selection measures

There are many approaches to the selection of attributes used for decision tree induction, and these approaches have been studied in detail by researchers in machine learning (Brieman et. al., 1984, Murthy et. al., 1994; Kononenko and Hong, 1997; Mingers, 1989 (b); Quinlan, 1993). Some approaches measure the "goodness of split" (Brieman et. al., 1984) while other approaches try to minimise the impurity of the training data.

The quality of an attribute in classification is defined in term of the purity of classes of training observations and most approaches assign a quality measure directly to the attribute. A set of observations is pure if all the observations belong to the same class, while the set is maximally impure if the proportion of observations in all classes is uniform. The *impurity function* measures the impurity of a set of observations and achieves the minimum for a pure set, and maximum for a maximally impure set. Impurity functions are mainly used in selecting the best attribute to further split the current node. The most frequently-used impurity measures in decision tree induction are:

1. Information Gain and Information Gain Ratio criterion (Quinlan, 1986, 1987, 1993).
2. Gini Index (Brieman et. al., 1984).
3. Twoing rule (Brieman et. al., 1984).
4. Chi-square statistics (Mingers, 1989 (b)).

3.4.2.1.1 Information Gain and Information Gain Ratio criterion

Quinlan (1993) proposed the use of the information gain and information gain ratio, based on a classic formula from information theory that measures the theoretical information content of a code as $-\sum p_i \log(p_i)$, where p_i is the probability of the i-th message. The value of this measure depends on the likelihood of the various possible messages. If they are all equally likely (i.e., the p_i are equal), there is the greatest amount of uncertainty and the information gained will be greatest. The less equal the probabilities, the less information there is to be gained. The value of the function also depends on the number of possible messages.

The information gain and information gain ratio measures (Quinlan, 1993) are developed in the following way:

For a given training set T, selecting one case at random and saying that it belongs to some class C_i , has the following probability of being correct:

$$f(C_i, T)/|T|$$

Where f (C_i, T) stands for the number of cases in T that belongs to class C_i and $|T|$ denotes the number of cases in T. So the information it conveys is:

$$-\log_2(f(C_i, T)/|T|) \text{ bits.} \qquad (3.1)$$

Then the amount of information required to identify the class for an observation in T can be quantified as

$$\text{info}(T) = -\sum_{i=1}^{m} f(C_i, T)/|T| \times \log_2 (f(C_i, T)/|T|) \text{ bits.} \qquad (3.2)$$

This quantity is known as the *entropy* of the set T.

If a test Z that can partition T into k outcomes is defined, then a similar measure can be defined that quantifies the total information content after applying Z:

$$\text{info}_z(T) = \sum_{j=1}^{k} \frac{|T_j|}{|T|} \times \text{info}(T_j) \qquad (3.3)$$

Using this approach, the information gained by splitting T using Z can be measured by the quantity:

$$\text{gain (Z)} = \text{info (T)} - \text{info}_z\text{(T)} \tag{3.4}$$

This criterion is called the *gain criterion* (Quinlan, 1993). The gain criterion, then, select a test to maximise the information gain. This is also known as the "mutual information between the test Z and the class"(Quinlan, 1993).

The major drawback of the gain criterion is that it has a strong bias in favour of tests with many outcomes. The bias inherent in the gain criterion can be rectified by a kind of normalisation in which the apparent gain with many outcomes is adjusted. If the information content of a message pertaining to a case that indicates not the class to which the case belongs but the outcome of the test then, by analogy with the definition of info (T) (Quinlan, 1993), the information generated by dividing Z into n subsets is given by

$$\text{Split info (Z)} = -\sum_{j=1}^{k} \frac{|T_j|}{|T|} \times \log_2\left(\frac{|T_j|}{|T|}\right) \tag{3.5}$$

This gives an idea of the potential information generated by dividing Z into k subsets, whereas the gain measures the information useful for classification that arises from the same division. Then, the ratio

$$\text{gain ratio (Z)} = \text{gain (Z)/split info (Z)} \tag{3.6}$$

gives the proportion of information generated by a split that is useful for classification.

Using this criterion, T is recursively split such that the gain ratio is maximised at each node of the tree. This procedure continues until each leaf node contains only observations from a single class, or further splitting yields no increase in information.

3.4.2.1.2 The Gini Index

Brieman et al. (1984) use a measure called the Gini index of diversity. The Gini function measures the impurity of an attribute with respect to the classes. For a given training set T, selecting one case at random and saying that it belongs to some class C_i has the following probability of being correct:

$$f(C_i, T)/|T| .$$

The general Gini function, or measure of impurity, is

$$\sum_{j \neq i}\sum (f(C_i, T)/|T|)(f(C_j, T)/|T|) \tag{3.7}$$

which can also be written as

$$\left(\sum_j f(C_j, T)/|T|\right)^2 - \sum_j f^2(C_j, T)/|T|$$

or

$$1 - \sum_j f^2(C_j, T)/|T| \tag{3.8}$$

The Gini index is simple and can be computed quickly. This index uses the rule that assigns an object selected at random from the node to the class i with probability f (C_i, T)/ |T|, instead of using the plurality rule to classify objects in a node.

3.4.2.1.3 The Twoing rule

The Twoing rule is described by Brieman et al. (1984). It uses a different approach to attribute selection in decision tree construction.

Denote the set of classes by C, i.e., C = {1,…., j}. At each node, separate the classes into two super-classes, C_1 = $\{j_1,...., j_n\}$, and $C_2 = C - C_1$. For a given split of a node, the decrease in impurity that results from this split of the node can be computed as:

$$\left(|T_L|/|T|\right)*\left(|T_R|/|T|\right)*\left(\sum_i \left| |L_i/|T_L| - R_i/|T_R|| \right|\right)^2 \tag{3.9}$$

Where $|T_L|$ and $|T_R|$ are the number of examples on the left and right of a split at the node and L_i and R_i are the number of examples in category i on the left and right side of the split. This decrease in impurity is known as the twoing value. The twoing value is actually a goodness of fit measure rather than an impurity measure.

3.4.2.1.4 The Chi-square Contingency Table statistic (χ^2)

Mingers (1989 (b)) discusses the use of this measure to select attributes for decision tree induction. It is based on traditional statistics for measuring the association between two variables in a contingency table, and is based on comparing the observed frequencies with the frequencies that one would expect if there were no association between the variables. The resulting statistic is distributed approximately as chi-square, with larger values indicating greater association. The basic equation for this function is

$$\chi^2 = \sum\sum \frac{(x_{ij} - E_{ij})^2}{E_{ij}} \tag{3.10}$$

Where $E_{ij} = x_i x_j / N$, i.e., the expected value for each cell in the contingency table.

The final stage in top-down decision tree classifier design is the determination of when splitting should be stopped. Initial approaches to selecting terminal nodes were of the form where a threshold $\beta > 0$ is set, and node t is declared as a terminal node if

$$\max_{S \in T} \Delta \text{ i (S (t),t)} < \beta$$

One way to accomplish this task is to define an *impurity function* i(t) (Breiman et al., 1984) at every internal node t. If a candidate split S divides the internal node t into left child node t_L and right child node t_R such that a proportion p_L of the cases in t go into t_L and a proportion p_R go into t_R, then the goodness of the split S can be measured by the decrease in impurity:

$$\Delta \text{ i (S, t)} = \text{i (t)} - \text{i} \, (t_L) \, p_L \text{ - i} \, (t_R) \, p_R$$

Hence a split is chosen that minimises Δ i (S, t) over all splits S in some set of data T.

The problem with this rule is that partitioning is frequently halted too soon at some nodes and too late at some others. Brieman et al. (1984) found that the stopping rule has a greater impact on the efficiency of decision tree classifier than the splitting rules. They suggested that, instead of using a stopping rule, one should continue splitting until all the terminal nodes are pure, or nearly pure, thus generating a large tree. This large tree is then selectively pruned, producing a decreasing sequence of subtrees. Finally, use cross validation to pick out the subtree that has the lowest estimated misclassification rate.

3.4.3 Hybrid approach

Hybrid methods of designing a decision tree classifier use both the bottom-up and top-down approaches sequentially (Kim and Landgrebe, 1991). The procedure for designing this type of classifier is as follows. First, considering the entire set of classes, a bottom-up approach is used to divide the data into two subgroups. Then the mean and covariance of each subgroup are calculated and used in a top-down approach to generate two new subgroups. Each subgroup is checked to see if it contains only one class. If so, that subgroup is labelled as terminal; otherwise, the previous procedure is repeated. The procedure terminates when all the subgroups are labelled as terminals.

Hybrid classifiers are found to have several advantages over both top-down and bottom-up approaches (Kim and Landgrebe, 1991). They are found to converge to classes of informational value, because the cluster initialisation provides early guidance in this direction, while the straightforward top-down approach does not guarantee such convergence. The hybrid approach can use overlapping classes, while there are no overlapping classes in the bottom-up approach. Covariance information can be applied in the hybrid approach to separate nonspherical subgroups.

3.4.4 Growing-pruning method

Gelfand et al. (1991) proposed this method of constructing a decision tree classifier for the following reasons:

1. A large decision tree is grown with the entire data set where partitioning continues until all terminal nodes have pure class membership. If we then attempt to prune it back by minimising an estimate of the error rate based on the same data set, then that estimate of the error rate will be biased and will result in selecting the large tree as the optimally pruned sub tree of itself.
2. The above problem can be avoided by splitting the entire data set into two subsets of nearly equal size, and using one data set for growing and other data set for pruning the tree. But it is not clear how to use this method both to grow and prune the tree with a small data set.
3. Brieman et. al. (1984) suggested a cost-complexity pruning method but Gelfand et. al. (1991) found that the problem of tree pruning is reduced to a problem of complexity parameter estimation so that cross validation may be used. They suggested that in this method a pruned sub-tree is selected by minimising over a parametric family of pruned sub-trees, and this parametric family may not include the optimal or even a good pruned sub-tree.

To overcome these difficulties, Gelfand et al. (1991) suggested the following method of tree growing and pruning, while using all of the data to both grow and prune a classification tree.

First, divide the entire data set into two subsets of nearly equal size. A large tree is grown with pure terminal nodes using first data subset. A pruned sub-tree is then selected by minimising an estimate of the error rate based on the second data subset over all pruned sub-trees. This procedure is then iterated, using the second subset to grow a tree starting from the terminal nodes of the previously selected pruned sub-tree. The first subset is now used to select a new pruned sub-tree, and so on. This process is continued till the sequence of selected pruned sub-trees converges.

3.5 Classification algorithms based on data splitting method

Decision tree classification algorithms can be defined according to whether a uniform or a heterogeneous set of algorithms is used to estimate the splits at internal nodes. Such algorithms are described as having homogenous or heterogeneous hypothesis space, respectively. Traditional approaches to the design of decision trees are based on homogenous classification models for which a single algorithm is used to estimate each split. Generally speaking, there are two types of decision trees based on homogenous hypothesis space: univariate decision trees and multivariate decision trees.

A hybrid hypothesis space is one that combines different homogenous hypothesis spaces. The learning algorithms used to estimate a hybrid tree allow different splitting methods to be applied within different subtrees of the larger decision tree (Friedl and Brodley, 1997).

3.5.1 Univariate decision trees

A univariate decision tree is a type of decision tree in which the decision boundaries at each node of the tree are defined by a single feature of the input data (Swain and Hauska, 1977). At each internal node in a univariate decision tree, the data are split into two or more subsets on the basis of a test on a single feature of the input data, and each test is required to have a discrete and finite number of outcomes. Thus, a univariate decision tree classification proceeds by recursively partitioning the input data until a leaf node is reached, and the class label associated with the leaf is then assigned to the observation. The specific values of the decision boundaries in a univariate decision tree are estimated empirically from the training data. In the case of continuous data, a boolean test of the form $x_i > b$ is estimated at each internal node of a decision tree from the training data, where x_i is a feature in the data space and b is a threshold in the observed range of x_i. The value of b can be estimated by using some objective measure that maximises dissimilarity or minimises similarity of the descendent nodes. As each test in univariate decision tree is based on one of the input variables, it is restricted to representing a split of the feature space that is orthogonal to the axis representing that variable axis, as shown in Figure 3.2.

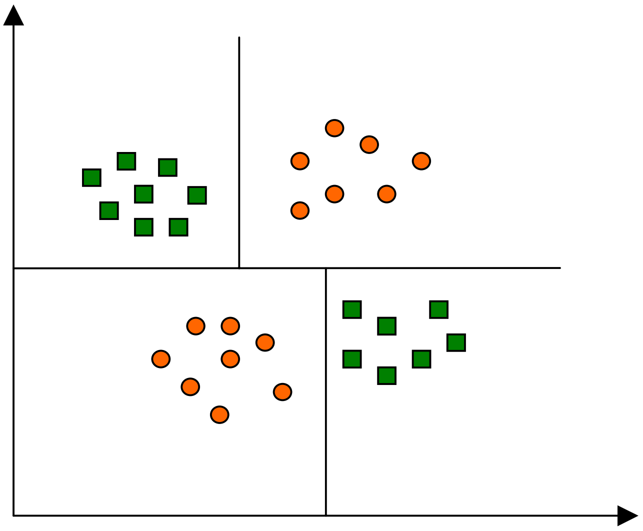

Figure 3. 2. Axis-parallel decision boundaries of a univariate decision tree.

3.5.2 Multivariate decision trees

Where the class structure can be revealed only by combinations of variables, a univariate decision tree will perform poorly at uncovering the structure of the data (Brieman et al, 1984; Utgoff and Brodley, 1990; Brodley and Utgoff,1992). In problems where a linear structure is suspected, the set of allowable splits is extended to include linear combinations of features in the input data (Figure 3.3).

Multivariate decision trees are similar to univariate decision trees except that the splitting test at each node is based on more than one feature of the input data. A set of linear discriminant functions is estimated at each interior node of a multivariate decision tree, and the coefficients for the linear discriminant function at each interior node are estimated from the training data. The test at each node has the form:

$$\sum_{i} a_i X_i \leq \mathrm{c}$$

Where X_i represent the features in the data space, *a* is the vector of coefficients of the linear discriminant functions, and *c* is a threshold value. Multivariate decision trees are often found to be more compact and can also be more accurate (Brodley and Utgoff, 1992). The higher complexity of multivariate relative to univariate decision tree algorithms introduces a number of factors that affect their performance. First, different algorithms can be used to estimate the splitting rule at internal nodes and each of these methods can have different degrees of performance depending on the data and classification problem. Second, as the split at each internal node of a multivariate decision tree is based on one or more features, so several different algorithms are available to perform feature selection at each internal node within a multivariate decision tree. These algorithms include sequential forward selection and sequential backward elimination. Another problem with multivariate decision tree algorithms is that these algorithms

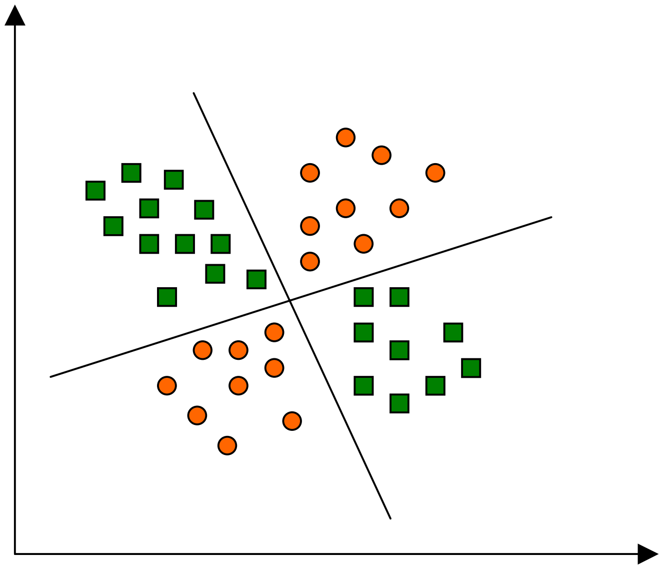

Figure 3. 3. Decision boundaries for a multivariate decision tree classifier.

perform local feature selection rather than global feature selection. They choose the features to include in each test on the basis of the data observed at a particular node, rather than selecting a uniform set of features on which to base tests for the entire tree.

3.5.3 Hybrid decision tree classifier

A hybrid decision tree is a decision tree in which different classification algorithms may be used in different subtrees of a larger tree. These algorithms can be linear discriminant functions, k nearest-neighbour classifiers, or any other classification algorithms. The motivation for implementing hybrid decision classification approach is based on the fact that different algorithms exhibit selective superiority in regard to their performance in classification (Friedl and Brodley, 1997) and the optimal classification algorithm depends on the data set to be classified. If different classification algorithms are allowed within the framework of a single hybrid tree, the data set can be partitioned in a fashion such that the different classifiers can be applied to different subsets of the data. Figure 3.4 shows an example of this type of classification structure in which three different types of classification algorithms LDF (linear discriminant function), K-NN (K-nearest neighbours) and UDT (univariate decision tree) are used to classify a data set within a single classification tree.

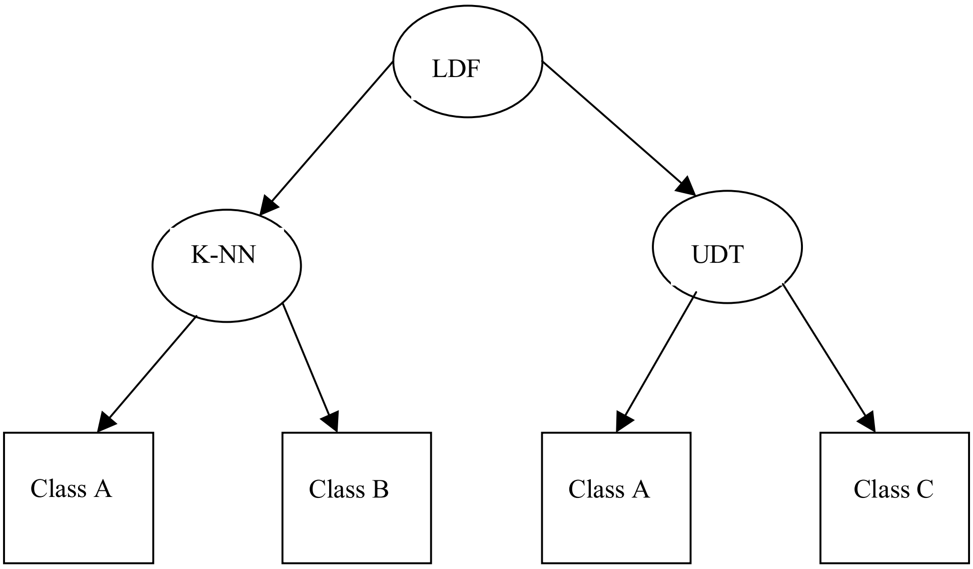

Figure 3. 4. A hybrid decision tree classifier (adapted from Friedl and Brodley, 1997).

3.6 Tests on continuous attributes

As continuous attributes contain arbitrary thresholds, it is necessary to have some test to find a threshold, which can be used to design a decision tree classifier. The algorithm for finding appropriate thresholds for continuous attributes (Brieman et al., 1984, and Quinlan, 1993) is as follows:

The training cases are first sorted on the values of the attribute being considered. As there are only a finite number of these values (m), they can be ordered as $\{v_1$, v_2, . . ., $v_m\}$. Any threshold value lying between v_i and v_{i+1} will have the same effect of dividing the cases into those whose value of the attribute lies in $\{v_1$, v_2,…., $v_i\}$ and those whose value is in $\{v_{i+1}$, v_{i+2}, …, $v_m\}$. There are thus *m*-1 possible splits on the attribute, all of which are examined. It is usual to choose the midpoint of each interval as the representative threshold, the *ith* such being

$$(v_i + v_{i+1})/2.$$

Each threshold divides the training data into two subsets, and so the value of the splitting criterion is a function of the threshold. The ability to choose the threshold so as to maximise the value of the splitting criterion gives a continuous attribute an advantage over a discrete attribute and also over other continuous attributes that have fewer distinct values in the training data set. That is, the choice of test will be biased towards continuous attributes with numerous distinct values.

Quinlan (1996) proposed a correction for this bias based on the Minimum Descriptive Length (MDL) principle (Rissanen, 1993), which adjust the apparent information gain from a test of a continuous attribute.

> Let a sender and receiver both possess an ordered list of the cases in the training data showing each case's attribute values. The sender also knows the class to which each case belongs and must transmit this information to the receiver. The person first encodes and sends a theory of how to classify the cases. Since this theory might be imperfect, the sender must also identify the exceptions to the theory that occurs in the training cases and state how their classes predicted by the theory should be corrected. The total length of the transmission is thus the number of bits required to encode the theory (the

> theory cost) plus the bits needed to identify and correct the exceptions (the exceptions cost). The sender may have a choice among several alternative theories, some being simple but leaving many errors to be corrected while other are more elaborate but more accurate. The minimum descriptive length principle may then be stated as: choose the theory that minimises the sum of the theory and exceptions costs (Quinlan, 1996, page 79-80).

MDL thus provides a framework for trading off the complexity of a theory against its accuracy on the training data T. The exceptions cost associated with a set of cases T is asymptotically equivalent to $|T| \times \inf o(T)$, so that $|T| \times \mathrm{gain}(T, Z)$ measures the reduction in exceptions cost when T is partitioned by a test Z. Partitioning T in this way, however, requires transmission of more complex theory that includes the definition of Z.

A test on continuous attributes with numerous distinct values will now be less likely to have the maximum value of the splitting criterion among the family of possible tests, and so is less likely to be selected. Further, if all thresholds on a continuous attribute have an adjusted gain that is less than zero, this attribute is not considered any further.

3.7 Softening thresholds

In the case where continuous attributes are used for testing, each value is compared against a threshold obtained by using a suitable attribute selection measure. Such a test acts as a switch that refers a case being classified to one or other of the subtrees, which may not resemble each other at all. Sending a case down one path or an other is reasonable when an attribute value lies clearly to one side of the threshold. If the value lies close to the threshold, however, so that small changes can move the value across the threshold, insignificant differences might produce radically different classifications. For some domains, this sudden change is quite appropriate. For other applications, though, it is more reasonable to expect classification decisions to change more slowly with changes in attribute values.

A simple scheme proposed by Quinlan (1993) defines subsidiary cutpoints Z^- and Z^+ below and above each threshold Z. If a test on continuous attribute A is encountered while classifying a case whose value of A is V, the probability of the outcome A ≤ Z is determined as follows:

1. If V is less than Z^-, the probability is 1.
2. If V lies between Z^- and Z, interpolate between 1 and 0.5.
3. If V lies between Z and Z^+, interpolate between 0.5 and 0.
4. If V is greater than Z^+, the probability is 0.

To calculate $Z^-$and Z^+Quinlan (1993) suggests that if the threshold Z were to be changed to a new value Z', the decision tree would classify some cases of the training set differently. The number of training cases misclassified by the tree can be determined for a value of Z' in the neighbourhood of Z. If E of the training cases T are misclassified when the threshold has its original value, the standard deviation of the number of errors can be estimated as

$$\sqrt{(E+0.5)\times(|T|-E-0.5)/|T|}\,.$$

$Z^-$and $Z^+$are then chosen so that, if the threshold were set to either of them, the number of misclassified training cases associated with this test would be one standard deviation more than E. This approach allows for either sharp or vague threshold effects. In the former situation, errors increase rapidly as Z is changed so that $Z^-$and $Z^+$are close to Z. In the latter situation, cases with values near the threshold might be expected to be classified equally well by the subtree associated with either outcome, so error increase relatively slowly and the interval from Z^- to $Z^+$is larger.

3.8 Pruning decision trees

Decision tree classifiers divide the training data into subsets, which contain only a single class. The result of this procedure is often a very large and complex tree. In most cases, fitting a decision tree until all leaves contain data for a single class may overfit to the noise in the training data, as the training samples may not be representative of the population they are intended to represent. If the training data contain errors, then overfitting the tree to the data in this manner can lead to poor performance on unseen cases. To reduce this problem, the original tree can be pruned to reduce classification errors when data outside of the training set are to be classified.

A decision tree is not usually simplified by deleting the whole tree in favour of a leaf. Instead, parts of the tree that do not contribute to classification accuracy on unseen cases are removed, thus producing a less complex and more comprehensible tree. There are two ways in which a decision tree classifier can be modified to produce a simpler tree (Breiman et al., 1984):

1. Deciding not to divide a set of training data any further, and
2. To remove retrospectively some part of the tree structure built by recursive partitioning.

The first approach, sometimes called stopping or pre-pruning, has the advantage that time is not wasted in assembling a structure that is not used in the final simplified tree. The approach is to look at the best way of splitting a dataset and to assess the split from the point of view of a factor such as information gain or error reduction. If this assessment falls below some threshold, the division is rejected and the tree for the data is just the most appropriate leaf. The problem with this approach is to specify a correct stopping rule (Breiman et al., 1984). If the threshold value is too high it can terminate division before the benefits of subsequent splits become evident, while too low a value results in little simplification of the tree.

In the second approach, the tree is allowed to grow to its full depth, when all leaves contain data for a single class. This overfitted tree is then pruned. This method needs more computation in building parts of the tree that are subsequently discarded, but this cost is offset against benefits due to more thorough exploration of possible partitions. Pruning a decision tree will cause it to misclassify more of the training data. Thus, the leaves of the pruned tree will not necessarily contain training data from a single class. Instead of a class associated with a leaf, there will be a class distribution specifying, for each class, the probability that a training data at the leaf belongs to that class.

The example below shows a decision tree before and after pruning .

Decision tree:

```
band2 <= 59 : 1 (343.0/2.0)
band2 > 59 :
|  band2 <= 61 : 2 (55.0/21.0)
|  band2 > 61 :
|  |  band1 <= 79 : 2 (293.0/18.0)
|  |  band1 > 79 :
|  |  |  band1 <= 87 : 2 (101.0/16.0)
|  |  |  band1 > 87 :
|  |  |  |  band2 <= 75 : 1 (3.0)
|  |  |  |  band2 > 75 : 2 (5.0/1.0)
```

Simplified decision tree:

```
band2 <= 59 : 1 (343.0/3.9)
band2 > 59 : 2 (457.0/64.7)
```

while the subtree

```
 band2 > 59 :
|  band2 <= 61 : 2 (55.0/21.0)
|  band2 > 61 :
|  |  band1 <= 79 : 2 (293.0/18.0)
|  |  band1 > 79 :
|  |  |  band1 <= 87 : 2 (101.0/16.0)
|  |  |  band1 > 87 :
|  |  |  |  band2 <= 75 : 1 (3.0)
|  |  |  |  band2 > 75 : 2 (5.0/1.0)
```

has been replaced by the leaf "class 2" in the simplified tree after pruning. As shown in the tree above every leaf is followed by a cryptic (n) or (n/m). For observation the last leaf of the simplified decision tree is 2 (457.0/64.7), for which *n* is 457 and *m* is 64.7. The value of *n* is the number of data that are mapped to this leaf, and *m* is the number of items that are classified incorrectly by the leaf. (A non-integral number of cases can arise because, when the value of an attribute in the tree is not known, the *See5.0* decision tree software splits the case and sends a fraction down each branch.)

Decision trees are usually simplified by removing one or more subtrees and replacing them with leaves if it is possible to predict the error rate of a tree and of its subtrees, including leaves. The process is started from the bottom of the tree and each nonleaf subtree is examined. This procedure is called the bottom-up approach. Alternatively, the process starts from the root and moves towards the leaves of the tree by examining the branches. This is called the top-down approach. The tree is pruned if replacement of a subtree with a leaf, or with its most frequently used branch, would lead to a lower predicted error rate. The error rate for whole tree decreases as the error rate of any of its subtrees is reduced, and this process will lead to a tree whose predicted error rate is minimal with respect to the allowable form of pruning. As mentioned earlier, pruning always increases error on training data, so it is necessary to have a suitable technique for predicting error rates.

Two families of techniques to predict error rates of a tree are available. In the first family, the error rate of the tree and its subtrees is predicted by using a new set of data that is separate from the training data. Since these cases were not examined at the time the tree was constructed, the estimate obtained from them will be unbiased and, if we have enough data, the estimate will also be reliable. In the second approach the training data are used to predict these error rates and pruning the tree. The techniques for pruning the decision tree are as follows:

1. Cost-complexity pruning (Breiman et al., 1984)
2. Reduced-error pruning (Quinlan, 1987)
3. Pessimistic pruning (Quinlan, 1993)

4. Error based pruning: (Quinlan, 1993)
5. Critical value pruning (Mingers, 1989 (a))

3.8.1 Cost-complexity pruning

In cost-complexity pruning, the predicted error rate of a tree is modelled as the weighted sum of its complexity and its error on training data, with the separate data set being used primarily to determine an appropriate weighting. This technique is a two-stage process in which a sequence of sub-trees $T_0, T_1, ..., T_k$ (denoted as $T_{max}(\alpha)$) of T_{max} (original decision tree generated by using training data set) is generated. Each sub-tree T_{i+1} is obtained by replacing one or more sub-trees of T_i with leaves until the final tree T_k is just a leaf.

Consider a decision tree T that is used to classify each of the *n(t)* data items in the training set from which T was generated, and let *e(t)* of them be misclassified. If L (T) is the number of leaves in T, then the cost-complexity of T is defined (Breiman et al., 1984) as the sum:

$$\frac{e(t)}{n(t)} + \alpha \times L\ (T)$$

for some parameter α. Now, suppose some sub-tree S of the tree T is replaced by the best possible leaf, the new tree would misclassify *m(t)* more of the cases in the training set but would contain L(S)-1 fewer leaves. This new tree would have the same cost-complexity as T if:

$$\alpha = \frac{m(t)}{n(t) \times (L(S) - 1)}$$

To produce T_{i+1} from T_i, each non-leaf subtree of T_i is examined to find the minimum value of α, as calculated above. Any subtrees with the values of α are then replaced by their respective best leaves.

In the second stage of this process, the best tree in $T_{max}(\alpha)$ with respect to the predictive accuracy criterion is chosen. There are two ways of estimating the true error rate of each tree in the family. One is based on cross-validation sets, and the other on an independent pruning set. Assume that some test set containing $N^{'}$ cases and use each T_i to classify all of the available test data. Let $E^{'}$ be the minimum number of errors observed with any T_i, with the standard error of $E^{'}$ being given by

$$\mathrm{Se}(E^{'}) = \sqrt{\frac{\mathrm{E}' \times (\mathrm{N}' - \mathrm{E}')}{\mathrm{N}'}}$$

The tree selected is the smallest T_i whose observed number of errors on the test set does not exceed $E^{'}$+ Se($E^{'}$).

3.8.2 Reduced-error pruning

This method assesses the error rates of the tree and its components directly on a separate set of test data. In this method, the original tree classifies all the test data. For every non-leaf subtree S of T, the changes in misclassification over the test data that would occur if S were replaced by the best possible leaf are examined. If the new tree would give an equal or smaller number of errors, and if S contains no subtree with the same property, then subtree S is replaced by the leaf. The process continues until any further replacements would increase the number of errors over the test set.

As with the cost-complexity pruning, this process generates a sequence of trees. The final tree is the most accurate subtree of the original tree with respect to the test data set and is the smallest tree with that accuracy. The disadvantages of this method are, first, it requires a separate test data set and, second, " …that part of the original tree corresponding to rarer special cases not represented in the test set may be excised" (Quinlan, 1987, pp. 226). These techniques of pruning may not be much of a disadvantage when training and test data are abundant, but can lead to poorer-performing trees when data are scarce. This makes it necessary to have a technique for pruning a tree which uses only the training set from which the tree was built.

3.8.3 Pessimistic pruning

This method increases the estimated error rates of subtrees to reflect the size and composition of the training subsets, then replaces every subtree whose predicted error rate is not significantly lower than that of a leaf. This method of pruning is described by Quinlan (1987). It aims to avoid the necessity of a separate test data set. A continuity correction for the binomial distribution is used to obtain a more realistic estimate of the misclassification rate.

If *n(t)* represents the number of training set examples at a node t in the tree and *e (t)* represents the number of examples misclassified at node t, then

$$r(t) = \frac{e(t)}{n(t)}$$

is an estimate of the misclassification rate. The rate with the continuity correction is

$$r'(t) = \frac{e(t) + 1/2}{n(t)} \tag{3.11}$$

For a sub-tree T_t, the misclassification rate will be:

$$r(T_t) = \frac{\sum e(i)}{\sum n(i)}$$

where *i* covers the leaves of the sub-tree. Thus, the corrected misclassification rate is:

$$r'(T_t) = \frac{\sum (e(i) + 1/2)}{\sum n(i)} = \frac{\sum e(i) + n_T / 2}{\sum n(i)} \tag{3.12}$$

where n_T is the number of leaves.

In equations (3.11) and (3.12), $n(t)=\sum n(i)$ as they refer to the same set of examples; therefore, the misclassification rates can be simplified to numbers of misclassifications:

$$n'(t)=e(t)+1/2 \quad \text{for a node}$$

$$n'(T_t)=\sum e(i)+n_T/2 \quad \text{for a sub-tree.}$$

Using training data, the sub-tree will always make fewer errors than the corresponding node, but this is not so when the corrected figures are used, since they depend on the number of leaves, not just on the number of errors. However, it is likely that even this corrected estimate of the number of misclassifications made by the sub-tree will be optimistic. Hence, the algorithm only keeps the sub-tree if its corrected figure is more than one standard error better than the figure for the node. The standard error for the number of misclassifications is derived from:

$$SE(n'(T_t))=\sqrt{\frac{n'(T_t)\times(n(t)-n'(T_t))}{n(t)}} \tag{3.13}$$

Quinlan (1993) suggests pruning the sub-tree unless its corrected number of misclassifications is lower than that for the node by at least one standard error. As this algorithm evaluates each node starting at the root of the tree. This means that it does not need to consider nodes that are in subtrees which have already been pruned.

3.8.4 Error based pruning

This pruning method is an improvement on the "pessimistic pruning" method, and it is based on a far more pessimistic estimate of the expected error rate. Unlike the method described in section 3.7.3, this method visits the nodes of the full-grown tree according to a bottom-up, post-order traversal strategy instead of a top-down strategy.

Taking the set of examples covered by a leaf *t* as a statistical sample, it is possible to estimate a confidence interval $[L_{CF}(t), U_{CF}(t)]$ for the posterior probability of misclassification of *t*. The upper limit of the interval is of particular interest for a worst case analysis, and is defined as the real value such that $P(e(t)/n(t) \le U_{CF}) = CF$, where CF is the confidence level. Under the further assumption that errors in the training set are binomially distributed with probability *p* in *n(t)* trials, it is possible to compute the exact value of U_{CF} as the value of *p* for which a binomially-distributed random variable X shows *e(t)* successes in *n(t)* trials with probability CF, that is, p (X≤e (t)) = CF. In other words, if X has a binomial distribution with parameters $(U_{CF}, n(t))$, the equality above must hold. The value of U_{CF} depends on both *e(t)* and *n(t)* so, having found the upper limit, the error estimates for leaves and subtrees are computed assuming that they are used to classify a set of unseen cases of the same size as the training set. Thus the predicted error rate for t will be n (t)· U_{CF} (Esposito et. al., 1997).

The sum of the predicted error rates of all the leaves in a branch T_t is considered to be an estimate of the error rate of the branch itself. Thus, by comparing the predicted error rate for *t* with that of the branch T_t and of the largest sub-branch $T_{t'}$ rooted in a child t' of parent of *t*, one can decide whether it is convenient to prune T_t, to graft $T_{t'}$ in place of parent of *t,* or to keep T_t.

3.8.5 Critical value pruning

This method relies on estimating the importance or strength of a node from classifications done at the tree creation stage. In creating the original tree, a goodness of split measure determines the attribute at a node. The value of the measure reflects how well the chosen attribute splits the data between the classes at the node. The pruning method specifies a critical value and prunes those nodes which do not reach the critical value, unless a node further along the branch does reach that value. The larger the critical value selected, the greater the degree of pruning and the smaller the resulting tree. In practice, a series of pruned trees is generated using increasing critical values (Mingers, 1989 (a)). A single tree can be chosen in the same way as for cost-complexity pruning. The particular critical value used depends on the measure used in creating the tree.

3.9 Problems in the use of decision tree classifiers

Although decision tree classifiers are an effective and general learning tool, and are used intensively in the field of machine learning research, few uses of decision trees have been reported in the field of remote sensing image classification. Like other classifiers based on different assumptions, these classifiers inevitably have some limitations that may have an impact on their performance. There are fewer factors affecting the accuracy of decision tree classifiers compared with the neural classifier, where a number of factors affect the classification accuracy. The factors affecting the decision tree classifiers can be summarised as:

1. Type of classifier, whether it is univariate or multivariate.
2. Attribute selection measure used in designing a classifier.
3. Pruning methods used to prune the tree.
4. Number of training pattern required for the optimum classification results.

A small number of studies report the effects of these factors on land cover classification accuracy. Friedl and Brodley (1997) studied the behaviour of different decision tree classifiers, such as univariate, multivariate and hybrid classifiers, for land cover classification. They found that hybrid decision classifiers outperform other types of decision tree. Except for this study, no other studies have used remotely sensed data to study the effects of other factors on classification accuracy. Brieman et al. (1984) and Mingers (1989 (a) (b)) use other types of data and suggest that it is the pruning method that most affects the classification accuracy. They also found that attribute selection measures have little or no effect on classification accuracy. Oates and Jenson (1997) studied the behaviour of a univariate decision tree classifier (C4.5) with five different pruning methods, and found that increasing training set size often results in a linear increase in tree size, even when that additional complexity results in no significant increase in classification accuracy. On the other hand, Quinlan (1993) found that in situations where the division of feature space by an oblique hyperplane (multivariate decision tree) is easier, the number of training cases required to approximate this oblique division by a collection of hyper-rectangles (univariate decision tree) will be large, which increases the complexity of the decision tree classifier.

3.10 Support Vector Machines (SVM)

This section gives an overview of another recent development in classification methodology, called *support vector machines (SVM)* or sometimes *support vector networks*. This classification system is based on statistical learning theory as proposed by Vapnik and Chervonenkis (1971), which is discussed in detail by Vapnik (1995, 1999). The SVM can be seen as a new way to train polynomial, radial basis function, or multilayer perceptron classifiers, in which the weights of the network are found by solving a Quadratric Programming (QP) problem with linear inequality and equality constraints using structural risk minimisation rather than by solving a non-convex, unconstrained minimisation problem, as in standard neural network training technique using empirical risk minimisation. Empirical risk minimises the misclassification error on the training set, whereas structural risk minimises the probability of misclassifying a previously unseen data point drawn randomly from a fixed but unknown probability distribution. The name SVM results from the fact that one of the outcomes of the algorithm, in addition to the parameters for the classifiers, is a set of data points (the "support vectors") which contain, in a sense, all the information relevant to the classification problem. A brief review of statistical learning theory is given in section 3.11.

3.11 Statistical learning theory

3.11.1 Empirical risk minimisation

In the case of two-class pattern recognition, the task of learning from examples can be formulated in the following way: given a set of decision functions

$$\{f_\alpha(\mathbf{x}) : \alpha \in \Lambda\}, \qquad f_\alpha : R^N \rightarrow \{-1, 1\}$$

where Λ is a set of abstract parameters (Osuna et. al., 1997), and a set of examples

$$(\mathbf{x}_1, y_1), \ldots\ldots\ldots\ldots, (\mathbf{x}_k, y_k), \qquad \mathbf{x}_i \in R^N, y_i \in \{-1, 1\}$$

drawn from an unknown distribution P(x, y). The aim is to find a function that provides the smallest possible value for the average error committed on independent examples randomly drawn from the same distribution P(x, y), called the *expected risk*:

$$R(\alpha) = \int \left| f_\alpha(\mathbf{x}) - y \right| P(\mathbf{x}, y) d\mathbf{x} dy \tag{3.14}$$

The functions f_α are usually called *hypotheses,* and the set $\{f_\alpha(\mathbf{x}) : \alpha \in \Lambda\}$ is called the *hypothesis space*, and is denoted by H. The expected risk is therefore a measure of the capability of a hypotheses to predict the correct label y for a point x. The set of functions f_α could be, for example, a set of radial basis functions or a multilayer perceptron with a certain number of hidden units. In this case, the set Λ is the set of weights of the network (Osuna et. al., 1997).

Since the probability distribution P(x, y) is unknown, it is not possible to compute, and therefore minimise, the expected risk R(α). Thus, the straightforward approach is to compute a stochastic approximation of R(α), the so called *empirical risk*:

$$R_{emp}(\alpha) = \frac{1}{k} \sum_{i=1}^{k} \left| f_\alpha(\mathbf{x}_i) - y_i \right| \tag{3.15}$$

A common approach consists in minimising the empirical risk rather than the expected risk. The value $R_{emp}(\alpha)$ is a fixed number for a particular choice of α and a particular training set. The term $(1/2)\left| f_\alpha(\mathbf{x}_i, \alpha) - y_i \right|$ is called the loss. If the number of training patterns (k) used to train the classifier is limited, the empirical risk calculated in equation 3.15 may not guarantee a small actual risk. This can be put another way: a low error value on a training set does not necessarily imply that the classifier has a high generalisation ability, and the empirical risk minimisation principle is therefore said to be non consistent. This problem is often referred to as *overfitting*.

Vapnik and Chervonenkis (1971, 1991) showed that necessary and sufficient condition for consistency of the empirical risk minimisation principle is the fitness of the *VC-dimension h* of the hypothesis space H. The VC-dimension of the hypothesis space H (or the VC-dimension of classifier f_α) is a natural number, which is, loosely speaking, the largest number of data points that can be separated in all possible ways by that set of functions f_α. The VC-dimension is a measure of the complexity of the set H, and it is often, but not necessarily, proportional to the number of free parameters of the classifier f_α.

The theory developed by Vapnik and Chervonenkis (1971) also provides a bound on the deviation of empirical risk from the expected risk. For the learning problem described, choosing some η such that $0 \le \eta \le 1$ (e.g. for a 95% confidence level, $\eta = 0.05$) the Vapnik and Chervonenkis bound, which holds with probability 1 - η, has the following form (Burges, 1998):

$$R(\alpha) \le R_{emp}(\alpha) + \phi\left(\frac{h}{k}, \frac{\log(\eta)}{k}\right) \tag{3.16}$$

where the confidence term ϕ is defined as

$$\phi\left(\frac{h}{k}, \frac{\log(\eta)}{k}\right) = \sqrt{\frac{h\left(\log\frac{2k}{h}+1\right) - \log(\eta/4)}{k}} \tag{3.17}$$

where *h* is the VC-dimension of a set of functions and the right hand side of inequality 3.16 can be called the "risk bound". This value describes the *capacity* of a set of functions. From this bound it is clear that, in order to achieve a small expected risk, that is, good generalisation performances, both the empirical risk and the ratio between the VC-dimension and the number of data points has to be small. The empirical risk is usually a decreasing function of *h*; thus, for a given number of data points, there is an optimal value of the VC-dimension. The choice of an appropriate value of *h* is crucial in order to get good performance, especially when the number of data points is small. When using a multilayer perceptron or a radial basis functions network, this is equivalent to the problem of finding the appropriate number of hidden units (Osuna et. al., 1997).

3.11.2 Structural risk minimisation

The technique of structural risk minimisation developed by Vapnik (1982) is an attempt to overcome the problem of choosing an appropriate VC-dimension. Equation 3.16 suggests that a small value of the empirical risk does not necessarily imply a small value of the expected risk. A different induction principle, called the S*tructural Risk Minimisation* (SRM) principle, was proposed by Vapnik (1982). The principle is based on the observation that, in order to make expected risk small, both sides in equation 3.16 should be small. Therefore, both the VC-dimension and the empirical risk should be minimised at the same time. In order to implement the SRM principle a nested structure of hypothesis space is introduced by dividing the entire class of functions into nested subsets

$$H_1 \subset H_2 \subset ..... \subset H_n \subset ......$$

with the property that h(n) ≤ h(n + 1) where h(n) is the VC-dimension of the set H_n. For each subset, a value of *h* or a bound on *h* is computed. SRM then finds that subset of function which maximise the bound on actual risk. This can be achieved by training a set of machines, one for each subset and choose that trained machine whose sum of empirical risk and VC confidence is minimal (Osuna et. al., 1997).

The SRM principle is well founded mathematically, but it is difficult to implement for the following reasons (Osuna et. al., 1997):

1. The VC-dimension of H_n could be difficult to compute, and there are only a small number of models for which it is possible to compute the VC-dimension.
2. Even, if it possible to compute the VC-dimension of H_n, it is not easy to solve the minimisation problem in equation 3.16. In most cases one will have to minimise the empirical risk for every set H_n, and then choose the H_n, that minimise the equation 3.17.

Therefore, the implementation of this principle is not easy, because it is not trivial to control the VC-dimension of a learning technique during the training phase.

The Support Vector Machine (SVM) algorithm achieves this goal of minimising a bound on the VC-dimension and the number of training errors at the same time.

3.12 Design of support vector machines

3.12.1 The linearly separable class

Linearly separable classes are the simplest case on which to train a support vector machine. Let the training data with k number of samples be represented by $\{\mathbf{x_i}, y_i\}$, i = 1, …, k, where $x \in \mathbf{R}^N$ is an N-dimensional space and $y \in \{-1, +1\}$ is the class label (Osuna et. al., 1997). These training patterns are said to be linearly separable if there exists a vector w (determining the orientation of a discriminating plane) and a scalar *b* (determine offset of the discriminating plane from origin) such that

$$\mathbf{w} \cdot \mathbf{x_i} + b \geq +1 \qquad \text{for all } y = +1 \tag{3.18}$$

$$\mathbf{w} \cdot \mathbf{x_i} + b \leq -1 \qquad \text{for all } y = -1 \tag{3.19}$$

inequalities 3.18 and 3.19 can be combined into a single inequality:

$$y_i(\mathbf{w} \cdot \mathbf{x}_i + b) - 1 \geq 0 \tag{3.20}$$

The hypothesis space in this case is therefore the set of functions given by

$$f_{\mathbf{w},b} = \operatorname{sign}(\mathbf{w} \cdot \mathbf{x} + b) \tag{3.21}$$

The decision surface in equation 3.21 will remain unchanged if the parameters w and b are scaled by the same quantity. In order to remove this redundancy, and to make each decision surface correspond to one unique pair (w, b), the following constraint is imposed:

$$\min_{i=1,\ldots,k} |\mathbf{w} \cdot \mathbf{x}_i + b| = 1 \tag{3.22}$$

where $\mathbf{x}_1, \ldots\ldots \mathbf{x}_k$ are the points in the dataset. The set of hyperplanes that satisfy equation 3.22 are called *canonical hyperplanes* (Osuna et. al., 1997). All linear decision surfaces can be represented by canonical hyperplanes, and the constraint in equation 3.22 is just a normalisation. Vapnik (1995) suggested that if no further constraints are imposed on the pair (w, b), the VC-dimension of the canonical hyperplanes will be (N + 1), that is, the total number of free parameters. In order to be able to apply the structural risk minimisation principle, one need to construct sets of hyperplanes of varying VC-dimension, and minimise both the empirical risk (the training classification error) and the VC-dimension at the same time.

It can be shown that the distance from a point x to the hyperplane associated to the pair (w, b) is:

$$d(\mathbf{x}; \mathbf{w}, b) = \frac{|\mathbf{x} \cdot \mathbf{w} + b|}{\|\mathbf{w}\|} \tag{3.23}$$

According to equation 3.22 the distance between the canonical hyperplane (w, b) and the closest of the data points is simply $1/\|\mathbf{w}\|$. If the set of examples is linearly separable, the goal of the SVM is to find, from among the canonical hyperplanes that correctly classify the data, the one with minimum norm, or equivalently minimum $\|\mathbf{w}\|^2$, because keeping this norm small will also keep the VC-dimension small. Minimising $\|\mathbf{w}\|^2$, in this case of linear separability, is equivalent to finding the separating hyperplanes for which the distance between the classes of training data, measured along a line perpendicular to the hyperplane, is maximised. This distance is called the margin (Burges, 1998).

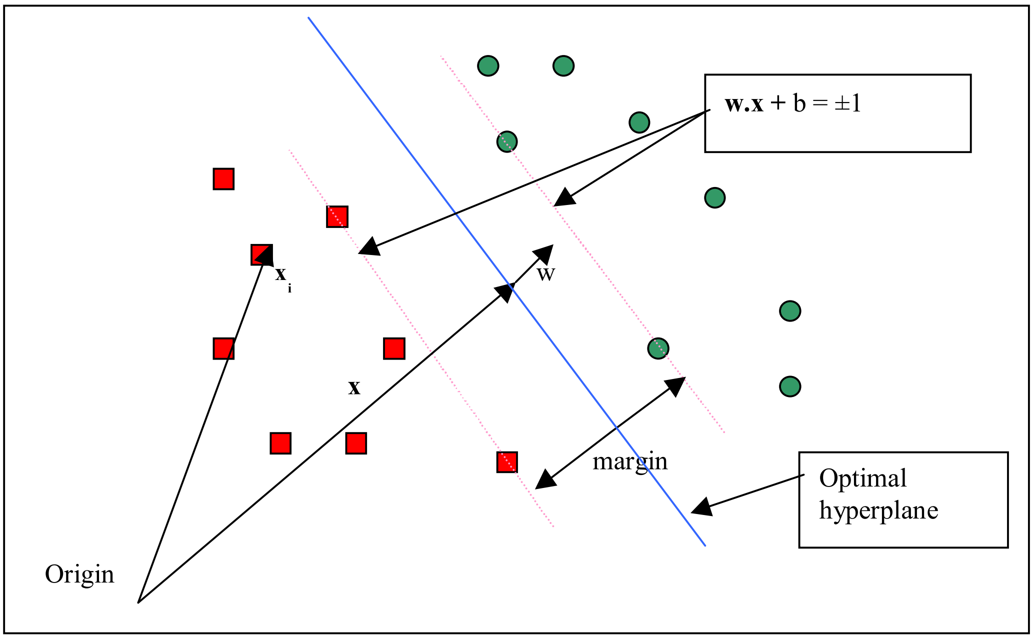

Figure 3. 5. Hyperplanes for the linearly separable data sets. Dashed line passes through the support vectors.

To construct the maximal margin or optimal separating hyperplane one needs to correctly classify a set of training data

$$(\mathbf{x}_1, y_1), \ldots\ldots\ldots\ldots, (\mathbf{x}_k, y_k) \quad \mathbf{x}_i \in \mathbf{R}^N, y_i \in \{-1, 1\}$$

into two different classes, using the smallest norm of coefficients. This can be formulated as follows:

$$\min_{\mathbf{w},b} \frac{1}{2}\|\mathbf{w}\|^2$$

subject to

$$y_i(\mathbf{w} \cdot \mathbf{x_i} + b) - 1 \geq 0 \qquad i = 1, \ldots..,k. \tag{3.24}$$

This problem can be solved using standard Quadratic Programming (QP) optimisation techniques and is not very complex since the dimensionality is N + 1, where N is the dimension of the input space. The quadratic optimisation problem in equation 3.24 can be solved by replacing the inequalities with a simpler form determined by transforming the problem to a dual space representation using Lagrangian multipliers. The Lagrangian is formed by introducing positive Lagrange multipliers λ_i, i = 1,….,k and multiplying the constraint equations by these Lagrange multipliers, and finally subtracting the results from the objective function (i.e, $(1/2)\|\mathbf{w}\|^2$). The solution of this optimisation problem can be obtained by locating the saddle point of the Lagrange function and, can be written as:

$$L(\mathbf{w}, b, \boldsymbol{\lambda}) = \frac{1}{2}\| w \|^2 - \sum_{i=1}^{k} \lambda_i y_i (\mathbf{w} \cdot \mathbf{x}_i + b) + \sum_{i=1}^{k} \lambda_i \tag{3.25}$$

The solution of this optimisation problem requires that $L(\mathbf{w}, b, \lambda)$ be minimised with respect to w and b and simultaneously, that the derivatives of $L(\mathbf{w}, b, \lambda)$ with respect to all α_i vanish, given $\lambda_i \geq 0$, thus generating the following conditions:

$$\mathbf{w} = \sum_{\mathbf{i}} \lambda_{\mathbf{i}} y_i \mathbf{x_i} \tag{3.26}$$

$$\sum_i \lambda_i y_i = 0 \tag{3.27}$$

By substituting equation 3.26 and 3.27 into equation 3.25, the optimisation problem becomes one of maximising:

$$L(\boldsymbol{\lambda}) = \sum_i \lambda_i - \frac{1}{2} \sum_{i,j} \lambda_i \lambda_j y_i y_j (\mathbf{x_i} \cdot \mathbf{x_j}) \tag{3.28}$$

under constraints $\lambda_i \geq 0$, i = 1, …..,k.

Once the vector solution $\lambda^a = (\lambda_1^a, ..., \lambda_k^a)$ of the maximisation problem in equation 3.28 has been found, the optimal separating hyperplane (hyperplane for which the distance to the closest point is maximal) has the following expansion:

$$\mathbf{w}^a = \sum_i y_i \lambda_i^a \mathbf{x}_i \tag{3.29}$$

The Karush-Kuhn-Tucker (KKT) conditions (Fletcher, 1987) play a central role in both the theory and practice of constrained optimisation. For the above problem, the KKT conditions may be stated as:

$$\begin{aligned}
&\frac{\partial L(\mathbf{w}, b, \boldsymbol{\lambda})}{\partial \mathbf{w}} = 0 \\
&\frac{\partial L(\mathbf{w}, b, \boldsymbol{\lambda})}{\partial b} = 0 \\
&y_i(\mathbf{w} \cdot \mathbf{x_i} + b) - 1 \geq 0 \qquad i = 1, \text{.....}k. \\
&\quad \lambda_i \geq 0, \text{ for } i = 1, \text{.....},k \\
&\quad \lambda_i(y_i(\mathbf{w} \cdot \mathbf{x}_i + b) - 1) \geq 0 \quad i = 1, \text{.....}k
\end{aligned} \tag{3.30}$$

According to KKT theory, only points that satisfy the equalities in equations 3.18 and 3.19 can have non-zero coefficients λ_i^a. These points lie on the two parallel hyperplanes shown in Figure 3.5 and are called support vectors. In other words, support vectors are the points for which $\lambda_i^a > 0$ and satisfy equalities in equation 3.18 and 3.19. For a two-class problem the decision rule that separates the two classes can be written as (Osuna et. al., 1997)

$$f(\mathbf{x}) = \operatorname{sign}\left(\sum_{i=1}^{k} \lambda_i y_i (\mathbf{x} \cdot \mathbf{x}_i) + b \right) \tag{3.31}$$

3.12.2 Non-separable data

Cortes and Vapnik (1995) generalised the method of finding the optimal hyperplane to the case of non-separable data, in which there is no opportunity to place a hyperplane such that data can be separated completely into two classes (Figure 3.6). For this type of problem, Cortes and Vapnik (1995) suggested that the restriction that every training vector of a given class lie on the same side of the optimal hyperplane be relaxed by introducing a positive "slack variable" ξ_i, that takes the value $\xi_i \geq 0$. Equation 3.20 can now be written as:

$$y_i(\mathbf{w} \cdot \mathbf{x_i} + b) - 1 + \xi_i \geq 0 \qquad (3.32)$$

In this case, the SVM algorithm searches for the hyperplane that maximises the margin and that, at the same time, minimises a quantity proportional to the number of misclassification errors. This trade-off between margin and misclassification error is controlled by introducing a positive constant C such that $\infty > C > 0$. Cortes and Vapnik (1995) introduce a new term $C\sum \xi_i$ with i = 1,…, k, into equation 3.24 that balances the contribution of minimising $(1/2)\|w\|^2$ with penalising solutions, for which ξ_i becomes large. The optimisation problem for non-separable data thus becomes:

$$\min_{\mathbf{w}, b, \xi_1, \ldots, \xi_k} \left[\frac{1}{2}\|w\|^2 + C\sum_{i=1}^{k} \xi_i \right] \qquad (3.33)$$

$$y_i(\mathbf{w} \cdot \mathbf{x}_i + b) - 1 + \xi_i \geq 0 \qquad (3.34)$$

$$\xi_i \geq 0 \qquad i = 1, \ldots\ldots k. \qquad (3.35)$$

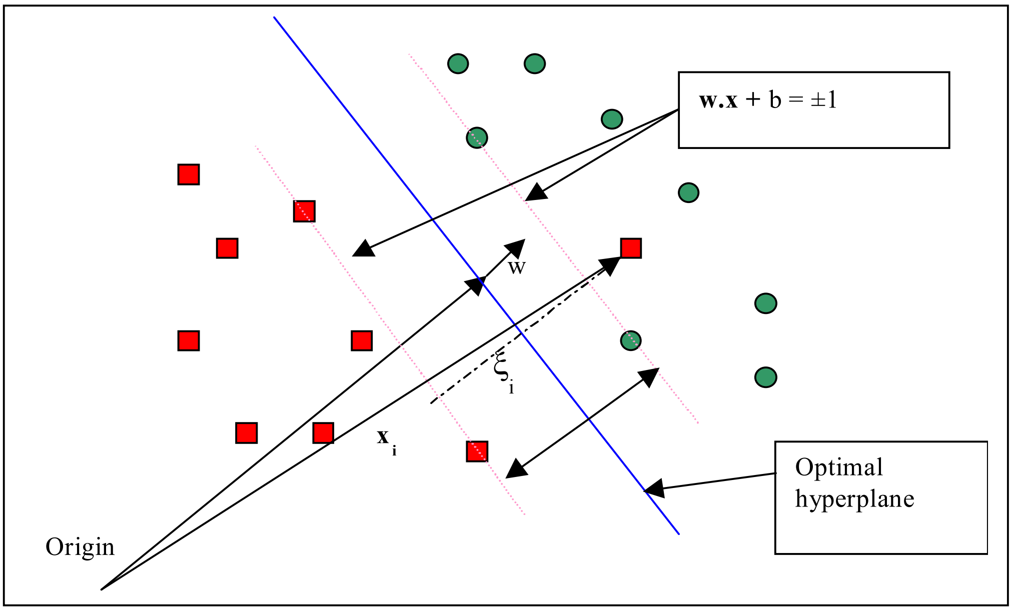

Figure 3. 6. Hyperplanes for non-separating data sets.

As $C \to \infty$ the effect of any ξ_i deviating from 0 becomes increasing more costly to the minimisation. In the situation when $C \to \infty$ the optimisation problem becomes a formulation for the separable data case. Thus, C is a parameter chosen by the user and a large C means assigning a higher penalty to errors. Minimising the first term in equation 3.33 means minimising the VC-dimension of the learning machine and minimising the second term in equation 3.33 controls the empirical risk, which is the first term on the right hand side of equation 3.16. This approach, therefore, constitutes a practical implementation of structural risk minimisation on the given set of functions. In order to solve the equation 3.33 for non separable data, equation 3.25 can be written as:

$$L(\mathbf{w},b,\boldsymbol{\lambda},\xi,\boldsymbol{\mu})=\frac{1}{2}\|\mathbf{w}\|^2+C\sum_i \xi_i-\sum_i \lambda_i \{y_i(\mathbf{w}\cdot\mathbf{x}_i+b)-1+\xi_i\}-\sum_i \mu_i\xi_i \quad (3.36)$$

where the μ_i are the Lagrange multipliers introduced to enforce positivity of the ξ_i.

The solution of equation 3.36 is determined by the saddle points of the Lagrangian (equation 3.36), by minimising with respect to w, ξ and b, and maximising with respect to $\lambda_i \geq 0$ and $\mu_i \geq 0$.

3.12.3 Nonlinear support vector machines

In the situations where it is not possible to have a decision surface (a hyperplane) defined by the linear equations on the training data, the techniques discussed in section 3.12.1 and section 3.12.2 can be extended to allow for non-linear decision surfaces. A technique introduced into machine learning as a part of the support vector machine by Boser et al. (1992) is discussed next.

Boser et al. (1992) propose that a feature vector, $\mathbf{x}\in\mathbf{R}^N$, is mapped into a higher dimensional Euclidean space (feature space) F (Figure 3.7), via a non-linear vector function $\boldsymbol{\Phi}:\mathbf{R}^N \mapsto F$. The optimal margin problem in the space F can be written by replacing $\mathbf{x}_i\cdot\mathbf{x}_j$ with $\boldsymbol{\Phi}(\mathbf{x}_i)\cdot\boldsymbol{\Phi}(\mathbf{x}_j)$, then solving the optimisation problem for λ_i in the transformed feature space by association with the $\lambda_i > 0$. By using this mapping, the solution of the SVM has the form:

$$f(\mathbf{x}) = \operatorname{sign}\left(\sum_i \lambda_i y_i \boldsymbol{\Phi}(\mathbf{x}) \cdot \boldsymbol{\Phi}(\mathbf{x}_i) + b\right) \tag{3.37}$$

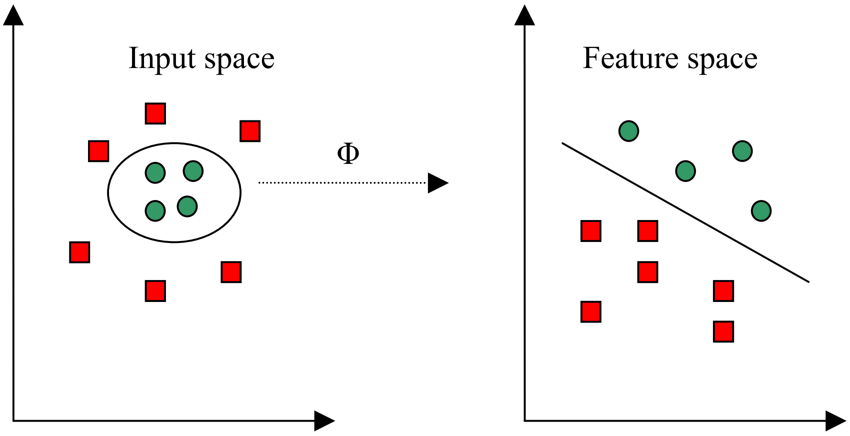

Figure 3. 7. The idea of a non-linear support vector machine.

As suggested by equation 3.37, the only quantities that one need to compute are the scalar products, of the form Φ(x) . Φ(y). It is therefore convenient to introduce the concept of the *kernel function* K (Vapnik, 1995) such that:

$$K(\mathbf{x}_i, \mathbf{x}_j) = \boldsymbol{\Phi}(\mathbf{x}_i) \cdot \boldsymbol{\Phi}(\mathbf{x}_j) \tag{3.38}$$

In this optimisation problem, only the kernel function is computed in place of computing $\boldsymbol{\Phi}(\mathbf{x})$, which could be computationally expensive. By doing this, the training data are moved into a higher-dimensional feature space where the training data may be spread further apart and a larger margin may be found for the optimal hyperplane. Thus, equation 3.28 can be written as:

$$L(\boldsymbol{\lambda}) = \sum_i \lambda_i - \frac{1}{2} \sum_{i,j} \lambda_i \lambda_j y_i y_j \left(\Phi(\mathbf{x}_i) \cdot \Phi(\mathbf{x}_j)\right) \tag{3.39}$$

A number of kernel functions are used within SVM. To find a way to choose among various kernels and the parameters of the kernel function, readers are referred to Vapnik (1995). For this study, several kernels are considered in order to compare the effect of choice of kernel type and associated parameters for land cover classification. The kernels used for this study are:

- The simple dot product: $K(\mathbf{x},\mathbf{y}) = \mathbf{x}\cdot\mathbf{y}$.
- The simple polynomial kernel of degree d: $K(\mathbf{x},\mathbf{y}) = ((\mathbf{x}\cdot\mathbf{y})+1)^d$.
- A radial basis function: $e^{-\gamma|x-y|^2}$ with γ defined by user.
- A two-layer neural network: $\tanh(b(\mathbf{x}\cdot\mathbf{y})-c)$ where b and c are user defined.
- A linear spline with an infinite number of points:

$$1+\mathbf{x}_i\mathbf{x}_j+\mathbf{x}_i\mathbf{x}_j\min(\mathbf{x}_i,\mathbf{x}_j)-\frac{\mathbf{x}_i+\mathbf{x}_j}{2}(\min(\mathbf{x}_i\mathbf{x}_j))^2+\frac{(\min(\mathbf{x}_i,\mathbf{x}_j))^3}{3}.$$

In order to find the optimal decision surface, the support vector training algorithm tries to separate, as best as possible, the clouds of data points representing each class. Data points closer to the boundary between the classes are more important in the classification than are data points that are far away, since data points closer to the boundary are harder to classify. These data points help shape and define better decision surface than other points. The support vector machine tries to find data points that are closest to the separating surfaces, therefore the support vectors are border points, and due to this reason support vectors are very few. Finally, SVMs are based on a QP optimisation problem that has only a global optimum. The absence of local minima is a significant difference from standard pattern recognition techniques such as neural networks (Osuna et. al., 1997).

3.13 Multi-class classifier

SVM was initially designed for binary (two-class) problems. When dealing with several classes, as the case of land cover classification, an appropriate multi-class method is needed. Different possibilities for this includes:

- Modify the design of SVM, such that it incorporate the multi-class learning directly in the quadratic solving algorithm (Weston and Watkins, 1998).

- Combine several binary classifiers: the "one against the rest" approach (Vapnik, 1995) compares a given class with all the others put together, thus generating n classifiers, where n is the number of classes. The final output of this SVM is the class that corresponds to the SVM with the largest margin, the value of the argument of the *sign* function in equation 3.37.
- Combine several classifiers: the "one against one" approach (Knerr et al., 1990) applies pairwise comparisons between classes. In this method, all possible two-class classifiers are evaluated from the training set of n classes, each classifier being trained on only two out of n classes. There would be a total of n(n-1)/2 classifiers. Applying each classifier to the vectors of the test data gives one vote to the winning class. The pixel is given the label of the class with most votes.

In this study, the "one against one" and "one against the rest" approaches are used so as to compare the results obtained. Two SVM based classification software systems were used. One was obtained from Royal Holloway College and AT&T, University of London; the other, LIBSVM, was provided by Chih-Chung Chang of the University of Taiwan.

3.13 Problems in the use of SVM

So far, few studies have reported the use of support vector machines for classification of remote sensing data (Huang et al., 2002; Zhu and Blumberg, 2002; Gualtieri and Cromp, 1998). In comparison to neural classifiers few factors affect the performance of these classifiers and Huang et al. (2002) discussed some of them in detail. Some of the factors that affect the classification accuracy of SVM classifiers are:

1. Choice of kernel used.
2. Choice of the parameters related to a particular kernel.
3. Method used to generate the SVM for multi-class classification problems.
4. Choice of parameter C.

This study is designed to study the effect of all these parameters on classification accuracy of remotely sensed data, details of which is provided in chapter 5 (section 5.2).

3.14 Ensemble of classifiers

In recent years, a number of papers proposing the combination of multiple classifiers to produce a single classification have been published in the remote sensing literature. The resulting classifier, referred to as an ensemble classifier, is generally found to be more accurate than any of the individual classifiers making up the ensemble. Some papers report the use of ensembles of neural networks (Giacinto and Roli, 1997) and the integration of classification results of different type of classifiers (Roli et al., 1997), and they find that this technique is effective in improving classification accuracy. Much of this research is focused on improving classification accuracy, as accuracy is the primary concern in all applications of learning. So far, very few works (Friedl et al., 1999) have reported the use of boosting, another technique that can improve the performance of any learning algorithm, in image classification. The basic difference between the use of ensembles of classifiers and boosting is that boosting uses the same learning algorithm that consistently generates multiple classifiers in an iterative manner.

3.14.1 Boosting

Boosting is a general method for improving the performance of any learning algorithm. Boosting can be used to reduce the error of any weak learning algorithm that consistently generates classifications on various distributions over the training data, and then combines the classifications produced by the weak learner into a single composite classification. Figure 3.8 illustrates the basic framework for a classifier ensemble.

In this study, a boosting algorithm called AdaBoost M1 (Freund and Schapire, 1996) is used with the C4.5 decision tree (Quinlan, 1993) as the base algorithm. Boosting assigns a weight to each observation - the higher the weight, the more that observation influences the classifier. At each trial, the vector of weights is adjusted to reflect the performance of the corresponding classifier, with the result that the weight of misclassified observations is increased. The final classifier aggregates the classifiers generated after each iteration by voting, but each classifier's vote is a function of its accuracy.

Following Freund and Schapire (1996), let $w^t{}_x$ be the weight assigned to observation x at trial t where, for every x, and t=1,

$$w^1{}_x = 1/N$$

where N is the total number of observations in the training set and t is the iteration or trial number (t = 1, 2, ……, T). At each trial, a classifier C^t is constructed from the given observations under the distribution w^t (i.e., as if the weight $w^t{}_x$ of observation x reflects the probability of its occurrence). The error ε^t of this classifier is also measured with respect to the weights, and consists of the sum of the weights of the observations that it misclassifies. If ε^t is greater than 0.5, the trials are terminated and the value of T becomes t-1. Conversely, if C^t correctly classifies all observations so that ε^t is zero, the trials terminate and the value of T becomes t. Otherwise, the weight vector $w^{t+1}{}_x$ for the next trial is generated by

$$w^{t+1}{}_x = w^t{}_x \times \varepsilon^t / \left(1 - \varepsilon^t\right)$$

Conversely, if the observation was not correctly classified, w_x is unchanged and at each iteration the weight w_x is normalised so that

$$\sum w_x = 1 .$$

By applying the above process, a new tree with a different error level is estimated at each step. The final, boosted classifier is the result of a voting procedure, where the vote for classifier C^t is worth

$\log\left(1/\beta^t\right)$ units.

with

$$\beta^t = \varepsilon^t / \left(1 - \varepsilon^t\right).$$

Studies carried out by Quinlan (1996) using a variety of data sets have shown that boosting tends to reduce misclassification error rate by 25% on average, and improvement in classification accuracy tends to stabilise by about 10 iterations. In remote sensing, only a few studies have been carried out (Friedl et al., 1999 and Muchoney et al., 2000), and these studies suggests that boosting helps to improve the accuracy of classification by 5-12%.

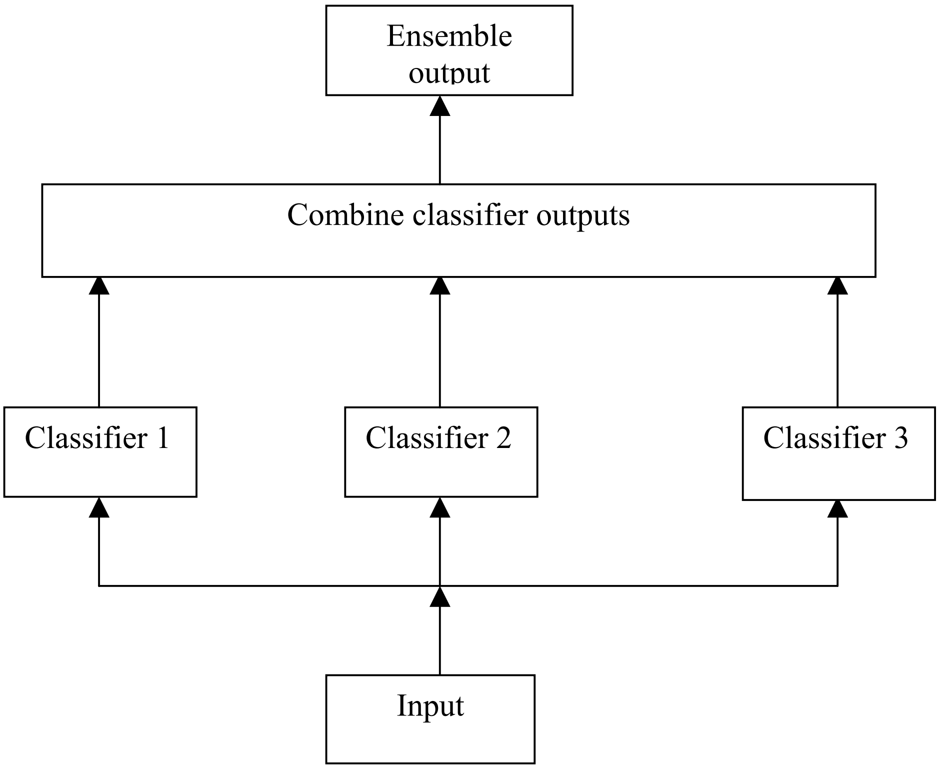

Figure 3. 8. A classifier ensemble of decision tree classifier.

3.14.2 Bagging

Brieman (1996) suggests another technique, called bootstrap aggregating or bagging, to improve the accuracy of a base classifier by creating a number of classifiers by manipulating the training data. In this method, each classifier's training set is generated by randomly drawing, with replacement, N examples, where N is the size of the original training set. In this situation, many of the original examples may be repeated in the resulting training set while others may be left out. The learning system generates a classifier from the sample and aggregates all the classifiers generated from the different trial to form the final classifier. To classify an instance, every classifier records a vote for the class to which it belongs, and the instance is labelled as a member of the class with the most votes.

3.15 Conclusions

The fundamental principles underlying the design and use of decision tree and support vector machine classifiers are discussed in this chapter. The main steps in the design of a decision tree classifier, such as the choice of an attribute selection measure, pruning methods, and various cases for the design of support vector machines are described in detail. Boosting is a new technique that is used to improve classification accuracy, and this technique is discussed in detail along with another technique, called bagging, to create ensemble of classifiers using the same classifier as the base classifier. So far few studies (Friedl and Brodley, 1997; Gahegan, 1998; Huang et al., 2002) have compared the behaviour of support vector machines and decision tree classifiers with statistical and neural classifiers. These studies suggested that SVM and DT classifiers outperform statistical classifiers but so far no study has attempted to compare the behaviour of SVM and DT classifiers with neural and statistical classifiers in detail.

The question of relative performance of statistical, neural network, support vector machines, and decision tree classifiers and various factors affecting these classifier in term of ease of use is examined in the following chapters of this thesis.

Chapter 4

Data Sets

4.1 Introduction

Several types of remote sensing data can be used in land cover classification. Data can be taken from the optical or microwave regions of the spectrum, and can be hyperspectral or multispectral in nature, depending on their availability and quality for a particular region. Usually medium spatial resolution satellite sensor data, such as Landsat TM/ETM+ and SPOT, have been used in several researches. Data acquired by these sensors, which operate in the visible and near-infrared part of the electromagnetic spectrum, are often hindered by clouds or haze. It may be difficult to acquire cloud free data when using conventional optical satellite sensors, thus impeding the regular updating of land cover maps, especially in areas like the UK. Active microwave sensors, however, acquire data independent of weather, cloud, solar angle, or solar illumination. This independence from weather and illumination conditions allows data to be collected by these sensors at any stage of the crop growth cycle.

Studies reporting on the use of optical and microwave data for land cover classification suggest that choice of data type has an effect on classification accuracy. This research is designed to evaluate the performance of both optical (ETM+) and microwave (InSAR) data for the same area in the UK for land cover classification, using different classification algorithms. DAIS hyperspectral data of an area in Spain are employed to study the behaviour of different classification algorithms with different training dataset sizes and increasing number of features. As few studies have used interferometric SAR data for land cover classification, a detailed description of the technique is given in this chapter.

4.2 Synthetic Aperture Radar(SAR)

A radar sensor operates by transmitting a pulse of electromagnetic energy and then intercepting the backscattered or reflected radiation with an aperture of some physical dimension. In traditional (non-SAR) systems, the angular resolution (the angular spread of the radar beam) is governed by the ratio of the wavelength of the electromagnetic radiation to the aperture size. The spatial resolution of the image is the angular resolution times the distance from the sensor to the earth's surface. Therefore, as the sensor altitude increases, the spatial resolution of the image decreases unless the physical size of the aperture is increased. At visible and near infrared wavelengths, a high resolution image can be obtained even from orbital altitudes for modest aperture sizes. However, for a microwave instrument, which uses wavelengths that are very long compared to those of visible light, high resolution imagery from a reasonably-sized antenna aperture is not possible. Hence, to improve resolution without increasing physical antenna size, Synthetic Aperture Radar (SAR) technology is employed. SAR is a coherent imaging system in that it retains both the phase and magnitude (amplitude) component of the backscattered signals. The value of a pixel in a complex SAR image may be divided into phase and intensity parts in the following way:

$$Z(x,y) = I(x,y)e^{i\phi(x,y)}$$

Where Z(x,y) is the complex pixel
x,y are image coordinates
I is the intensity of the pixel
Φ is the phase of the pixel
i is the imaginary unit

The phase information contained in a single SAR image is practically useless and SAR intensity is generally used.

SAR operates on the principle of using the along track sensor motion to transform a single physically short antenna into an array of such antennae that can be linked together mathematically as part of the data recording and processing procedures (Curlander and Mcdonough, 1991; Elachi, 1987). The successive positions of the real antenna along the flight line are treated mathematically as if they were simply successive elements of a single, long synthetic antenna. Points on the ground at near range are viewed by proportionately fewer antenna elements than those at far range, meaning effective antenna length increases with range. Through this process, long antennas can be synthesised with spaceborne SAR systems. A SAR system is therefore capable of achieving a given resolution independent of sensor altitude. This characteristic makes SAR an extremely valuable instrument for remote sensing. The major advantages of SAR are that it can provide high resolution images of extensive areas of the earth's surface irrespective of weather conditions or solar illumination. The resistance to weather conditions derives from the use of wavelengths of the order of centimetres, with X-band (3 cm), C-band (6 cm) and L-band (24 cm) being favoured. This all-weather and day/night capability makes SAR a most attractive tool for environmental monitoring in regions affected by clouds or darkness. An essential element of monitoring changes in the earth's environment is the ability to observe a study area on a regular and reliable basis. Over many parts of the globe this is not possible using optical and infrared radiation, so SAR not only has the ability to operate at all the times of the year but also has sufficient resolution to detect environmental changes. A spaceborne SAR generates a radar backscatter map by scanning the earth's surface in a side-looking fashion as shown in figure 4.1. While the sensor is moving along its orbital path it transmits microwave pulses at the rate of pulse repetition frequency and receives the echoes from each pulse via the same antenna. The spot on the ground that is illuminated by a single pulse is referred to as the antenna footprint, and the entire imaged strip is the swath.

In remote sensing radars, the size of a resolution cell on the surface is always much larger than the signal wavelength and is generally significantly larger than the size of the individual scattering objects. Microwave signals returning from a given resolution cell on the earth's surface can be in phase or out of phase by varying degree when received by the sensor. The image thus obtained has a random pattern of brighter and darker pixels, giving them a distinctly grainy appearance called speckle. Speckle can be reduced through the application of image processing techniques such as averaging neighbouring pixel values, or by special filtering and averaging techniques but it is more difficult to remove from the image than is additive noise. One technique useful for reducing speckle is multi-look processing (Lillesand and Kiefer 1994).

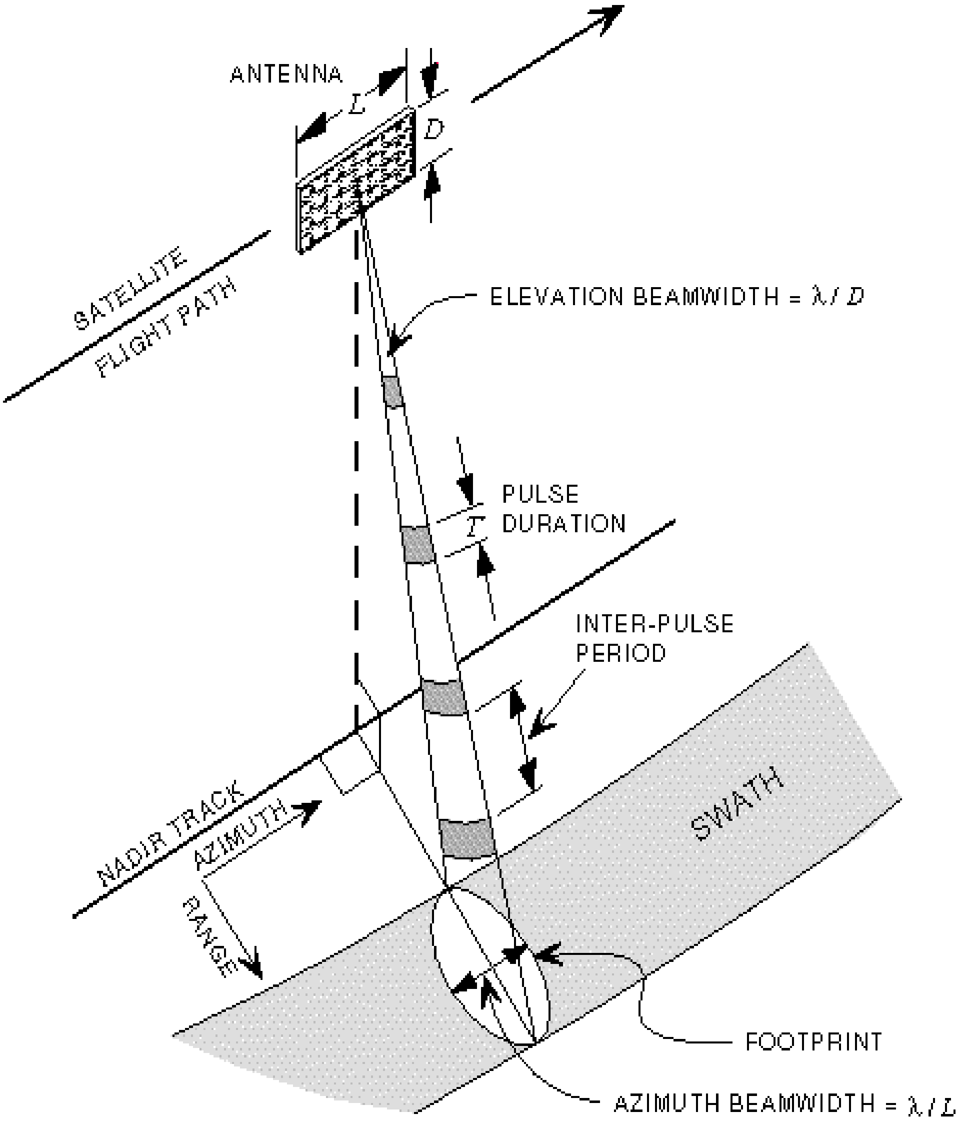

Figure 4. 1. Geometry of a SAR (adapted from http://www.ccrs.nrcan.gc.ca/ccrs).

This is usually done by computing some number of nominally independent images (looks) of the same scene produced by different portions of the synthetic aperture, and averaging them, pixel by pixel to produce a smoother image. The image thus obtained will be called as multi-look image. Multi-looking is thus a method for reducing speckle noise in SAR data. The SAR data can be multi-looked to a specified number of looks, number of lines and samples, or azimuth and range resolution. In addition to speckle reduction, multi-looking is often used to give SAR data square pixels.

4.3 Interferometric Synthetic Aperture Radar

Global high-resolution digital topographic information is necessary for many geographical applications. The simultaneous requirements of global coverage, high spatial resolution, and high vertical accuracy pose severe demands that cannot be met easily with conventional mapping techniques. A technique which may meet these requirements, Interferometric Synthetic Aperture Radar (InSAR) mapping was introduced by Graham (1974). Radar interferometry is a technique for extracting three-dimensional information about the earth's surface by using the relative phase difference of two coherent synthetic aperture radar images obtained by two receivers separated by a cross-track baseline to derive an estimate of the earth surface deviation. The horizontal resolution (range and azimuth resolution) of the system is dictated by the SAR bandwidth (frequency range contained in a signal) and the antenna length. These parameters can be selected so as to satisfy topographic resolution requirements. The vertical accuracy of the system is ultimately limited by the wavelength used by the SAR which, for microwaves, is on the centimetric scale. The general geometry of SAR interferometry is illustrated in figure 4.2.

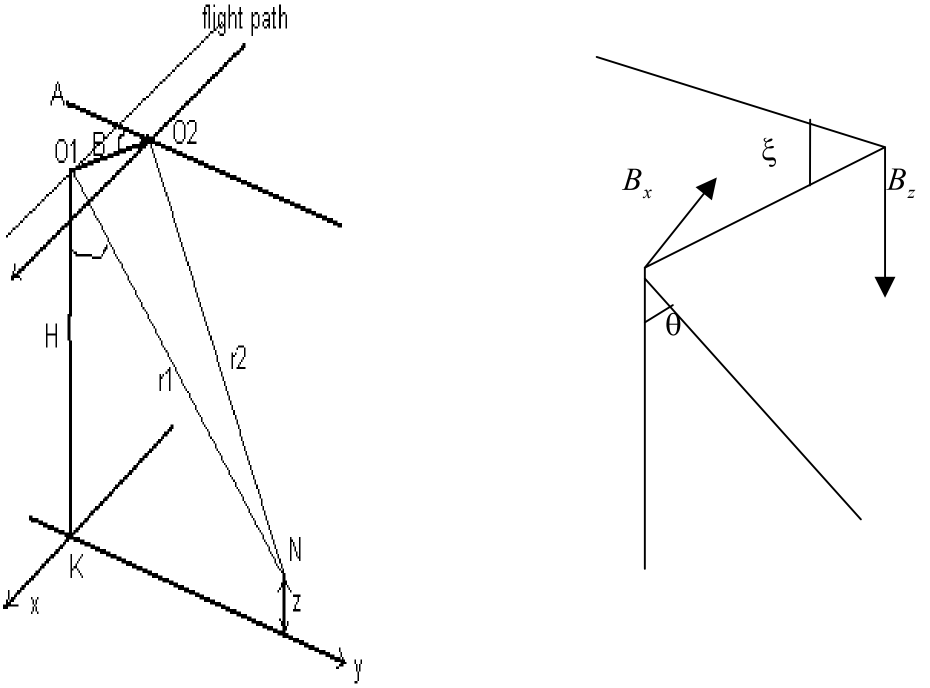

Figure 4. 2. Principle of interferometric synthetic aperture radar (adapted from Gens and Van Genderen, 1996).

The phase difference ϕ between the signals received from the same surface element at the two antenna positions is

$$\Phi = 4\pi(r2 - r1)/\lambda \tag{4.1}$$

$$\Phi = \frac{4\pi}{\lambda}\left(B_x \sin\theta - B_z \cos\theta\right) \tag{4.2}$$

Where λ is the SAR wavelength (which must be the same for the two observations) and r1 and r2 are the distances between the radar antenna and the scatterers for platform positions O1 and O2 in figure 4.2, B_x and B_z are the baseline components and θ is the local incident angle.

The height of the point N can then be determined by

$$Z = H - r1\cos\theta$$

$$= H - r1\ \left(\cos\xi\sqrt{1-\sin^2(\theta-\xi)} - \sin\xi\sin(\theta-\xi)\right) \tag{4.3}$$

where H is the flying height and ξ is the baseline tilt angle.

There are three main ways to acquire SAR interferometric data. These are by the use of along track, across track, and repeat-track (multi-pass) interferometry. In across-track interferometry two SAR antenna systems are mounted simultaneously on a single platform, which can be an aircraft or a space shuttle. The geometry of the across-track interferometry is shown in Figure 4.3.

The terrain height can be calculated by

$$h = H - r1\cos\theta_1 \tag{4.4}$$

The ground range is determined by

$$y = r1 \sin\theta_1 \qquad (4.5)$$

and the phase difference can be calculated by equation 4.1.

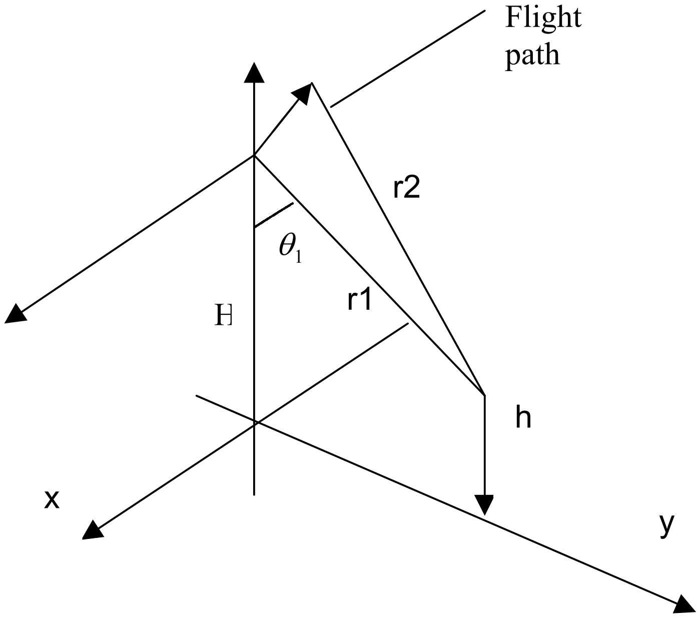

Figure 4. 3. Geometry of across-track interferometry (adapted from Gens and van Genderen, 1996).

Along-track interferometry does not differ very much from across-track interferometry in term of geometry. In principle, only the x- and y-axes are changed, as shown in Figure 4.4.

The phase difference between the corresponding pixels in the two SAR images in this geometry is caused by the movement of the object during measurement. The velocity of the object, u can be derived from the expression

$$u = \frac{\phi\lambda V}{4\pi B_x} \qquad (4.6)$$

where λ is the radar wavelength, ϕ is the phase, V is the velocity of the aircraft and B_x is the baseline component.

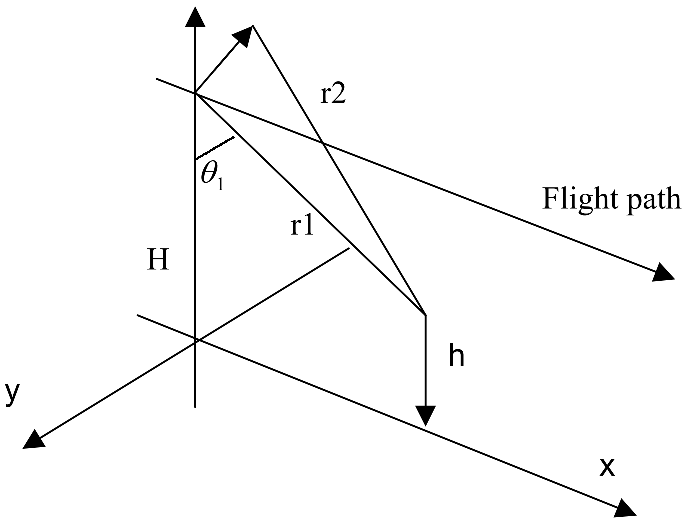

Figure 4. 4. Geometry of along-track interferometry (adapted from Gens and van Genderen, 1996).

Repeat-pass interferometry requires only one antenna and is therefore most suited to spaceborne SAR sensors. The satellite has to accomplish two close orbits giving coverage of the area of interest in order to acquire two images of the area with slightly different viewing geometry within a short space of time (usually a few days). Alternatively, images from two identical instruments carried onboard different satellites can be used. This is called "tandem mode" operation (e.g. ERS-1 and ERS-2).The geometry of repeat-pass interferometry is shown in Figure 4.5. In Figure 4.5, " ….the two observation points O1 and O2 are not antenna phase centre positions but points on the motion compensation reference paths which dictates the cycles in phase difference across the swath" (Gens and van Genderen 1996). The separation of the sensor locations O1 and O2 determines the correlation in the two complex images (contains both backscatter amplitude and phase information and in mathematical sense it has a real and imaginary part).

The interferometric baseline can be described by the horizontal separation h and vertical separation v of the reference paths, assuming that the reference paths are parallel. The values of h and v are often not differentiated, but this approximation is acceptable to show the principle of repeat-pass interferometry. The difference in slant range r is given by

$$r = r1 - r2 = \frac{gh - (H-h)v}{\bar{r}} - \frac{B^2}{2\bar{r}} \qquad (4.7)$$

where

$$\bar{r} = (r1 + r2)/2$$

$$B = \sqrt{h^2 + v^2}$$

The phase difference can be derived from the path difference by the equation

$$\phi = -4\pi r/\lambda \qquad (4.8)$$

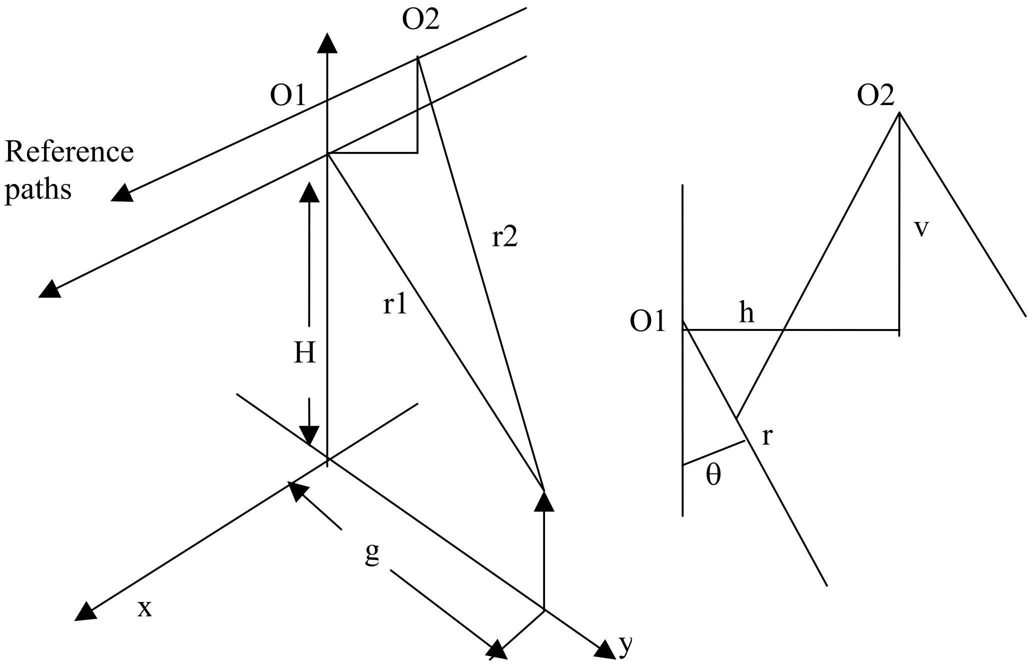

Figure 4. 5. Geometry of repeat-pass interferometry (adapted from Gens and van Genderen, 1996).

4.4 Differential interferometry

In addition to measuring the topography, an interferometric SAR may be used to measure surface motion, provided that such motion is coherent. Coherence is maintained if the group of scatterers within one resolution cell do not change significantly from the first pass to the second pass of the SAR sensor, and provided that the scattering mechanism of the individual scatterers does not change significantly between the two passes. If these assumptions are valid, then it is possible to measure surface motion between the two passes of the SAR sensor using repeat-pass interferometry. Differential interferometry provides relative measures in the order of a few centimetres, or less, for movements in the vertical and planimetric directions. In this technique a differential interferogram is generated by the difference of two interferograms, which contains information about small-scale displacements that occur between the times of data acquisition. A differential interferogram can be produced in two different ways. Based on two phase-unwrapped interferograms, the difference of these interferograms can be calculated. Alternatively, an existing digital elevation model can be registered to the viewing geometry of a calculated interferogram. The result of this approach is a simulated interferogram. The difference of the original and simulated interferogram is the required differential interferogram.

4.5 Coherence

The phase component in conventional SAR imagery is determined by two terms. Firstly, the two-way electrical path length from the sensor to a specific resolution cell and, secondly, the interference between different scatterers within the cell. Constructive and destructive interference will introduce speckle and therefore produces no useful phase information in one single SAR image. A second observation from a different angle will, in principle, have the same speckle interference term provided that the change of angle is small. The phase difference between the two images will therefore be determined by the path length difference between the two observation points to the resolution cell. The two images can either be obtained by using two different sensors or the same platform (single-pass interferometry) or by using the same sensor at two different parallel or nearly parallel passes over the area (repeat-pass interferometry) as described above.

In SAR interferometry, coherence is defined as a measure of the degree of resemblance of radar phase between two SAR images of the same area, and the degree of correlation that exists between the two SAR images is called the complex degree of coherence. The value of this coefficient varies between zero and one, where a zero value means no interference, which implies that there will be no interferometric fringes.

4.5.1 Coherence magnitude estimation

The complex coherence of two zero-mean complex signals g_1 and g_2 for stationary random processes is defined as (Born and Wolf, 1980):

$$\gamma = \frac{E\left[g_1 g_2^*\right]}{\sqrt{E\left[\left|g_1\right|^2\right]E\left[\left|g_2\right|^2\right]}} \tag{4.9}$$

Where g_2^* is the conjugate value of signal g_2 and E[ ] denotes the expectation value. The magnitude of γ ($|\gamma|$) is called the degree of coherence and the phase of γ is called interferometric phase. Under the assumption that the processes involved in equation (4.9) are ergodic in mean,[1] the ensemble average is found by coherently averaging the complex values of N single look pixels. The coherence is then defined as:

$$\bar{\gamma} = \frac{\left|\sum_{i=1}^{N} g_{1,i} g_{2,i}^*\right|}{\sqrt{\sum_{i=1}^{N}\left|g_{1,i}\right|^2 \sum_{i=1}^{N}\left|g_{2,i}\right|^2}} \tag{4.10}$$

In equation (4.9), it can be noted that g_1 and g_2,which are assumed to be stationary, are also jointly stationary.

[1] There are two ways to calculate the mean of a random variable: 1. Time average: by integrating a particular member function over all time or 2. Ensemble average: average together the values of all member functions evaluated at some particular point in time. A random variable is ergodic if and only if (1) the time averages of all member functions are equal, (2) the ensemble average is constant in time, and (3) the time average and the ensemble average are numerically equal. Thus, for ergodic random variables, time average and ensemble average are interchangeable.

Stationarity of the processes (g_1, g_2 and $g_1g_2^*$) is required such that the time average of each process converges to a finite limit. Ergodicity in mean is also required so that different time averages of each process converge to the same limit, i.e. the ensemble average. The ensemble averages can then be substituted in equation (4.9) with the time average and sample coherence of equation (4.10) to provide an estimate of coherence. The coherence estimation considered above is for stationary scenes in which the processes (g_1, g_2 and $g_1g_2^*$) involved in equation (4.9) are stationary. Such conditions are satisfied in homogeneous scenes (Touzi et al., 1999).

In nonstationary areas, the processes (g_1, g_2 and $g_1g_2^*$) involved in equation (4.9) may not be stationary in mean and the sample coherence of equation (4.10) will lead to a meaningless result (Foster and Guinzy, 1967). In practice, stationarity in mean (the assumption that the mean E[ ] does not vary) may be relaxed: all that is required is that E[ ] does not change within the observation interval (Foster and Guinzy, 1967). If this condition is satisfied by each of the processes involved in equation (4.9), the nonstationary processes can be considered to be locally stationary (also called "stationary in increment") and the coherence can be estimated over a moving window.

In certain nonstationary areas, the processes involved in equation (4.9) cannot be assumed to be stationary in increments, and coherence cannot be estimated even locally. In some applications, the source of signal nonstationarity might be removed and coherence can then be estimated. Especially in SAR interferometry, nonstationarity of the cross channel product $g_1g_2^*$ is assigned to the phase changes due to topographic variations. The phase nonstationarity is compensated at the spatial position i with a phase factor $e^{-j\phi_i}$ for the local imaging geometry, and the sample phase corrected coherence is used instead of sample coherence of equation (4.10) (Touzi et al., 1999)

$$\bar{\gamma} = \frac{\left| \sum_{i=1}^{N} g_{1,i} g^*_{2,i} \; e^{-j\phi_i} \right|}{\sqrt{\sum_{i=1}^{N} \left| g_{1,i} \right|^2 \sum_{i=1}^{N} \left| g_{2,i} \right|^2}} \tag{4.11}$$

After phase compensation, and under the assumption that the unique source of signal nonstationarity is topographic phase variations, all processes involved in equation (4.11) are stationary in the region of interest and the channels can still be assumed to be zero-mean jointly gaussian. The results obtained in stationary regions with the sample coherence of equation (4.10) can then be extended to the modified sample coherence as given in equation (4.11) (Touzi et al. 1999).

The statistical confidence level of the sampled coherence depends on the number of independent samples N that are combined to produce the coherence estimate. Sampled coherence is usually estimated using a square estimator window. As a first approximation, the standard deviation of the estimator is defined as (Prati et al., 1994)

$$\sigma_{\bar{\gamma}} = \frac{1}{\sqrt{N}} \tag{4.12}$$

where N is the number of pixels in the window.

In practice, coherence has to be estimated from the combination of many pixels in order to limit the statistical errors. The effects of the topography of the target inside the estimator window have to be compensated for. This was not necessary in this study due to extremely flat topography.

Another coherence estimator, suggested by Guarnieri and Prati (1997), is intended for selection of interferometric pairs with good coherence, as its implementation is quick. It is described as

$$\overline{\gamma_a} = \sqrt{2\rho - 1} \qquad \text{For } \rho > 1/2$$

$$\text{Otherwise} \quad \overline{\gamma_a} = 0$$

where

$$\rho = \frac{\sum_{i=1}^{N} \left| g_{1,i} \right|^2 \left| g_{2,i} \right|^2}{\sqrt{\sum_{i=1}^{N} \left| g_{1,i} \right|^4 \sum_{i=1}^{N} \left| g_{2,i} \right|^4}} \tag{4.13}$$

In SAR interferometry, interferometric correlation or degree of coherence as expressed in a coherence image has potential as an input to classification for different land surfaces. The degradation of coherence between two images is due to several effects. The most important are spatial decorrelation (due to observation angle change) and temporal decorrelation (due to changing scatterer characteristics between the two images).

4.5.2 Image processing and generation of coherence images

4.5.2.1 Co-registration and common band filtering

In interferometric processing, two single-look complex images (SLC) are co-registered at sub-pixel accuracy; an accuracy better than 0.2 pixels is required in order not to degrade the interferometric correlation by more than 5%. In this study, the GAMMA interferometric software was used for all interferometric processing. The co-registration of the images in an interferometric pair was done by calculating the local spatial correlation of the image intensities for at least 100 small square areas throughout the two images. The offset polynomial relating the geometries of the two images was determined by finding the image offsets, which maximises the local correlation in these small areas. The advantage of this method is that it is possible to co-register images that have no interferometric correlation into a common geometry, the only requirement being that there is some contrast in the SAR intensity images. Before interferogram generation, common band filtering (Gatelli et al., 1994) was performed in order to include only the parts of the range and azimuth spectra common to the two interfering images. Common band filtering improves the coherence estimate by minimising the effects of the baseline geometry.

4.5.2.2 Interferogram generation and flat earth correction

After co-registration and common-band filtering, normalised interferograms and intensity images were generated by cross-correlating the two co-registered images. At this stage, multi-looking in the range and azimuth direction was also performed to improve the estimate of interferometric phase and coherence. The resulting multi-look interferogram was then flattened by removing the phase trend corresponding to a flat earth. Flattening was performed by estimating the local fringe frequency on a topographically flat area using a 2-D fast Fourier transform, and subtracting this estimated phase trend from the unflattened interferogram. Supposing that there are no atmospheric artefacts, the interferometric phase of a flattened interferogram is related to the surface topography. On an extremely flat area, such as the study area near Littleport the phase of the flattened interferogram is related to differential phase effects, such as changes in the dielectric constant of the land surface.

Figure 4. 6. Interferograms of the study area. (a) without flat earth correction and (b) with flat earth correction.

4.5.2.3 Coherence estimation

The interferometric correlation or coherence was estimated from the flattened multi-look interferograms and the co-registered intensity images. In this study, a maximum likelihood coherence estimator with a square estimator window is used. There is always a trade-off between spatial resolution and estimation accuracy at low coherence values when choosing the estimator window size. In addition, a weighing function, decreasing linearly with increasing distance from the central pixel, was applied in the coherence estimation. With the data sets shown in Table 4.1, the following coherence images were generated (Figure 4.7):

1 1-day coherence image using 02/05/1996 and 03/05/1996 SLC.
2 35-day coherence image using 16/08/1996 and 20/09/1996 SLC.
3 70-day coherence image using 07/06/1996 and 16/08/1996 SLC.

Table 4. 1. The date and corresponding sensor of the SLC used in the study.

Sensor	**Date**
ERS-1	02 May 1996
ERS-2	03 May 1996
ERS-2	07 June 1996
ERS-2	16 August 1996
ERS-2	20 September 1996

Due to the large base line length (>1000 m) and the time interval involved, the phase coherence obtained at 35 days and 70 days was not very good. Hence, in this study, only the 1-day coherence image and five intensity images produced during the interferometric processing of the single look complex images are used for land use classification.

4.5.2.4 Image coregistration

The 1-day coherence image used in this study was registered to the Ordnance Survey (OS) of Great Britain's National Grid using the ERDAS Imagine image processing software by applying a first-order polynomial transformation using fifteen ground control points. The RMS error value estimated for image transformation was of the order of 0.87 pixels. Later, all the five intensity images were co-registered to the coherence image. The nearest neighbour resampling method was used and the spatial resolution (i.e. pixel size) of the image was reduced to 20 metres. A 286-pixel by 386-pixel portion of the image covering the area of interest was extracted and used for further stages of classification and texture extraction.

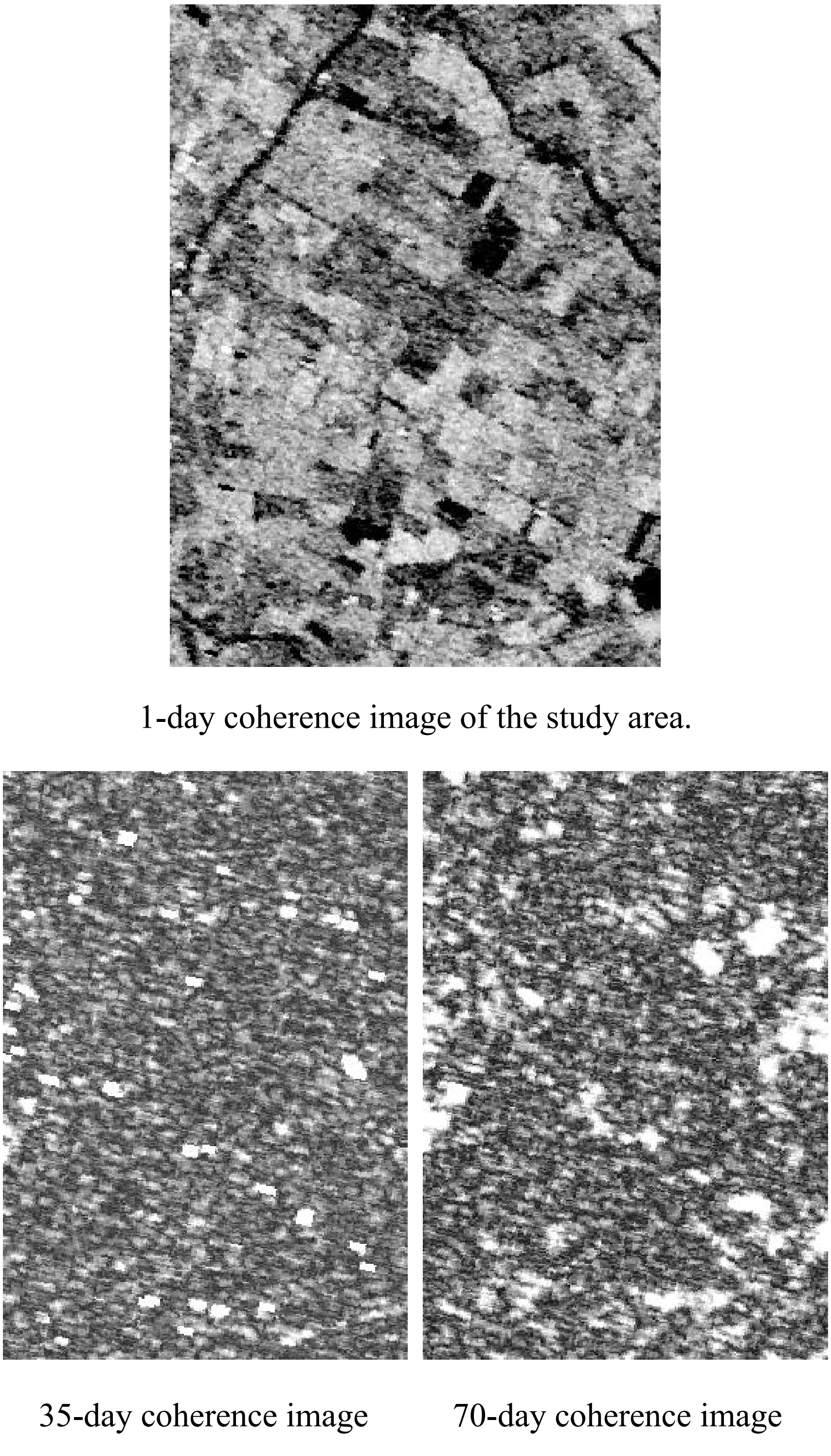

1-day coherence image of the study area.

35-day coherence image

70-day coherence image

Figure 4. 7. Coherence images of the study area.

4.5.2.5 Speckle suppression

In remote sensing radar images, the size of a resolution cell on the surface is always much larger than the signal wavelength and is generally significantly larger than the size of individual scattering objects. Because of the random orientation of terrain surface elements, returns from multiple scatterers within a resolution cell add incoherently to give a net backscattering coefficient, which has a random distribution in the image plane. The image thus obtained has a randomly fluctuating intensity at each pixel, which leads to a grainy appearance. This random multiplicative noise/grainy appearance within a SAR resolution element is called speckle. Speckle is one of the main problems in the use of synthetic aperture radar image interpretation and classification because a zone that is homogeneous on the ground has a granular appearance on image. For the purpose of classification, it is desirable to reduce these fluctuations and to cluster the observed intensities closer to the mean intensity, since it is the mean intensity that expresses the required image information. In order to decrease the effects of speckle, several different approaches can be used. These includes averaging of images (Ulaby et al., 1986), filtering of images using adaptive filters (Nezry et al., 1996), the use of texture features (Ulaby et al., 1986).

In this study, all of the intensity images obtained from interferometric processes are single look images. A number of filters (Lee (Lee, 1986) Frost (Frost et al., 1982) and Kuan (Kuan et al., 1985)) have been developed and tested for speckle reduction in radar data. When applying the speckle filter, selection of window size is important, because speckle suppression will not be satisfactory with a small window size and with a large window size, the original image will also be degraded by oversmoothing. There is a trade-off between speckle reduction and preservation of image quality. In this study, a median filter with a window size of 5×5 is used for speckle reduction in all intensity and coherence images. The median filter operates on the image so that the centre pixel of the filter window is replaced by the median value of the pixels in window. In other words, low and high valued pixels are considered as noise and are removed (Richards, 1993). These filtered images were then used for classification studies.

4.5.3 Factors affecting coherence

As mentioned earlier, interferometric coherence is a by-product of SAR interferometry and it provides a measure of the phase correlation between two images of the same target obtained from two different positions, possibly at different times. Phase coherence is affected by a number of factors, the most important being:

1. Instrument parameters, including wavelength, signal to noise ratio, range resolution, and number of independent looks.
2. Parameters related to the geometry, such as the baseline length and incidence angle. The spatial extent of the baseline is one of the major performance drivers in an interferometric radar system. If the baseline is too short the sensitivity to signal phase differences will be undetectable, while if the baseline is too long then additional noise due to spatial decorrelation corrupts the signal. It can be shown that coherence (phase correlation) decreases approximately linearly with the increase in baseline length (Rodriquez et al., 1992). The length of the baseline for which the attainable coherence is zero is called the critical baseline length, which occurs when the change in look angle between the interfering images is sufficient to cause backscatter from each pixel to become completely uncorrelated. The critical baseline length for ERS-1/2 interferometry on flat terrain is approximately 1100m. The effect of baseline decorrelation may be reduced by the use of spectral filtering during interferometric processing.
3. Volume scattering and temporal changes, i.e., movement of the scatterers due to wind effects, growth, and loss of foliage. In other words, it is not possible to illuminate the same patch of surface from two different aspect angles and expect the signals to be fully correlated. This is also called decorrelation due to the rotation of the targets with respect to the radar look direction. Temporal effects which follows from physical changes in the surface over the time period between observations. In practice, the amount of temporal decorrelation depends on the soil and vegetation type

of the target area, as well as the weather conditions between the radar passes.

4. Variation in the dielectric constant due to freezing, wetting, and drying of surface, thus causing temporal decorrelation.

As long as the data used are from same system, instrument parameters remain the same and have no effect on coherence. Common spectral band filtering[2] (Gatelli et al., 1994) of the SAR image pair before computation of the interferogram helps to reduce the decorrelation introduced by baseline geometry[3], if baseline length is within an acceptable range. Repeat pass SAR interferometry is very sensitive to temporal changes, i.e., change occurring between the two data acquisition times.

4.6 ETM+ data

The main instrument carried by Landsat 7 is the Enhanced Thematic Mapper Plus (ETM+). This instrument maintains the essential characteristics of Thematic Mapper carried by Landsats 4 and 5 (Table 4.2). Ground resolution for ETM+ data remains unchanged at 30 m, except for the thermal band in which the resolution is increased from 120 to 60 m. A panchromatic band with 15 meter resolution is also added for rectification and image sharpening. Landsat 7 provides data with a swath width of 185 km and a repeat coverage interval of 16 days. For this study, ETM+ multispectral data for both study areas in the UK and Spain acquired on 19 June 2000 and 28 June 2000 respectively, are used. Panchromatic data for the UK study area is used to study its influence on classification accuracy in combination with multispectral data.

[2] Accounting for the spectral shift induced by the slight difference in incidence angle between two SLC images. After this processing only the range spectrum interval common to the two SLC images is retained.

[3] The distance between the satellite on the first pass and second pass should not be too large. As this distance increases, the coherence is increasingly lost. The loss of coherence in this way is called baseline decorrelation.

Table 4. 2. Landsat 7 ETM+ data characteristics.

Band number	Spectral range (microns)	Ground resolution (m)
1	0.450 - 0.515	30
2	0.525 - 0.605	30
3	0.630 - 0.690	30
4	0.750 - 0.900	30
5	1.550 - 1.750	30
6	10.40 - 12.50	60
7	2.090 - 2.350	30
Panchromatic	0.520 - 0.900	15

4.7 DAIS hyperspectral data

The DAIS (Digital Airborne Imaging Spectrometer) sensor is a new generation hyperspectral sensor, designed by the Geophysical Environmental Research Corporation (GER) and funded by the European Union (EU). The development was initiated in 1993 after European Remote Sensing Capabilities (EARSEC) and European Commission (EC) decided to fund and support the development of an imaging spectrometer. The sensor is operated by the German Space Agency or German Aerospace Research Establishment, which is also known as the German Aerospace Centre (DLR) since 1995 (Strobl and Zhukov 1998). Between 1996 to 1999, the Large-Scale Facility was developed. In the framework of the DAIS Large-Scale Facility, DLR operates its Digital Airborne Imaging Spectrometer (DAIS 7915) on board a DO-228 aircraft**.** It is a 79 channel imaging spectrometer (Table 4.2) which measures energy in the range from visible to the thermal infrared wavelengths. The spatial resolution of the sensor can vary from 5 to 20 m, depending on the altitude of the aircraft. The DAIS is a whisk broom scanning instrument with an optomechanical scanner. The scanning principle is of Kennedy type with a four-sided rotating polygon mirror. The advantages of this technique are mainly the solely reflective optics, the large aperture realisable and the high scan efficiency. These advantages are counterweighted by the high susceptibility to produce striping (Strobl et al. 1997) and the presence of intrinsic background signals ((Strobl and Zhukov 1998).

Table 4. 3. The DAIS 7915 system specifications.

Spectrometer	Bands	Wavelength range (micrometer)
VIS/NIR	32	0.50 - 1.05
SWIR I	8	1.50 - 1.80
SWIR II	32	1.90 - 2.50
MIR	1	3.00 - 5.00
TIR	6	8.70 - 12.50

The DAIS data show moderate to severe striping problems in the optical infrared region between bands 41 and 72. Initially, the first 72 bands in the wavelength range 0.4 µm to 2.5 µm were selected. All 72 bands were visually examined to determine the severity of striping. Seven bands with very severe striping (bands 41, 42 and 68 to 72) were removed from further study. The striping in the remaining bands was removed by automatically enhancing the Fourier transform of the image (Cannon et al., 1983; Srinivasan et al., 1988). The input image is first divided into overlapping 128-by-128-pixel blocks. The Fourier transform of each block is calculated and the log-magnitudes of each FFT block are averaged. The averaging removes all frequency domain quantities except those which are present in each block; i.e., some sort of periodic interference. The average power spectrum is then used as a filter to adjust the FFT of the entire image. When the inverse Fourier transform is performed, the result is an image with periodic noise eliminated or significantly reduced.

4.8 Conclusion

This chapter gives a brief introduction to the data used for this study. Interferometric SAR and the way interferometric coherence is calculated by using the phase information in the radar return is discussed in detail. The factors affecting the coherence are also discussed because - as mentioned in this chapter - coherence is a by-product of SAR interferometry and it very important to know these factors before selecting the Single Look Complex images to generate coherence maps.

Some details of ETM+ and DAIS hypespectral data as well as the problems of striping in DAIS data and the method used to remove these striping using Fourier transformation are also discussed.

Chapter 5

Crop classification using decision tree and support vector machine classifiers

5.1. Decision tree classifiers

5.1.1 Introduction

The effective management and use of land resources requires knowledge of the properties and spatial distribution of these resources. The rapid evolution and increasing number of applications of remote sensing methods in the last 20 years shows that such methods are becoming more widely accepted for the purposes of terrestrial resource survey, especially for the observation of land cover that comprises the base for development projects. The cost of surveys using remote sensing is less than that of ground-based methods. Other advantages include large area of coverage under the same atmospheric conditions, and repeatability. Multispectral and multitemporal properties are of great importance to land cover studies. Nowadays, satellite products are widely used for the study and classification of land cover, using data from the Landsat, SPOT, ERS and IRS systems.

Accurate classification of terrain from remotely sensed data is essential, especially for agricultural and forest monitoring, ecological monitoring of vegetation communities, land cover mapping and monitoring, and many other similar applications. Much work related to the classification of land use/land cover categories using satellite data is reported in the literature. To achieve an accurate classification of terrain, an image at a suitable resolution for the terrain needs to be acquired first, and then the characteristics of each small segment of the image must be classified accurately. A number of different types of classifiers are now in routine use in remote sensing. The classification methodology implemented in remote sensing has so far used statistical-based approaches, such as the maximum likelihood classifier, unsupervised classifiers such as the ISODATA clustering algorithm, and neural network classifiers, which offer a non-parametric classification approach. Statistical classifiers basically depend on some pre-defined data model (e.g. Gaussian normal distribution), and, therefore, the performance of these classifiers will depend on how well the data match the pre-defined model. The performance of these classifiers can be good if the distribution of input data are approximately normal. For clustering algorithms, knowledge of the area is very important because these classifiers basically depend on input from the analyst. Within the last ten years, neural classifiers have been extensively tested by the remote sensing community (Benediktsson et al., 1990; Civco, 1991; Heermann and Khazenie, 1992; Foody, 1995(a)(b)) due to their non-parametric nature (independence of frequency distribution), ability to handle data acquired at different levels of measurement, precision, and - once trained - rapid data processing. Although neural networks may generally be used to classify data at least as accurately as statistical classification approaches, there are a range of factors that limits their use (Wilkinson, 1997). Some of these factors are discussed in section 2.3.4.3. Perhaps one of the most important problems is that classification is highly subjective (Johnston, 1968). Despite the apparent objectivity of the method, the analyst has control over a range of network parameters that influences network performance and, even if these parameters are selected judiciously, there is no guarantee that the neural network will provide an acceptable optimal solution.

Decision tree classification techniques have been used successfully for a wide range of classification problems but have not been tested in detail by the remote sensing community (Safavian and Landgrebe, 1991). These techniques have substantial advantages for remote sensing classification problems because of their flexibility, nonparametric nature, and ability to handle nonlinear relations between features and classes. Just like other classification algorithms, the accuracy of a classification produced by a decision tree classifier can be a function of a number of factors, such as size and composition of the training set, attribute selection methods, various pruning methods, and boosting. So far, few studies have been carried out to study the effects of these factors. Friedl et al. (1999) and Muchoney et al. (2000) studied the effect of boosting of classifications using decision trees on land cover classification accuracy. No study in remote sensing has tried to assess the effects of training data size, various pruning methods, and attribute selection measures on land cover classification accuracy. Studies carried out by Brieman et. al., (1984) and Mingers (1989 a) suggest that the pruning method affects the classification accuracy, whatever may be the attribute selection measure. Oates and Jenson (1997) suggest that increasing the number of training data only affects the size of the tree but has a little affect on the classification accuracy.

This chapter presents an investigation into the effects of these factors on the accuracy of crop classification using decision tree classifiers. Besides decision tree classifier, maximum likelihood and neural classifiers have been used for comparison, because these classifiers have already been used in numbers of studies and give acceptable results.

5.1. 2 Study area

The study area selected is an agricultural area located near the town of Littleport in Cambridgeshire, in the eastern part of England. ETM+ data acquired on 19 June 2000 are used. The classification problem involved the identification of seven land cover types, namely, wheat, potato, sugar beet, onion, peas, lettuce and beans that cover the bulk of the area of interest.

The ERDAS Imagine image processing software (version 8.4) was used to register the images to the Ordnance Survey of Great Britain's National Grid by applying a linear transformation. The RMSE (Root Mean Square Error) values estimated for image transformations were less than one pixel. An area of 307-pixel (columns) by 330-pixel (rows) covering the area of interest was then extracted for further analyses.

For this study field data for the relevant crops were collected from farmers and their representative agencies, and other areas were surveyed on the ground. The field boundaries visible on the multispectral image were then digitised using Arc Info software. A polygon file was created by applying a buffering operation of one pixel width to remove the boundary pixels during the classification process and each polygon is assigned a label corresponding to the crop it contained.

Finally a ground reference image is generated by using the polygon file (Figure 5.1.1).

5.1.3 Methods

A series of classifications was performed in order to evaluate the effects of training set size, attribute selection measure, pruning methods and boosting on the accuracy of the output from a decision tree classifier. To study the effects of various attribute selection measures, error based pruning was used while for the purposes of studying the effects of pruning methods on classification accuracy, the gain ratio was used as a selection measure. The effects of training set size were evaluated using two different decision tree classifiers, See5.0, a univariate classifier, and QUEST (Loh and Shih, 1997), a multivarite decision tree classifier.

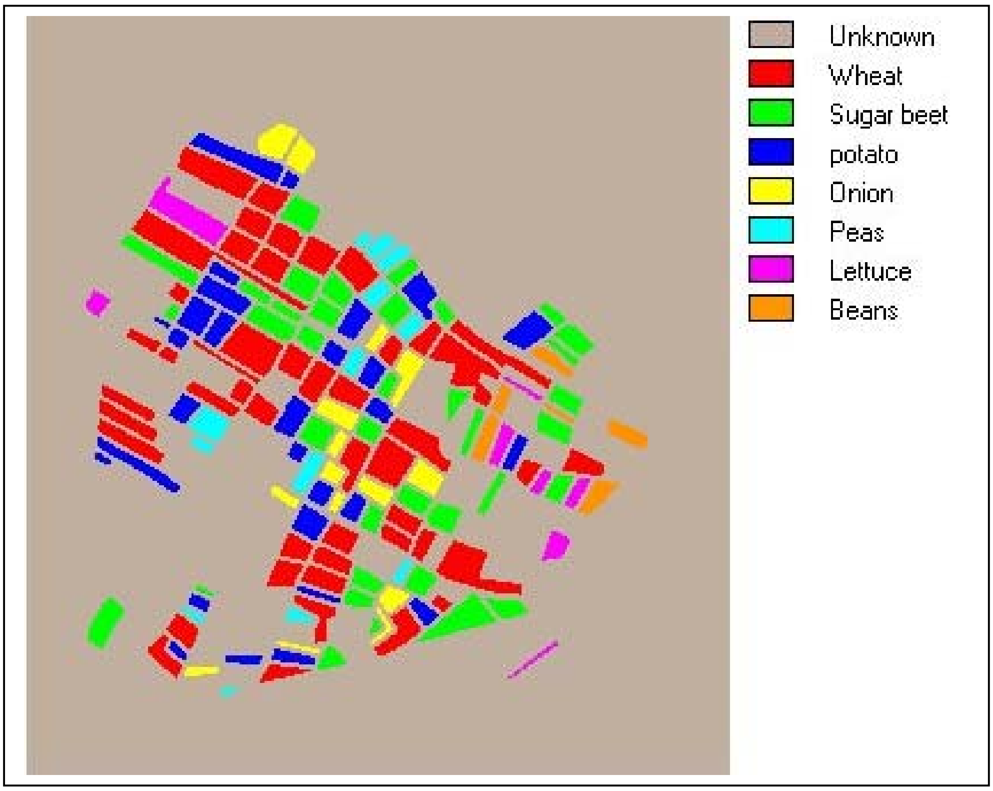

Figure 5.1.1. The ground reference image of the ETM+ data.

5.1.3.1 Training set size

The characteristics of the data used to train a supervised classification have a considerable influence on the quality of the resulting classification (Campbell, 1981, Labovitz, 1986). It is essential that the training data provide a representative description of each class. For the maximum likelihood classifier, a key requirement is to have the training data size for each class equal to from 10-30 times the number of features (Mather, 1999). The required training set size may therefore be large, and acquiring such training sets may be difficult where a large number of classes is involved or utilising data acquired in many wavebands. Consequently, many investigations have been based on a sample size that is less than the generally accepted guidelines and thus the information content of remotely sensed data may not have been fully exploited. The lack of distributional assumptions makes neural classifiers an attractive alternative to the conventional statistical techniques. It has been proposed that neural network classification can be performed successfully using smaller training data sets (Hepner et al., 1990; Foody et al., 1995 (b)). Further investigations into the effects of training set characteristics on the performance on neural network classification have revealed that the training set size has a major effects on the classification accuracy (Foody et al., 1995 (b); Foody and Arora, 1997; Kavazoglu, 2001).

So far few studies (Huang et al., 2002) have discussed the effects of training set size on classification of remote sensing data using decision tree classifiers. It is therefore important to investigate the effect of training set size on these classifiers for crop classification problems. For this study, seven categories of training set size were formed. Each category contains randomly selected pixels representative of each class. The training sets contained 700, 1050, 1400, 1750, 2100, 2450 and 2700 pixels in total, respectively and a total of 2037 pixels was used for testing the classifier. Figure 5.1.2 shows the variation of accuracy with increase in training set using a univariate decision tree classifier.

For each of the training data sets a classification was performed and a confusion matrix was generated to calculate the overall accuracy and the Kappa coefficient. Comparing the classification accuracies obtained from different training sets revealed that the rate of increase in classification accuracy with increasing training set size is linear up to fifth data set (300 pixels per class). As the training set size increases from 700 to 2100 pixels (100 per class to 300 pixels per class), there is a marked increase in overall classification accuracy ranging from 78.3 to 84.1%

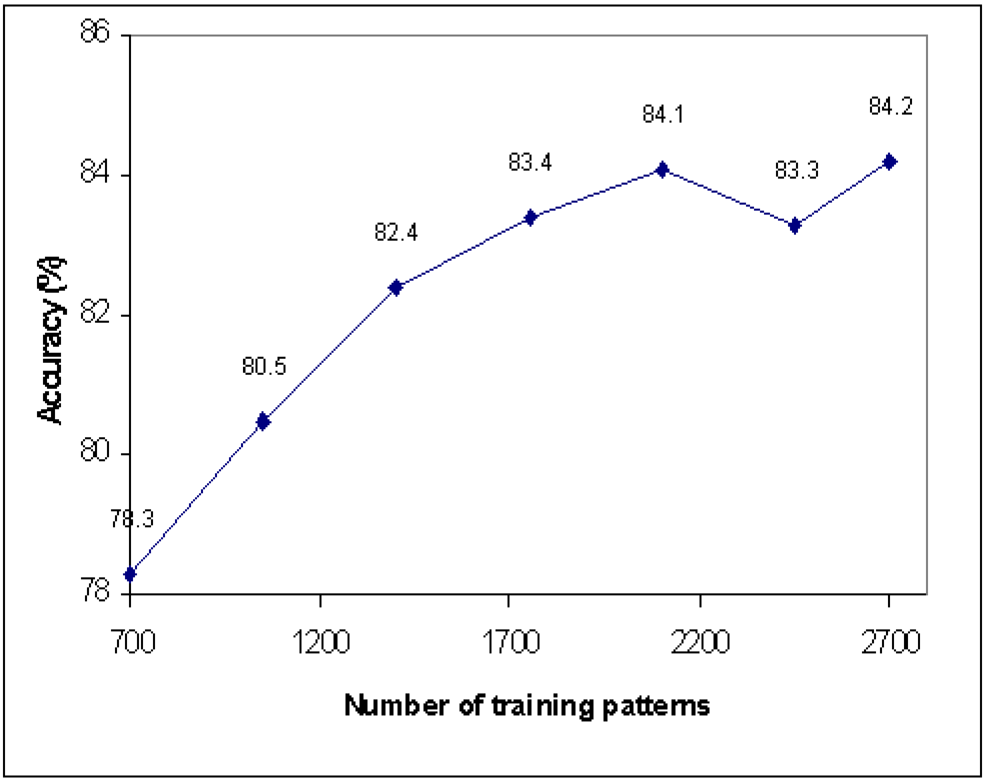

Figure 5.1.2. Variation of classification accuracy with increasing number of training patterns using a univariate decision tree classifier.

and the Kappa values increase from 0.746 to 0.815. However, further increases in training set size, using the sixth and seventh data sets , produced a lesser increase in classification accuracy and even shows a slight decrease in classification accuracy with the sixth data set (using 2450 pixels for all classes). These results indicate that the accuracy of a univariate decision tree classification increases as the size of the training set is increased but suggests that there is no requirement of very large training sets to be used. These results do not concur with the study carried out by Oates and Jenson (1997) in that the rate of increase in classification accuracy was found to be independent of training set size.

A second study was carried out to study the behaviour of a multivariate decision tree classifier ((Figure 5.1.3) with increasing number of training patterns using the same set of training and test data as were used to test the univariate decision tree classifier. It was concluded that classification accuracy increases with the increase in training set size and this increase is almost linear up to fourth data set (100 pixels per class to 250 pixels per class). Accuracy then starts to fall with the fifth and sixth data sets but rises again so that the highest classification accuracy is achieved by the seventh data set. These results suggest that classification accuracy increases with the size of the training set, but only up to a point.

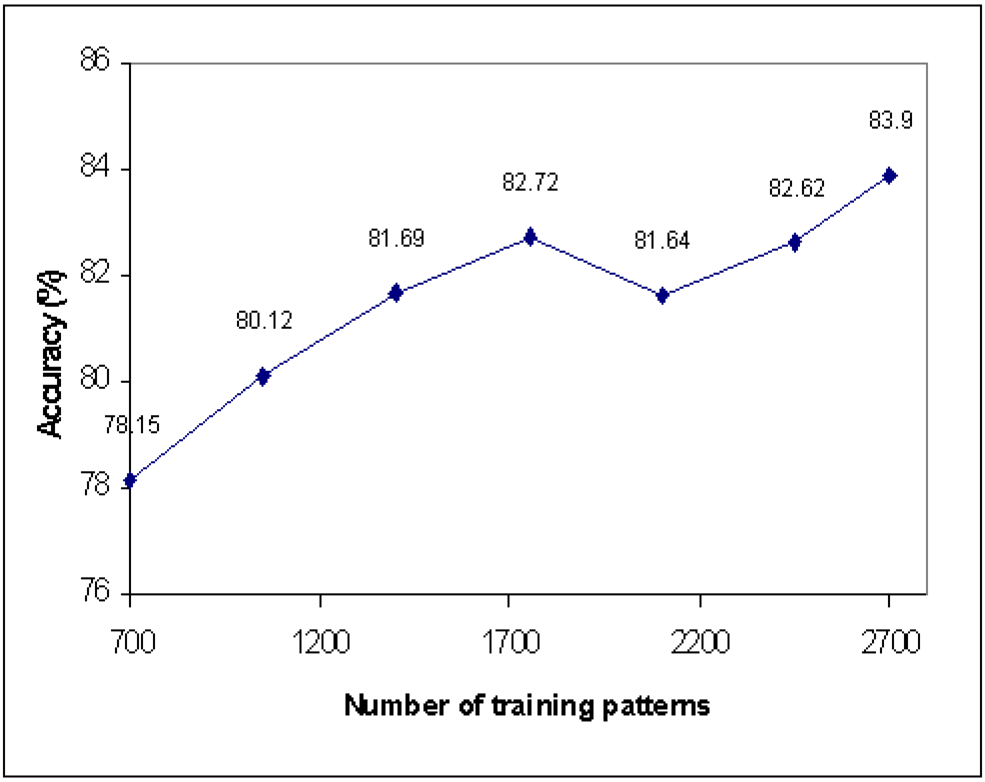

Figure 5.1.3. Variation of classification accuracy with increasing number of training patterns using mulivariate decision tree classifier.

The behaviour of the multivariate classifier was found to be somewhat unpredictable as the training pattern increases beyond a certain limit. It is evident also that the performance of the multivariate classifier is no better than the univariate classifier for this data set. As the training time is always greater with a multivariate decision tree classifier, it is suggested that the use of univariate decision tree classifiers may be adequate for this type of data.

5.1.3.2 Attribute selection measure

It is reasonable to choose the attribute that best divides the data into their classes, and then partition the data according to the value of that attribute. At each node in the development of a decision tree there will be a set of data and a number of attributes available to classify the data. One selects the best attribute for splitting by seeing how well each one separates the data into the various classes. A number of these splitting measures have been proposed by various authors in the literature and are discussed in detail in section 3.4.2.1. The purpose of this section is to examine the various attribute selection measures in terms of comparative performance for land cover classification studies. Earlier studies carried out by Breiman et al. (1984) and Mingers (1989 b) suggest that the predictive accuracy of decision trees is not sensitive to the goodness of split measure or attribute selection measures. For the present study, a univariate decision tree classifier with error-based pruning and four different attribute selection measures is used. A total of 2700 patterns for training and 2037 for testing were used for this study (Figure 5.1.4).

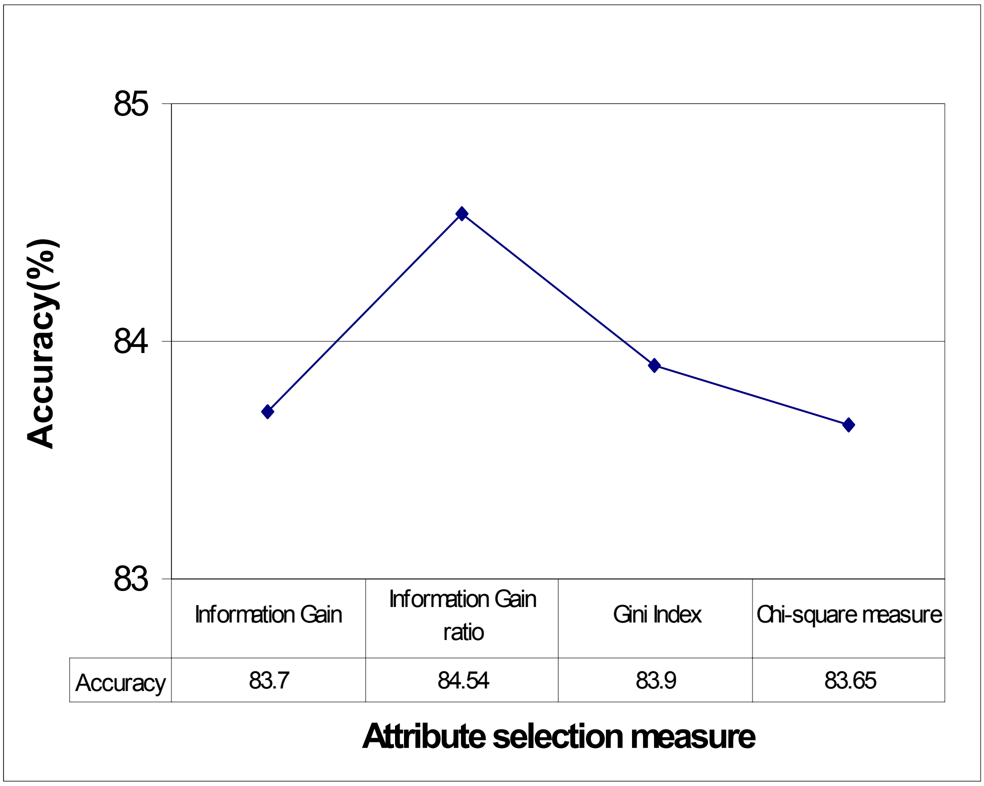

Figure 5.1.4. Variation of accuracy with different attribute selection measures.

Figure 5.1.4 essentially confirms the findings of Breiman et al. (1984) and Mingers (1989 b) that classification accuracy is not seriously affected by the choice of attribute selection measure, and shows that this conclusion applies to remote sensing data also. Except for the information gain ratio, the accuracy obtained with all four selection measure is almost the same, and the increase in accuracy resulting from the use of the information gain ratio is less than 1%. It is therefore concluded that the selection measure does not affect the predictive accuracy of the decision tree.

5.1.3.3 Pruning methods

Studies carried out by the machine learning community and described in section 5.1.3.2 show that overall accuracy of a decision tree classifier on unseen data is not sensitive to the goodness of the split. It is further suggested that the predictive accuracy of the decision tree classifier depends on the pruning methods used in the design of the tree. This section examines the effect of various pruning methods on classification accuracy. Five different pruning methods are used with the information gain ratio as the attribute selection measure in a univariate decision tree classifer (C4.5). The pruning methods employed are: Reduced Error Pruning (REP), Pessimistic Error Pruning (PEP) Error-Based Pruning (EBP) proposed by Quinlan (1987,1993); Critical Value Pruning (CVP) proposed by Mingers (1989 a); and Cost-Complexity Pruning (CCP) proposed by Brieman et al. (1984). Figure 5.1.5 show the variation in classification accuracy with respect to the different pruning methods used.

As suggested by Figure 5.1.5, each of the five pruning methods produces a different classification accuracy. The performance of the REP method is worst of all the pruning methods employed in this study. The reason for this could be the requirement of separate data set for pruning, a conclusion also suggested by Esposito et al. (1997). Pessimistic error pruning gives the highest accuracy of 82.9% as compared to other four pruning methods but the study carried out by Esposito et al. (1997) suggests that the introduction of the continuity correction (section 3.8.3) in the estimation of error rate has no theoretical justification and such a factor is improperly compared to an error rate, which may lead to either underpruning or overpruning of the tree. The performance of CVP is affected by the choice of the critical value set to prune a tree. CCP uses a separate data set or a *cross validation* approach for pruning, while EBP uses training data for pruning the tree. These results suggests that the choice of pruning method is important in the design of a decision tree classifier. Error-based pruning, which gives an accuracy of 82.8%, is used in this research for further studies.

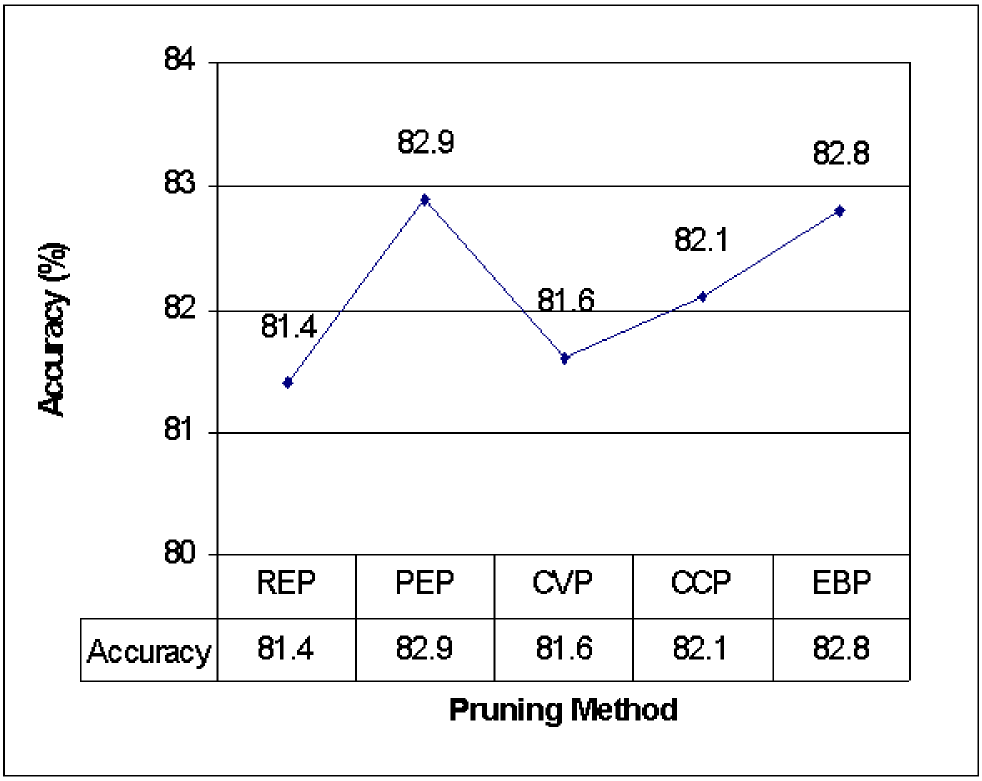

	REP	PEP	CVP	CCP	EBP
Accuracy	81.4	82.9	81.6	82.1	82.8

Figure 5.1.5. Variation of classification accuracy with different pruning methods.

5.1.3.4 Boosting

Classification accuracies and Kappa values obtained from unboosted and boosted decision trees, estimated by using 2700 training and 2037 test data, are shown in Table 5.1.1. The boosted decision tree classifications were estimated using

Table 5.1.1. Results from boosted and unboosted decision tree.

	Accuracy (%)	Kappa value
Unboosted decision tree	84.24	0.816
Boosted decision tree	88.46	0.865

fourteen iterations of the base decision tree algorithm. In this study, different numbers of boosting iterations varying from 2 to 20 were used to see how variation in the number of iterations affects accuracy. It was found that little change in accuracy is gained by performing different boosting runs after fourteen iterations (Figure 5.1.6). These results confirm that the degree of accuracy improvement achieved through the use of boosting starts to stabilise after eight iterations and results indicates that relatively little increase in accuracy is

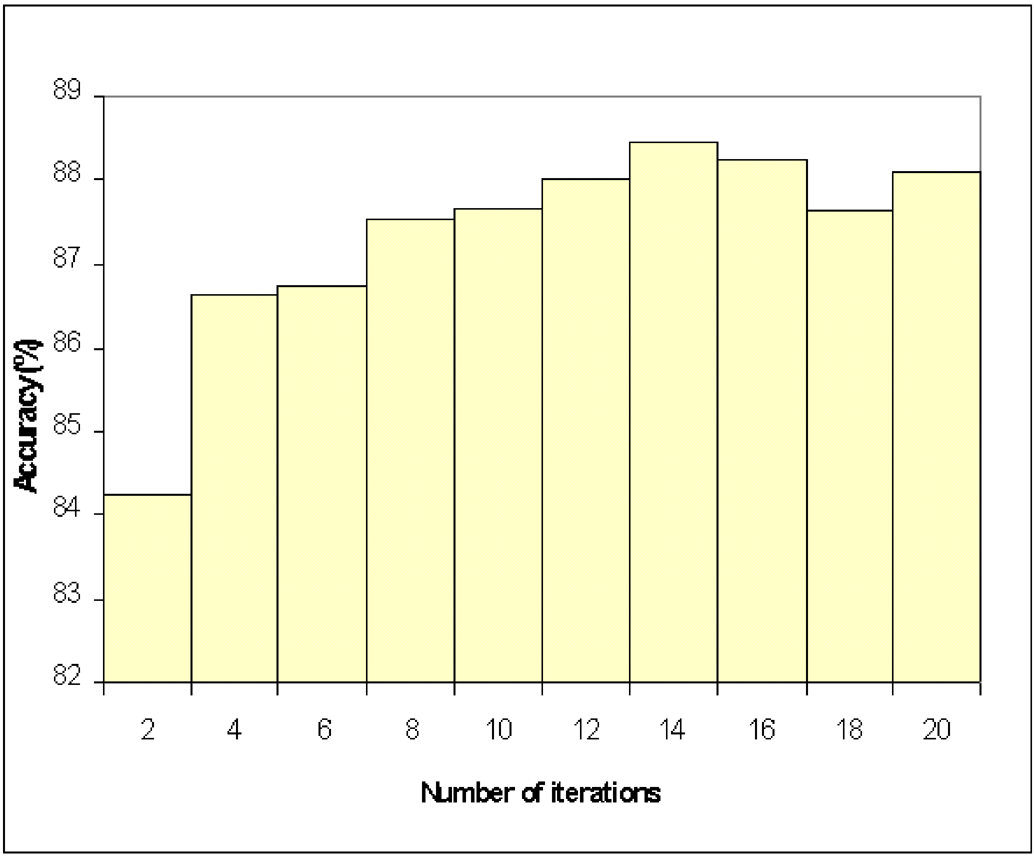

Figure 5.1.6. Classification accuracies for boosted decision trees for varying number of boosting iterations.

gained beyond the twelfth iterations. This result suggests that ten to fifteen boosting iterations is enough to achieve the best attainable accuracy for this type of data. The result also concurs with those studies carried out using non-remote sensing data. Quinlan (1996) concludes that about ten iterations provide the maximum improvement in classification accuracy, and that little is gained by performing additional boosting runs.

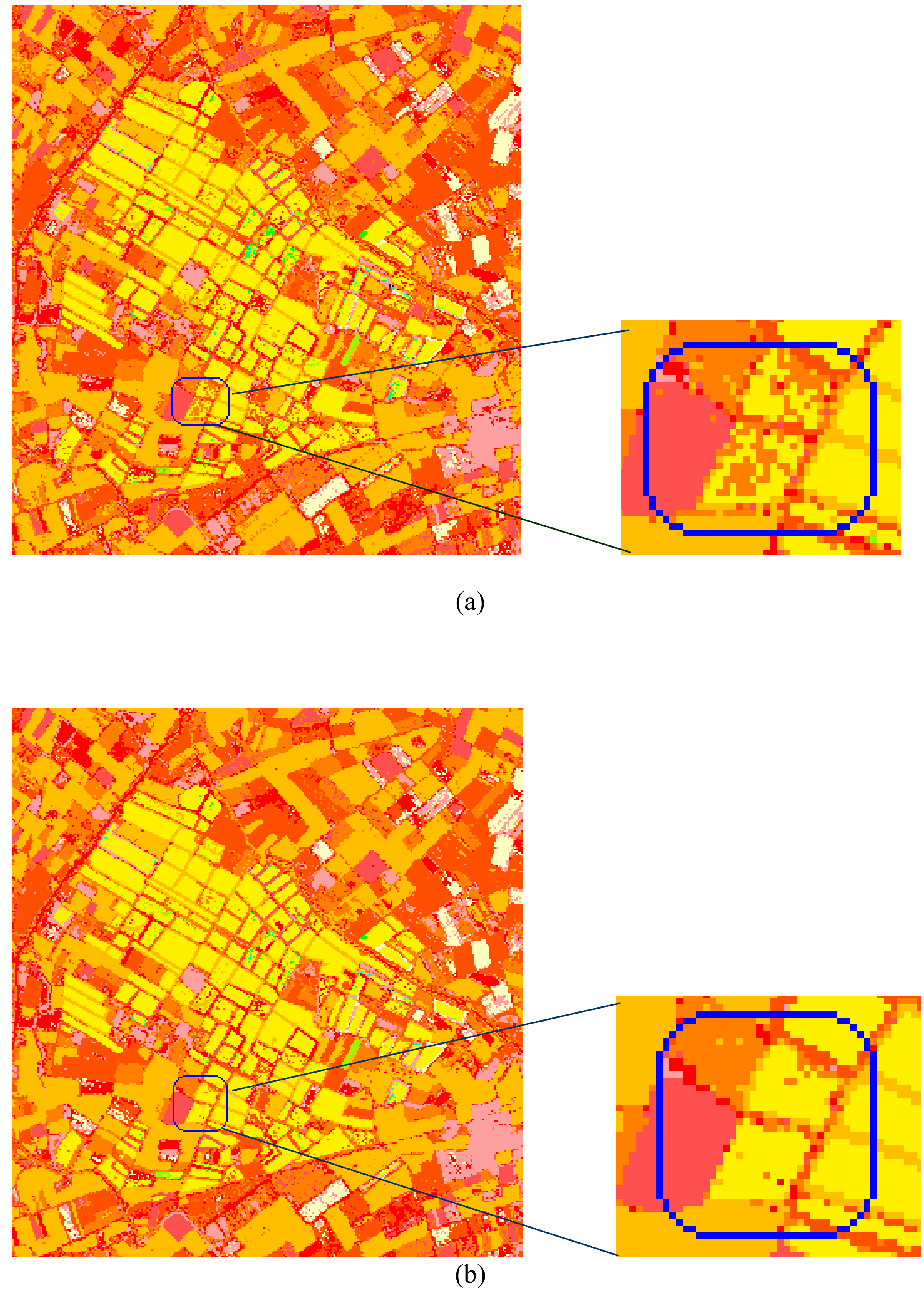

(a)

(b)

Figure 5.1.7. Difference of classified images with ground reference image (a) unboosted decision tree classifier (b) boosted decision tree classifier. Visual comparison of individual fields shows that within-field variation is reduced by boosting.

It is apparent that classification accuracy increases by more than four percent following boosting (confusion matrices are listed in Appendix A). Although 4% may appear to be a small increase, it should be borne in mind that even small percentage increases are difficult to generate when the overall classification accuracy level exceeds 80%. We can, therefore, conclude that boosting is a useful technique for improving the performance of decision tree classifiers. As can be seen from Figure 5.1.7(a), there are number of incorrectly classified pixels in several fields. After boosting the classifier, the number of incorrectly classified pixels reduces significantly (Figure 5.1.7 (b)), as this boosting algorithm assigns a weight to each training observation and those observations that were misclassified in the previous iteration are assigned a higher weight value in the next iteration. Thus, boosting forces the classification algorithm to concentrate on those observations that are more difficult to classify.

5.1.4 Results with ML and neural classifiers

In order to compare the results obtained from decision tree classifier and avoid the situation in which the observed results may be classifier dependent, the data set used in the decision tree experiments was inputted to both maximum likelihood and neural network classifiers. For this study, a standard back-propagation neural classifier with one hidden layer having twenty six nodes was used. Table 5.1.2 and Figure 5.1.8 show the results obtained by using the same number of training and test data, as used with decision tree classifier (confusion matrices are listed in appendix A).

Table 5.1.2. Results from Maximum likelihood and neural network classifier.

Classifier	Accuracy (%)	Kappa value
Maximum Likelihood	82.9	0.801
Neural network	85.1	0.829

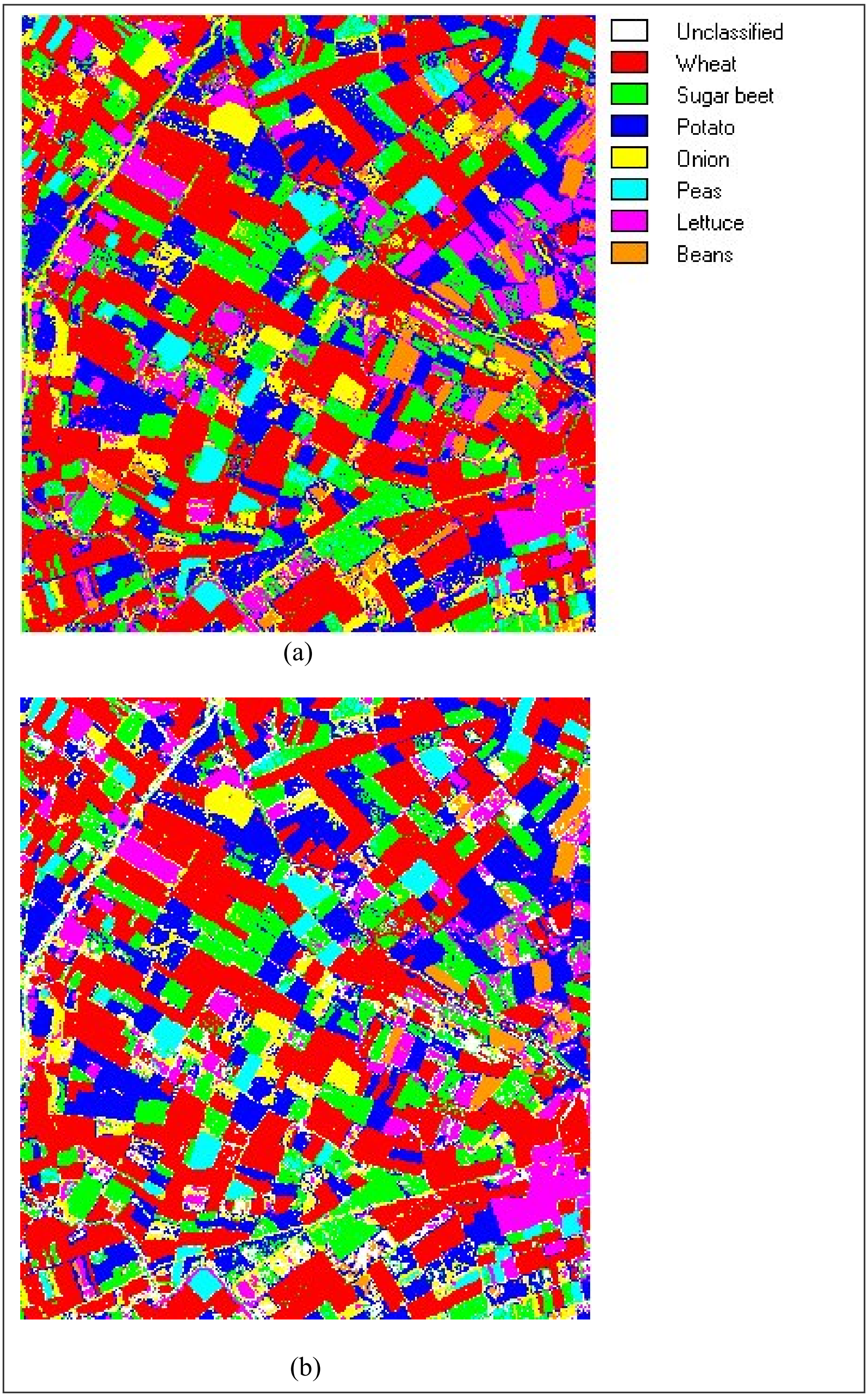

Figure 5.1.8. Classified images of the study area using (a) Maximum Likelihood classifier and (b) Neural network classifier. The colour palette is the same as in Figure 5.1.8 (a).

Results shown in Tables 5.1.1 and 5.1.2 shows that the decision tree classifier performs better than a maximum-likelihood classifier, and its performance is comparable to a neural network, even without boosting. As suggested by Table 5.1.1, after boosting, the performance of the decision tree classifier improves by about 3.26 percent as compared to the neural network classifier. Thus, these results indicates that the boosted decision tree classifier performs better than the neural network classifier. As discussed in section 2.3.4.3, a number of factors affect the classification accuracy achievable by a neural network classifier (Kavzoglu, 2001). The use of a decision tree classifier requires only the choice of attribute selection measure and pruning method. This study suggests that only the pruning method affects the predictive accuracy of a decision tree classifier, not the attribute selection measure.

Another study was carried out to compare the training time of the decision tree and neural classifier using the same training data. All other factors affecting the neural network classifier were set as recommended by Kavzoglu (2001). The training time for the neural network classifier was about 58 CPU minutes on a Sun machine as compared to 0.7 CPU second using a personal computer with a Pentium II processor by a decision tree without boosting. Even after using boosting the decision tree classifier took about 7.1 CPU seconds for 14 iterations, which is still far less than the time taken by a neural network classifier.

5.1.5 Inclusion of panchromatic band and its texture

Further studies were carried out to include information derived from the ETM+ panchromatic band with multispectral data for classification. In order to evaluate the performance of different data sets, a statistical separability measure called the Jeffreys-Matusita distance (JM distance) is used. Signature separability is a measure of the statistical distance between two signatures. Separability can be calculated for any combination of bands that is used in the classification enabling the user to compare the contribution made by each or band combination to the class separability using, the spectral distance between the mean vectors of each pair of signatures. If the spectral distance between two samples is not significant for any pair of bands, then signatures may not be distinct enough to produce a successful classification.

Generally, three different formulae are used for calculating separability. These three formulae take into account the covariances of the signatures of the bands being compared as well as the mean vectors of the signatures. The first separability index is called divergence and is denoted by D_{ij}. It is derived from the likelihood ratio of any pair of classes i and j. For multivariate Gaussian distributions, D_{ij} for classes i , j is defined by:

$$D_{ij} = \frac{1}{2}\mathrm{tr}((C_i - C_j).(C_j^{-1} - C_i^{-1})) + \frac{1}{2}\mathrm{tr}((C_i^{-1} + C_j^{-1}).(\mu_i - \mu_j).(\mu_i - \mu_j)^T) \qquad (5.1.1)$$

where tr denotes the trace of a matrix, C is the sample class covariance matrix, μ is the class mean vector, and T denotes the transpose of a matrix. The second separability measure is called Transformed Divergence, represented by TD_{ij} and is calculated from

$$TD_{ij} = 2000.[1 - \exp(D_{ij}/8)] \qquad (5.1.2)$$

where D_{ij} is the divergence index. Transformed Divergence gives an exponentially decreasing weight to increasing distance between the classes. The scale of divergence values can range from 0 to 2000. According to Jenson (1996) if the value is more than 1900, then the classes can be separated easily. Between 1700 and 1900, the class separation is fairly good and if this value is below 1700, the class separation is poor.

A third method of computing the separability is to calculate the JM distance between two classes i and j as

$$JM_{ij} = \sqrt{2.\left(1 - \exp^{-\alpha}\right)} \qquad (5.1.3)$$

in which α (the Bhattacharyya distance) is given by

$$\alpha = \frac{1}{8}\left(\mu_i - \mu_j\right)^T \left(\frac{C_i + C_j}{2}\right)^{-1} \left(\mu_i - \mu_j\right) + \frac{1}{2}\ln\left[\frac{\left|(C_i + C_j)/2\right|}{\sqrt{\left|C_i\right| \times \left|C_j\right|}}\right] \qquad (5.1.4)$$

where $|C_i|$ is the determinant of C_i (covariance matrix). The Bhattacharyya distance is widely used as a measure of class separability because of its analytical form and its relation to the Bayes error (obtained from the Bayes classifier designed with an infinite number of training samples). The first terms and the second term represent the class separability due to the mean difference and due to the covariance difference, respectively. Note that the "mean difference" used here is in the sense of the Mahalanobis "distance" rather than the Euclidean distance. JM distance is used in this research to measure how class separability changes with the addition of extra features with ETM+ multispectral data.

Initially a texture measure called *internal texture* was extracted from the panchromatic band in a way to reduce the image to 30m resolution. A program to calculate the difference between the maximum and minimum value in a 2×2 window was used. The movement of the pointer after each iteration is shown in Figure 5.1.9. In this way the image size is reduced from 15m to 30m resolution while simultaneously generating the texture image. The image generated by this procedure is georeferenced to the multispectral image and an area of 307 column and 330 rows was extracted for further study in combination with multispectral

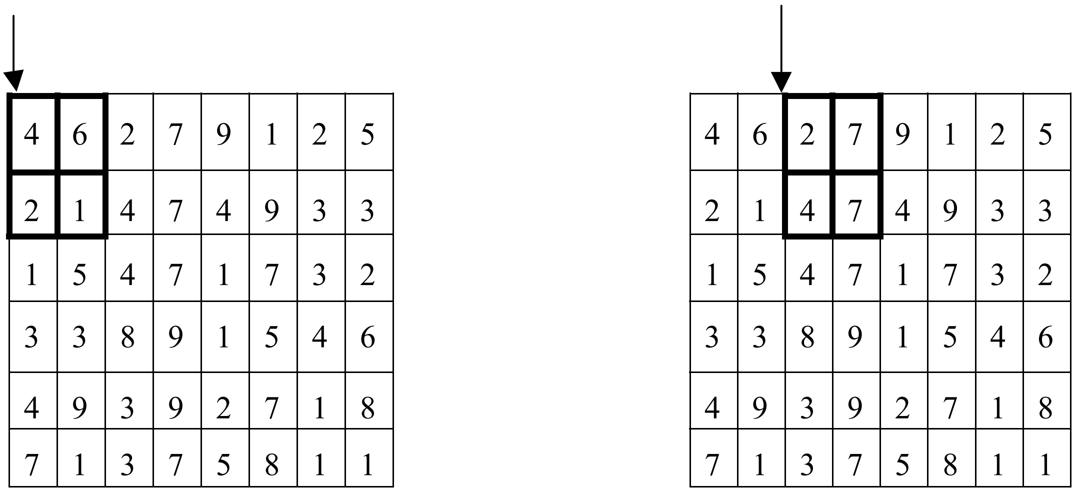

4	6	2	7	9	1	2	5
2	1	4	7	4	9	3	3
1	5	4	7	1	7	3	2
3	3	8	9	1	5	4	6
4	9	3	9	2	7	1	8
7	1	3	7	5	8	1	1

4	6	2	7	9	1	2	5
2	1	4	7	4	9	3	3
1	5	4	7	1	7	3	2
3	3	8	9	1	5	4	6
4	9	3	9	2	7	1	8
7	1	3	7	5	8	1	1

Figure 5.1.9. Movement of pointer to extract internal texture of the panchromatic image.

data. All the three classifiers were used to evaluate the effect of the inclusion of internal texture on classification accuracy (Table 5.1.3).

Comparing the results shown in Table 5.1.3 with those shown in Tables 5.1.1 and 5.1.2 suggests that there is little or no increase (in the case of decision tree classifier this increase is only 0.06%) in classification accuracy with all the three classification systems used in this study, thus indicating that the addition of an internal texture feature derived from the panchromatic band of ETM+ does not help in increasing the classification accuracy. The JM distance for this data set was 1329 as compared to 1320 for ETM+ data alone.

Table 5.1.3. Results obtained by using internal texture of panchromatic band with ETM+ multispectral data.

Classifier	Accuracy (%)	Kappa value
Maximum Likelihood	83.1	0.803
Neural Network	85.4	0.832
Decision Tree	84.3	0.816

Further studies were carried out to include the panchromatic band, internal texture and GLCM features derived from the panchromatic band in combination with ETM+ multispectral data. As the resolution of the ETM+ panchromatic data is 15m, bilinear resampling was used in this study to reduce the resolution to 30m (i.e. the resolution of ETM+ multispectral data). The texture features used for this study were extracted from the 30m resolution resampled panchromatic image. For this study two different data sets were used. These are:

1. Combination of multispectral, panchromatic band and internal texture of panchromatic band referred to as data set 1.

2. Combination of data set 1 and three GLCM based texture features (correlation, entropy, and inverse different moment) of panchromatic band, referred to as data set 2.

Table 5.1.4. JM distance for data set 1 and data set 2.

Data set	JM distance
1	1330
2	1369

Table 5.1.5. Results obtained by using data set 1 (Table 5.1.5 (a)) and data set 2 (Table 5.1.5 (b)).

Table 5.1.5 (a)

Classifier	Accuracy (%)	Kappa value
Maximum Likelihood	82.6	0.798
Neural Network	85.6	0.836
Decision Tree	85.1	0.829

Table 5.1.5(b)

Classifier	Accuracy (%)	Kappa value
Maximum Likelihood	84.8	0.823
Neural Network	87.7	0.858
Decision Tree	86.1	0.838
Decision Tree (boosted)	89.6	0.879

Though the value of the JM distance for the data set 1 is greater than the value obtained from the ETM+ data but the results from Table 5.1.5 (a) suggest that the inclusion of the panchromatic band and internal texture feature with multispectral data does not increase classification accuracy by a large amount and may even result in a poorer performance. For example, the performance of ML classifier decreases by a small amount as compared to the results obtained by using multispectral data alone. Otherwise, the results obtained from the neural and decision tree classifiers improve by about one percent. Further, using data set 2 (Table 5.1.5(b)) gives the highest JM distance of 1369 but the classification accuracies with all the three classification algorithms improve by about 1 to 2.5%, thus suggesting the limited utility of panchromatic data and its texture for land cover classification.

5.1.6 Conclusions

The main objective of the work reported in this section is to assess the utility of decision tree classifiers for land cover classification. The specific objectives are to study the behaviour of decision tree classifiers with changes in training data size, different attribute selection measures, pruning methods, and boosting. The results suggest several main conclusions. First, in spite of being non-parametric in nature, the performance of the decision tree classifier is always affected by the size of the training data set used. This study also concludes that it is the pruning method that has the most significant effect on classification accuracy and not the attribute selection measure, as suggested by some earlier studies. Boosting is found to improve classification accuracy by about 3-4%. We can conclude that boosting is a useful technique and should be used for crop classification problems using remotely sensed data.

Studies carried out using maximum likelihood and neural classifiers for the same data sets used with decision tree classifier show that the decision tree performs better than the maximum likelihood classifier, while the performance of neural classifier is better (but not significant in the statistical sense) than the unboosted decision tree classifier for this type of data in crop classification studies. As suggested by a number of earlier studies (Kavzoglu, 2001; Foody and Arora, 1997), the performance of a neural classifier depends on a number of user-determined factors, and the training time is very large compared to that of the decision tree classifier. Training time increases only slightly if boosting is used. Inclusion of the ETM+ panchromatic band and its texture measures increases the classification accuracy by about 1 to 2.5%.

5.2 Support vector machine classifiers

5.2.1 Introduction

Much research effort in the past ten years has been devoted to analysis of the performance of artificial neural networks, particularly the feed-forward multi-layer perceptron using back-propagation, due to their ability to handle any kind of numerical data, and to their freedom from distributional assumptions (section 2.3.4.3). A number of studies have reported that uses of neural classifiers have problems in setting various parameters during training. The choice of architecture of the network, the sample size for training, choice of learning algorithms, and number of iterations required for training are some of these problems. Within the last few years, another nonparametric classification algorithm - the decision tree classifier (chapter 3) has become more popular, due to its simplicity in use and their performance, which is comparable and even better than neural classifiers. Despite their simplicity in use, decision tree classifiers present some problems which influence classification accuracy (section 3.9 and section 5.1.3).

This section gives the results of another recent development in classification methodology, called *support vector machines* (SVM) using ETM+ data. Some of the factors affecting support vector machines are discussed and the value of some parameters affecting these classifier are suggested for this type of data.

5.2.2 Study area and methods

Details of the study area used in this part of the research are given in section 5.1.2. As the main aim of this study is to compare the performance of decision tree, neural network and SVM classifiers for land cover classification, the training and testing data sets for the SVM classifier are the same as those used for the DT and neural classifiers. To investigate the behaviour of the SVM classifier with the variation in number of training patterns, seven training data set were used (section 5.1.3.1).

5.2.2.1 Effect of kernel choice

As discussed in section 3.12.3, in situations with non-linear decision surfaces, support vector classifiers use a mapping to project the data in a higher dimensional feature space, while to make computation simpler, the concept of the kernel was introduced. A number of kernels are discussed in the literature, but it is difficult to choose one which gives the best generalisation. In this study, five different kernels are used in order to investigate the effect of kernel choice on classification accuracy. Both the chosen kernel type and the values of other parameters associated with these kernels affect the level of classification accuracies. Another factor that affects the level of classification accuracy is the choice of the value of the parameter C (section 3.12.2). After a number of trials, the values of C used with various kernels are given in Table 5.2.1.

This comparison suggests that a value of C within the range 1000 to 5000 is effective for this type of land cover classification study, depending on the type of kernel used. Training time also increases as the value of C rises. The parameter values found to be suitable for the various kernel functions are as follows:

- degree of polynomial = 5 for the polynomial kernel.
- $\gamma = 2$ for the radial basis function.
- b = 0.04 and c = 0.001 for the neural network.

Table 5.2.1. Values of parameter C with different kernels.

Kernel	Parameter C
Polynomial	1000
Radial basis function	5000
Linear splines	10000
Simple dot product	5000
Neural network	5000

The classification accuracies achieved using the above values of C and the user-defined parameters for different kernels are shown in Figure 5.2.1. For a polynomial kernel, increasing the degree of the polynomial increases training time but not the classification accuracy.

Figure 5.2.1 suggests that the radial basis and the linear splines perform equally well and achieve the highest accuracy. The poor performance of the simple dot product kernel function may be due to the fact that decision boundaries between the classes may be non-linear. The reason of poor performance of neural network kernel function may lie in the selection of appropriate values of the user defined parameters, which is a topic that needs further study. The performance of the polynomial function is comparable to that of the radial basis function. A radial basis kernel function is used for the evaluations of SVM in the remainder of this section.

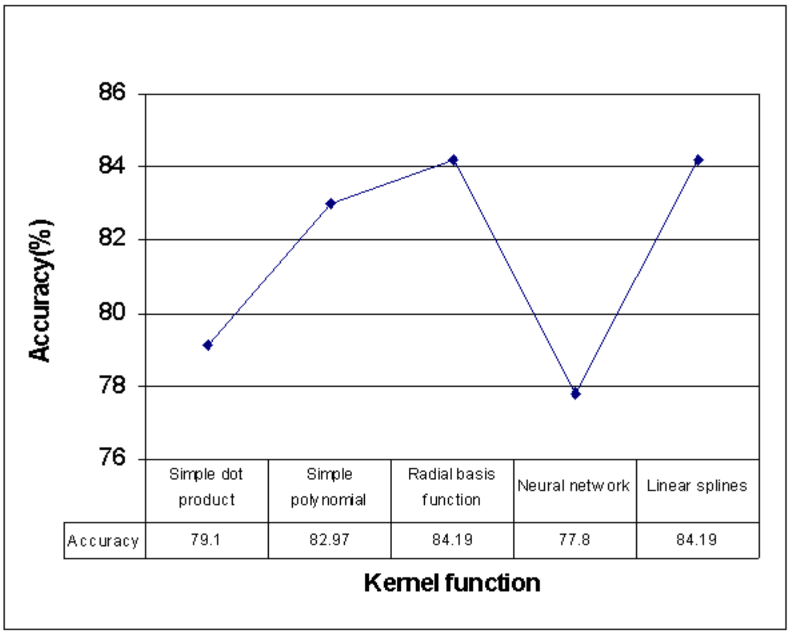

	Simple dot product	Simple polynomial	Radial basis function	Neural network	Linear splines
Accuracy	79.1	82.97	84.19	77.8	84.19

Figure 5.2.1. Variation in classification accuracy with different kernel functions.

5.2.2.2 Training sample size

A support vector machine works on the principle of optimal separation of the training data, if the classes are separable, the optimum solution hyperplane is that which maximally separates the classes. The training of the SVM defines the optimal hyperplanes and, in doing so, selects the data points which lie on or near the class boundary closest to the neighbouring classes. It follows that by using these pixels (the support vectors) for defining the decision surfaces, the use of a very small number of training pixels can provide a good degree of generalisation. To check this deduction, seven data sets containing 700, 1050, 1400, 1750, 2100, 2450 and 2700 training pixels in total, and a set of 2037 pixels was used for testing the results of the SVM classifier. For all these data sets a "one against one" multi-class technique and a radial basis kernel were used in generating SVM. The accuracy of classification obtained using each data set is plotted in Figure 5.2.2 (confusion matrices are listed in appendix B).

Figure 5.2.2 suggests that classification accuracy increases as the number of training patterns increases, thus indicating that SVM-based classification is affected by training data size, in spite of the fact that this classification system uses very few pixels to create decision surfaces. The probable reason for this increase in classification accuracy with increasing number of training patterns could be due to the quality of training pixels used, so that as the number of pixels increases the system finds pixels that define better discriminating surfaces.

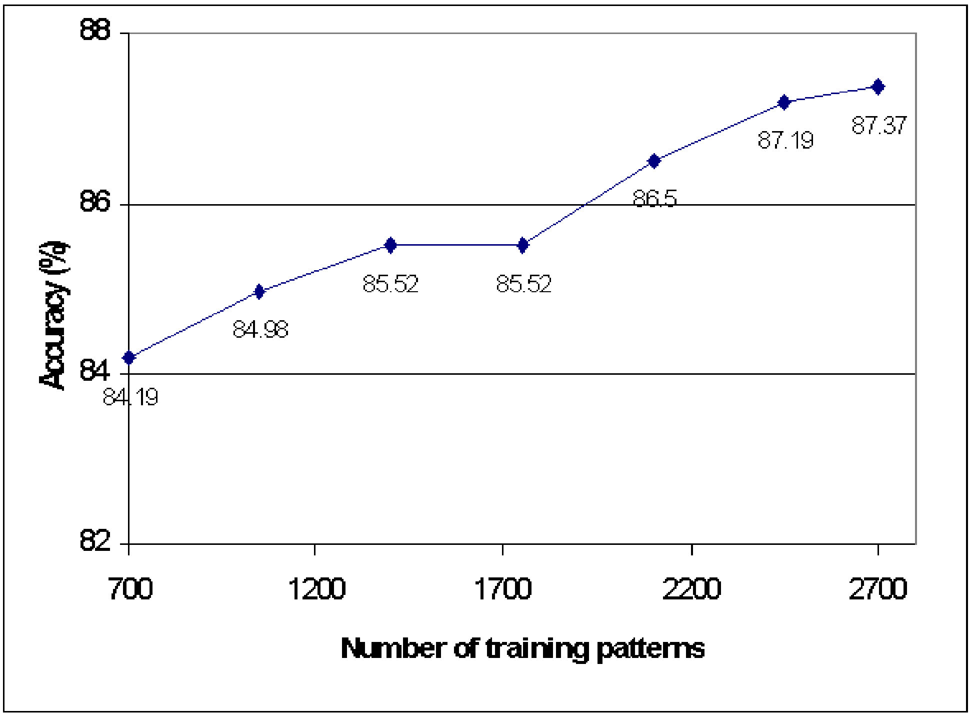

Figure 5.2.2. Variation in classification accuracy with change in training patterns.

5.2.2.3 Use of different multi-class methods

In this part of the study, two methods of generating multi-class support vector machines are discussed, with respect to training time and classification accuracy. Table 5.2.2 gives the classification accuracy as well as the training time taken using SVM classifier from Royal Holloway College, University of London, running on a Sun workstation.

The results shown in the Table 5.2.2 suggest that the time taken by using *one against the rest* method is much higher than the *one against one* technique, thus suggesting the use of *one against one* method for generating multi-class support vector machines. Further, the accuracy obtained by using *one against the rest* method is not as high as with the *one against one* method. One possible reason could be unbalanced training data sizes in two classes while using the *one against the rest* multi-class method and not finding suitable decision boundaries which may affect the performance of classifier and affecting the final classification accuracy.

Further studies carried out using the LIBSVM classifier using a *one against one* multi-class technique suggests that this classifier takes only 0.30 CPU minutes to train the SVM using 2700 training pixels and attains an accuracy of 87.9% accuracy. Figure 5.2.3 shows a SVM classified image of the study area.

Table 5.2.2. Classification accuracy and training time using different SVMs and different multi-class methods.

Multi-class method	Number of training pixels	Accuracy (%)	Training time (CPU minutes)
One against rest	700	76.19	6.09
	2700	79.73	505.27
One against one	700	84.19	0.27
	2700	87.37	21.54

5.2.3 Conclusions

The main objective of this part of the study is to investigate the utility of a support vector machine for crop classification studies. It can be concluded from the results of this study that this algorithm can be very useful in land cover classification. Comparison of results obtained by SVM with the results of other classifiers (Tables 5.1.1 and 5.1.2) suggests that SVM performance is better than all other classifiers, and approaches that of the boosted decision tree classifier. Like neural classifiers, the effective use of an SVM depends on the values of a few user defined parameters. This study suggests values for these parameters for this type of classification problem. The performance of the SVM is also affected by the number of training pixels as well the type of the kernel used. A recent study carried out by Huang et al. (2002) suggests that the training time for a SVM can be very high. This could be due to two reasons: (1) for their study they replicated the sample size of smaller class, thus increasing number of training patterns, and (2) they used a *one against the rest* strategy for generating the SVM, which is not a good choice for multi-class problems.

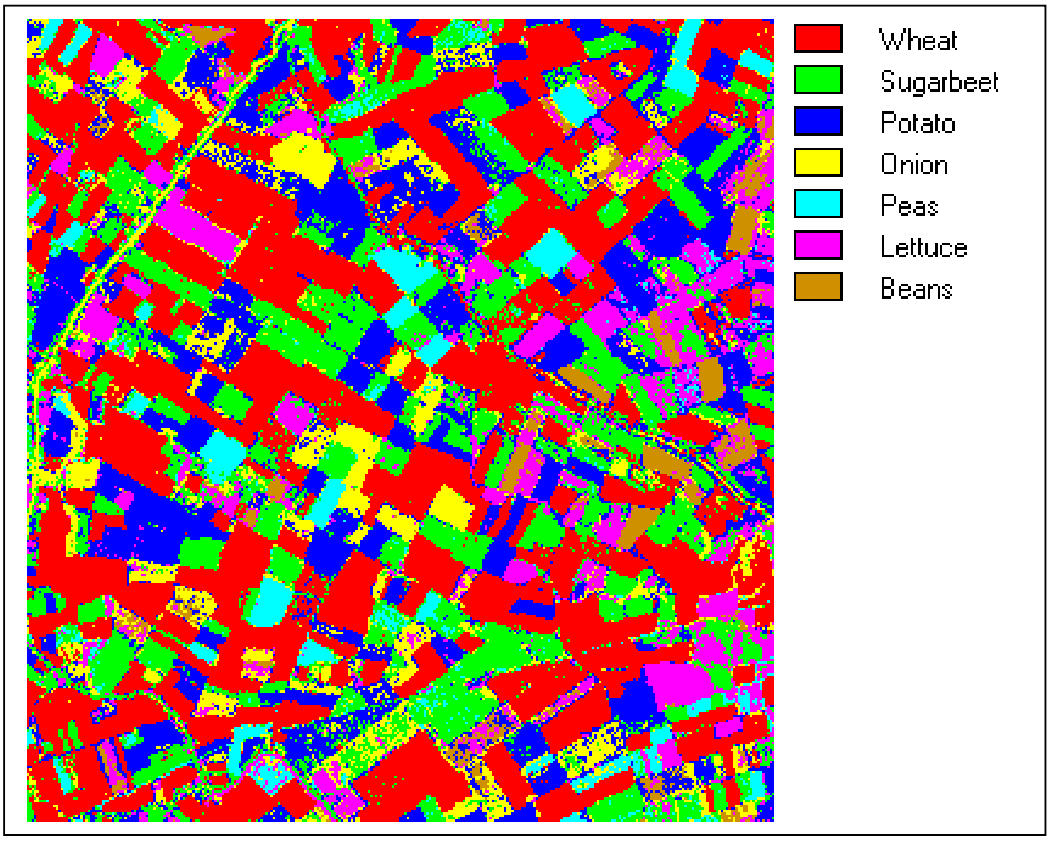

Figure 5.2.3. Classified image of the study area.

This study also suggests that training time taken by SVM generated by using *one against one* technique is far less than that with the *one against the rest* strategy used by Huang et al. (2002). Even the performance of SVM by using *one against the rest* is found to be very poor as compared to that with *one against one* multi-class strategy. Further, a probable reason for the small training time using LIBSVM could be the use of a good optimisation strategy to solve the QP optimisation problem.

1. **Decision tree classifier performance is affected by the choice of pruning method to be used, while the performance of a neural classifier is affected by several user defined parameters.**

2. **Performance of decision tree classifiers, both univariate and multivariate, is affected by number of training patterns used:**

   - Accuracy of a univariate decision tree classifier varies from 78.3% to 84.1% when training data size varies from 100 pixels/class to 300 pixels/class. Further addition of training data has no significant change in classification accuracy.

   - Multivariate decision tree classifier accuracy changes from 78.15 % to 82.72% as data size changes from 100 pixels/class to 250 pixels/class.

   - Univariate decision trees perform as well as or better than the multivariate classifier with this type of data.

3. **Performance of a DT classifier is better than that of a maximum likelihood classifier, while neural classifier performed better than a univariate decision tree classifier.**

4. **Boosting a decision tree gives a significant improvement in classification accuracy as compared to neural classifier.**

5. **Training time of a univariate decision tree classifier is quite small, even after applying boosting, in comparison with neural classifier.**

6. **Performance of SVM is affected by several factors such as:**

- Choice of kernel
- Choice of multi-class method used
- Parameters for a particular kernel
- Parameter C

7. **SVM perform significantly better than decision tree and neural classifier, even with very small training datasets.**

8. **Training time for SVM is small, even comparable with the training time taken by the boosted decision tree classifier, if the *one against one* technique is used to generate multi-class output.**

9. **The *one against the rest* technique is not suitable to generate multi-class outputs.**

Chapter 6

Crop Classification Using INSAR Data

6.1 Introduction

The ERS-1/2 SAR is a coherent sensor measuring both the magnitude and phase of the backscattered signal. It operates at 5.3 GHz, vv-polarisation, at incidence angles between 20 and 26 degrees, with a swath of 100 km and with a repeat cycle of 35 days. Traditionally, only the backscatter intensity was interpreted. Now, by means of SAR interferometry, the phase component has proven to be a very valuable source of information. More recently, it has been demonstrated (Askne and Hagberg, 1993; Wegmueller and Werner, 1994, 1995, 1996, 1997) that the coherence component (which is a measure of accuracy of estimation of interferometric phase) derived by using phase information from an interferometric image pair gives useful information that can be used effectively for land cover classification.

In this chapter, a classification scheme using both intensity and coherence information derived from INSAR data is developed. In order to evaluate the capability of SAR intensity and coherence images to discriminate between agricultural crops, the classification experiments reported in this study are carried out by using statistical, neural and decision tree classifiers. In particular, the usefulness of texture features derived by using GLCM, the MAR model, and fractal geometry from the intensity and coherence images for land cover classification is also studied. The limitations of tandem and 35-day repeat-pass interferometry for this application are also discussed.

6.2 Description of study area

The study area is located near Littleport, Ely Cambridgeshire, in the eastern part of England. This area is close to sea level and the agriculture of the region is characterised by the use of rotational crop planting techniques. Five SLC images, from 2nd May to 20th September 1996, are selected for land cover classification.

Since the main purpose of this study is crop discrimination, it is necessary to ensure that the selected images cover the entire crop growing period, which helps to identify various crops during their growth period. After a detailed study of the cropping pattern of the area, the SLC images listed in Table 4.1 were selected. As mentioned in sections 4.5.2.3 and 4.5.2.4, one coherence and five intensity images and an area of interest covering 286 pixels (columns) and 386 pixels (rows) was used for further studies.

6.3 Ground reference image generation

The purpose of generating a ground reference image is to allow the collection of pixels for training and testing the classifiers. Before creating a ground reference image, field boundaries should first be defined. If no map reference data are available, image segmentation can be used to identify the field boundaries. In this study, the field boundaries were generated through on screen digitisation of images. Reference data for the crop types in the year 1996 were collected from farmers. On the basis of examination of the areas covered by each crop and the geographical scale of the study, seven cover categories were selected. These are: potatoes, sugar beet, wheat, barley, carrot, onions and peas. The field boundaries were digitised using ARC-INFO software, by using a colour composite of all the five intensity images generated by interferometric processing. The field boundary file was transformed from arc into polygon format by applying a buffering operation of 1 pixel width so as to remove the boundary pixels during the classification process. This polygon file is then used to assign a unique label to each of the polygons according to the crop type associated with that parcel. By using the crop map, digital identifiers from “1” to “7” (each number represents a particular class as shown in the Table 6.1) are assigned to the corresponding fields. The digital identifier “0” is assigned to the unknown fields. The final ground reference image is shown in Figure 6.1, which also shows the colours used to represent each crop.

Table 6. 1. Crops being used for classification with digital numbers in reference image.

Digital Number	Crop type
1	Barley
2	Wheat
3	Sugar Beet
4	Potato
5	Onion
6	Peas
7	Carrot

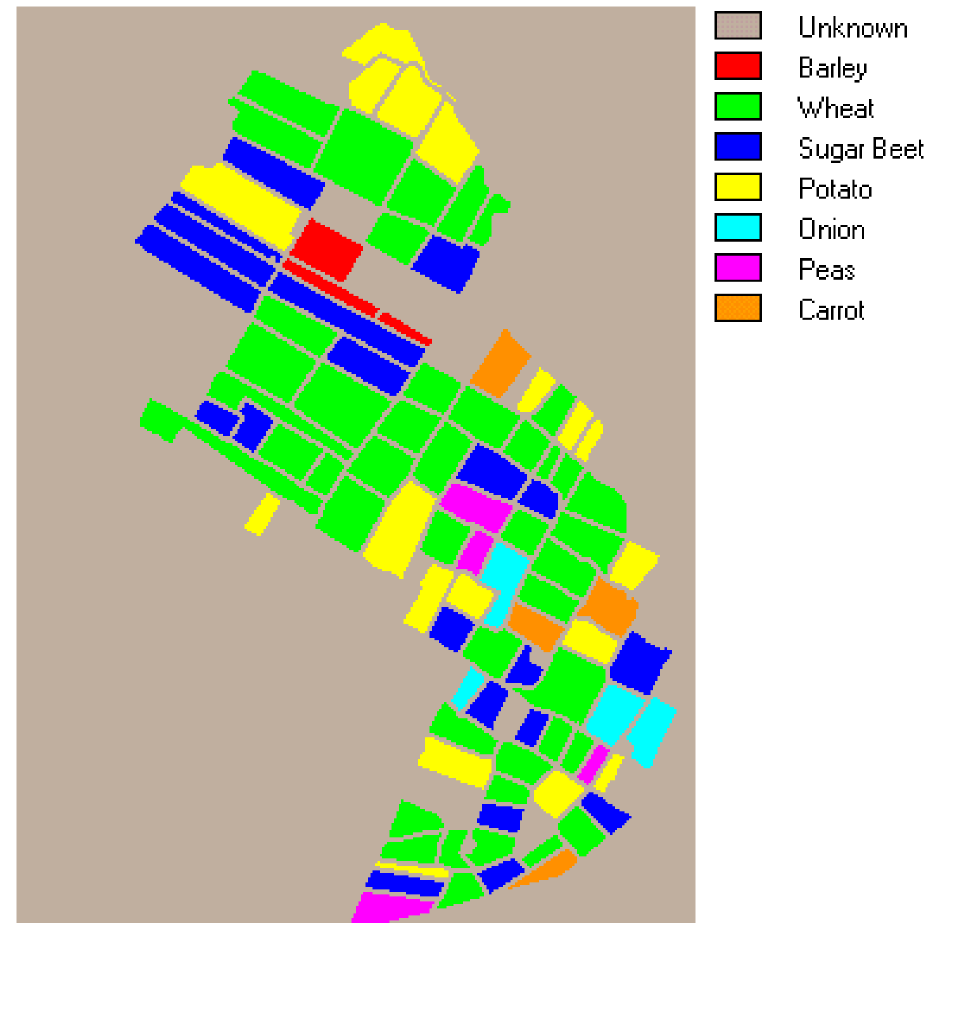

Figure 6. 1. Ground reference image of the study area.

6.4 Feature extraction and selection

Methods to generate features based on combinations or transformations of primary features are called feature extraction methods. Image derived features, such as measures of spatial and spectral features, may provide useful information for classification. Some features obtained by transforming primary features tend to suppress undesirable variability in remote sensing signatures, such as noise, so it is wise to use such features in classification because they allow the classifier to better distinguish spectral classes.

Spectral and spatial features are not independent. They always simultaneously exist in the image, although sometimes one will dominate the other, depending on how fine or how rough the object is. Spectral features describe average tonal variation, whilst spatial features reflect the spatial distribution of tonal variation. Generally the words texture and context are used to represent this form of spatial relationship in tonal variation. Texture features contain information about the spatial distribution of tonal variations within a band while contextual features contain information derived from blocks of image data surrounding the area being analysed.

The concept of tone is based on the varying shades of the grey of the resolution cells making up an image and the texture is concerned with the spatial distribution of grey tones. Texture and tone are not independent concepts; rather, they bear a very close relationship to one another. Texture is a natural property of objects. It contains important information about the structural arrangement of surfaces and their relationship to the surrounding environment.

A number of methods have been developed to deal with spectral and spatial information, in order to achieve improved classification performance. In comparison with tonal measures, the definition of texture features appears more difficult. The main difficulty faced by the researcher is to define a set of meaningful features to characterise texture properties.

Based on the texture descriptors available in the literature, four approaches are used in this study. The first approach uses the grey-level co-occurrence matrix (Haralick et al., 1973). The second approach uses the features derived from local statistics. The third approach is based on the fractal geometry of the image (Sarkar and Chaudhuri, 1994), and the fourth approach is based on the multiplicative autoregressive random field model (Frankot and Chellapa, 1987).

6.5 Grey Level Co-occurrence Matrix (GLCM)

This section describes texture feature extraction based on the Grey Level Co-occurrence Matrix (GLCM), or the grey-tone spatial-dependency matrix. A co-occurrence matrix for an image region contains partial second order statistical information about the image pixel intensities. When generating a co-occurrence matrix, it is assumed that the intensity distribution is in a wide sense stationary over a region of uniform texture. The main concept of the GLCM is that the texture information contained in an image is defined by the adjacency relationships that the grey tones in an image have to one another. In other words, it is assumed that the texture information is specified by values f_{ij}^{d} within the matrix, where f_{ij}^{d} denotes the frequency of occurrence of two cells of grey tone i and j respectively separated by distance d with a specific direction on the image. Values of f_{ij}^{d} can be calculated by any direction and distance *d* inside the image but only four directions corresponding to angles 0^0, 45^0, 90^0, and 135^0 are generally used.

The appropriate frequency normalisation for each cell inside the matrices are easily computed. For the horizontal direction process, with d = 1 and angle equals to 0^0, and the if the image to be analysed has N_C resolution cells in the horizontal direction (number of columns) and N_R resolution cells in the vertical direction (number of rows), there will be 2× (N_C – 1) neighbouring resolution cell pairs in each row. As a result, the total number of nearest horizontal neighbour pairs can be obtained by the expression 2× (N_C – 1) × N_C. When the relationship between the cells is nearest right-diagonal neighbour, with d=1 and angle = 45^0, there will be 2(N_C-1) 45^0 neighbouring resolution cell pairs for each row except the first, for which there are none. This provides a total of 2(N_C-1)(N_R-1) nearest right-diagonal neighbour pairs. By symmetry there will be $2(N_R-1)N_C$ nearest neighbour pairs for the vertical direction and $2(N_R-1)(N_C-1)$ nearest left-diagonal neighbour pairs. For the right-diagonal direction, by symmetry, the number of nearest pairs is the same as left diagonal. After the total number of neighbouring resolution cell pairs used in computing a particular GLCM has been obtained, the matrix is normalised by dividing each cell in the matrix by the total number of pairs. Figure 6.2 shows a generated GLCM for a small image segment.

1	1	2
2	0	2
0	1	1

(a)

0	1	2
1	4	1
2	1	0

(b)

2	0	1
0	0	2
1	2	0

(c)

0	2	1
2	0	2
1	2	2

(d)

0	2	0
2	0	2
0	2	0

(e)

Figure 6. 2. (a) A 3×3 image with three grey levels; (b)-(e) GLCM for angles of angles 0^0, 45^0, 90^0, and 135^0 respectively.

6.5.1 Texture extraction from GLCM

If the texture contained in an image is coarse, and the measured distance *d* is relatively small in comparison with texture structure, the neighbouring pairs being measured should have very similar grey levels. As a result, the joint neighbouring pair distribution within the GLCM will produce higher values concentrated around its left diagonal direction (i.e. cells (i, j), i = j). Conversely, for a fine texture, if the measured distance d is comparable to the texture structure or is relatively large in scale, the grey level of points separated by distance *d* will be quite different. Therefore, the values in the GLCM should be spread out more uniformly.

Haralick et. al. (1973) proposed fourteen texture measures based on the GLCM. These texture measures, called textural features, are found to be very useful for image classification. Some of these measures relate to specific textural characteristics of the image such as homogeneity, contrast, and the presence of organised structure within the image. Other measures characterise the complexity and nature of gray level transitions which occur in the image. In this study, five indices are used as texture measures obtained from coherence and intensity images. In what follows, g(i, j) denotes the (i, j)th entry in a normalised GLCM, and N_g denotes number of distinct grey levels in the quantised image. The selected texture methods are:

(1) Angular Second Moment (ASM):

$$\text{ASM} = \sum_i \sum_j [g(i,j)]^2 \tag{6.1}$$

The measure is smallest when the g(i, j) are all as equal as possible and is largest when some values are high and others low, e.g., when the values are concentrated near the origin. This parameter measures the homogeneity of the image.

(2) Contrast (Con):

$$\text{Con} = \sum_{n=0}^{N_g-1} n^2 \left\{ \sum_{i=1}^{N_g} \sum_{j=1}^{N_g} g(i,j) \right\} \tag{6.2}$$

This is the second moment of g(i, j), i.e., its moment of inertia about the origin. This is a measure of the contrast or the amount of local variation present in an image.

(3) Correlation (Cor):

$$\text{Cor} = \frac{\sum_i \sum_j (i,j) g(i,j) - \mu_x \mu_y}{\sigma_x \sigma_y} \tag{6.3}$$

where μ_x and σ_x are the means and standard deviations of the rows of GLCM, and μ_y and σ_y are means and standard deviations of the columns. This feature is used to reflect the degree to which the rows or columns resemble each other. It is high when the values are uniformly distributed in the GLCM matrix, and low otherwise, e.g., when the values off the diagonal are small. This is a measure of gray-tone linear dependencies in the image.

(4) Inverse Different Moment (IDM):

$$\text{IDM} = \sum_i \sum_j \frac{1}{1 + (i-j)^2} g(i,j) \tag{6.4}$$

This measure will generate higher values for an image having large homogenous patches because such an image will show high values on the main diagonal of the GLCM. It gives lower weight to those elements g(i, j) that are away from the main diagonal.

(5) Entropy (Ent):

$$\text{Ent} = -\sum_i \sum_j g(i,j) \log(g(i,j)) \tag{6.5}$$

This measure is largest for equal g(i, j) and small when the values of g(i, j) are very unequal.

6.5.2 Feature based on local statistics

Only one feature, “variance”, is calculated based on local statistics. It can be calculated from the following formula using a moving window:

$$\text{Variance} = \frac{\sum \left(DN_{ij} - \mu\right)^2}{n-1} \tag{6.6}$$

where DN_{ij} represents the DN value of pixel at position (i, j), n is the number of pixels in a moving window and μ represents the mean of the moving window, which is calculated from:

$$\mu = \frac{\sum DN_{ij}}{n}.$$

6.6 Fractal dimension

Simple objects can be described by the ideal shapes such as cubes, cones and cylinders, but most natural objects are complex and so they can not be described by these simple shapes. Hence, the concept of self-similarity found an important role in the description of nature. When each piece of a shape is geometrically similar to the whole, that is, when an object is composed of copies of itself and each copy is scaled down by the same ratio in all directions from the whole, both the shape and the cascading process that generates it are said to be self-similar. The complex and erratic shape description in term of self-similarity was introduced by Mandelbrot (1983), who proposed the fractal geometry of nature and defined a fractal as"… a shape made of parts similar to the whole in some way" (Mandelbrot, 1986, p. 8). One of the most important properties of fractals is scaling. Mandelbrot (1983) defined scaling to mean invariance under certain transformations of scale.

Self-similarity is manifested in two ways: it can be exact or statistical. The concept of exact self-similarity is defined as follows: if one were to take a portion of the perimeter of an object and look at it under a microscope, the magnified portion would look exactly the same as the original large part of the boundary. Objects in nature rarely exhibit such exact self-similarity. Nevertheless, they do often posses a related property, statistical self-similarity. Statistical self-similarity means that upon magnification a small portion of an objects looks very much like, but never exactly like, the configurations at other scales. The simplest example of statistically self-similar fractals is a coastline.

An important concept in fractal geometry is fractal dimension. In the Euclidean universe, the dimension of an object is defined as the number of distinct coordinates needed to specify a position on or within the object. A point object has zero dimension; a line, whether straight or curved, has one dimension. Any point on the line can be represented by a single parameter. However, this definition of dimension is not satisfactory for a proper understanding of irregularity or fragmentation in nature. The fractal concept provides a more appropriate mathematical framework to study the irregular, complex shapes found in nature. Fractal geometry has had a major impact in modelling and analysis in the natural and physical sciences.

Two important types of dimension are commonly used in fractal research: the topological dimension and the fractional dimension (D) (Xia and Clarke, 1997). The topological dimension is always an integer and coincides with the intuitive dimension in Euclidean geometry. The notion of a fractional dimension was introduced by Hausdorff (1919) in order to put a size to a highly irregular non-rectifiable sets. Thus the fractional dimension is sometimes called the "Hausdorff dimension" or "Hausdorff-Besicovitch dimension". The Hausdorff-Besicovitch dimensions of all cases studied in fractal geometry are greater than their topological dimensions. In order to emphasise the fact that a fractal may also have an integer dimension and to avoid the confusion of Hausdorff-Besicovitch dimension with the dimension of the Hausdorff topological space, Mandelbrot (1983, p. 15-17) proposed to call D the fractal dimension. On the other hand, most people continue using the terms fractional dimension, Hausdorff dimension, Hausdorff-Besicovitch dimension and fractal dimension interchangeably. The fractal dimension is a real number that measures the degree of irregularity or level of complexity of an object.

The concept of fractal dimension can be useful in the measurement, analysis, and classification of shape and texture. The characterisation of surface roughness by a fractal dimension has been applied to fracture surfaces and it has been used to obtain shape information and to distinguish between rough textured regions for imaged three-dimensional surfaces (Pentland, 1984, 1986).

A number of approaches exists in literature to estimate the fractal dimension (D). Peleg et al. (1984) used the ε-blanket method, in which an image can be viewed as a hilly terrain surface whose height above a datum is proportional to the image gray value. All points at a distance ε from the surface on both sides creates a blanket of thickness 2ε. The estimated surface area is the volume of the blanket divided by 2ε. For different ε, the blanket area is iteratively estimated and fractal dimension can be derived from least squares linear fit of the log-log plot of A(ε) and ε, where A(ε) is defined as

$$A(\varepsilon) = F \cdot e^{2-D} \tag{6.7}$$

where F is a positive constant.

This approach is a 2-D generalisation of the original approach suggested by Mandelbrot (1983). Pentland (1984) considered the image intensity surface as a fractal Brownian function and estimated the fractal dimension from Fourier power spectrum of fractal Brownian function. Gangepain and Roques-Carmes (1986), Keller and Chen (1989) and Sarkar and Chaudhuri (1994) used variations of the box-counting approach to estimate the fractal dimension. This method uses different scale boxes denoted by B_l to cover the data set and measures the number of boxes needed to cover the whole set. The slope of the regression line of these $\log B_l - \log N_l$ pairs gives an estimate of the fractal dimension. In this study the method based on box-counting proposed by Sarkar and Chaudhri (1994) and found to perform well with SAR data (Tso, 1997) is used.

This method is described as follows: consider that the image of size M×M pixels has been divided into grids of size s×s, where M/2 ≥ s > 1 and s is an integer.

Consider the image as a 3D surface with (x, y) denoting 2-D position and the third co-ordinate (z) being grey level. The (x, y) space is divided into grids of size s×s. Thus for each grid there is a column of boxes of size $s \times s \times s'$, where s can be a multiple of the side length of a pixel in (x, y) and s' can be a multiple of the grey level in z-direction. If the total number of grey level is G then s' is calculated from the expression

$$\left\lfloor \frac{G}{s'} \right\rfloor = \left\lfloor \frac{M}{s} \right\rfloor \tag{6.8}$$

where symbol $\lfloor \ \rfloor$ indicates the integer part of the argument.

Assign the numbers 1, 2, …., n in turn to each box in the column from bottom to top. Let the minimum and maximum grey level of the image on the (i, j)th grid fall in boxes number p and k, respectively. Then the number of boxes needed to cover the surface on the (i, j)th grid is

$$n_r(i,j) = \ = p - k + 1 \tag{6.9}$$

where

$$r = s/M$$

Because of the differential nature of computing n_r, this method is called differential box-counting approach. After taking contributions from all grids, the total number of boxes needed to cover the whole image with box size $s \times s \times s'$ is

$$N_r = \sum_{i,j} n_r(i,j) \tag{6.10}$$

N_r is counted for different values of s. The fractal dimension D is estimated from the least square linear fit of log (N_r) against log (1/r). This method is computationally efficient and counting N_r in this manner gives a better approximation to the boxes intersecting the image intensity surface when there is sharp grey level variation in neighbouring pixels in the images.

6.7 Multiplicative Autoregressive Random Field (MAR) model

Research carried out to study the behaviour of the radar returns have found that radar returns are corrupted by speckle (Ulaby, 1980). Thus, the use of lognormal models for radar have been suggested for homomorphic filtering to separate multiplicative illumination and reflective components (Stockham, 1972).

Frankot and Chellapa (1987) proposed the gaussian autoregressive random field models for the logarithm of radar image intensity in two dimensions, which they called the lognormal multiplicative autoregressive (MAR) model and suggested that these models are useful for estimating spatial correlation structures which, together with the image intensity distribution model, fits a variety of radar imagery. Initially, the MAR concept was originally used to model image data, and the parameters of the model have been found to be highly correlated with the spatial distribution of image intensities. For this reason, they can be used as a texture descriptors for image classification (Solberg and Jain, 1997; Tso, 1997). Lognormal random fields with multiplicative spatial interaction are a special case of the gaussian autoregressive random fields.

Let an image p(s), $s \in \Omega$, with size M×M, be represented by the following white-noise-driven multiplicative system:

$$p(s) = \prod_{r \in N} [p(s+r)]^{\theta_r} \cdot v(s) \tag{6.11}$$

where $\Omega = \{0, 1, \ldots., M\text{-}1\} \times \{0, 1, \ldots.., M\text{-}1\}$, N is the neighbourhood set defining model support (i.e., the number and location of pixels contributing to the central pixel, as shown in Figure 6.3, v(s) is a lognormal white-noise process referred to as the driving process, θ_r is an exponent weighting factor for neighbourhood r, and s = (m, n), a 2-D index to an image.

The random field p(s) is said to obey a lognormal MAR model if q(s) = ln p(s) obeys the following gaussian autoregressive random field model with w(s) = ln v(s):

$$q(s) = \sum_{r \in N} \theta_r \cdot q(s+r) + w(s) \tag{6.12}$$

where w(s) is zero mean white gaussian noise. The covariance of w(s) is given by

$$\mathrm{cov}_w(r) = \begin{cases} \sigma_w{}^2, & r=(0,0) \\ 0, & r\neq(0,0) \end{cases}$$

where σ_w denotes the variance of w.

6.7.1 Estimation of parameters in the MAR model

The parameters of the MAR model, the neighbourhood weighting parameter vector θ, the noise variance $\sigma_w{}^2$, and the mean value m_q of the stationary random process q are estimated for each image, using a least squares estimation method (Kashyap and Chellappa, 1983) and used as texture features. The neighbourhood N = {(0,-1), (-1,-1), (-1,0)} is used to compute these three parameters (Figure 6.3).

N= {(0,1), (-1,-1), (-1,0)} $\longrightarrow$

(-1,-1)	(-1,0)	
(0,-1)	(i,j)	

Figure 6. 3. Neighbourhood support of central pixel.

For MAR models, the least squares estimates based on p(s) are as:

Covariance:

$$\sigma_w{}^2 = \frac{1}{M^2}\sum_{s\in\Omega}\left[q(s)-m_q-\theta^T z(s)\right]^2 \qquad (6.13)$$

where

$$\theta = \left[\sum_{s\in\Omega} z(s)\cdot z^T(s)\right]^{-1}\left[\sum_{s\in\Omega} z(s)\left(q(s)-m_q\right)\right]$$

while mean is defined as:

$$m_q = \frac{1}{M^2} \sum_{s \in \Omega} q(s) \tag{6.14}$$

where

$$z(s) = q(s + r) - m_q, \quad r \in N$$

6.8 Feature selection

In real-world situations, all features relevant to the classification of an object are often unknown a priori. Therefore, a number of candidate features are often introduced to better represent the image classification problem. Unfortunately, many of these features are either partially or completely irrelevant or redundant for the problem concerned. A relevant feature is neither irrelevant nor redundant while an irrelevant feature does not affect the results in any way, and a redundant feature does not add anything new to the results. In many applications, the size of a dataset is so large that learning might not work well unless these unwanted features are removed. Reducing the number of irrelevant/redundant features drastically reduces the running time of a learning algorithm as well as increasing its effectiveness. Feature selection methods try to pick a subset of features that are relevant to the problem.

A basic problem in pattern classification is to determine which features should be employed for minimum error and maximum efficiency in classification. A large number of pattern classification problems involve classification of patterns into one of a set of classes, which are defined only by a limited number of labelled representative patterns (which are pixel vectors in remote sensing). Feature extraction can be viewed as finding a set of vectors that adequately represent an observation but in a lower dimensional feature space. In pattern recognition, it is desirable to extract features that have the highest discriminating power between classes. Although a reduction in dimensionality is desirable, the error resulting from the reduction in dimension has to be acceptably low. The development of feature extraction methods has been a prominent research area in the field of pattern analysis.

Feature selection is defined by many authors by looking at the problem from various angles. But, as expected, many of the solutions are similar in intuition and/or content. The following are some of the definitions those are conceptually different and cover a range of definitions.

1. Idealised: find the minimally sized feature subset that is necessary and sufficient to the target concept (Kira and Rendell, 1992).
2. Classical: select a subset of M features from a set of N features, M < N, such that the value of a criterion function is optimised over all subsets of size M (Narendra and Fukunaga, 1977).
3. Improving prediction accuracy: the aim of feature selection is to choose a subset of features for improving prediction accuracy or decreasing the size of the structure without significantly decreasing prediction accuracy of the classifier built using only the selected features (Koller and Sahami, 1996).
4. Approximating original class distribution: the goal of feature selection is to select a small subset such that the resulting class distribution, given only the values for the selected features, is as close as possible to the original class distribution given all feature values (Koller and Sahami, 1996).

The third definition emphasises the prediction accuracy of a classifier, using only the selected features, whereas the last definition emphasises the class distribution given the training data set. These two approaches are quite different conceptually.

Feature selection is a difficult task in classification because it is both dependent on the input data and on the classifier used. The quality of a feature is measured by its relevance, discriminative power, and ease of computation. Additionally, by excluding redundant, irrelevant, or inconsistent features from the training set, higher accuracy on an independent validation dataset can often be achieved.

The problem of feature selection is defined as follows: given a set of candidate features, select a subset that performs best (according to some criterion) under some classification system. This procedure can reduce both the cost of classification by reducing the number of features that need to be collected and, in some cases it can provide a higher classification accuracy due to finite sample size effects. The term "feature selection" is taken to refer to algorithms that output a subset of the input feature set. The procedure of feature selection must be based on two components. First, a criterion must be defined by which it is possible to judge the performance of each feature. Second, a systematic procedure must be found for searching through candidate subsets of features. In principle, the feature selection criterion should be the same as that used to assess the misclassification rate for a image classification problem. Similarly, the search procedure could simply consist of an exhaustive search for all possible subsets of features since this is, in general, the only approach that is guaranteed to find the optimal subset. In a practical application, however, a simplified selection criterion as well as a non-exhaustive search procedure is used in order to limit the computational complexity of the search procedure. A number of studies of feature selection methods have been carried out in image classification (Jain and Zongker, 1997; Kavzoglu, 2001). In this study, following Kavzoglu's (2001) guidelines, Hotelling's T^2 statistical method is used to determine the best three texture features out of the ten features of each intensity and coherence image.

6.8.1 Hotelling's T^2

Several multivariate statistical techniques can be used to determine the degree of discrimination between the classes present in a given dataset, by using the means and co-variance matrices of the classes. Hotelling's T^2 statistic (Hotelling, 1931) is one of the most popular statistical tests to estimate the discriminating power of a feature or relative importance of a feature.

Hotelling's T^2 statistic is used to test the null hypothesis that the (population) multivariate means of the two groups under study do not differ significantly. It provides a multivariate generalisation of the Student's t test and is related to the problem of how best to discriminate between two groups. T^2 is calculated from:

$$T^2 = \frac{n_1 n_2}{n_1 + n_2} . D^2 \tag{6.15}$$

$$D^2 = (m_1 - m_2)^T \sum{}^{-1} (m_1 - m_2)$$

where D^2 is the measure known as Mahalanobis' D-squared, which measures the overall similarity between the two groups. $\sum^{-1}$ is the inverse matrix of the pooled co-variance matrix $\sum$, and m_1 and m_2 are the mean vectors for the groups, which contain n_1 and n_2 individuals, respectively.

The value of Hotelling's T^2 increases as inter-class separation increases. The statistical significance of T^2 can be evaluated using a transformation to the F distribution. It should be noted that the number of observations need not be the same for the two samples, but the number of features must be the same.

Hotelling's T^2 is used to identify only three best texture features for each image (five intensity images and one coherence image) to be used for land cover classification. For intensity and coherence images, nine texture features, including five grey-level co-occurance features (asm, con, crr, ent and idm), two features from the MAR model (markov mean and covariance), one feature calculated from fractal geometry and one feature from first order statistics (variance) are used for feature selection. With intensity images, the four best features selected for use in further classification are the fractal dimension, the intensity image itself, contrast from GLCM and variance from first order statistics. For the coherence image, the four features selected are coherence, markov mean, plus correlation and entropy from GLCM (Table 6.2).

6.9 Classification results and discussion

6.9.1 Results

Extensive experiments were carried out in order to test the performance of classifiers using intensity images, the coherence image, and the texture features derived from these, for crop classification. In order to achieve a comprehensive analysis, different data types derived from the original intensity and coherence images are included in the experimental process. Besides using the median-filtered intensity and coherence images, other data sets used in this study include texture features derived from coherence and intensity images based on GLCM, local statistics, the MAR model and the fractal models. For each intensity and coherence image, five features from GLCM, one feature from local statistics, two features from the Markov autoregressive model and one feature from the fractal model are derived (discussed in section 6.7). As the number of features becomes large, a feature selection method is used to reduce the dimensionalty of the data used for classification. For this study the different data sets used for classification are:

1. All five median filtered intensity images.
2. A combination of filtered coherence image with all five intensity images.
3. Coherence, one intensity image obtained from 02 and 03 May 1996 (tandem pair of SLC) and the difference between the two intensity images obtained from this pair.
4. A combination of the coherence image and its three best texture features with all five median-filtered intensity images.
5. A combination of the coherence image and five intensity images with the two best texture features for each of the coherence and intensity images.
6. All five intensity images in combination with the texture features of all these five intensity images.
7. The coherence image, all five intensity images, and the three best texture features for each of the coherence and intensity images.

Three different classifiers (maximum likelihood, neural network and decision tree) were used. The user-defined parameters (section 2.3.4.3) for the neural network are set according to the recommendations made by Kavzuglu (2001). The best three texture features used to recognise land cover classes in the classification process and obtained by employing the Hotelling's T^2 statistic are shown in Table 6.2.

Table 6. 2. Various features obtained by applying Hotelling's T^2 feature selection method and used in final classification process.

Image	Features selected	Hotelling's T^2 value
Coherence image	Correlation and entropy from GLCM and MAR mean	709.15
Intensity images	Variance from local statistics, contrast from GLCM and fractal dimension	476.18

Random sampling was used to collect the training and test pixels from the ground reference image for all datasets. These pixels were divided into two subsets, one for training and one for testing the classifiers, so as to remove any bias resulting from the use of the same set of pixels during training and testing. The number of observations to be used in training the classifiers should be enough so as to assure that each class is properly sampled and the analysis performed for accuracy assessment is statistically valid. Mather (1999) recommend that to generate a representative training sample for the statistical classifier (multivariate case), there should be at least 30 training pixels for each features per class, and preferably more. In this study, different numbers of training data for every combination of features were used to examine the above requirement. The same number of training and test pixels was used for all the three classifiers.

To analyse the results, confusion matrices were generated using the three classifiers for each of the combinations listed above. Overall classification accuracy (in percentage) and Kappa coefficients are shown in Table 6.3. Figure 6.4 shows the classified images using coherence with five intensity images and three best texture features for each, using neural and decision tree classifiers respectively. The confusion matrices are listed in appendix C.

Table 6. 3. Total classification accuracies for different data sets used in the classification process. Table 6.3(a) is for maximum likelihood, Table 6.3 (b) for the neural network and Table 6.3(c) for decision tree classifier.

Table 6.3(a)

Data sets used	Number of features	Overall Classification accuracy	Kappa value
1	5	59.2	0.524
2	6	68.7	0.635
3	3	49.7	0.413
4	9	70.6	0.657
5	18	78.0	0.744
6	20	68.7	0.634
7	24	77.1	0.733

Table 6.3(b)

Data sets used	Number of features	Overall classification accuracy	Kappa value
1	5	60.8	0.572
2	6	69.7	0.664
3	3	30.5	0.279
4	9	73.7	0.705
5	18	79.1	0.765
6	20	73.1	0.701
7	24	82.9	0.805

Table 6.3(c)

Data sets used	Number of features	Overall classification accuracy	Kappa value
1	5	69.9	0.650
2	6	77.8	0.741
3	3	47.4	0.390
4	9	77.9	0.742
5	18	80.2	0.769
6	20	78.6	0.750
7	24	82.7	0.797

6.9.2 Discussion

Comparison of the results shown in Table 6.3 (data sets 1 and 2) suggests that the inclusion of coherence information with the intensity images results in a substantial improvement in overall classification accuracy for all of the three classifiers used. The increase in accuracy with the maximum likelihood classifier is from 59.2% to 68.7% (Kappa value 0.524 to 0.635), for the neural classifier the increase is from 60.8% to 69.7% (Kappa value 0.572 to 0.664), while the overall accuracies from the decision tree classifier rises from 69.9% to 77.8% (Kappa value 0.65 to 0.741). There is an increase of about 8-9% in accuracy when coherence information is added, irrespective of the classifier used. Wegmuller and Werner (1994) found that the combination of coherence, one intensity and the difference of intensity images obtained by interferometric processing of a tandem pair to be very promising for land cover classification studies, so we carried out classification using this combination also (data set 3). This combination performs badly for this particular land cover classification problem. It gives a maximum accuracy of 49.7% using a decision tree classifier, a result that is far lower than the accuracy obtained with data set 1.

Evaluation of the results presented so far in this study suggests that the decision tree classifier performs better than either the maximum likelihood or the neural classifiers. It gives a considerable increase in accuracy (of about 10%) as compared to both of the other classification systems with data sets 1 and 2.

The study further suggests that the inclusion of texture measures helps to improve classification accuracy. A total of nine features per intensity and coherence image was extracted using GLCM (five features), MAR model (two features), the variance based on first order statistics, and the fractal model (one feature) making a total of sixty features. It is necessary to apply feature selection so as to reduce the dimensionality of the input feature space and to overcome the problem of dimensionality (Hughes, 1968). For this study, the three best texture features are selected for each intensity and coherence image. Initially, data set 4, which includes texture features obtained from the coherence image, was used for classification. The results suggests that an improvement of 4% in classification accuracy is achieved by using the neural network classifier as compared to data

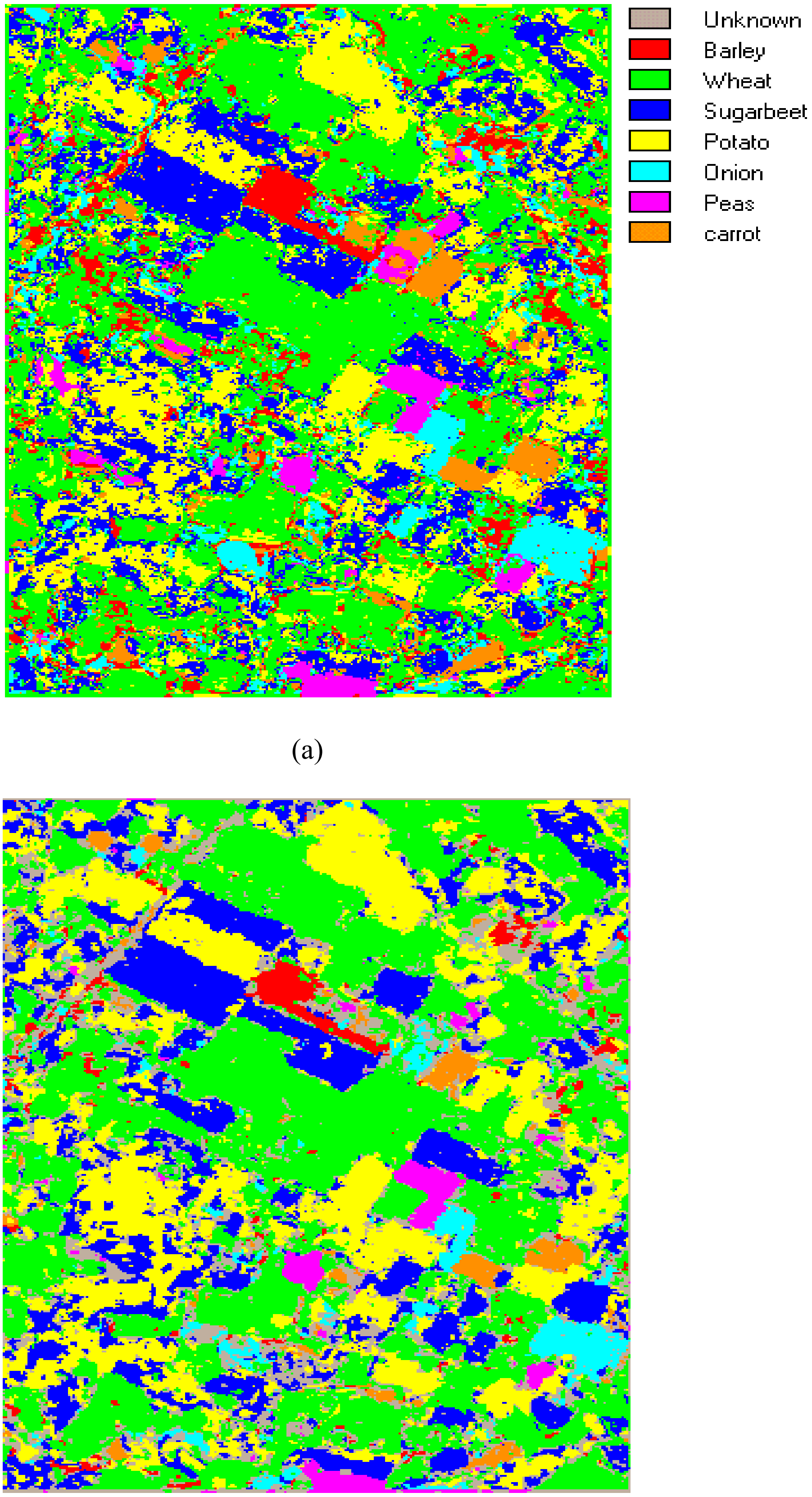

(a)

(b)

Figure 6. 4. Classified images of data set 7 using (a) decision tree classifier and (b) with neural classifier.

set 2, while use of the maximum likelihood and the decision tree classifiers suggests no major improvement in classification accuracy.

When all five intensity images with their associated texture features (data set 6) are used, a significant improvement in classification accuracy is shown as compared to the data set 1. Classification accuracy increases by an amount ranging from 8.7% to 12.3% depending on the classifier used, suggesting the importance of texture features with InSAR intensity images in land cover classification. Further studies were carried out after adding the coherence and its texture features with dataset 6 (data set 7). An increase of between 4 and 9% in classification accuracy as compared to data set 6 suggests that the coherence image provides discriminating information about the land surface and can be used effectively for land cover classification in combination with intensity images obtained from interferometric SAR data. The highest accuracy obtained by this combination (data set 7) is 82.9% with a neural classifier, which is slightly higher than the overall accuracy of the decision tree classifier (82.7%). Another study using data set 5 was carried out, using only two texture features per coherence and intensity image. The results in Table 6.3 suggest that the accuracy reached by this combination is not comparable to the performance of data set 7. The highest accuracy of 80.2% was achieved by the decision tree classifier, but the accuracy is still less than the highest accuracy achieved with data set 7.

6.10 Conclusions

A number of combinations of data sets derived from interferometric SAR intensity and coherence images have been evaluated for crop discrimination. The results obtained from seven different datasets (Table 6.3) shows that the use of the coherence image in combination with the intensity images provides additional discriminating power in land cover classification studies. The performance of dataset 3 was found to be the worst among the different combination tested, which contrasts with the results for land cover classification reported by Wegmuller and Werner (1997). The highest accuracy obtained is about 82.9% while using 24 features, justifying the importance of the texture features, as suggested by earlier work by Dutra and Huber (1999). However, in practice, one often encounters the so-called dimensionality problem, i.e., with a fixed relatively small sample size, the classification accuracy may actually decrease when the number of features is increased (Hughes, 1968). This means that the use of a larger number of features requires a corresponding increase in the number of training samples, so that the results obtained are reliable.

It has also been found that decision tree classifier achieves better results (in terms of overall accuracy) than the statistical and neural classifiers in almost all cases, except with dataset 7, where the overall classification accuracy achieved with a decision tree classifier is slightly less than that of the neural classifier. The same number of training data were used for the three classifiers for dataset 7, thus indicating the limitations of univariate decision tree with limited training data size as the number of features increases.

1. **Coherence information provides additional discriminating power in land cover classification studies.**
2. **Texture information is quite useful in improving classification accuracy of InSAR data.**
3. **Tandem SLC pair is more suitable for good coherence information.**

CHAPTER 7

Issues in the classification of remote sensing data

7.1 Introduction

One of the fundamental characteristics of a remotely sensed image is its spatial resolution, or the size of the area on the ground from which the measurements that comprise the image are derived. Spatial resolution is analogous to the scale of the observations. In most scientific works, the investigator selects the scale at which observations are collected but, in case of remotely sensed imagery obtained from space-borne sensors, investigators are limited to specific scales of observations. Until 1990, this choice was extremely limited, with data being available at medium resolution (such as 80m for Landsat MSS and 20m for SPOT) as well as coarse resolution (NOAA). With the availability of airborne scanners and space-borne sensors providing data at up to one-metre resolution, a problem of choice is created. There are considerations beyond spatial resolution concerning the spectral, temporal, and radiometric characteristics of the data, as well as the sample size and sampling plan used for collection of test and training datasets. The dimensionality of the dataset poses additional problem. Accuracy assessment requires that an adequate number of samples per class be gathered so that any analysis performed is statistically valid. In addition to the sample size, choice of sampling scheme plays an important part in any accuracy assessment by generating an error matrix that is representative of the entire map. Different sampling schemes assume different sampling models and also determine the distribution of the samples across the landscape, which in turn will significantly affect accuracy assessment.

While sample size and sampling plan have been recognised as important factors in classification accuracy assessment, it is becoming apparent that the factor of scale also plays an important role in the planning of remote sensing investigations. In the past, the selection of an appropriate scale has been left to the experience of individual investigators. A series of studies (Sadowski et al., 1977; Markham and

Townshend, 1981; Irons et al., 1985; Cushnie, 1987) has assessed the effect of spatial resolution on the ability to classify land use/land cover types using digital classification techniques. The conclusions of these studies are that a change in spatial resolution could significantly affect the classification accuracies and that, in many cases, the use of higher spatial resolution data resulted in lower classification accuracy. Woodcock and Strahler (1987) suggested that this may be due to an increase in within-class spectral variability which confuses per-pixel classifiers.

The aim of this chapter is to study the behaviour of different classification algorithms in term of their overall classification accuracy, with fixed number of training data and varying number of features as well as with fixed number of features and varying number of training data. This study also considers the effect of sampling plan on the classification accuracy of a classifier. Further, this study investigate the effect of scale on classification accuracy, using data for the same region at two different resolutions.

7.2 Scale

In general sense, scale refers to the spatial, temporal, quantitative, or analytical dimensions used to measure and study objects and processes. The problem in defining scale is that its meaning varies between disciplines. Conceptually, "..scale represents the window of perception, the filter or the measuring tool through which a landscape may be viewed or perceived" (Levin, 1992). Thus, changing the scale changes the view of reality, which has obvious implications for understanding the dynamics of any environmental system. The term "scale" has a variety of meanings and has been used in different contexts in various disciplines. Landscape ecologists define scale as having two components: grain and extent. Grain corresponds to the smallest spatial sampling units used to gather a series of observations. Extent is the total area over which observations of a particular grain are made. To a cartographer, scale is defined simply as the ratio between distance on the map and the distance on the ground. This issue is complicated further by the use of scale as a basic dimension of generalisation. The effect of generalisation is to introduce the uncertainty into the representation of a real phenomenon that could only be mapped perfectly at a much larger scale.

To most scientists, the term "scale" is likely to imply a small linear dimension. For remote sensing data, scale corresponds to spatial resolution (Woodcock and Strahler, 1987) which refers to the ability of a sensor to record and display fine spatial detail as separated from its surroundings. For other data types it may be more difficult to identify a single linear dimension to characterise the observations. In short, a small linear dimension representing spatial data "scale" is well defined for some types of digital data, but not well defined for other types. Geographic scale is important because it defines the limit to our observations of the earth. All earth observation must have a small linear dimension, defined as the limiting spatial resolution, the size of the smallest observable objects, the pixel size, the grain of the photographic emulsion, or some similarly defined parameter. Geographic scale is also important because it is often a parameter in the physical and social processes that shape geographic phenomenon.

Further to the use of scale in spatial context, scale may also be used in a temporal context. This is important in many remote sensing investigations where an ability to monitor changes over time periods that ranges from hours (e.g., in meteorology) through years (e.g., in urban growth) to centuries (e.g., soil development) is vital. For a variety of reasons, notably practical constraints of data handling and manipulation, the spatial and temporal aspects of scale need to be considered together in many remote sensing applications.

7.2.1 Definition

Scale is one of the primary attributes in describing geographic data. As discussed earlier, the concept of scale has a variety of meanings. Marceau (1999) defines scale in relation to the absolute and relative representations of space. In an absolute framework, scale can be defined in operational terms and refers to a practical, standard system used to partition geographical space into operational spatial units. In a relative framework, scale becomes a variable intrinsically linked to the spatial entities, patterns, forms, functions, processes, and the rate under investigation. In this study, the focus is on spatial scale. Within the spatial domain, at least four meanings of the term scale can be identified in the literature (Cao and Lam, 1997) (Figure 7.1):

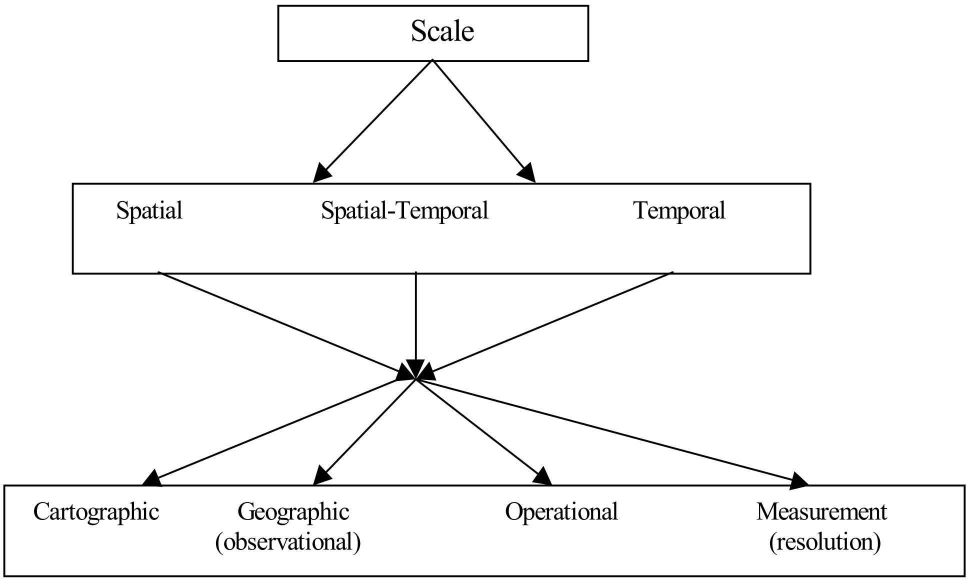

Figure 7. 1. Meaning of scale (adapted from Cao and Lam, 1997).

(1) The cartographic or map scale refers to the proportion of a distance on a map to the corresponding distance on the ground. A large scale may cover a small area and show more detailed information. On the other hand, a small-scale map covers a larger area and the map often contains less detailed information.

(2) The geographic or observational scale refers to the size or spatial extent of the study. A large scale (geographic) study covers a larger area, as opposed to a small scale study which covers a smaller area. For example, a study of the distribution of forests on a global level is considered a large scale study compared with a study of crop classification in some part of Cambridgeshire, UK.

(3) The operational scale refers to the scale at which certain processes operate in the environment. This scale is referred as the scale of action by some researchers, and methods have been suggested to determine this scale of action. The operational scale is inherited from the geographic phenomena,

as it is compared to the observational scale, which could be rather subjective depending on the observer. Finding the operational scale of phenomena is an important step in determining the observational scale of the study because a phenomenon is best observed at its operational scale. Also, a phenomenon observed at one scale may not exist at another scale.

(4) Spatial resolution refers to the smallest distinguishable parts of an object, such as a pixel in remotely sensed imagery, and can be considered as a measurable scale.

These four meanings of scale are closely related. Thus, small scale cartographic maps are often used in large scale geographic studies, and only certain processes can be observed from a map with a specific cartographic scale. In remote sensing, a measurement scale of 30 m (in ETM+ data) results in a pixel size (spatial resolution) of 30 m, but it takes a number of pixels (operational scale) for a feature to be recognised and much larger area (geographical scale) to understand the spatial pattern of the feature. The main concern in all the definitions of the scale is the relative size of the object and its spatial representation or generalisation. Scale dependency is an inherent property of geographic phenomena. If the geographic pattern under consideration varies with scale, the geographic phenomenon is considered scale dependent. If, however, the pattern does not change across scale, the phenomenon is regarded as scale independent. In reality, very few geographical phenomenon are scale independent.

Of the four definitions of scale, cartographic scale has been studied most intensively. A large volume of literature in this field has contributed to the proper use of both paper maps and their digital equivalents. Studies of resolution are second to those of cartographic scale, with most of this research being done in the last two decades. Resolution is explicitly linked to areal units. Most resolution studies have focused on regular grid data such as remotely sensed images or raster GIS data, such as digital elevation models.

7.3 Scaling

One of the major use of geographical information systems (GIS) is to provide an environment that facilitates distributed modelling. Such modelling frequently requires the integration of diverse datasets such as point ground measurements, thematic maps, and areal remotely-sensed observations. The required input parameters are rarely available at the desired modelling scale and their use at a scale other than at which they were observed is not always straightforward. Conversely, if the data are allowed to determine the scale at which the modelling is to take place, the resulting model outputs may not be suitable for addressing the research problem in question. In general, the modeller tends to find some middle ground and make decisions on modelling scale based on the resolution of the available input data, computational resources, and their perception of the required resolution of the outputs. However, these decisions are not without consequences, the most important of which is that model output may vary as a function of scale. The scale of observation and measurement is thus one of the most essential considerations to be made in the interpretation and analysis of remote sensing data. It is widely recognised that many environmental processes and patterns are scale-dependent. The recognition of such scale effect has led to research into the scaling properties of environment fields. The term "scaling" has come to have multiple definitions, depending not only on the general discipline (e.g., in geography, and ecology) but the application within the discipline (e.g., within geography, remote sensing as opposed to cartography).

7.3.1 The scaling process

The scaling process involves taking information at one scale and uses it to derive information at another scale (Figure 7.2). As we have only a limited ability to make representative measurements, integration and scaling techniques are used to apply small-scale, short-term measurements to make larger-scale, longer-term inferences. Although it is possible to make measurements at a large scale, by using remote sensing data, applying these results to other ecosystems, locations, time, or weather conditions has proven difficult for two reasons:

1. Limited resources constrain measurements periods and conditions, so less-than representative observations are available.
2. The system behaviour is the result of interactions among many factors on small and large scales and, without accommodating the most important of these interactions, generalisations are difficult.

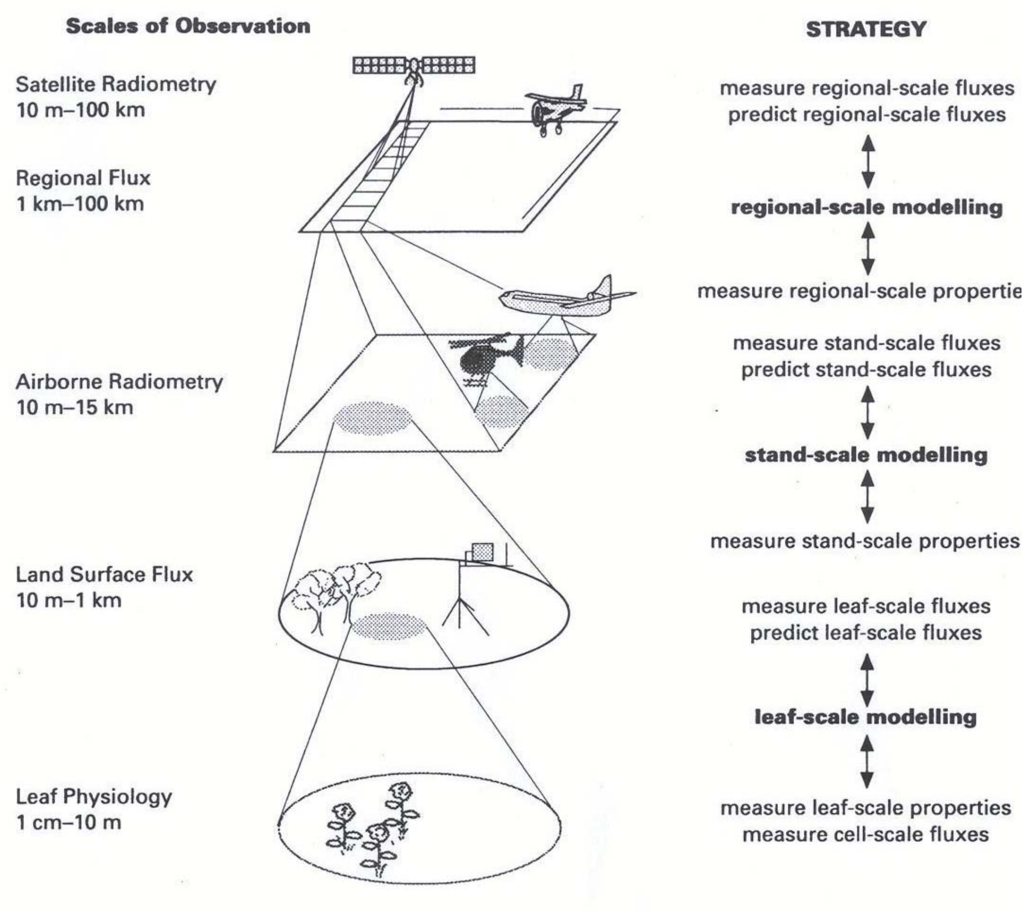
Scales of Observation
Satellite Radiometry
10 m–100 km
Regional Flux
1 km–100 km
Airborne Radiometry
10 m–15 km
Land Surface Flux
10 m–1 km
Leaf Physiology
1 cm–10 m
STRATEGY
measure regional-scale fluxes
predict regional-scale fluxes
regional-scale modelling
measure regional-scale propertie
measure stand-scale fluxes
predict stand-scale fluxes
stand-scale modelling
measure stand-scale properties
measure leaf-scale fluxes
predict leaf-scale fluxes
leaf-scale modelling
measure leaf-scale properties
measure cell-scale fluxes

Figure 7. 2. The strategy of up- and downscaling across the four spatial scales of interest in relation to global environmental change (adapted from Jarvis, 1995).

Scaling is not simply integration or aggregation of values at one level to achieve values at different level. Rather, scaling represents the concepts that link processes at different levels of space and time. Scaling also involves not being distracted by those factors that are less important in the transitions among scales.

Upscaling consists of taking information at smaller spatial and shorter temporal scales and using that information to derive information at larger spatial and longer temporal scales. A widely-used example of upscaling is to take a description of the process of photo-synthesis at the scale of biochemical processes in the chloroplast, combine that with a description of leaf structure and carbon dioxide diffusion, and use that information to derive a description of the fluxes of carbon dioxide at the leaf scale. Combination of leaf scale fluxes with information about the physical structure of the vegetation canopy, together with appropriate driving variables, can then lead to a description of carbon dioxide fluxes at the canopy scale.

Generally, the objective of upscaling is to preserve the rate of the processes involved, usually flux densities, such that the rate at the larger spatial and longer temporal scales is equal to the sum of the rates of all the individual components in the system. This would clearly be a very easy objective to achieve if all the process involved were linear. But non-linearity between processes and variables, and heterogeneity in properties, makes upscaling a challenge. For example, the measurement of area of land cover from remote sensing images is heavily influenced by the pixel size, because of the changes in the degree of heterogeneity of the land cover across scales. Heterogeneous landscapes also lead to more rapid information loss as the data are aggregated and analysed at coarser scales (Meentemeyer and Box, 1987).

Downscaling consists of decomposing information at one scale into its constituents at smaller spatial and shorter temporal scales. The information may be a description of a process at a larger scale. Downscaling may also be usefully applied to both state and environmental driving variables. For example, it may be desirable to downscale a crude estimate of canopy structure, such as leaf area index, to a more detailed description of the spatial distribution of leaf area density for the purpose of radiative transfer modelling.

For many purposes, it is adequate, if not desirable, to seek to understand processes at one particular scale and it is almost impossible to perform large scale experiments at the scale of natural ecosystems, regional landscapes etc as well as very small scale experiments at the scale of metres. That is why a need exists for upscaling and downscaling of data.

A variety of tools are available for scaling, involving a combination of correlation, extrapolation, and modelling, all of which being designed to relate patterns across wide range of scale. For short-term or small-scale predictions, direct extrapolation of observed trends may be the best technique, but the application of such methods can give no hints about when the method will break down or about how patterns will change beyond observed ranges or in response to environmental changes.

Some guidelines for scaling suggested by Caldwell et al. (1993) are:

1. Assess the scale of the phenomenon in question,
2. Identify the boundary conditions and constraints,
3. Search for consistencies at different scales,
4. Streamline the upscaling models to incorporate only salient features,
5. Incorporate feedback, both positive and negative, that may operate on some scale but not necessarily on other scales, and
6. Test the results at different scales with independent estimates.

7.4 Sample size

After selecting data at a suitable scale for the study, the next task in assessing the accuracy of the land use/land cover maps depends on the selection of samples for training and testing a classifier that gives reliable results applicable both to the whole land use map and to the individual land use/land cover categories (Fitzpatrick-Lins, 1981). Due to time and cost constraints involving the collection of reference data, it would be virtually impossible to consider the entire population of pixels for classification. Therefore, a sample of pixels is required for each of the land use class to estimate classification accuracy. Too large a sample implies a waste of resources, and too small a sample diminishes the utility of the results. A number of studies carried out by Fitzpatrick-Lins (1981), Hay (1979), Hord and Brooner (1976), Rosenfield (1982) and Van Genderen and Lock (1977) have reported a number of equations and guidelines for choosing an appropriate sample size. The majority of these equations are based on assumption that the data follow a binomial distribution or the normal approximation to the binomial distribution.

The equation for the determination of the appropriate sample size, N, suggested by Snedecor and Cochran (1967) (later used by Fitzpatrick-Lins, 1981) is based on the binomial distribution and depends on the allowable error at a given confidence level. This equation is:

$$N = \frac{K^2 \left(ab\right)}{L^2} \tag{7.1}$$

where *a* is expected percent accuracy, *b* = 100 - *a*, *L* is the allowable error, and *K* is the standard normal deviate for a desired confidence level (e.g. the value of *K* = 2 is generalised from the standard normal deviate of 1.96 for the 95% two sided confidence level). This formula assumes that pixels are selected by using a simple random sampling technique. When more complex sampling methods such as stratified sampling are employed, a useful quantity known as the *design effect* of the sampling plan enable simple random sampling formulae to be used more extensively (Snedecor and Cochran, 1967). The design effect is defined as the ratio of the variance of the estimate given by the complex sampling plan to the variance of the estimate given by a simple random sample of the same size.

Tortora (1978) suggested another method of estimating the sample size for multinomial distribution based on the approximate large sample equations for the simultaneous confidence limits. The equation has the form

$$N = \frac{\chi_{1,1-\alpha/k}{}^{2} \lambda_i \left(1 - \lambda_1\right)}{\delta_i{}^{2}} \tag{7.2}$$

where λ_i i = 1, 2 ,. . . . , *c*, is the proportion of the image area in the i^{th} class, parameter δ_i is the half width of the desired confidence interval, and the value of $\chi_{1,1-\alpha/k}$ can be found from the tables of percentage points for the unit normal distribution i.e. "…, the χ^2 distribution, with one degree of freedom is the distribution of the square of a normal deviate: the 5% significance level of χ^2, 3.84, is simply the square of 1.96" (Snedecor and Cochran, 1967).

These techniques are statistically sound for computing the sample size needed to compute the overall accuracy of a classification or the overall accuracy of a single class. As suggested by Congalton (1991), these techniques are not designed to chose a sample size for filling in a confusion matrix. In the case of a confusion matrix, it is not a matter of correct or incorrect but it a matter of which categories are being confused. Due to the large number of pixels in remotely sensed datasets, practical considerations more often dictate the sample size selection than the traditional methods of sampling. The sample size selected this way should be such that a balance between what is statistically sound and what is practically attainable must be maintained. Mather (1999) and Swain and Davis (1978) recommended that a minimum sample of at least 30 times the number of features (discriminating variable or wavebands) per class would be suitable, while Congalton (1991) suggested a minimum of 50 samples for each land use class. Lillesend and Kiefer (1994) suggested a minimum of from 10 to 100 times the number of pixels should be used since the estimates of the mean vectors and covariance matrices improves (if data are normally distributed) as the number of training pixels increases. The number of pixels selected for each class can also be adjusted based on the relative importance of the class or by the inherent variability within each of the class. It is also useful to collect fewer number of pixels from the classes having little or no within class variability (like water and snow) and increase the number of sampled pixels in the classes that have more within class variability.

7.5 Sampling plan

The nature of the sampling plan is an important part of any accuracy assessment, due to the large volume of remotely sensed data in digital format. In remote sensing, sampling consists of (i) the creation of sub-areas from large scenes and (ii) the generation of pixel coordinate lists for use in various image processing tasks (Franklin et al., 1991). The output of pixel sampling is usually a table which is a compilation of image values and in some cases these values are referenced by their location (coordinates). These pixel values can be subjected to various statistical, image processing, and geographic information systems-type operations.

Selection of a proper sampling plan is important for assessing the accuracy of a classification system because a poor choice of sampling plan may introduce bias into the confusion matrix, which then may finally over- or under-estimate the actual accuracy of the classification (Congalton, 1991). The most commonly used sampling plans used in remote sensing studies are simple random sampling, cluster sampling, stratified random sampling, and systematic sampling. A number of studies have been carried out using different sampling plans, producing different opinions about each of the plans used (Hord and Brooner, 1976; Fitzpatrick-Lins, 1981; Congalton, 1988; Franklin et al., 1991; Stehman, 1992).

Simple random sampling is a method of selecting a sample of pixels from the total number of pixels available of a particular class such that every one of the possible distinct pixels has an equal chance of being selected (Cochran, 1977). In practice, a random number generator is used to identify a random coordinate pairs in the image to select the samples. At any stage, the process used must give an equal chance of selection to any pixel in the population not already drawn. The sample estimates (i.e. mean, variance) derived from simple random sampling are consistent and unbiased. An estimate is said to be consistent if the estimate equals the population parameter when the entire population is sampled. An estimate is said to be unbiased if the average value of the estimate at a given sample size over all possible samples is equal to the population average.

In cluster sampling, a group of pixels is selected. Each pixel must be unique to only one cluster of pixels. This method of sampling is much easier and cheaper than random sampling, but the disadvantages of cluster sampling are that the variance for a given sample is greater as compared to simple random sampling due to the homogeneity of elements in the clusters, and the complexity of subsequent statistical analysis is greater (Congalton, 1988).

In stratified sampling *a priori* knowledge is used to subdivide the population into non-overlapping categories. A number of samples is then selected from each strata. This selection should be made independently for each stratum. Stratified sampling is used when it is necessary to make sure that small, but important, areas are represented in the sample.

In systematic sampling, pixels are selected at some equal interval over time or space. The first sample drawn from the population is located at random and each successive pixel is collected at a specified interval thereafter. Due to the uniform spread of the sampled pixels over the entire population, systematic sampling is more accurate than stratified random sampling (Cochran, 1977). Its major disadvantage is that each sample in the entire population does not have an equal chance of being included in the sample and, if the population contained some periodicity, then the regular spacing of the sampling units might result in unrepresentative samples (Berry and Baker, 1968).

For this study two different sampling plans, - random sampling and systematic random sampling - were selected to collect pixels for training and testing the classifiers. A reference image generated after a field visit of the study area was used to select the pixels from the remotely sensed image.

7.6 Study area and data

The study area for this research is located within an area known as 'La Mancha Alta' that covers an area of approximately 8000 km^2 to the south of Madrid, Spain (Figures 7.3 and 7.4). This is an area of semi-arid wetlands that is typical of a Mediterranean environment. It is important as an area for migrating birds and rain-fed agricultural activities, such as cultivation of wheat and barley and other crops such as vines, and olives. However, the process of land degradation is increasing due to intensive agricultural practices. For this study, hyperspectral data acquired by the DAIS 7915 airborne imaging spectrometer taken on 29th June 2000, at five meter resolution were used. The data were collected for Prof. J. Gumuzzio of the Autonomous University of Madrid, who has kindly made them available for this study. This spectrometer was developed by the German

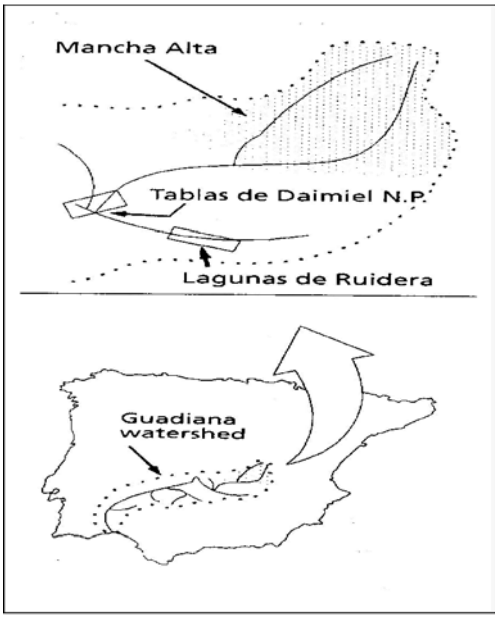

Figure 7. 3. La Mancha Alta region, Central Spain (adapted from Oliver and Florin, 1995).

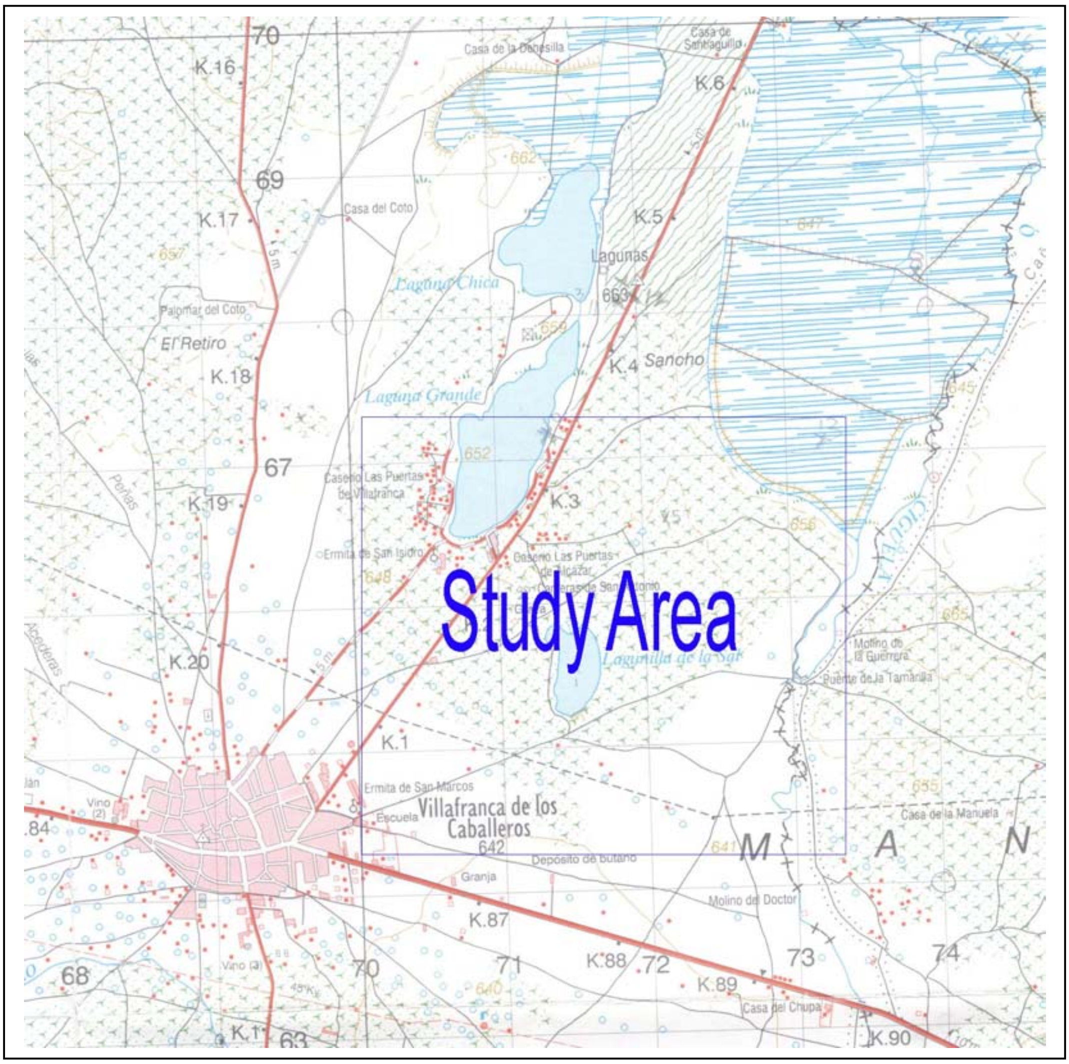

Figure 7. 4. Study area in La Mancha region.

Space Agency and the European Union. DAIS 7915 is a 79 channel high-resolution optical spectrometer operating in the wavelength range from 0.4 µm to 12.5 µm. The spatial resolution of the sensor can vary from 5 to 20 m depending on the altitude of the aircraft. With the exception of the 1.1 µm to the 1.4 µm region, all atmospheric windows from visible to the thermal infrared wavelengths are covered. The advantage of this system is that it has solely reflective optics with a large aperture, which gives high scan efficiency. The disadvantage is that it is highly susceptible to striping that results from intrinsic background radiation to the detector (Muller et al., 1998).

Eight different land cover types, namely wheat, water body, salt lake, hydrophytic vegetation, vineyards, bare soil, pasture lands and built up area were used for this study. An area of 512 pixels by 512 pixels in 65 bands covering the area of interest was extracted. As one aim of this study is to find out the effect of scale (resolution) of data on land cover classification accuracy, another data set for the same area from the ETM+ at 30 m resolution, acquired on 28th June 2000 was also used.

To collect the ground reference information required for land cover classification, field studies were carried out on 30th June 2001 with Prof. José Gumuzzio and Thomas Schmid of UAM, Madrid, Spain. Due to non-availability of field data for the year 2000 from the local farmers, a reference image was generated from the 2001 field data. While digitising the boundaries to create polygons for training data, only those fields which were most likely to have the same crop as in the previous year were used. Each polygon is assigned a label corresponding to the land cover it contains (Figure 7.5).

7.7 Classification

Multispectral sensors have been used to gather data about the Earth's surface since the 1960's. The number of spectral bands used by these sensors ranged from three to seven for space-borne sensors and up to 18 for airborne sensors. In contrast to such multispectral sensors, the new generation of remote sensing instruments, referred to as hyperspectral sensors, have tens or hundreds of contiguous narrow spectral bands. Data in ten or more bands are termed hyperspectral data, as opposed to multispectral data, in less than about 20 bands. Hyperspectral data potentially contain more information than multispectral data because hyperspectral data have higher spectral resolution. In statistical classifiers, the characteristics of a class are modelled using a set of parameters (such as the mean and covariance matrices) which are estimated based on some prior knowledge, such as data with known class labels. These class-labelled pixels, used to estimate class parameters and design a classifier, are called training samples (or training pixels). The accuracy of parameter estimation depends substantially on the ratio of the number of training samples to the dimensionality of the spectral bands. As the dimensionality increases, the number of training samples needed to characterise the classes increases. If the number of training samples becomes inadequate, which may be the case for hyperspectral data, parameter estimation becomes inaccurate (Hsiegh and Landgrebe, 1998).

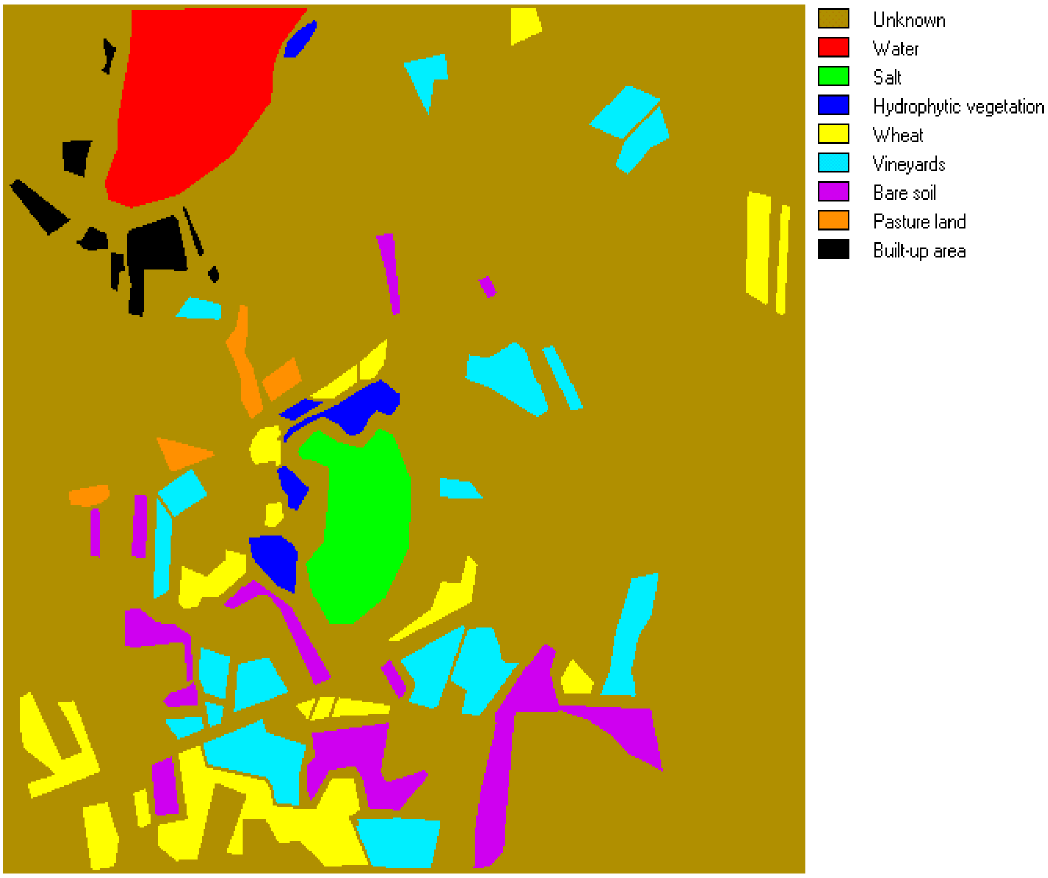

Figure 7. 5. The "ground reference" image for the test area.

Although increasing the number of spectral bands (dimensionality) potentially provides more information about class separability, this positive effect is diluted by poor parameter estimation performance due to an inadequate number of training pixels. As a result, classification accuracy first increases and then declines as the number of spectral bands increases. This behaviour is often referred to as the "Hughes phenomenon" (Hughes, 1968). In short, a small ratio of training samples to dimensionality may result in unreliable parameter estimation, leading to poor classification performance.

In general, classification performance depends on the following factors (Raudys, and Pikelis, 1980):

1. Class separability,
2. training sample size,
3. dimensionality, and
4. classifier type.

Classification performance improves if (a) more precise class parameter values are used (in case of a statistical classifier), (b) class separability increases, (c) the ratio of training sample size to dimensionality increases, and/or (d) a more appropriate classifier is chosen.

This research is designed to study the effects of change in number of training pixels on classification accuracy with the change in dimensionality of the data. Further, this study is extended to evaluate the effect of different sampling plans on classification accuracy using different classifiers. Data sets having 100, 200, 250, 300, 350, 400, and 500 pixels per class, using random sampling methods, and 400 pixels per class using systematic sampling methods were selected to train different classifiers. To generate the confusion matrix (which is used to compare the performance of different trained classifiers) a total of 3800 and 3880 pixels respectively were selected by random sampling and systematic sampling. Four different classification schemes were used - maximum likelihood, neural network, support vector machines, and decision tree classifiers. To compare the classification results obtained using different sampling schemes all of the above mentioned classifiers were employed.

7.7.1 Results and discussions

Figure 7.6 summarises the classification results obtained using different data sets with increasing number of bands. In this figure, the classification accuracies were obtained using Maximum Likelihood (ML), Artificial Neural Networks (ANN), Decision Tree (DT), and Support Vector Machine (SVM) classifiers, respectively. A total of sixty five features was used. Beginning with five bands, an additional five bands were added at each cycle, thus generating thirteen accuracy values for each data set. Figure 7.7 shows the variation in classification accuracy for different classification systems with varying number of bands and training patterns.

Results from Figure 7.6 suggests that there is no sharp fall in classification accuracy, even with ML classifier, as the number of features increases for a fixed number of training data, as suggested by earlier studies (Hughes, 1968). The accuracy value begins to stabilise after forty features with different numbers of training patterns. There is no significant change in classification accuracy as more features are added. Figure 7.6 suggests that maximum accuracy achieved with a small training data set occurs at lower dimensionality (number of features), as compared to the higher dimensionality when a larger training data set is used. One possible reason for this may be that a larger number of training patterns allows a better estimation of ML parameters, thus giving better classification accuracy. Generally, maximum accuracy is achieved at higher dimensions with more training data, supporting the view that more training data is needed as the number of features increases.

The results from neural and decision tree classifiers show a similar trend of variation in accuracy as the ML classifier. The performance of the NN classifier is almost quite similar to that of the ML classifier with all datasets and there is no significant difference in accuracy, except in a few cases. The accuracy achieved

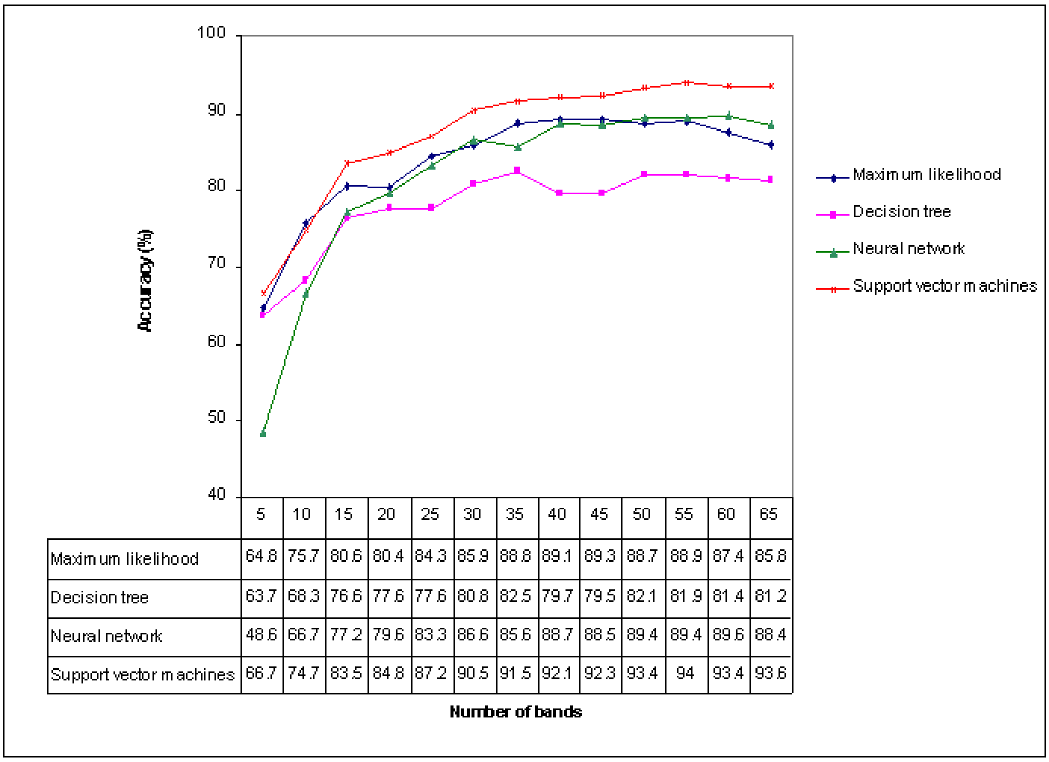

	5	10	15	20	25	30	35	40	45	50	55	60	65
Maximum likelihood	64.8	75.7	80.6	80.4	84.3	85.9	88.8	89.1	89.3	88.7	88.9	87.4	85.8
Decision tree	63.7	68.3	76.6	77.6	77.6	80.8	82.5	79.7	79.5	82.1	81.9	81.4	81.2
Neural network	48.6	66.7	77.2	79.6	83.3	86.6	85.6	88.7	88.5	89.4	89.4	89.6	88.4
Support vector machines	66.7	74.7	83.5	84.8	87.2	90.5	91.5	92.1	92.3	93.4	94	93.4	93.6

Figure 7.6 (a). Classification accuracies with 100 pixels/class.

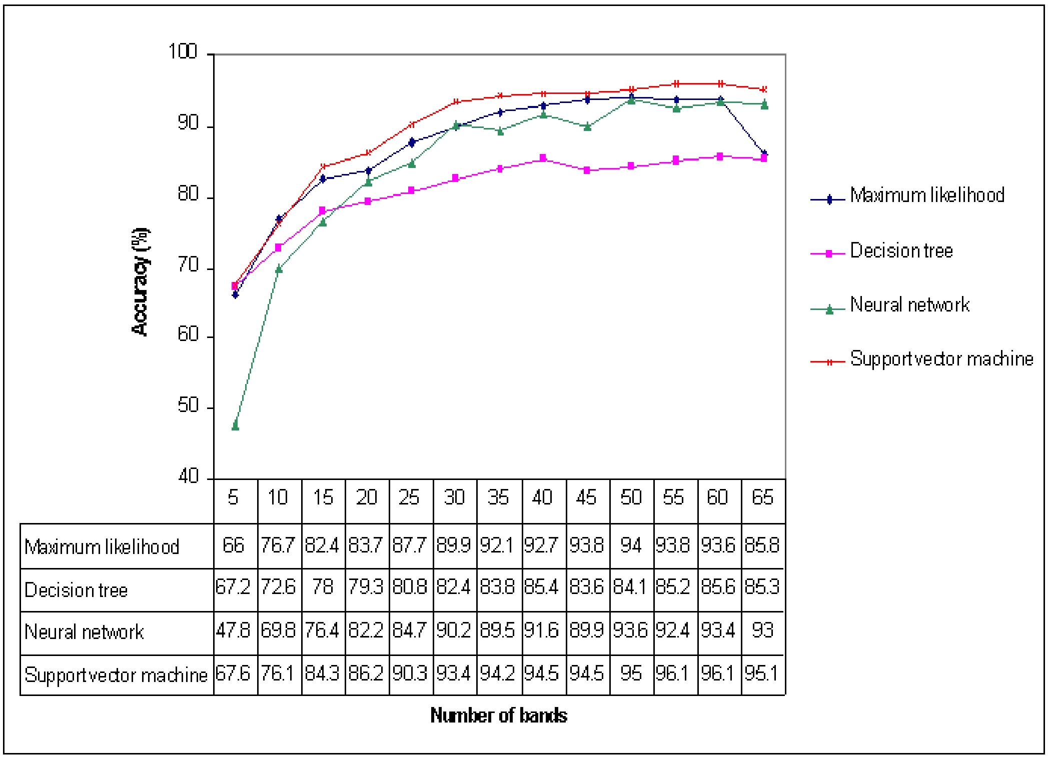

	5	10	15	20	25	30	35	40	45	50	55	60	65
Maximum likelihood	66	76.7	82.4	83.7	87.7	89.9	92.1	92.7	93.8	94	93.8	93.6	85.8
Decision tree	67.2	72.6	78	79.3	80.8	82.4	83.8	85.4	83.6	84.1	85.2	85.6	85.3
Neural network	47.8	69.8	76.4	82.2	84.7	90.2	89.5	91.6	89.9	93.6	92.4	93.4	93
Supportvector machine	67.6	76.1	84.3	86.2	90.3	93.4	94.2	94.5	94.5	95	96.1	96.1	95.1

Figure 7.6 (b). Classification accuracies with 200 pixels/class.

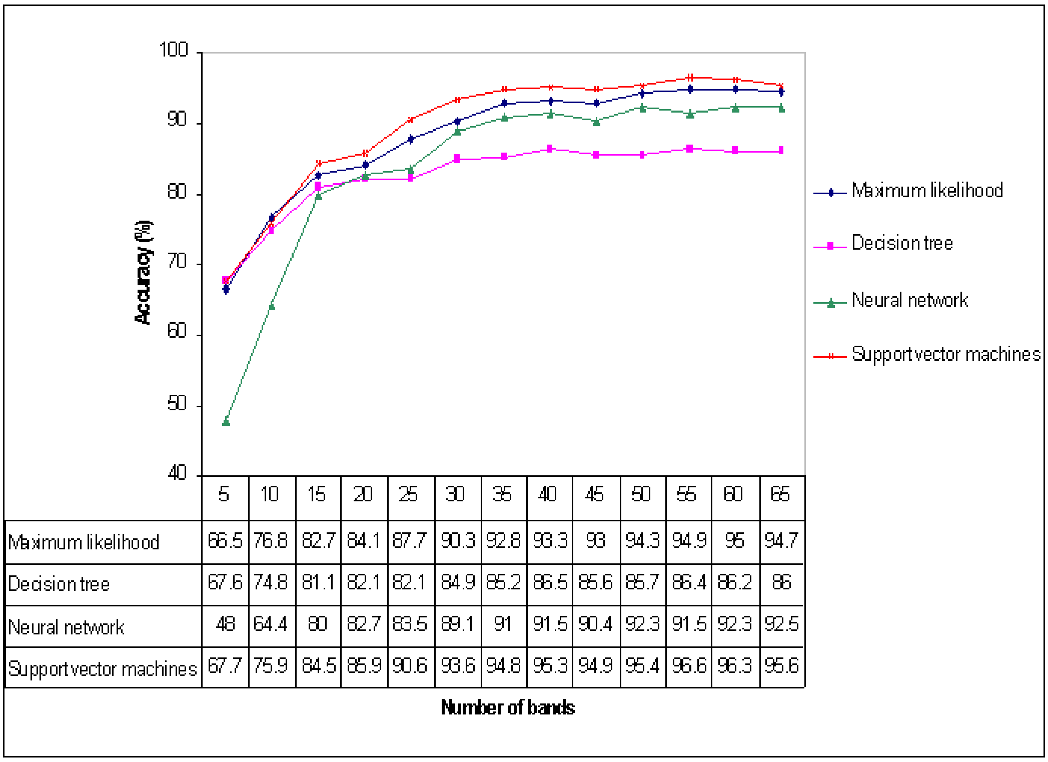

	5	10	15	20	25	30	35	40	45	50	55	60	65
Maximum likelihood	66.5	76.8	82.7	84.1	87.7	90.3	92.8	93.3	93	94.3	94.9	95	94.7
Decision tree	67.6	74.8	81.1	82.1	82.1	84.9	85.2	86.5	85.6	85.7	86.4	86.2	86
Neural network	48	64.4	80	82.7	83.5	89.1	91	91.5	90.4	92.3	91.5	92.3	92.5
Support vector machines	67.7	75.9	84.5	85.9	90.6	93.6	94.8	95.3	94.9	95.4	96.6	96.3	95.6

Figure 7.6(c) Classification accuracies with 250 pixels/class

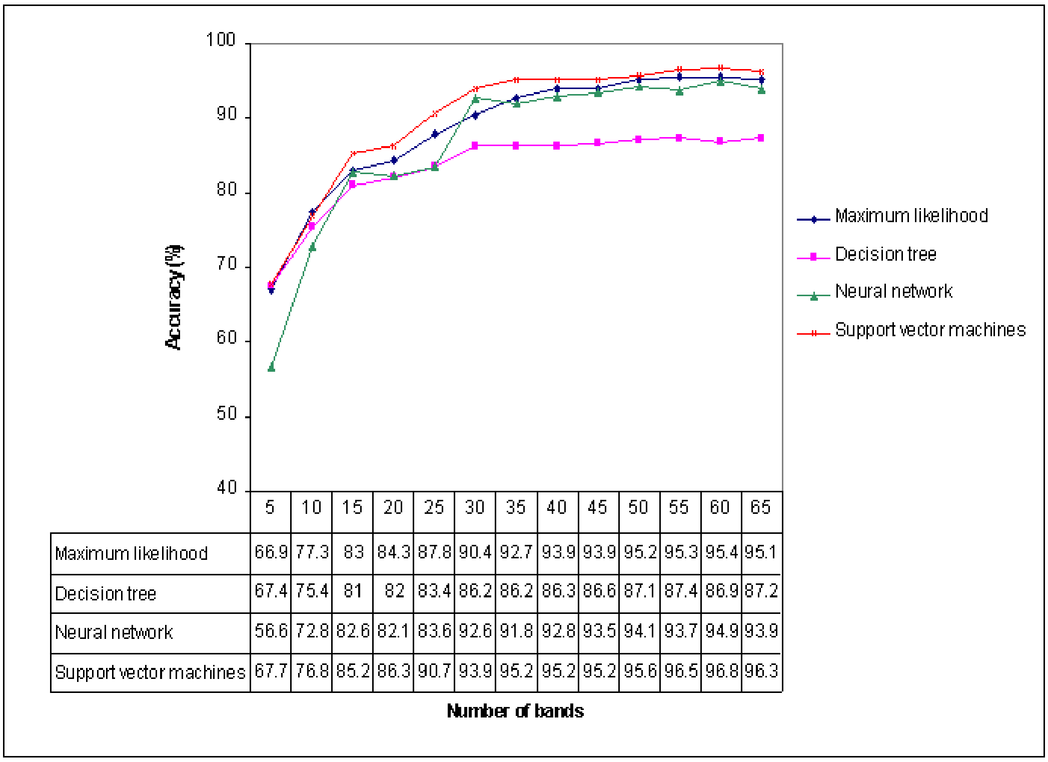

	5	10	15	20	25	30	35	40	45	50	55	60	65
Maximum likelihood	66.9	77.3	83	84.3	87.8	90.4	92.7	93.9	93.9	95.2	95.3	95.4	95.1
Decision tree	67.4	75.4	81	82	83.4	86.2	86.2	86.3	86.6	87.1	87.4	86.9	87.2
Neural network	56.6	72.8	82.6	82.1	83.6	92.6	91.8	92.8	93.5	94.1	93.7	94.9	93.9
Support vector machines	67.7	76.8	85.2	86.3	90.7	93.9	95.2	95.2	95.2	95.6	96.5	96.8	96.3

Figure 7.6(d) Classification accuracies with 300 pixels/class

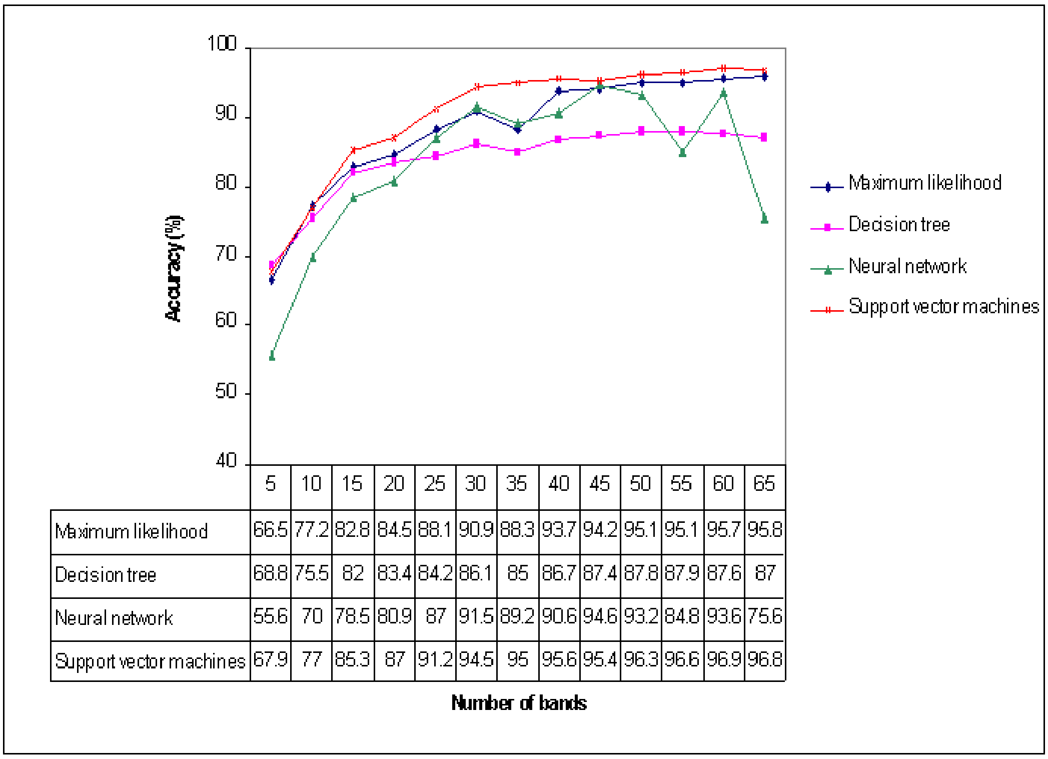

	5	10	15	20	25	30	35	40	45	50	55	60	65
Maximum likelihood	66.5	77.2	82.8	84.5	88.1	90.9	88.3	93.7	94.2	95.1	95.1	95.7	95.8
Decision tree	68.8	75.5	82	83.4	84.2	86.1	85	86.7	87.4	87.8	87.9	87.6	87
Neural network	55.6	70	78.5	80.9	87	91.5	89.2	90.6	94.6	93.2	84.8	93.6	75.6
Support vector machines	67.9	77	85.3	87	91.2	94.5	95	95.6	95.4	96.3	96.6	96.9	96.8

Figure 7.6(e) Classification accuracies with 350 pixels/class

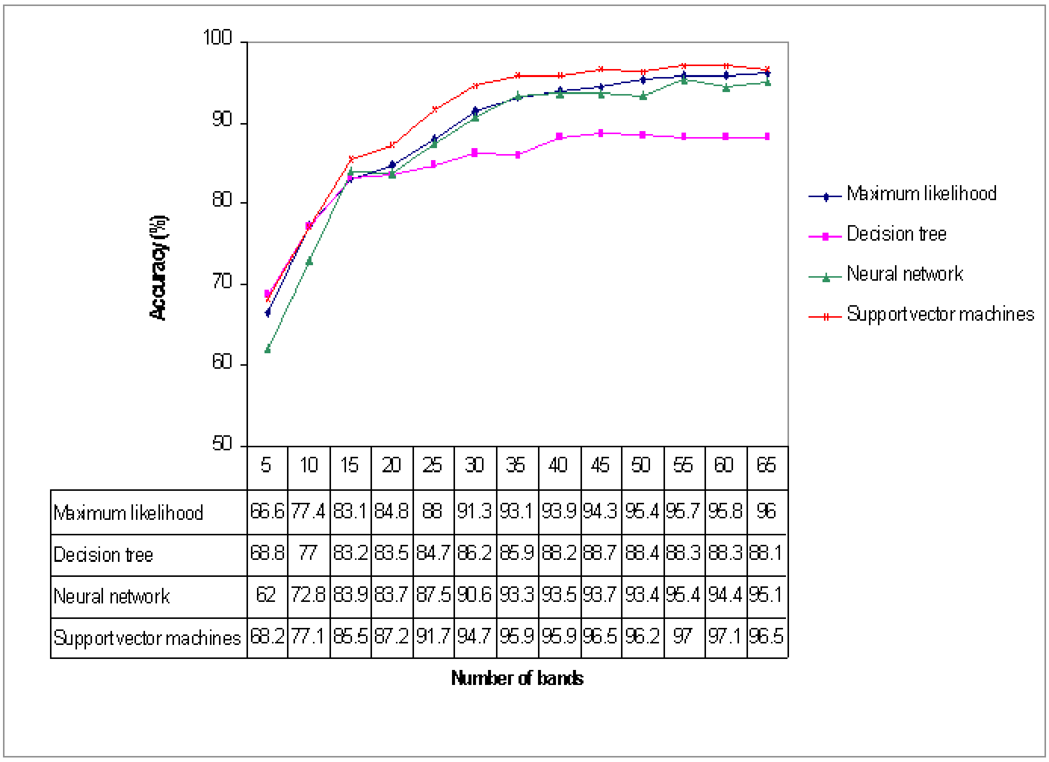

	5	10	15	20	25	30	35	40	45	50	55	60	65
Maximum likelihood	66.6	77.4	83.1	84.8	88	91.3	93.1	93.9	94.3	95.4	95.7	95.8	96
Decision tree	68.8	77	83.2	83.5	84.7	86.2	85.9	88.2	88.7	88.4	88.3	88.3	88.1
Neural network	62	72.8	83.9	83.7	87.5	90.6	93.3	93.5	93.7	93.4	95.4	94.4	95.1
Support vector machines	68.2	77.1	85.5	87.2	91.7	94.7	95.9	95.9	96.5	96.2	97	97.1	96.5

Figure 7.6(f) Classification accuracies with 400 pixels/class

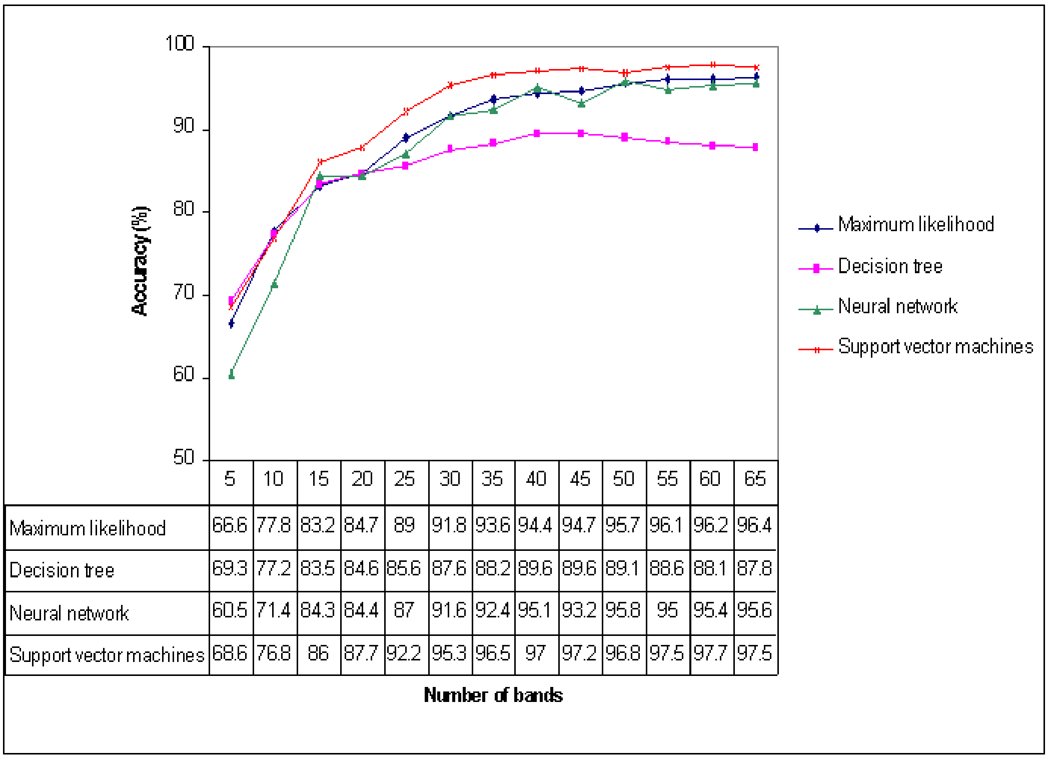

	5	10	15	20	25	30	35	40	45	50	55	60	65
Maximum likelihood	66.6	77.8	83.2	84.7	89	91.8	93.6	94.4	94.7	95.7	96.1	96.2	96.4
Decision tree	69.3	77.2	83.5	84.6	85.6	87.6	88.2	89.6	89.6	89.1	88.6	88.1	87.8
Neural network	60.5	71.4	84.3	84.4	87	91.6	92.4	95.1	93.2	95.8	95	95.4	95.6
Support vector machines	68.6	76.8	86	87.7	92.2	95.3	96.5	97	97.2	96.8	97.5	97.7	97.5

Figure 7.6(g) Classification accuracies with 500 pixels/class

Figure 7. 6. Variation in classification accuracy with change in number of bands with different training sets.

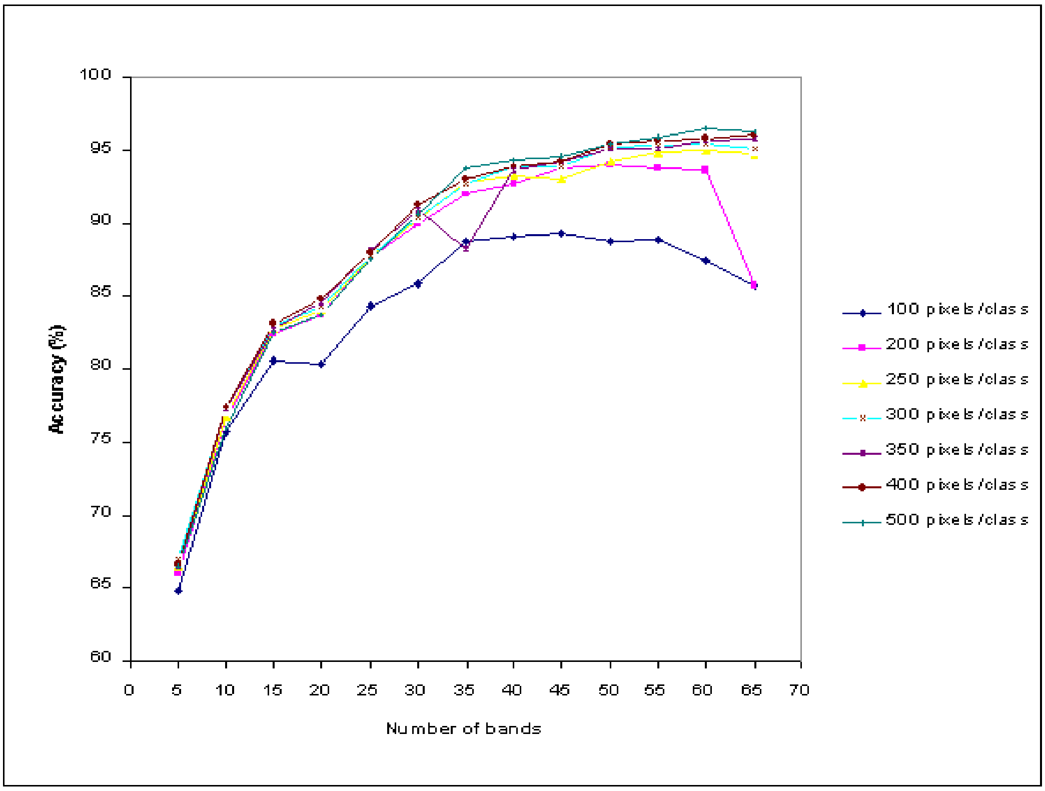

Figure 7.7(a) Classification accuracies with maximum likelihood classifier

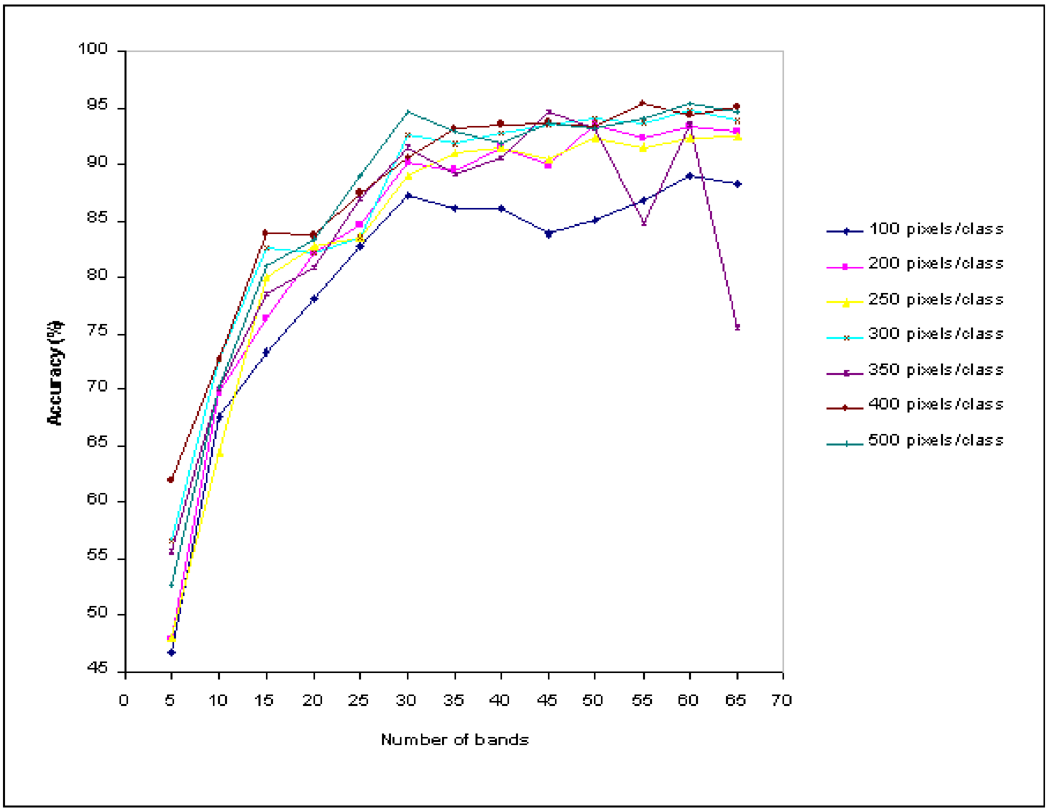

Figure 7.7(b) Classification accuracies with neural network classifier

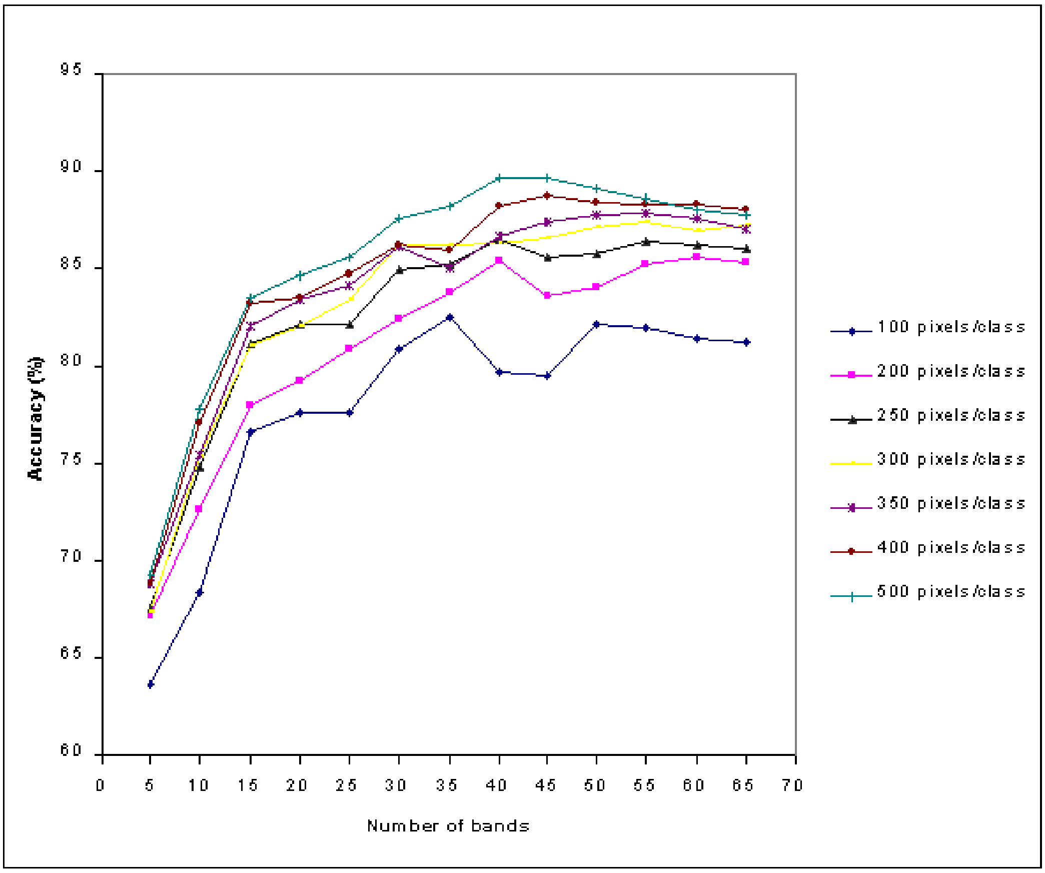

Figure 7.7(c) Classification accuracies with decision tree classifier

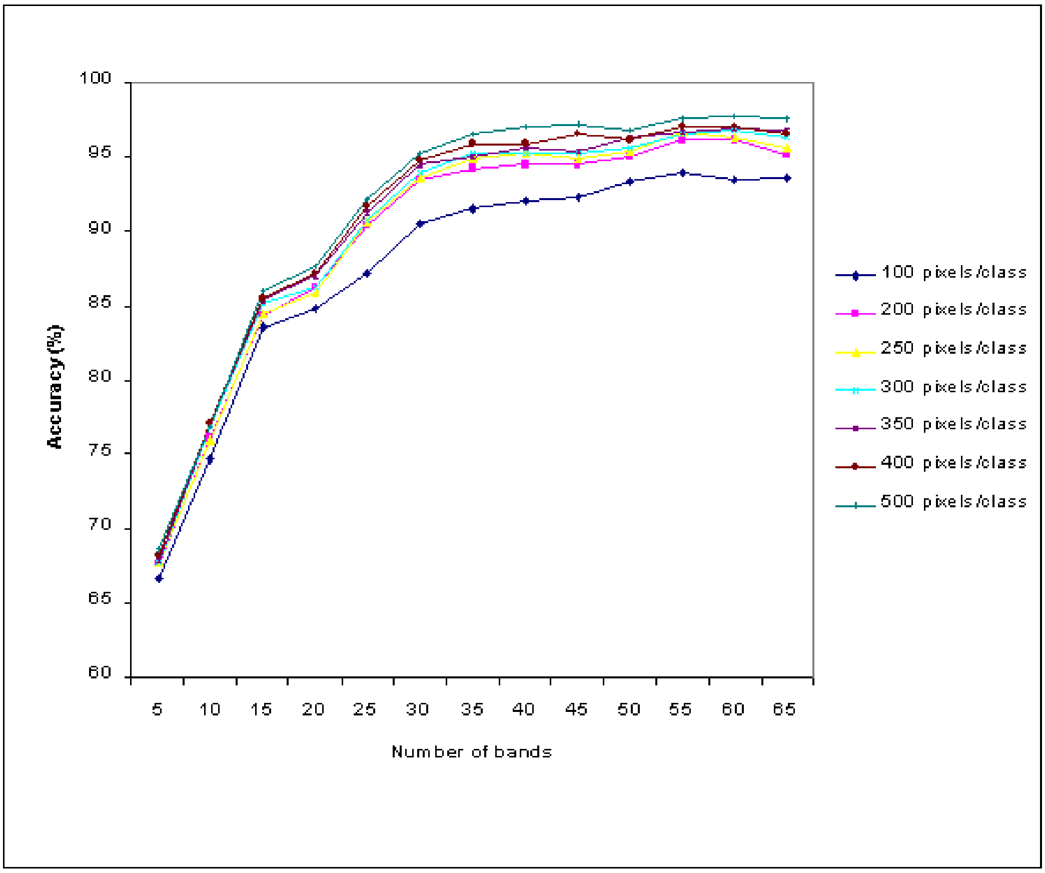

Figure 7.7(d) Classification accuracies with support vector machines

Figure 7. 7. Variation in classification accuracy with different classifiers using different number of bands and training datasets.

using the NN classifier with a small number of training data is higher than the ML classifier, suggesting that the NN classifier performs better with a small number of training data. Further, this study suggests that the performance of the DT classifier declines as the number of features increases using different data sets. The possible reasons may be (1) the performance of the DT classifier is always affected by the number of training patterns used (section 4.3.1) and (2) a univariate DT classifier performs better with a small number of features. As the number of training data increases, the performance of the DT classifier becomes better and comparable to the ML and NN classifiers up to a certain number of features. For this data set, as the number of features (dimensionality) increases, class structure becomes more dependent on a combinations of features, thus making it difficult for a univariate DT classifier to perform well.

One remarkable property of SVM is that their ability to learn is independent of the dimensionality of the feature space. SVMs measure the complexity of hypotheses based on the margin with which they separate the data, not on the number of features. This means that it is possible to generalise even in the presence of very many features, if our data are separable with a wider margin using functions from the feature space. Figure 7.6 suggests that the performance of an SVM is good even with a small number of training data in comparison with other classifiers. Further, results form Figure 7.7 suggests that classification accuracy increases continuously with few exceptions in all datasets, with a fixed number of training data and the increasing number of features, thus suggesting that this classification system is unaffected by the Hughes (1968) phenomenon.

Figure 7.7 suggests that classification accuracy always increases as the number of training data increases, irrespective of number of features and classifier used, suggesting that the performances of all four classification algorithms used in this study are affected by the number of training patterns, even with a fixed number of features. Further, Figure 7.7 suggests that peak in classification accuracy occurs at a much higher dimensionality as suggested by Hughes (1968). The results reported here concur with the suggestion of Abend and Harley (1969) that highest classification accuracy occurs when the number of features is higher than the number suggested by Hughes (1968).

Further studies were carried out to compare the results of random and systematic sampling plans used to collect pixels for training and for testing classifier performances. For this study, Maximum Likelihood (ML), Neural Network (NN), Decision Tree (DT), and Support Vector Machine (SVM) classifiers and 400 training pixels/class collected using both sampling methods were used. A total of 3800 pixels were selected by random sampling, and 3880 by systematic random sampling for testing the classifiers. A pairwise statistic for testing the significance of the classifiers is used (equation 2.8, where κ_1 and κ_2 correspond to kappa values calculated from the random and the systematic random sampling plans respectively). The results are summarised in Table 7.1.

This table shows that, there are “positive” improvements (grey coloured values) in maximum likelihood classifier performances using the random sampling plan (e.g., for the ML and 20 features, *Z* = 2.201 > 1.96 while *Z* = 2.186 > 1.96 using 45 features). Overall, the majority of experiments suggest that the use of a random sampling strategy produces a higher classification accuracy than does the systematic sampling plan, for the maximum likelihood classifier. Results obtained with the neural network classifier are not consistent and suggest that the results from both the systematic and the random sampling depend on the number of features used (e.g., Z = 3.25 > 1.96 for 30 features, suggesting better results with systematic random sampling).

Table 7. 1. Calculated Z values for comparison among the different sampling plans using Kappa analysis. Shaded values indicate significant improvements in the performance of the classifiers at the 95% confidence level *(Z* critical value = 1.96). Negative value indicates better performance of the systematic random sampling plan over the random sampling plan.

Number of features	ML classifier	NN classifier	DT classifier	SVM
5	0.569	5.190	-1.004	0.33
10	0.548	1.114	1.620	-0.64
15	1.015	0.755	0.920	-1.21
20	2.201	-0.434	0.310	-1.77
25	2.080	-0.970	0.530	-1.71
30	2.100	-3.250	-0.110	-1.23
35	1.470	0.463	-1.690	-0.39
40	0.000	-1.622	0.360	-1.60
45	2.186	2.590	0.120	1.00
50	2.263	-.801	0.710	-0.82
55	2.155	3.087	0.810	-0.22
60	2.008	-0.857	1.180	-0.46
65	1.732	1.740	0.590	-1.28

Results obtained using DT and SVM suggests that these classifier perform equally well with random and systematic random sampling plans. Thus, this study gives an idea that NN, DT, and SVM classifiers perform comparably well with both sampling plans as compared to maximum likelihood classifier, which works well with a random sampling scheme only.

7.8 Dimensionality reduction

The recent development of more sophisticated sensors for remote sensing systems enables the measurement of radiation in many more spectral intervals than was previous possible. An example of this technology is the AVIRIS system, which collects image data in 220 bands. The increased dimensionality of such hyperspectral data provides a challenge to current techniques for analysing such data. As the number of dimensions of high spectral resolution data increases, the capability to detect more detailed classes should also increase, although, with the increase of the number of features, with corresponding increase in the cost and complexity of the feature extraction and classifier, it is expected that the classification accuracy will also increase.

Usually the number of training samples is limited. It has been observed frequently in practice that beyond a certain point, if the number of training samples per feature is small, the addition of more dimensions leads to a worse performance in terms of a penalty in the test samples classification accuracy. Hughes (1968) suggested that the basic source of the problem is the limited number of training samples. The problem becomes more serious in high dimensional cases. In order to avoid what has been named the Hughes phenomenon, there have been some empirical and analytical studies to find a relationship in the number of training samples and the number of features. Fukunaga and Hays (1989) demonstrated that the required number of training samples is linearly related to the dimensionality for a linear classifier and to the square of the dimensionality for a quadratic classifier.

The negative impact of high dimensionality on classifier performance means that it is generally agreed that some form of dimensionality reduction, or feature selection, is considered appropriate. A number of techniques for feature extraction including Principal Components (Watanabe, 1965), maximum noise fraction transformation (Green at al., 1988) and non-orthogonal techniques such as projection pursuit (Jiminez and Landgrebe, 1999) have been developed to reduce the dimensionality of the data. In this study the maximum noise fraction (MNF) transformation is used to reduce the dimensionality of the hyperspectral data set, but a brief description of principal component analysis (PCA) is also given, as the MNF transform is a variant or development of PCA.

7.8.1 Principal Components Analysis

The principal component transformation is also known as the eigenvector transformation, the Hotelling transformation, or the Karhunen-Loēve (K-L) transformation in the remote sensing and pattern recognition literature. It is a multivariate statistical technique that essentially consists of choosing uncorrelated linear combinations of the variables in such a way that each successively extracted linear combination, called a principal component, has a smaller variance than its predecessor. If the variables have significant linear intercorrelations, the first few components will accounts for a large part of the total variance. Principal components transformation is based on pixel wise operation that does not take the spatial nature of image data into account. Also, PCA does not always produce components that show decreasing image quality with increasing component number.

The application of this transformation requires an estimate of the variance-covariance matrix of the features. The principal components maximise the variance represented by each component. PC-1 is the linear combination of the original bands that explains the maximum variance in the original data. A higher order PC is the combination of the original bands that explains maximum variance subject to the constraint that it is uncorrelated with lower order PCs.

Let A and D denotes the multiband image mean and pixel value vectors, respectively. The covariance matrix σ can be calculated by the expression:

$$\sigma = \frac{\sum_{i=1}^{n}(D_i - A)\times(D_i - A)^T}{n-1} \tag{7.3}$$

where n is the number of pixels. If the correlation matrix is used, each entry in variance-covariance matrix is divided by the product of the standard deviations of the features represented by the corresponding row and column.

The second step is the calculation of the eigenvectors of σ, which can be achieved by solving the following equation:

$$(\sigma - \lambda_j I)\times K_j = 0 \tag{7.4}$$

where K_j is the eigenvector corresponding to the eigenvalue λ_j, and I is the identity matrix. The new coordinate system is formed by the normalised eigenvectors of the variance-covariance matrix and each pixel value is then projected on this new coordinate system to get a new pixel value.

A drawback of principal components analysis is that its results depend on the unit of measurement of the original variables. This problem can be circumvented by performing the PC transformation on a correlation matrix instead of on the covariance matrix. For details of principal components transformation, readers are referred to Mather (1999).

7.8.2 Maximum Noise Fraction (MNF) transform

Principal components do not always produce components of decreasing image quality with increasing component number (Townshend, 1984). While working with spatial data, the maximisation of variance across bands is not an optimal approach if the issue is ordering in term of image quality rather than variance. One of the most common measures of image quality is the signal-to-noise ratio. Thus, instead of choosing new components to maximise variance, as the principal components transform does, the MNF transform choose components to maximise the signal-to-noise ratio.

This transformation can be defined in several ways. It can be shown that the same set of eigenvectors is obtained by procedures that maximise the signal-to-noise ratio and the noise fraction. The procedure was first introduced by Green et al. (1988) in continuation of the work on Minimum/maximum autocorrelation factors by Switzer and Green (1984). Hence the name maximum noise fraction (MNF).

The application of the MNF transformation requires estimates of the signal and noise covariance matrices. MNF number one is the linear combination of the original bands that contains the minimum signal-to-noise ratio. A higher order MNF is the linear combination of the original bands that contains minimum signal-to-noise ratio subject to the constraint that it is orthogonal to the lower order MNFs. The MNF transform is equivalent to a transformation of the data to a coordinate system in which the noise covariance matrix is the identity matrix followed by a principal component transformation. To deduce the maximum noise transformation, consider a multivariate data set of p-bands with grey levels

$$Z_i(x), \qquad i = 1, \ldots, p$$

where x gives the coordinates of the sample. If it is assumed that

$$Z(x) = S(x) + N(x) \tag{7.5}$$

where $Z^T(x) = \{Z_1(x), \ldots\ldots, Z_p(x)\}$, and S(x) and N(x) are the uncorrelated signal and noise component of Z(x). Thus

$$\mathrm{Cov}\{Z(x)\} = \sum = \sum{}_S + \sum{}_N \tag{7.6}$$

where Σ_S and Σ_N are the covariance matrices of S(x) and N(x), respectively. This noise is assumed to be additive but this technique can be applied to multiplicative noise by first taking logarithms of the observations.

The noise fraction of the i^{th} band can be defined as:

$$\mathrm{Var}\{N_i(x)\}/\mathrm{Var}\{Z_i(x)\} \tag{7.7}$$

the ratio of the noise variance to the total variance for that band. The maximum noise fraction can be defined as the linear transformations:

$$Y_i(x) = a_i^T Z(x),\ \mathrm{i} = 1, \ldots, \mathrm{p} \tag{7.8}$$

such that the signal-to-noise ratio for $Y_i(x)$ is maximum among all linear transformations orthogonal to $Y_j(x), j = 1,\ldots\ldots, i$. Furthermore it is assumed that eigenvectors a_i are normalised so that

$$a_i^T \sum a_i = 1, \quad \mathrm{i} = 1, \ldots, \mathrm{p} \tag{7.9}$$

Using arguments similar to those used in the derivation of principal components, it can be shown that the vectors a_i are the left-hand eigenvectors of $\Sigma_N \Sigma^{-1}$, and that μ_i, the eigenvalue corresponding to a_i, equals the noise fraction in $Y_i(x)$. Hence, from the definition of the MNF transform, MNF components will show steadily increasing image quality, with increasing component number.

An important property of the MNF transform, which is not shared by principal components, is that - because it depends on signal-to-noise ratios - it is invariant under scale changes to any feature. Another useful property is that it orthogonalises S(x) and N(x), as well as Z(x). The central problem in the calculation of the MNF transformation is the estimation of the noise component with the purpose of generation a covariance matrix that approximates Σ_N.

A number of methods to calculate the noise covariance matrix are suggested in the literature (Olsen, 1993). These are as follows:

1. Simple differencing. The noise is estimated as the difference between the current and neighbouring pixel.
2. Differencing with the local mean. More pixels could be entered to the estimation by differencing between the current pixel and the local mean of a window.
3. The noise is estimated as the residual in simultaneous autoregressive (SAR) model involving the neighbouring pixel to the W, NW, N and NE of the current pixel.
4. Differencing with local median. To avoid the blurring of edges and other details, the local median could be used instead of the local mean as in (2).
5. Quadratic surface. The noise is estimated as the residual from a fitted quadratic surface in a neighbourhood.

For this study, a simple differencing method as suggested by Green et al. (1988) was used to estimate the noise covariance matrix. The noise is estimated as the difference between the current and a neighbouring pixel (horizontal neighbour). In this case $\sum_{N}$ is referred as $\sum_{\Delta}$.

The hyperspectral data set contained 65 features (bands). A total of thirteen maximum noise fraction components was extracted using the criterion of image quality. A total of 4000 pixels for training and 3200 pixels for testing was selected using a random sampling plan. The results obtained with four different classification schemes used are shown in Table 7.2 (the corresponding confusion matrices are provided in appendix D).

The results shown in Table 7.2 suggest that the maximum likelihood classifier performs the worst of all four classifiers used with MNF transformed data. The possible reason for this poor performance may be due to zero noise covariance of two classes (water and salt) while calculating the MNF components which finally affects the calculation of ML parameters for these two classes. The decision tree classifier performs well, compared to the support vector machine, maximum likelihood, and neural classifiers. Nevertheless the accuracy achieved is lower than the highest accuracy achieved using the original hyperspectral data.

Table 7. 2. Results with MNF transformed image.

Classifier	Accuracy (%)	Kappa value
Maximum likelihood	61.10	0.556
Neural network	87.10	0.854
Decision tree	88.56	0.869
Support vector machine	88.20	0.865

Decision tree classifiers can be used to uncover structures in data (Breiman et al. 1984, Safavian and Landgrebe 1991) and the hierarchical relationships revealed by partitioning feature space, thus, decision tree classifier can be used to eliminate redundant or noisy features in input data. Feature selection was therefore attempted, using the tree-based approach (using *See 5.0* software) to reduce the dimensionality of hyperspectral data. Initially, decision trees of maximum size were generated using all sixty-five input features. By inspection of the full tree, those features that contributed most of the variance in the training data were retained for the subsequent classification phase. A total of 25 features was selected this way and used to compare the capabilities of four different classification systems (maximum likelihood, neural, support vector machines, and decision tree classifiers). For this study a total of 3200 pixels (for 8 classes, with 400 pixels/class) and 3800 pixels, all randomly selected, were used for training and testing, respectively. Table 7.3 gives the classification accuracy and Kappa value achieved with this data set. The corresponding confusion matrix is listed in appendix E.

The results listed in Table 7.3 suggest that feature selection using decision trees is effective in reducing the dimensionality of input feature space. Although the decision tree method reduced the number of input features by about 60%, classification accuracies were not significantly degraded. No classifier performed as well or better with the feature subsets than with the total number of features, yet the accuracies achieved are quite high and comparable to the accuracies obtained with a full complement of features.

Table 7. 3. Results obtained by applying decision tree based feature selection.

Classifier	Accuracy (%)	Kappa value
Maximum likelihood	94.10	0.935
Neural network	92.10	0.911
Decision tree	87.60	0.858
Support vector machine	95.30	0.946

Further studies were carried out to find out the effect of scale (resolution) on classification accuracy. For this study, ETM+ data (30 m resolution) of the same area in Spain, acquired on 28th June 2000, were used. Figure 7.8 gives an idea of the quality of the images at two different resolutions for same study area and indicating how difficult is to locate field boundaries in the ETM+ data to prepare a ground reference image. Thus, for this study, a ground reference image generated using hyperspectral data was used to collect the pixels for training and testing the different classifiers. The image shown in Figure 7.5 was resampled at 30m resolution so as to make it compatible with ETM+ data. Six classes (water, salt, wheat, vineyards, bare soil, and built-up area) were used in place of the eight classes used with DAIS data due to the lack of a sufficient number of pixels for two classes - pasture land and hydrophytic vegetation. A total of 1395 pixels were collected using a random sampling plan, out of which 600 pixels were used for training and remaining 795 pixels for testing the classifiers.

The results shown in Table 7.4 (and in the corresponding confusion matrices, listed in appendix F) suggest that, even at this scale, high accuracy can be obtained. The highest accuracy of 91.1% is achieved with support vector machine. However, comparison of the classified images (Figures 7.9 (a) 7.9 (b)) suggests that, except for the water and salt classes, no other class boundary is properly located and it is very difficult to locate the area covered by other classes in the

Table 7. 4. Classification results obtained with ETM+ data for the La Mancha test area of Spain.

Classifier	Accuracy (%)	Kappa value
Maximum likelihood	83.9	0.797
Neural network	89.4	0.869
Decision tree	84.7	0.810
Support vector machine	91.1	0.880

classified image (Figure 7.9 (b)). Thus, one possible reason of achieving very high classification accuracy may be due the small number and nature of data used for testing the different Classifiers, as suggested by Congalton (1988), the nature of the testing set can have a significant affect on the resulting classification accuracy. As with the training data, the testing set must also be representative of the classes and the test samples should be drawn from across the test area and the sample large enough for a rigorous evaluation of the classification accuracy.

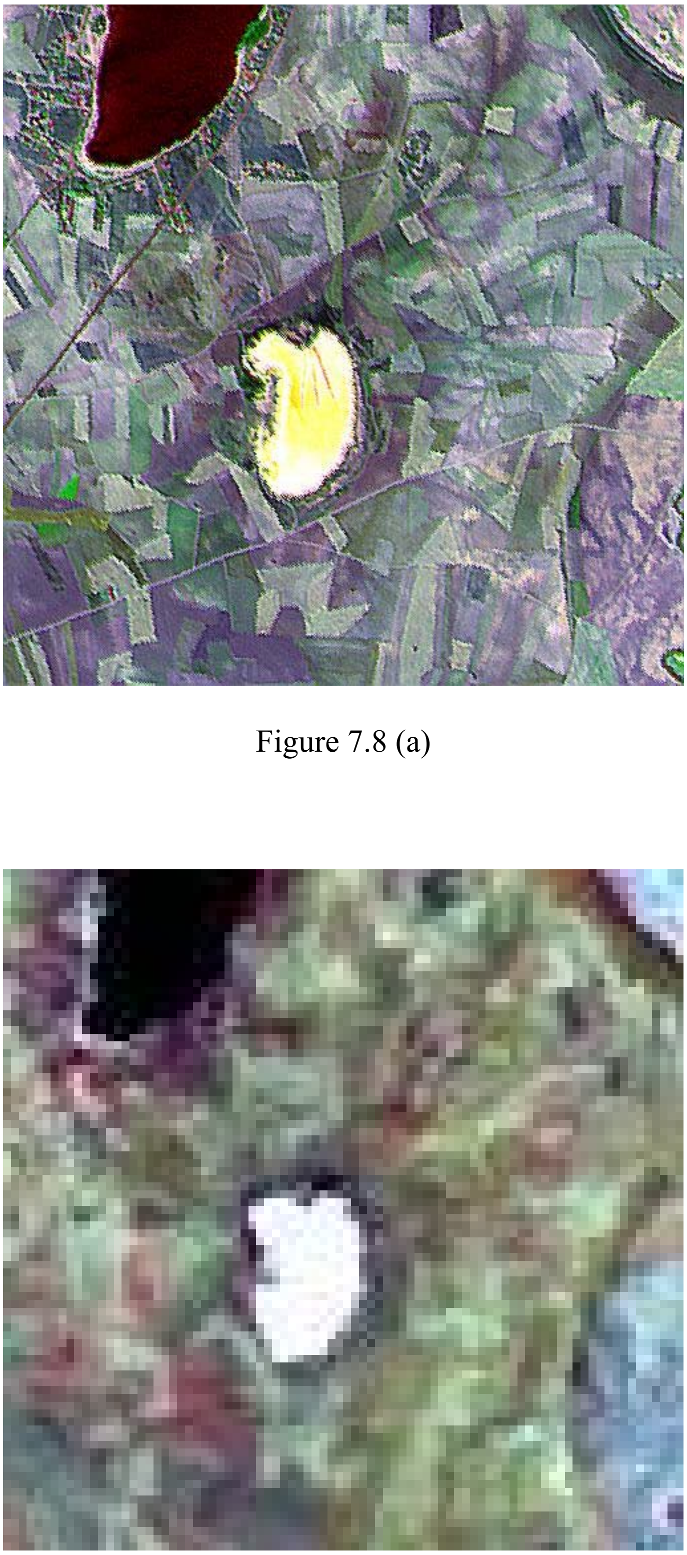

Figure 7.8 (a)

Figure 7.8 (b)

Figure 7. 8. Images of the study area (a) DAIS hyperspectral image (5m resolution) and (b) ETM+ image (30m resolution).

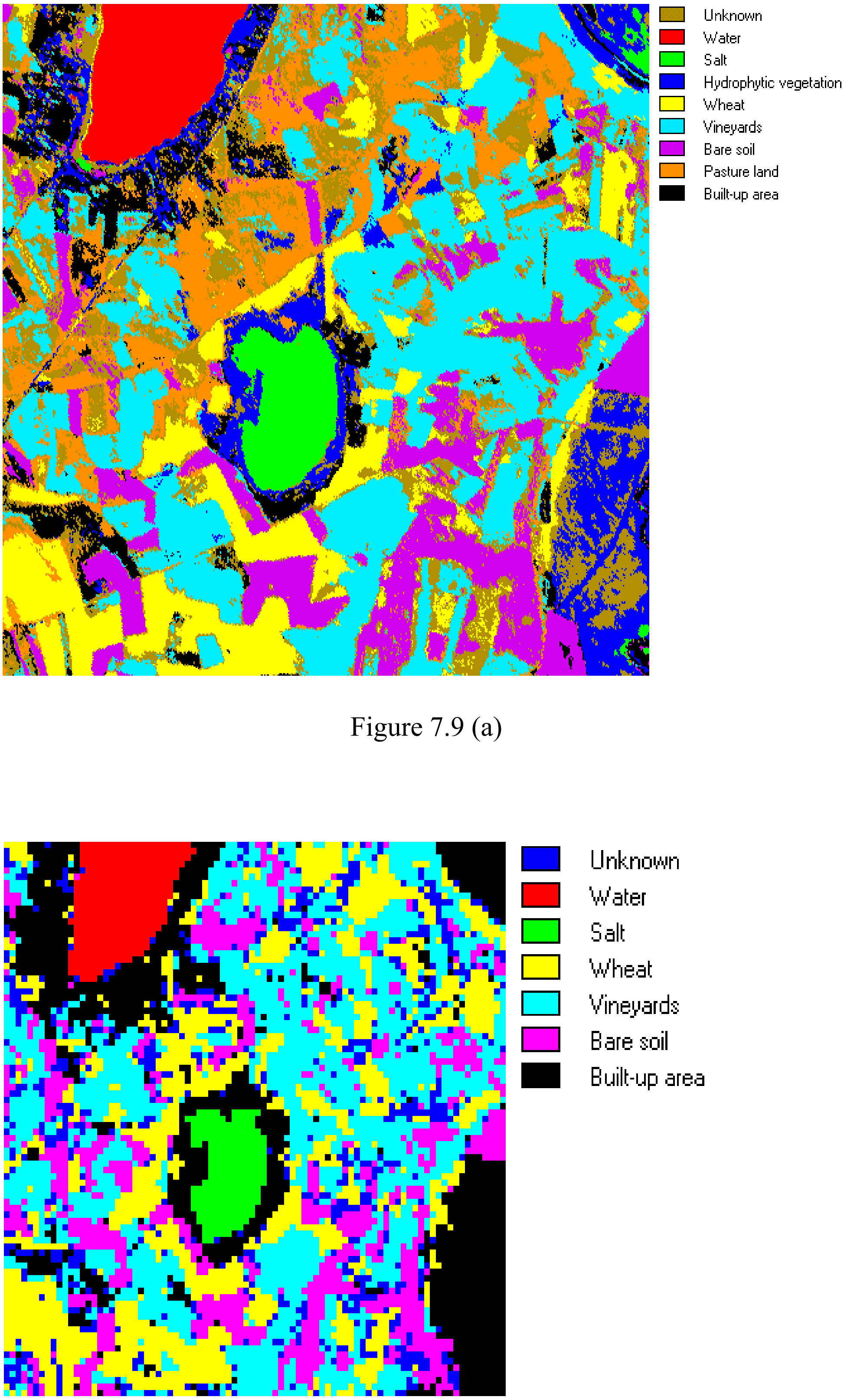

Figure 7.9 (a)

Figure 7.9 (b)

Figure 7. 9. Classified images using neural network classifier (a) DAIS hyperspectral image (5m resolution) and (b) ETM+ image (30m resolution).

7.9 Conclusions

This work was carried out to study the effect of the factors of sample size, sampling plan, number of features in relation with sample size, dimensionality reduction, and scale (resolution) of the data on land cover classification accuracy using different classification algorithms. First, this study suggests no sudden change in classification accuracy after a peak value, even with a small number of training data, with increasing numbers of features as suggested by Hughes (1968) while using maximum likelihood, neural and decision tree classifiers. Otherwise, the results suggest that accuracy starts to stabilise once a maximum value is reached. This study also suggests that highest accuracy is achieved at higher dimensionality with different data sets, contrary to the study carried out by Hughes (1968), thus justifying the suggestions made by Abend and Harley (1969). The results with support vector machines suggests its insensitivity to the Hughes phenomenon. Further, this study suggests, that for the maximum likelihood classifier, training and test data collected using a random sampling plan produce higher classification accuracies than those achieved using a systematic sampling plan. Both sampling plans perform well with support vector machine, decision tree, and neural network classifiers for this type of data.

By applying an MNF transformation, the dimensionality of the hyperspectral dataset reduces to thirteen features, but the level of classification accuracy achieved is not comparable with that obtained from the use of all of the features of DAIS data. This result suggests that the MNF technique may not be used effectively for dimensionality reduction for this type of data. On the other hand, decision tree (DT)-based dimensionality reduction techniques perform well, and the accuracy achieved is higher than that achieved by using MNF transformation. The accuracy achieved with features obtained using the DT-based dimensionality reduction technique is comparable to the accuracy achieved by using the full set of features, suggesting that the DT approach can be effectively used for feature selection with hyperspectral data.

Further studies suggest that classification accuracy is always affected by the scale (resolution) of the data used for a particular type of area because scale has an influence on observed variability both within and between classes (Markham and Townshend, 1981). Changes in classification accuracies using data at different scales show the dependence of classification accuracy on scale or resolution of the data used, suggesting a need to consider the spatial resolution of remotely sensed data relative to the inherent characteristics of the study area.

1. **SVM classifier is not affected by Hughes (1968) phenomenon.**
2. **Training dataset size affects all classification algorithms.**
3. **MNF did not work well with this dataset.**
4. **DT, ANN, and SVM works well with both random and systematic sampling plans.**
5. **ML works well with random sampling plans.**
6. **Decision tree provides an effective way for dimensionality reduction.**
7. **Scale of remote sensing data affects the classification accuracy as suggested by several other studies.**

Chapter 8

Overview of results and future research directions

8.1 Introduction

Identifying land cover type and change in land cover is an important task for land and resource management at local and regional scales. However, detecting and monitoring these changes using ground measurements is limited by logistics and cost. Remote sensing provides an alternate and useful perspective for collecting the information for studying these changes, and producing land cover maps using various classification methods. A number of statistical and neural classification methods have been developed and used for classification of remotely sensed data. However, each method has its limitations; for example, statistical classifiers, being parametric in nature, assume that the data follow a particular frequency distribution. Artificial neural networks, a nonparametric technique, have been used extensively in a variety of problems in the remote sensing field, and perform well when compared to statistical classifiers. However, a range of factors limit their use in land use classification studies. Decision tree (DT) and support vector machine (SVM) classifiers, new nonparametric techniques for analysing remote sensing images, have the potential to improve the land cover classification accuracy. It is worth mentioning that choice of scale (resolution), number of features, type of data (optical or radar), training data as well as sampling plan have as much as influence as the classifier on classification results.

The main aim of this chapter is to summarise the results presented in previous chapters. The first part of this research demonstrates the utility of decision tree classification methods for land cover classification derived from remotely sensed images. This stage also involved a comparison of results obtained with decision tree classifiers with the most widely-used methods (statistical and neural classifiers) for classifying agricultural crops. The second stage of this study involves assessing the behaviour of support vector machines for land cover classification studies. The third part of this work involves the assessment of the utility of interferometric SAR coherence measurements for land cover classification. This stage also discusses some methods of feature extraction and selection. Finally, a detailed study is carried out to analyse the performance of various classifiers using different sampling plans, different numbers of training data with changes in number of features, and data at different scales as well as the effect of orthogonal transformation on classification accuracy using hyperspectral data. Conclusions drawn from this research are summarised and presented in the following subsections**.**

8.1.1 The usefulness of decision tree classifiers and support vector machines

Chapter 3 describes the decision tree classifier, which is a multi-stage classification technique that decomposes a complex classification problem into several stages, finally simplifying the decision-making process by taking partial decisions at each stage of classification. This chapter also introduces support vector machines, a classification technique which maximises the margin between the class boundaries and based on structural risk minimisation techniques. Classification results using decision tree classifiers are discussed in chapters 5 (section 5.1), 6 and 7. Chapters 5 (section 5.2) and 7 discuss the results obtained using support vector machines. A critical assessment of the problems encountered in the use and design of decision tree classifiers and support vector machines is also presented in chapter 3.

The decision-tree and support vector machines-based classification approach, used for classifying agricultural crops using various type of remotely sensed data, have been found to be effective in identifying general agricultural crop classes, with acceptable levels of overall classification accuracy in comparison with neural and statistical classifiers.

The conclusions reached from this study using the three datasets described in chapters 5 (sections 5.1, 5.2), 6 and 7 are presented in the conclusion section of each chapter. The most important conclusions of this study are:

- The performance of DT classifiers (both univariate and multivariate) is affected by the number of training patterns used to train the classifier.

- In spite of being nonparametric in nature, DT classifiers perform poorly in comparison with neural and statistical classifier when using small training datasets. This observation suggests that a sufficient number of training data is required for DT classifiers.

- When a sufficient number of training data and small number of features are used (e. g., data from ETM+), classification results achieved by a univariate DT classifier are invariably better than those from a ML classifier.

- SVM perform well - in fact, better than DT, ANN and ML classifiers - with small training datasets, but classification accuracy improves as the number of training pixels increases.

- As the number of features increases, with training dataset size held constant, the performance of a univariate DT classifier starts to degrade, and classification accuracy falls below that produced by the maximum likelihood classifier, indicating that the univariate DT classifier performs less well in high dimension feature space, where class information is dependent on a combination of features. In contrast, support vector machines perform well and better than DT, ANN, and ML classifiers with a fixed training dataset size and increasing number of features.

- Results obtained employing various attribute selection measures with the error based pruning method, and employing various pruning methods with the information gain ratio as the attribute selection measure, suggest that the performance of a DT classifier is affected by the pruning method used, and not by the attribute selection methods.

- Assessment of the effect of boosting on the level of classification accuracy achieved by the DT classifier indicates that classification accuracy is increased by about 3-4%. The study also concludes that about 10 to 15 boosting iteration are enough to attain this increase in classification accuracy.

- The DT classifier performance is slightly inferior to that of the ANN classifier using ETM+ data. However, it performs better with InSAR data even without boosting. After boosting, the DT classifier always perform better than the ANN classifier. Performance of the SVM classifier is always better than either the DT or the ANN with ETM+ data.

- Assessment of the effect of the number of factors affecting classification accuracy using ANN and DT classifiers shows that the number of factors affecting the performance of the ANN classifier is high in comparison to the DT classifier, which is affected by only two factors. Classification accuracy obtained using SVM is affected by a number of factors, such as: choice of kernel, user-defined parameters for various kernels, number of training data, and multi-class method used. This suggests that a skilled and experienced person is needed to work with ANN and SVM, requiring extra financial resources for training.

- This study suggests that when the SVM classifier is used, the "one against one" multi-class method performs better than the " one against rest" multi-class strategy.

- The time taken to train and test a DT classifier is very short compared to an ANN classifier. For an ETM+ data set of the Littleport area, the training time for a DT classifier is 0.7 seconds compared to 58 minutes for an ANN. Even the use of boosting (14 iterations) increases the training time for the DT by only a small amount (to 7.1 seconds).

- The time taken for training a SVM depends on the multi-class method used. The o*ne against the rest* multi-class method requires several hours of training time, while the *one against one* multi-class method needs a significantly smaller training time, which is almost same as the time taken by a ML.

- Further studies carried out include the use of the internal texture of panchromatic ETM+ band with multispectral data using DT, ANN, and ML classifiers suggest no significant improvement in classification accuracy.

- A DT can be used effectively for feature selection.

8.1.2 Use of coherence for land use classification

Another important issue reviewed in this thesis is the use of InSAR data for land cover classification studies. SAR data are now available with phase and intensity information. It is possible to utilise the phase information to generate a coherence image for use in land cover classification studies in combination with the intensity images obtained during InSAR processing. Relatively few studies have used coherence information in land cover studies; one reason may be that obtaining a good quality coherence image depends on several factors. The value of texture measures (e.g. GLCM, the MAR model, and fractals) and feature selection using Hotelling's T^2 test were assessed. The results obtained from this study using DT, ANN and ML classifiers are discussed in chapter 6. The main conclusions are summarised below:

- The combination of coherence and intensity images results in an improved classification accuracy of the order of 8-9%, as compared to using intensity images alone.

- The quality of coherence information depends on several factors (that is why only one acceptably good coherence image was obtained from the five Single Look Complex (SLC) used in this study). This, suggests that tandem interferometric pairs are more suitable for good quality coherence images.

- Inclusion of texture information with coherence and intensity images was found to be effective in improving classification accuracy. By using three texture features per coherence and intensity image, obtained after feature selection, an increase in classification accuracy by an amount of 10% to 12% (depending on the classifier used) was observed.

- The highest accuracy obtained was from a data set with a total of 24 features is 82.9%, which justifies the value of texture information but at the cost of increase in computation time as well as the requirement for a large number of training data.

8.1.3 Issues in remote sensing image classification

Advancement in sensor technology provides data with a much higher dimensionality than before. Although such high-dimensional data have the potential to provide increased amounts of information, new problems arises that have not been encountered in the analysis of relatively low dimensional data. The more important of these problems in analysing high dimensional data are investigated in chapter 7. Conclusions drawn from this study are as follows:

- Classification accuracy stabilises after reaching a peak as the number of features increases, when the number of training data is fixed. Accuracy increases with the increase in number of training patterns for a fixed number of features with all four classifiers used in this study, suggesting that performance of all of these classifiers depends on the number of training data.

- A random sampling plan for training data selection was found to perform well as compared to a systematic sampling plan when using a ML classifier.

- The ANN classifier performs well with both random and systematic sampling plans, depending on the number of features used, while SVM and DT work well with both random and systematic random sampling plans irrespective of the number of features used.

- The MNF transformation reduces the dimensionality of 65-band DAIS hyperspectral data to thirteen features, but classification results suggests that this method is not very suitable for this type of study.

- DT-based feature extraction methods, using twenty five features, perform well with this data set. The level of accuracy obtained with this data set is comparable with the highest accuracy achieved by using all features of hyperspectral data, and results are better that those using the MNF transformation.

- Classification accuracy is always affected by the scale of the data used as well as the classifier used for a particular type of data, thus confirming that the type of data and classifier used for classification studies are dependent on the characteristics of the study area.

- Performance of the SVM classifier for hyperspectral data is very encouraging, and is far better than ML, ANN and DT classifiers, with a small training dataset sizes and with increasing number of features. Further, this study suggests that the SVM classifier is not affected by the Hughes phenomenon.

Work reported in this thesis provides evidence that the expected classification accuracy for remotely sensed data is directly affected by a number of factors. Tables 8.1 and 8.2 provide a comparison of classifier performance and various factors affecting the classification accuracy with different classification algorithms used in this study.

8.2 Suggestions for future research

Results obtained from this study suggests a considerable potential for extending the investigating into developing new strategies for the design of DT and ANN classifiers. In the design of multilayer feedforward neural networks, the structure of the network (the number of hidden layer and number of neurons in each hidden layer) is not known in advance, and is often chosen heuristically and by trial and error. Studies carried out by Sethi (1990) offer a way to uncover the structure of the network. This study suggests the use of a neural network design methodology (called an entropy net) by exploiting the similarities between the hierarchical classifiers and the multiple-layer neural network. The main advantage of this approach is to eliminate the guess-work involved in the design of ANN classifiers.

Table 8. 1. Classification accuracies obtained using various algorithms and the factor affecting the classifier.

Number of training pixels	Classifier used	Assumption	User-defined parameters	Classification accuracy (%) and Kappa value	Training time (CPU time)
2700 randomly selected using ETM+ data	Neural Network (back propagation algorithm)	Nonparametric	1. Number of Hidden units and layers 2. Number of iterations 3. Learning parameters, such as momentum and learning rate 4. Initial weight setting	85.1(0.829)	58 minutes (SUN machine)
	Decision Tree	Nonparametric	1. Attribute selection measure and 2. Pruning method	84.24 (0.816) without boosting 88.46 (0.865) with boosting	0.7 seconds (PC Pentium II) 7.1 seconds (PC Pentium II)
	Support Vector Machines	Nonparametric	1. Kernel type 2. Parameter for kernel used 3. Multi-class method used 4. Parameter C	79.13 (0.77) with "one against rest" multi-class method 87.37 (0.86) "one against one" multi-class method using Royal Holloway and AT&T software 87.92 (0.87) "one against one" multi-class method using LIBSVM software	505.27 minutes (SUN machine) 21.54 minutes (SUN machine) 0.30 minutes (SUN machine)
	Maximum Likelihood	Parametric	None	82.9 (0.801)	0.20 minutes (SUN machine)

Table 8. 2. Calculated Z values for comparison between different classification systems. Shaded values indicate significant improvements in the performance of first classifier at the 95% confidence level (Z critical value = 1.96). While unshaded value indicates that both classifiers perform equally well. WB means "without boosting" and B means "boosting" a decision tree classifier.

Classifiers	Z value
Decision tree(WB) vs. Maximum likelihood	2.13
Decision tree (WB) vs. Neural network	1.01
Decision tree (B) vs. Neural network	2.54
SVM vs. Neural network	2.46
SVM vs. Decision tree (WB)	3.40
SVM vs. Decision tree (B)	-0.08

Studies carried out by Gelfand and Guo (1991) suggest that ANNs can be used as internal nodes of a decision tree to perform the task of feature selection. It is therefore suggested that further work is needed to evaluate a classification system obtained by combining both neural and decision tree classifiers. In order to improve and extend the use of decision tree classifiers for land cover classification studies of complex data sets, fuzzy representation of inexact and uncertain information about the area should be examined (Jenikow, 1998).

Studies carried out in chapters 5.1 and 7 concludes that DT classifiers require a large training dataset size in order to achieve good classification results, irrespective of the data used. With hyperspectral data, such as the DAIS data set used in this study, the training set requirement for correct application of these classification is very high. Requirement of a large training set for mapping runs contrary to a major goal of remote sensing, which involves extrapolation over large areas from limited ground data. SVM offer a possibility to train a generalisable, nonlinear, classifier in high-dimension space using a small training data set, which can be very useful for mapping from regional to global scale, where availability of ground truth information is limited. Further, the use of boosting, a new methodology being used to generate ensembles of classifiers, is also suggested with SVM.

8.3 Algorithm choice - some guidelines

The conclusions drawn and the experiments carried out during this study can be used to form a number of guidelines that can greatly facilitate the use of various classification algorithms with different datasets. It should be noted that these guidelines are valid for similar datasets and classification problems used in this study. The list of the guidelines is given as follows:

A. Ease of use:

1. Maximum likelihood and decision tree classifier - easiest
2. Support vector machines
3. Neural Network. - required skilled analyst

B. Accuracy (multispectral / InSAR data):

1. Support vector machines - highest
2. Neural network
3. Decision tree
4. Maximum likelihood - lowest

C. Accuracy (hyperspectral data):

1. Support vector machines - highest
2. Maximum likelihood
3. Neural network
4. Decision tree - lowest

D. Computational demand:

    1. Neural network - high
    2. Support vector machines / Maximum likelihood - medium
    3. Decision tree - low

E. sensitivity to sample size and sampling plan:

    1. Maximum likelihood - very sensitive to both sample size and sampling plan.
    2. Decision tree - very sensitive to sample size, not to sampling plan.
    3. Neural network - sensitive to sample size, not to sampling plan.
    4. Support vector machines - sensitive to sample size but performs very well with small dataset; not sensitive to sampling plan.

F. Availability

    1. Maximum likelihood - provided with almost all commercial image processing software.
    2. Decision tree - provided with statistical software packages. Some freely downloadable from the internet. Some commercial (stand alone) software packages.
    3. Neural network - SNNS software free from internet; ENVI, and some commercial (standalone) softwares.
    4. Support vector machines - some freely downloadable software from internet.

Figure 8.1 gives a graphical representation of the effects of the factors listed above on the choice of a classification algorithm. A scale of 1-5 is chosen to grade different factors. Two different choice of algorithms is represented in the Figure 8.1, one for multispectral/radar and other for hyperspectral data. The result suggests that support vector machine classifier are the best choice for all datasets.

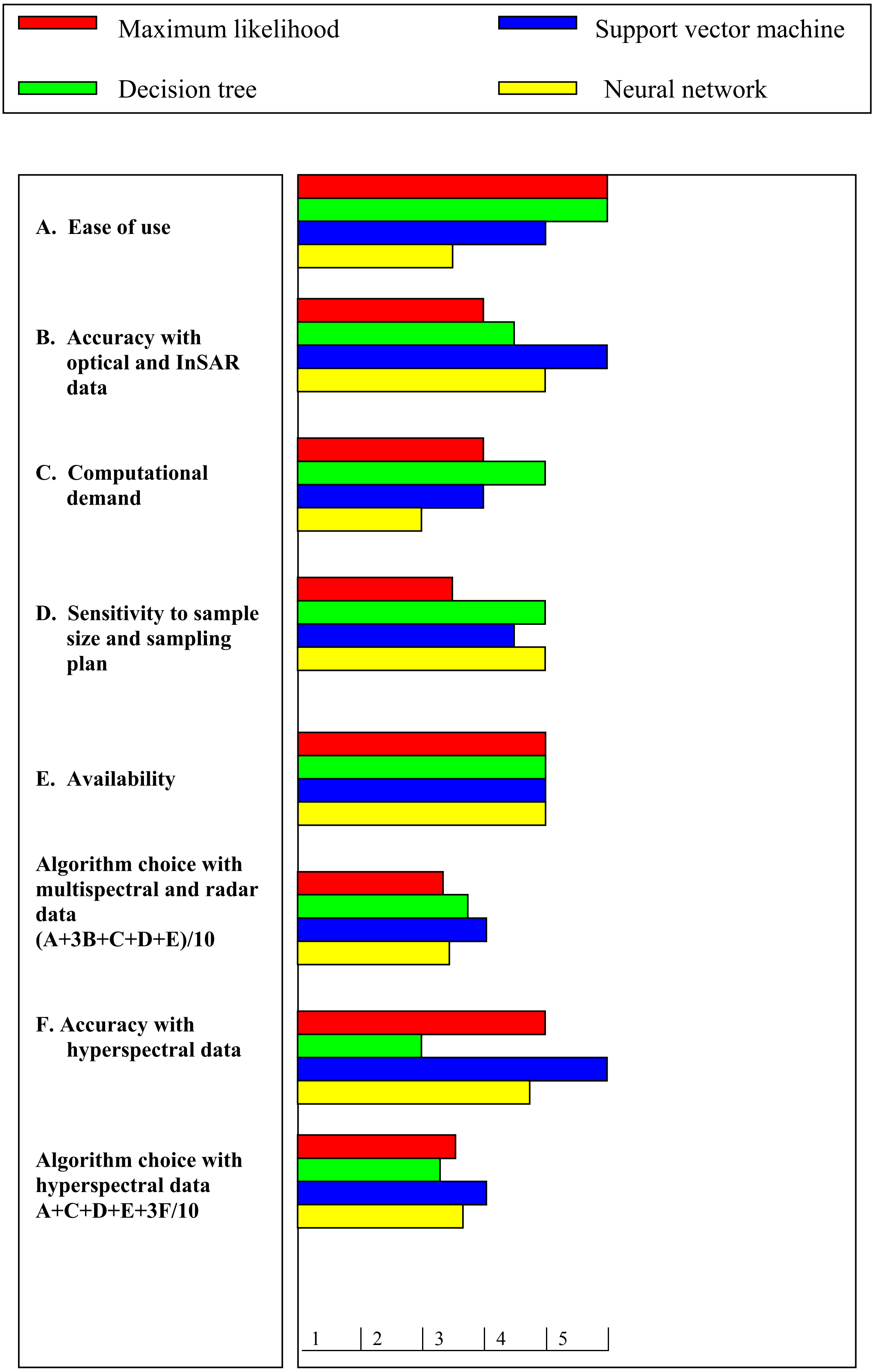

Figure 8. 1. Algorithm choice for different type of data depending on different factors. Higher grading is given to the classifier, which provides high accuracy and easy in use. A classifier that requires small computational time and less sensitive to both sampling plan and sample size is given high grading.

Bibliography

Abend, K., and Harley, T. J. (1969) Comments "On the mean accuracy of statistical pattern recognisers". *IEEE Transactions of Information Theory*, May, 420-421.

Aleksander, I., and Morton, H. (1991) *An Introduction to Neural Computing*. London: Chapman and Hall.

Antikidis, E., Arino, O., Laur, H., and Arnaud, A. (1998) ERS SAR coherence and ATS R Hot Spots: a synergy for mapping deforested areas. The special case of the 1997 fire event in Indonesia. *Retrieval of Bio- and Physical Parameters from SAR Data for Land Application Workshop.* ESTEC, The Netherlands, 21- 23 October 1998, http://www.estec.esa.nl/CONFANNOUN/98c07/.

Askne, J., and Hagberg, J. O. (1993) Potential of interferometric SAR for classification of land surfaces. *Proceedings of the International Geoscience and Remote Sensing Symposium* (IGARSS`93), Tokyo, Japan, 18-21 August, 985-987.

Askne, J., Dammert, P., and Smith, G. (1996) Interferometric SAR observations of forested areas. *FRINGE-ESA Workshop on Application of ERS SAR Interferometry*, University of Zurich, 30 September to 2 October, http://www.geo.unizh.ch/rsl/fringe96/.

Atlas, L., Cole, R., Muthusamy, Y., Lippman, A., Connor, J., Park, D., El-Sharkawi, M., and Mark Ii, R. J. (1990) A performance comparison of trained multilayer perceptrons and trained classification trees. *Proceedings of the IEEE*, **78**, 1614-1619.

Ball, G. H., and Hall, D. J. (1965) *A Novel Method of Data Analysis and Pattern Classification*. Menlo Park, CA: Stanford Research Institute.

Bao, M. (1999) Classification of multi-temporal SAR images and InSAR coherence images using adaptive neighbourhood model and simulated annealing approach. *Proceedings of 20th Asian Conference on Remote Sensing*. 22-25 November 1999, Hongkong, China.

Barber, D. G., and LeDrew, E. F. (1991) SAR sea ice discrimination using texture statistics: A multivariate approach. *Photogrammetric Engineering and Remote Sensin*g, **57**, 385-395.

Baraldi, A., and Parmiggiani, F. (1995) A neural network for unsupervised categorisation of multivalued input patterns: an application to satellite image clustering. *I.E.E.E. Transactions on Geoscience and Remote Sensing*, **33**, 305-316.

Belward, A. S., and Hoyos, A. D. (1987) A comparison of supervised maximum likelihood and decision tree classification for crop cover estimation from multitemporal LANDSAT MSS data. *International Journal of Remote Sensing,* **8**, 229-235.

Benediktsson, J. A., Swain, P. H., and Erase, O. K. (1990) Neural network approaches versus statistical methods in classification of multisource remote sensing data. *IEEE Transactions on Geoscience and Remote Sensing*, **28**,540-551.

Berry, B. J. L., and Baker, A. M. (1968) Geographical sampling. *Spatial Analysis: A Reader in Statistical Geography*, (Berry, B. J. L., and Marble, D. F. eds.), Englewood Cliffs, N. J.: Prentice-Hall.

Bezdek, J. (1981) *Pattern Recognition with Fuzzy Objective Function Algorithms*. New York: Plenum Press.

Bishop, Y., Fienberg, S., and Holland, P. (1975) *Discrete Multivariate Analysis-Theory and Practice*. Cambridge, MA: MIT Press.

Bishop, C. M. (1995) *Neural Networks for Pattern Recognition*. Oxford: Clarendon Press.

Booth, D. J., and Oldfield, R. B. (1989) A comparision of classification algorithms in term of speed and accuracy after the application of a post-classification model filter. *International Journal of Remote Sensing,* **10**, 1271-1276.

Borak, J. S., and Strahler, A. H. (1999) Feature selection and land cover classification of a MODIS-like data set for semi-arid environment. *International Journal of Remote Sensing*, **20**, 919-938.

Born, M., and Wolf, E. (1980) P*rinciples of Optics*. Oxford: Pergamon Press.

Boser, B., Guyon, I., and Vapnik, V. N. (1992) A training algorithm for optimal margin classifiers. *Proceedings of 5th Annual Workshop on Computer Learning Theory*, Pittsburgh, PA: ACM, 144-152.

Borgelt, C., Gebhardt, J., and Kruse, R. (1996) Concepts for Probabilistic and Possibilistic Induction of Decision Trees on Real World Data. *Proceedings of 4th European Congress on Intelligent Techniques and Soft Computing*, Aachen, Germany, **3**, 1556-1560.

Breiman, L. (1996) Bagging predictors. *Machine Learning,* **24**, 123-140.

Breiman, L., Friedman, J. H., Olshen, R. A., and Stone, C. J. (1984) *Classification and Regression Trees.* Monterey, CA: Wadsworth.

Brodley, C. E., and Utgoff, P. E. (1992) Multivariate versus univariate decision trees. *Technical Report 92-8*. Department of Computer Science, University of Massachusetts, Amherst, Massachusetts, USA.

Bryan, M. L. (1974) Extraction of urban land cover data from multiplexed synthetic aperture radar imagery. *Proceedings of the Ninth International Symposium on Remote Sensing of the Environment*, ERIM, Ann Arbor, Michgan, 271-288.

Buck, C. H., and Monni, S. (1999) Application of SAR Interferometer to Flood Damage Assessment. *CEOS SAR Workshop*, ESA-CNES Toulouse, 26-29 October, http://www.estec.esa.nl/ceos99/.

Burges, C. J. C. (1998) A tutorial on support vector machines for pattern recognition. *Data Mining and Knowledge Discovery*, **2**, 121-167.

Caldwell, M. M., Matson, P. A., Wessman, C., and Gamon, J. (1993) *Prospects for scaling. Scaling Physiological Processes: Leaf to Globe*, Academic Press, San Diego, 1993, 223-230.

Campbell, J. B. (1981) Spatial correlation effects upon accuracy of supervised classification of land cover. *Photogrammetric Engineering and Remote Sensin*g, **47**, 355-363.

Canada Centre for Remote Sensing (CCRS), *CCRS Remote Sensing Tutorials: Radar and Stereoscopy*, http:/www.ccrs.nrcan.gc.ca/ccrs/eduref/sradar/.

Cannon., M., Lehar, A., and Preston, F. (1983) Background pattern removal by power spectral filtering. *Applied Optics*, **22(6)**, 777-779.

Cao, C., and Lam, N. S. (1997) Understanding the scale and resolution effects in remote sensing and GIS. *Scale in Remote Sensing and GIS,* Quattrochi, D. A., and Goodchild, M. A. ed., Boca Raton: CRC Press, 57-72.

Casey, R. G., and Nagy, G. (1984) Decision tree design using a probabilistic model. *IEEE Transactions on Information Theory*. **IT-30**, 93-99.

Chapelle, O., Haffner, P., and Vapnik, V. N. (1999) Support vector machines for histogram-based image classification. *IEEE Transactions on Neural Networks*, **10**, 1055-1064.

Civco, D. L. (1993) Artificial neural networks for land-cover classification and mapping. *International Journal of Geographical Information Systems*, **7**, 173-186.

Chang, C., and Lin, C. (2001) *LIBSVM: A Library for Support Vector Machines*. Computer Science and Information Engineering, National Taiwan University, Taiwan.

Chorley, R. J., and Haggett, P. (1967) *Models in Geography*. London: Methuen and Company Ltd..

Civco, D. (1989) Knowledge-based land use and land cover mapping. Proceeding of Annual Convention of American Society for Photogrammetry and Remote Sensing, **3**, 276-291.

Cochran, W. G. (1977) *Sampling techniques*. New York, John Wiley and Sons.

Cohen, J. (1960) A coefficient of agreement for nominal scales. *Educational and Psychlogical Measurement*, **20**, 37-40.

Congalton, R. G. (1991) A review of assessing the accuracy of classifications of remotely sensed data. *Remote Sensing of Environment*, **37**, 35-46.

Congalton, R. G. (1988) A comparison of sampling schemes used in generating error matrices for assessing the accuracy of maps generated from remotely sensed data. *Photogrammetric Engineering and Remote Sensing*, **54**, 593-600.

Cortes, C., and Vapnik, V. N. (1995) Support vector networks. *Machine Learn*ing, **20**, 273-297.

Curlander, J. C., and Mcdonough, R. N. (1991) *Synthetic Aperture Radar*: *System and Signal Processing.* New York: John Wiley and Sons.

Cushnie, J. L. (1987) The interactive effect of spatial resolution and degree of internal variability with land-cover types on classification accuracies. *International Journal of Remote Sensing*, **8**, 15-29.

Dammert, P. B. G., Lepparanta, M., and Askne, J. (1998) SAR interferometery over Baltic Sea ice. *International Journal of Remote Sensing,* **19**, 3019-3037.

Defries, R. S., Hansen, M., Townshend, J. R. G., and Sohlberg, R. (1998) Global land cover classification at 8 km spatial resolution: the use of training data derived from Landsat imagery in decision tree classifiers. *International Journal of Remote Sensing,* **19**, 3141-3168.

Dobson, M. C., Ulaby F. T., and Pierce L. E. (1995) Land-cover classification and estimation of terrain attributes using synthetic aperture radar, *Remote Sensing of Environment*, **51**, 199-214.

Durand, J.M., Gimonet, B.J., and Perbos, J.R. (1987) SAR data filtering for classification. *IEEE Transactions of Geoscience and. Remote Sensing*, **25**, 629-637.

Dutra, L. V., and Huber, R. (1999) Feature extraction and selection for ERS-1/2 InSAR classification. *International Journal of Remote Sensing*, **20**, 993-1016.

Elachi, C. (1987) *Spaceborne Radar Remote Sensing: Applications and Techniques*. New York, IEEE Press.

Engdahl, M., and Borgeaud, M. (1998) ERS-1/2 tandem interferometric coherence and agricultural crop height. Retrieval of Bio- and Physical Parameters from SAR *Data for Land Application Workshop*. ESTEC, The Netherlands, 21-23 October 1998, http://www.estec.esa.nl/CONFANNOUN/98c07/.

Estes, J., Sailor, C., and Tinney, L. (1986) Applications of artificial intelligence techniques to remote sensing. *Professional Geographer*, **38**, 133-141.

Esposito, F., Malerba, D., and Semeraro, G. (1997) A comparative analysis of methods for pruning decision trees. *IEEE Transactions on Pattern Analysis and Machine Intelligence,* **19**, 476-491.

Evans, F. (1998) *An Investigation into the Use of Maximum Likelihood Classifiers, Decision Trees, Neural Networks and Conditional Probabilistic Network for Mapping and Predicting Salinity*. M. Sc. Thesis, Department of Computer Science, Curtin University of Technology, Australia.

Fischer, M. M. (1996) Computational neural networks: a new paradigm for spatial analysis. *Proceedings of First International Conference on Geocomputation*, University of Leeds, UK, **1**, 297-314.

Fitzgerald, R. W., and Lees, B. G. (1994) Assessing the classification accuracy of multisource remote sensing data. *Remote Sensing of the Environment*, **47**, 362-368.

Fitzpatrick-Lins, K. (1981) Comaparision of sampling procedures and data analysis for a land use and land cover map. *Photogrammetric Engineering and Remote Sensing*, **47**, 343-351.

Fletcher, R. (1987) *Practical Methods of Optimisation*. John Wiley and Sons, 2nd edition.

Floury, N., Toan, T. L., Souyris, J. C., Singh, K., Stussi, N., Hsu, C. C., and Kong, J. A. (1996) Interferometry for forest studies. *FRINGE-ESA Workshop on Application of ERS SAR Interferometry*, University of Zurich, 30 September to 2 October, http://www.geo.unizh.ch/rsl/fringe96/.

Foody, G. M. (1995 a) Land cover classification by an artificial neural network with ancillary information. *International Journal of Geographical Information Systems*, **9**, 527-542.

Foody , G. M., Mcculloch, M. B., and Yates, W. B. (1995 b) The effects of training set size and composition on artificial neural network. *Photogrammetric Engineering and Remote Sensin*g, **58**, 1459-1460.

Foody, G. M., and Arora, M. K. (1997) An evaluation of some factors affecting the accuracy of classification by an artificial neural network. *International Journal of Remote Sensin*g, **18,** 799-810.

Foster, M. R., and Guinzy, N. J. (1967) The coefficient of coherence: Its estimation and use in geophysical data processing. *Geophysics*, **XXXII**, 602-616.

Franklin, S. E., Peddle, D. R., Wilson, B. A., and Blodgett, C. F. (1991) Pixel sampling of remotely sensed digital imagery. *Computers and Geosciences*, **17**, 759-775.

Friedl, M., Estes, J., and Star, J. (1988) Advanced information-extraction tools in remote sensing, for earth science applications: AI and GIS. *AI Applications*, **2**, 17-31.

Friedl, M. A., Brodley, C. E., and Strahler, A. H. (1999) Maximizing land cover classification accuracies produced by decision tree at continental to global scales. *IEEE Transactions on Geoscience and Remote Sensing*. **37**, 969-977.

Friedl, M. A., and Brodley, C. E. (1997) Decision tree classification of land cover from remotely sensed data. *Remote Sensing of Environment*. **61**, 399-409.

Frankot, R. T., and Chellappa, R. (1987) Log Normal random field models and their applications to radar image synthesis. *IEEE Transactions on Geoscience and Remote Sensing*, **25**, 195-207.

Freund, Y., and Schapire, R. E. (1996) Experiments with new boosting algorithm. *Machine Learning: Proceedings of the Thirteenth International Conference*. Bari, Italy, July 3-6.

Friedman, J. H. (1977) A recursive partitioning decision rule for non-parametric classification. *IEEE Transactions on Computers*, **C-26**, 163-168.

Frost, V. S., Stiles, J. A., Shanmugan, K. S., and Hotzman, J. C. (1982) A model for radar images and its application to adaptive digital filtering of multiplicative noise. *IEEE Transactions on Pattern Analysis and Machine Intelligence*, **4**, 157-165.

Fu, K. S. (1968) *Sequential Methods in Pattern Recognition and Machine Learning*. New York: Academic Press.

Fukuda, S., and Hirosawa, H. (1999) A wavelet-based texture feature set applied to classification of multifrequency polarimetric SAR images. *IEEE Transactions on Geoscience and Remote Sensing*, **37**, 2282-2286.

Fukunaga, K., and Hayes, R. R. (1989) Effects of Sample Size in Classifier Design. *IEEE Transactions on Pattern Analysis and Machine Intelligenc*e, **11**, 873-885.

Gabriel, A. K, and Goldstein, R. M. (1988) Crossed Orbit Interferometry: Theory and Experimental Results from SIR-B, *International Journal of Remote Sensing,* **9**, 857-872.

Gahegan, M., and West, G. (1998) The classification of complex data sets: an operational comparison of artificial neural networks and decision tree classifiers. *Proceedings of the 3rd International Conference on Geocomputation*, University of Bristol, UK, 17-19 September 1998, http://divcom.otago.ac.nz/sirc/webpages/conferences/GeoComp/GeoComp98/geocomp98.htm.

Gangepain, J., and Roques-Carmes, C. (1986) Fractal approach to two dimensional and three dimensional surface roughness. *Wear*, **109**, 119-126.

Gatelli F., Guarnieri A. M., Parizzi F., Pasquali P., Prati C., and Rocca F. (1994) The wavenumber shift in SAR interferometry , *IEEE Transactions on Geoscience and Remote Sensing*, **32**, 855-865.

Gelfand, S., and Guo, H. (1991) *Tree Classifiers with Multilayer Perceptron Feature Extraction*. Ph. D. dissertation, School of Electrical Engineering, Purdue University, West Lafayette, Indiana.

Gelfand, S. B., Ravishankar, C. S., and Delp, E. J. (1991) An iterative growing and pruning algorithms for classification tree design. *IEEE Transactions on Pattern Analysis and Machine Intelligence,* **13**, 163-174.

Gens, R., and Van Genderen, J. L. (1996) SAR interferometry - issue, techniques, applications. *International Journal of Remote Sensing,* **17,** 1803-1835.

Giacinto, G., and Roli, F. (1997) Ensembles of neural networks for soft classification of remote sensing images, *Proceedings of the European Symposium on Intelligent Techniques*, European Network for Fuzzy Logic and Uncertainty Modelling in Information Technology, Bari, Italy, 166-170.

Goldberg, M., Karam, G., and Alvo, M. (1983) A production rule-based expert system for interpreting multi-temporal Landsat imagery. *Proceedings of IEEE Computer Society Conference on Computer Vision and Pattern recognition*. 77-82.

Graham, L. C. (1974) Synthetic Interferometer Radar for topographic mapping. *Proceedings of the IEEE*, **62**, 763-768.

Green, A. A., Berman, M., Switzer, P., and Craig, M. D. (1988) A transformation for ordering multispectral data in term of image quality with implications for noise removal. *IEEE Transactions on Geoscience and Remote Sensing*, **26**, 65-74.

Guarnieri, A. M., and Prati, C. (1997) SAR Interferometry: A ”quick and dirty” coherence estimator for data browsing. *IEEE Transactions on Geoscience and Remote Sensing*. **35**, 660-669.

Gualtieri, J. A., and Cromp, R. F. (1998) Support vector machines for hyperspectral remote sensing classification. *Proceedings of the of the SPIE, 27th AIPR Workshop: Advances in Computer Assisted Recognition*, Washington, DC, October 14-16, 221-232.

Hagberg, J. O., and Ulander, L. M. H. (1993) On the optimisation of interferometric SAR for topographic mapping. *IEEE Transactions of Geoscience and Remote Sensing*, **31**, 303-306.

Hansen, M., Dubayah, R., and Defries, R. (1996) Classification trees: an alternative to traditional land cover classifiers. *International Journal of Remote Sensing,* **17,** 1075-1081.

Hansen, M., Defries, R., Townshend, J. R. G., and Sohlberg, R. (2000) Global land cover classification at 1 km spatial resolution using a classification tree approach. *International Journal of Remote Sensing,* **21,** 1331-1364.

Harlick, R.M., Shanmugam, K., and Dinstein, I. (1973) Texture features for image classification. *IEEE Transactions on System, Man, and Cybernetics*, **3(6)**, 610-621.

Hausdorff, F. (1919) Dimension und ausseres mass. *Mathematische Annalen*, **79**, 157.

Hay, A. M. (1979) Sampling design to test land use map accuracy. *Photogrammetric Engineering and Remote Sensing*, **45**, 529-533.

Heerman, P. D., and Khazenie, N. (1992) Classification of multispectral remote sensing data using a back propagation neural network. *IEEE Transactions on Geoscience and Remote Sensing*, **30**, 81-88.

Henderson, F. M. (1975) Radar for small-scale land-use mapping. *Photogrammetric Engineering and Remote Sensing*, **41**, 307.

Henebry, G. M., and Kux, H. J. H. (1995) Lacunarity as texture measure for SAR imagery. *International Journal of Remote Sensing*, **16**, 565-571.

Hepner, G. F., Logan, T., Ritter, N., and Bryant, N. (1990) Artificial neural network classification using a minimal training set: comparison to conventional supervised classification. *Photogrammetric Engineering and Remote Sensin*g, **56,** 469-473.

Herland, E. A. (1996) Operational use of SAR interferometer for DEM generation and land use mapping. *FRINGE-ESA Workshop on Application of ERS SAR Interferometry*, University of Zurich, 30 September to 2 October, http://www.geo.unizh.ch/rsl/fringe96/.

Hord, R. M., and Brooner, W. (1976) Land use map accuracy criteria. *Photogrammetric Engineering and Remote Sensing*, **42**, 671-677.

Hochschild, V., Klenke, M., Bartsch, A., and Flügel, W. A. (1999) Land cover classification in hilly watersheds using SAR backscatter intensity and interferometric coherence information. *Second international symposium on operationalization of remote sensing*, ITC, The Netherlands, 16-20 August 1999, http://www.itc.nl/ags/research/ors99/abstracts.

Hotelling, H. (1931) The generalisation of students's ratio. *Annals of Mathematical Statistics*, **2**, 360-378.

Hsieh, P., and Landgrebe, D. (1998) *Classification of high dimensional data*. Technical Report - **ECE 98-4**, School of Electrical and Computer Engineering Purdue University West Lafayette, Indiana.

Huang, C., Davis, L. S., and Townshend, J. R. G. (2002) An assessment of support vector machines for land cover classification. *International Journal of Remote Sensing,* **23**, 725-749.

Hughes, G. F. (1968) On the mean accuracy of statistical pattern recognizers. *IEEE Transactions on Information Theory,* **IT-14,** 55-63.

Hunt, E. B., Marian, J., and Stone, P. J. (1966) *Experiments in Induction*. New York: Academic Press.

Hwang, J., Lay, S., and Lippman, A. (1994) Nonparametric Multivariate Density Estimation: A Comparative Study. *IEEE Transactions on Signal Processin*g, **42**, 2795-2810.

Ichoku, C., Karnieli, A., Arkin, Y., Chorowicz, J., Fleury, T., and Rudent, J. P. (1998) Exploring the utility potential of SAR interferometric coherence images. *International Journal of Remote Sensing*, **19**, 1147-1160.

Ince, F. (1987) Maximum likelihood classification, optimal or problematic: A comparision with nearest neighbour classification. *International Journal of Remote Sensing*, **8**, 1829-1838.

Irons, J. R., Markham, B. L., Nelson, R. F., Toll, D. L., Williams, D. L., Latty, R. S., and Stauffer, M. L. (1985) The effects of spatial resolution on the classification of Thematic mapper data. *International Journal of Remote Sensing*, **6**, 1385-1403.

Jain, A. K., and Dubes, R. C. (1988) *Algorithms for Clustering Data*. Englewood Cliff, Prentice-Hall.

Jain, A. K., and Chandrasekaran, B. (1982) Dimensionality and sample size considerations in pattern recognition practice. *Handbook of Statistics*, Amsterdam: North-Holland.

Jain, A., and Zongker, D. (1997) Feature selection: evaluation, application, and small sample performance. *IEEE Transactions on pattern Analysis and Machine Intelligence*, **19**, 153-158.

Jarvis, P. G. (1995) Scaling processes and problems. *Plant, Cell and Environment*, **18**, 1079-1089.

Jenikow, C. Z. (1998) Fuzzy decision trees: issue and methods. *IEEE Transactions on Systems, Man, and Cybernetics*. Part-B, **28**, 1-14.

Jensen, J. R. (1 996) *Introductory Digital Image Processing - A Remote Sensing Perspective*. London: Prentice Hall.

Jiminez, L., and Landgrebe, D. A. (1998) Supervised classification in high dimensional space: Geometrical, statistical and asymptotical properties of multivariate data. *IEEE Transactions on System, Man, and Cybernetics*, **28**, **Part C**, 39-54.

Johnston, R. J., Gregory, D., and Smith, D. M. (1981) *The Dictionary of Human Geography*. Oxford: Blackwell.

Johnston, R. J. (1968) Choice in classification: the subjectivity of objective methods. *Annals of the Association of American geographers*, **58**, 575-589.

Kashyap, R. L., and Chellappa, R. (1983) Estimation and choice of neighbours in spatial-interaction models of images. *IEEE Transactions on Information Theory*, **IT-29**, 60-72.

Kavzoglu, T. (2001) *An Investigation of the Design and Use of Feed-forward Artificial Neural Networks in the Classification of Remotely Sensed Images*. PhD thesis. School of Geography, The University of Nottingham, Nottingham, UK.

Keller, J., and Chen, S. (1989) Texture description and segmentation through fractal geometry. *Computer Vision, Graphics, and Image Processing*, **45**, 150-166.

Kim, B., and Landgrebe, D. A. (1991) Hierarchical classifier design in high-dimensional, numerous class cases. *IEEE Transactions on Geoscience and Remote Sensing*. **29**, 518-528.

Kira, K., and Rendell, L.A. (1992) The feature selection problem: Traditional methods and a new algorithm. *Proceedings of Ninth National Conference on Artificial Intelligence*, American Association for Artificial Intelligence, San Jose, California, 129-134.

Koller, D., and Sahami, M. (1996) Toward optimal feature selection. *Machine Learning: Proceedings of the Thirteenth International Conference*. Department of Informatics, University of Bari, Italy, 284-292.

Knerr, S., Personnaz, L., and Dreyfus, G. (1990) Single-layer learning revisited: A stepwise procedure for building and training neural network. *Neurocomputing: Algorithms, Architectures and Applications*, NATO ASI, Berlin: Springer-Verlag.

Knuth, D. E. (1971) Optimum binary search tree. *Acta Inform*atica, **1**, 14-25.

Kononenko, I., and Hong, J. S. (1997) Attribute selection for modelling. *Future Generation Computer Systems*, **13**, 181-195.

Kohonen, T. (1989) *Self-organisation and Associative Memory*. New York: Springer-Verlag.

Koskinen, J., Pullianen, J., and Hallikainen, M. (1995) Land-use classification employing ERS-1 SAR data. *Photogrammetric Journal of Finland*, **14**, 23-34.

Kuan, D. T., Sawchuk, A. A., Strand, T. C., and Chavel, P. (1985) Adaptive noise smoothing filter for image with signal-dependent noise. *IEEE Transactions on Pattern Analysis and Machine Intelligence*, **7**, 165-177.

Kurzynski, M. W. (1983) The optimal strategy of a tree classifier. *Pattern Recognition,* **16**, 81-87.

Labivitz, M. L. (1986) Issue arising from sampling designs and the band selection in discriminating ground reference attributes using remotely sensed data. *Photogrammetric Engineering and Remote Sensin*g, **52**, 201-211.

Landeweerd, G. H., Timmers, T., and Gelsema, E. S. (1983) Binary tree verses single level tree classification of white blood cells. *Pattern Recognition*, **16**, 571-577.

Lee, J. S., Hoppel, K. W., Mango, S. A., and Miller, A. R. (1994 a) Intensity and phase statistics of multilook polarimetric and interferometric SAR imagery. *IEEE Transaction of Geoscience and Remote Sensing*, **32**, 1017-1028.

Lee, J. S., Jurkewich, I., Dewaele, P., Wambacq, P., and Oosterlinck, A. (1994 b) Specle filtering of synthetic aperture radar images: A review. *Remote Sensing Reviews*, **8**, 313-340.

Lee, J. S. (1986) Speckle suppression and analysis for Synthetic Aperture Radar. *Optical Engineering*, **25**, 636-643.

Levin, S. A. (1992) The problem of pattern and scale in ecology. *Ecology*, **73**, 1943-1967.

Li, S., Benson, C., Shapiro, L., and Dean, K. (1997) Aufeis in the Ivishak river, Alaska, mapped from satellite radar interferometer. *Remote Sensing of Environment*, **60**, 131-139.

Liew, S. C., Kwoh, L. K., Padmanabhan, K., Lim, O. K., and Lim, H. (1999) Delineating land/forest fire burnt scars with ERS interferometric SAR. *Geophysical Research Letters*, **26**, 2409-2412.

Lillesand, T. M., and Kiefer, R. W. (1994) *Remote Sensing and Image Interpretation*. New York: John Wiley and Sons.

Lim, H. H., Swartz, A. A., Yueh, H. A., Kong, J. A., and Shin, R. T. (1989) Classification of earth terrain using polarimetric synthetic aperture radar images. ***Journal of Geophysical Research***, **94**, 7049-7057.

Lin, Y. K., and Fu, K. S. (1983) Automatic classification of cervical cells using a binary tree classifier. *Pattern Recognition*, **16**, 69-80.

Loh, W.-Y., and Shih, Y.-S. (1997) Split selection methods for classification trees. *Statistica Sinica*, **7**, 815-840.

Mandelbrot, B. B. (1977) *Fractals: Form, Chance and Dimension*. San Francisco, CA: Freeman.

Mandelbrot, B. B. (1983) *The Fractal Geometry of Nature*. San Francisco, CA: Freeman.

Mandelbrot, B. B. (1986) Self-affine fractal sets I: the basic fractal dimensions. *Fractals in Physics* (ed.), Amsterdam: North-Holland Physics Publishing.

Markham, B. L., and Towenshend, J. R. G. (1981) land cover classification accuracy as function of sensor spatial resolution. *Proceedings of the Fifteenth International Symposium on Remote Sensing of Environment*, ERIM, Ann Arbor, Michigan, 1075-1090.

Marceau, D. J. (1999) The scale issue in the social and natural sciences. *Canadian Journal of Remote Sensing*, **25**, 347-356.

Marinelli, L., Michel, R., Beaudoin, A., and Astier, J. (1997) Flood mapping using ERS tandem coherence images: A case study in south France. *Proceedings of Third ERS Symposium*, Florence, Italy, http://earth1.esa.it/florence/papers/ .

Mather, P. M. (1999) *Computer Processing of Remotely-Sensed Images: An Introduction*. Second Edition, Chichester: John Wiley and Sons.

Mather, P. M., Tso, B., and Koch, M. (1998) An evaluation of Landsat TM spectral data and SAR-derived textural information for lithological discrimination in the Red Sea Hills, Sudan. *International Journal of Remote Sensing*, **19**, 587-604.

Meentemeyer, V., and Box, E. O. (1987) Scale effects in landscape studies. *Ecological Studies*, **64**, 15-20.

Meisel, W. S., and Michalopoulos, D. S. (1973) A partitioning algorithm with application in pattern classification and the optimisation of decision trees. *IEEE transaction on computers*, **C-22**, 93-103.

Mingers, J. (1989 a) An empirical comparison of pruning methods for decision tree induction. *Machine Learning*, **4**, 227-243.

Mingers, J. (1989 b) An empirical comparison of selection measures for decision tree induction. *Machine Learning*, **3**, 319-342.

Morgan, J., and Sonquist, J. A. (1963) Problem in the analysis of survey data, and a proposal. *Journal of American Statistical Association*, **58**, 415-435.

Morley, J., Muller, J. P., and Madden, S. (1996) Wetland monitoring in Mali using SAR interferometry. *FRINGE-ESA Workshop on Application of ERS SAR Interferometry*, University of Zurich, 30 September to 2 October, http://www.geo.unizh.ch/rsl/fringe96/.

Muchoney, D., Borak, J., Chi, H., Friedl, M., Gopal, S., Hodges, J., Morrow, N., and Strahler, A. (2000) Application of MODIS global supervised classification model to vegetation and land cover mapping of Central America. *International Journal of Remote Sensing,* **21**, 1115-1138.

Mui, J. K., and Fu, K. S. (1980) Automated classification of nucleated blood cells using a binary tree classifier. *IEEE Transactions on Pattern Analysis and Machine Intelligence,* **PAMI-2**, 429-443.

Muller, A., Oertel, D., Richter, R., Strobl, P., Beran, D., Fries, J., Boehl, R., Obermeier, P., Housold, A., and Reinhaeckel, G. (1998) The DIAS 7915 - Three years operating airborne imaging spectrometer. *First EARSeL Workshop on Imaging Spectroscopy*, University of Zurich, Zurich, 21-28.

Mumford, B., Muller, J, P., and Mandanayke, A. (1996) Assessment of land cover mapping potential in Africa using tandem ERS interferometry. *FRINGE-ESA Workshop on Application of ERS SAR Interferometry*, University of Zurich, 30 September to 2 October, http://www.geo.unizh.ch/rsl/fringe96/

Murthy, S. K., Kasif, S., and Salzberg, S. (1994) A system for induction of oblique decision trees. *Journal of Artificial Intelligence Research*, **2**, 1-32.

Nagao, M., and Matsuyama, T. (1980) *A Structural Analysis of Complex Aerial Photographs*. New York: Plenum Press.

Narendra, P. M., and Fukunaga, K. (1977) A branch and bound algorithm for feature selection. *IEEE Transactions on Computers*, **26**, 917-922.

Nezry, E., Lopes, A., Ducrot-Gambart, D., Nezry, G., and Lee, J. S. (1996) Supervised classification of K-distributed SAR images of natural targets and probability of error estimation. *IEEE Transactions of Geoscience and Remote Sensing*, **84**, 1233-1242.

Nilsson, N. J. (1965) *Learning Machines*. New York: McGraw-Hill.

Oates, T., and Jenson, D. (1997) The effects of training set size on decision tree complexity. Machine Learning, *Proceedings of 14th International Conference on Machine Learning*. San Francisco, CA: Morgan Kaufmann, 254 - 262.

Oliver, G., and Florín, M. (1995) The wetlands of La Mancha, Central Spain: Opportunities and problems concerning restoration. In *Bases Ecologicas para la Restauracion de Humedales en la Cuneca Mediterranea,* edited by G. Oliver, F. Moline and J. Cobos (Junta de Andalucia: Consejeria de Medioambiente), 197-216.

Olsen, S. I. (1993) Estimation of noise in images: an evaluation. *Graphical Models and Image Processing*, **55**, 319-323.

Osuna, E. E., Freund, R., and Girosi, F. (1997) *Support vector machines: training and applications*. A. I. Memo No. 1602, CBCL paper No. 144, Artificial Intelligence laboratory, Massachusetts Institute of Technology, ftp://publications.ai.mit.edu/ai-publications/pdf/AIM-1602.pdf

Papathanassiou, K. P., Reigber, A., and Coltelli. M. (1996) On the interferometric coherence: A multifrequency and multitemporal analysis. *RINGE-ESA Workshop on Application of ERS SAR Interferometry,* University of Zurich, 30 September to 2 October http://www.geo.unizh.ch/rsl/fringe96/ .

Peddle, D. R., and Franklin, S. E. (1991) Image texture processing and data integration for surface pattern discrimination. *Photogrammetric Engineering and Remote Sensing*, **57**, 413-420.

Peleg, S., Naor, J., Hartley, R., and Avnir, D. (1984) Multiple resolution texture analysis and classification, *IEEE Transactions on Pattern Analysis and Machine Intelligence*, **6**, 518-523.

Pentland, A. P. (1984) Fractal based description of natural scenes. *IEEE Transactions of Pattern Analysis and Machine Intelligence*, **6**, 661-674.

Pentland, A. P. (1986) Shading into texture. *Journal of Artificial Intelligence*,**29**, 147-170.

Pierce, L. E., Ulaby, F. T., Sarabandi, K., and Dobson, M. C. (1994) Knowledge-based classification of polarimetric SAR images, *IEEE Transactions of Geoscience and. Remote Sensing*, **32,** 1081-1086.

Piper, J. (1992) Variability and bias in experimentally measured classifier error rates. *Pattern Recognition Letters*, **13**, 685-692.

Prati, C., Rocca, F., and Mouti Guaruieri, A. (1992) SAR Interferometry Experiments with ERS-1. F*irst ERS-1 Symposium--Space at the Service of our Environment, Cannes, France, 4-6 November,* 211-217.

Prati, C., Rocca, F., Guarnieri, A. M., and Pasquali, P (1994) Report on ERS-1 SAR interferometric techniques and applications. *ESA Study Contract Report*, ESA Contract No.:3-7439/92/HE-1.

Quinlan, J. R. (1987) Simplifying decision trees. *International Journal of Man-Machine Studies*. **27**, 221-234.

Quinlan, J. R., and Rivest, R. L. (1989) Inferring decision trees using minimum description length principle. *Information and Computation*. **80**, 227-248.

Quinlan, J. R. ((1990) Decision tree and decision making. *IEEE Transactions on Systems, Man, and Cybernetics*. **20**, 339-346.

Quinlan, J. R. (1993) *C4.5: Programs for Machine Learning*. San Mateo: Morgan Kaufmann.

Quinlan, J. R. (1996) Bagging, boosting and C4.5. *Thirteenth National Conference of Artificial Intelligence*. American Association for Artificial Intelligence Portland, August 4 - 8, Oregon, USA.

Quinlan, J. R. (1996) Improved use of continuous attributes in C4.5. *Journal of Artificial Intelligence Research*, **4,** 77-90.

Raffy, M. (1992) Change of scale in models of remote sensing: a general method for spatialization of models. *Remote Sensing of Environment*, **40**, 101-112.

Raudys, S., and Pikelis, V. (1980) On dimensionality, sample size, classification error, and complexity of classification algorithms in pattern recognition. *IEEE Transactions of Pattern Analysis and Machine Intelligence*, **3**, 242-252.

Raudys, S. J., and Jain, A. K. (1991) Small sample size effects in statistical pattern recognition: Recommendations for practitioners. *IEEE Transactions of Pattern Analysis and Machine Intelligence*, **13**, 252-264.

Ribbes, F., Toan, T. L., Bruniquel, J., Floury, N., Stussi, N., Liew, S. C., and Wasrin, U. R. (1997) Forest mapping in tropical region using multitemporal and Interferometric ERS-1/2 data. *Proceedings of Third ERS Symposium*, Florence, Italy, http://earth1.esa.it/florence/papers/.

Richards, J. A. (1993) *Remote Sensing Digital Image Analysis- An Introduction*. Berlin : Springer-Verlag.

Rissanen, J. (1983) A universal prior for integers and estimation by minimum description length. *Annals of Statistics*, **11**, 416-431.

Rodriquez, E., Martin, J. M. (1992) Theory and design of interferometric synthetic aperture radars. *IEE Proceedings-F*, **139**, 147-159.

Roli, F., Giacinto, G., and Vernazza, G. (1997) Comparison and combination of statistical and neural networks algorithms for remote-sensing image classification. *Neurocomputation in Remote Sensing Data Analysi*s, Austin, J., Kanellopoulos, I., Roli, F. and Wilkinson G. (Eds.), Berlin: Springer-Verlag, 117-124.

Rosenfield, G. H. (1982) Sample design for estimating changes in land use and land cover. *Photogrammetric Engineering and Remote Sensing*, **48**, 793-801.

Rott, H., and Seigal, A. (1996) Glaciological studies in the Alps and in Antarctica using ERS interferometric SAR. *FRINGE-ESA Workshop on Application of ERS SAR Interferometry*, University of Zurich, 30 September to 2 October, http://www.geo.unizh.ch/rsl/fringe96/.

Rounds, E. M. (1980) A combined nonparametric approach to feature selection and binary decision tree design. *Pattern Recognition*, **12**, 313-317.

Roven, E., and Alvarez, L. (1998) Multitemporal coherence mapping for classification of land surfaces around the Gulf of California. *Proceedings of the 24th Annual Conference and Exhibition of Remote Sensing Society*, The University of Greenwich, 9-11 September.

Rumelhart, D. E., Hinton, G. E., and Williams, R. J. (1996) Learning internal representation by error propagation. *Parallel Distributed Processing: Explorations in the Microstructure of Cognition*, Volume 1: Foundations (ed.), Cambridge, MA: The MIT Press, 318-362.

Sadowski, F. G., Malila, D. A., Sarno, J. E., and Nalepka, R. F. (1977) The influence of multispectral scanner spatial resolution on forest feature classification. *Proceedings of the Eleventh International Symposium on Remote Sensing of Environment*, ERIM, Ann Arbor, Michigan, 1279-1288.

Safavian, S. R., and Landgrebe, D. (1991) A survey of decision tree classifier methodology. *IEEE Transactions of Systems, Man, and Cybernetics*, **21**, 660-675.

Saint-Jean, R., Singhroy, V., and Khalifa, S. M. (1995) Geological interpretation of integrated SAR images in Azraq area of Jordan. *Canadian Journal of Remote Sensing*, **21**, 511-517.

Sarkar, N., and Chaudhuri, B. B. (1994) An efficient differential box-counting approach to compute the fractal dimension of images. *IEEE Transactions on System, Man, and Cybernetics*, **24**, 115-120.

Saunders, C., Stitson, M. O., Weston, J., Bottou, L., Schölkopf, B., and Smola, A. (1998) *Support Vector Machine - Reference Manual*. Technical Report, CSD-TR-98-03, Royal Holloway and AT&T, University of London.

Schowengerdt, R. A. (1997) *Remote Sensing Models and Methods for Image Processing*. New York: Academic Press.

Schalkoff, R. J. (1992) *Pattern Recognition: Statistical, Structural and Neural Approaches*. New York: Wiley.

Schaale, M., and Furrer, R. (1995) Land surface classification by neural networks. *International Journal of Remote Sensing*, **16**, 3003-3031.

Schistad, S. A. H., Jain, A. K., and Taxt, T. (1994) Multisource classification of remotely sensed data: Fusion of Landsat-TM and SAR images. *IEEE Transactions of Geoscience and Remote Sensing*, **32**, 768-778.

Scholkopf, B. (1997) *Support Vector Learning*. Ph. D. thesis, Technische Universitat, Berlin.

Schwabisch, M., Lehner, S., and Winkel, N. (1997) Coastline extraction using ERS SAR interferometry. *Proceedings of Third ERS Symposium*, Florence, Italy, http://earth1.esa.it/florence/papers/.

Sethi, I. K. (1990) Entropy nets: from decision tree to neural networks. *Proceedings of the IEEE*, **78**, 1605-1613.

Sethi, I. K., and Chatterjee, B. (1977) Efficient decision tree design for discrete variable pattern recognition problems. *Pattern Recognition*, **9**, 197-206.

Seynat, C., and Hobbs, S. (1998) Crop parameter retrieval with multi-temporal SAR coherence images. *Retrieval of Bio- and Physical Parameters from SAR Data for Land Application Workshop.* ESTEC, The Netherlands, 21- 23 October 1998, http://www.estec.esa.nl/CONFANNOUN/98c07/.

Sharkawi, M., and Mark II, R. J. (1990) A performance comparison of trained multilayer perceptrons and trained classification trees. *Proceeding of the IEEE*, **78**, 1614-1619.

Snedecor, G. W., and Cochran, W. G. (1967) *Statistical Methods*. Ames, Iowa: The Iowa State University Press.

Solberg, A. H. S., and Jain, A. K. (1997) Texture fusion and feature selection applied to SAR imagery. *IEEE Transactions on Geoscience and Remote Sensing*, **35**, 475-479.

Srinivasan, R., Cannon, M., and White, J. (1988) Landsat data destriping using power spectral filtering. *Optical Engineering*, **27**, 939-943.

Stehman, S. V. (1192) Comparison of systematic and random sampling for estimating the accuracy of maps generated from remotely sensed data. *Photogrammetric Engineering and Remote Sensing*, **58**, 1343-1350.

Stockham, T. G. (1972) Image processing in the context of a visual model. Proceeding of the IEEE, **60**, 828-842.

Stoffel, J. C. (1974) A classifier design technique for discrete variable pattern recognition problems. *IEEE Transactions on Computers*, **C-23**, 428-441.

Story, M., and Congalton, R. G. (1986) Accuracy assessment: a user's perspective. *Photogrammetric Engineering and Remote Sensing*, **52**, 397-399.

Stozzi, T., Dammert, P., Wegmuller, Martinez, J. M., Beaudoin, A., Askne, J., and Hallikainen, M. (1998) European forest mapping with SAR interferometry. *Retrieval of Bio- and Physical Parameters from SAR Data for Land Application Workshop.* ESTEC, The Netherlands, 21- 23 October 1998, http://www.estec.esa.nl/CONFANNOUN/98c07/.

Stussi, N., Liew, S. C., Kwoh, L. K., Lim, H., Nicol, J., and Goh, K. C. (1997) Landcover classification using ERS SAR/INSAR data on coastal region of central Sumatra. *Proceedings of Third ERS Symposium*, Florence, Italy, http://earth1.esa.it/florence/papers/.

Strahler, A. H., Woodcock, C. E., and Smith, J. A. (1986) On the nature of models in remote sensing. *Remote Sensing of Environment*, **20**, 121-139.

Strobl, P., and Zhukov, B. (1998) Recent developments in 3-12 μm radiometric calibration of the DAIS 7915. *Ist EARSeL Workshop on Imaging Spectroscopy*, Remote Sensing Laboratories, University of Zurich, 6-8 October.

Strobl, P., Muller, A., Schlaepfer, D., and Schaepman, M. (1997) Laboratory calibration and in-flight validation of DAIS 7915 data. *Proceedings of SPIE: Algorithms for Multispectral and Hyperspectral Imagery III*, **3071**, 225-236.

Swain, P., and Davis, S. (1978) *Remote Sensing: The Quantitative Approach*. New York: McGraw-Hill.

Swain, P. H., and Hauska, H. (1977) The decision tree classifier: design and potential. *IEEE Transactions on Geoscience Electronics,* **3**, 142-147.

Switzer, P., and Green, A. (1984) *Min/max autocorrelation factors for multivariate spatial imagery*. Technical Report *6*, Department of Statistics, Stanford University.

Tell, B. R., and Walker, N. P. (1998) Examining the effect of satellite repeat pass times on interferometric coherence for land classification applications. *Retrieval of Bio- and Physical Parameters from SAR Data for Land Application Workshop.* ESTEC, The Netherlands, 21- 23 October 1998, http://www.estec.esa.nl/CONFANNOUN/98c07/.

Tortora, R. D. (1978) A note on sample size estimation for multinomial populations. *The American Statistician*, **32**, 100-102.

Tou, J., and Gonzalez, R. (1974) *Pattern Recognition Principles*. Reading, Massachusetts: Addison-Wesley.

Touzi, R., Lopes, A., Bruniquel, J., and Vachon, P. W. (1999) Coherence estimation of SAR imagery. *IEEE Transactions on Geoscience and Remote Sensing*, **37**, 135-149.

Townshend, J. R. G. (1984) Agriculture land-cover discrimination using thematic mapper spectral bands. *International Journal of Remote Sensing*, **5**, 681-698.

Townshend, F. E. (1986) The enhancement of computer classifications by logical smoothing. *Photogrammetric Engineering and Remote Sensin*g, **52**, 213-221.

Townshend, J. R. G., and Justice, C. (1981) Information extraction from remotely sensed data: a user view. *International Journal of Remote Sensing*, **2**, 313-329.

Townshend, J. R. G. (1992) Land cover. *International Journal of Remote Sensing*, **13**, 1319-1328.

Tso, B. C. K. (1997) *An Investigation of Alternate Strategies for Incorporating Spectral, Textural, and Contextual Information in Remote Sensing Image Classification*. PhD Thesis. School of Geography, The University of Nottingham, Nottingham, UK.

Tso, B. C. K., and Mather, P. M., (2001) *Classification Methods for Remotely sensed Data*. London: Taylor and Francis.

Ulaby, F. T. (1980) Vegetation clutter model. *IEEE Transactions of Antennas and Propagation*, **28**, 538-545.

Ulaby, F. T., Kouyate, F., brisco, B., and Williams, L. (1986) Textural information in SAR images. *IEEE Transactions of Geoscience and. Remote Sensing*, **24**, 235-245.

Ulbricht, A. (1998) Evaluation of the potential of full-polarimetic airborne repeat-pass- SAR- interferometery for classification of changes detected by the coherence. *Retrieval of Bio- and Physical Parameters from SAR Data for Land Application Workshop.* ESTEC, The Netherlands, 21-23 October 1998, http://www.estec.esa.nl/CONFANNOUN/98c07/.

Usai, S., and Hanssen, R. (1997) Long time scale INSAR by means of high coherence features. *Proceedings of Third ERS Symposium*, Florence, Italy, http://earth1.esa.it/florence/papers/.

Utgoff, P. E., and Brodley, C. E., (1990) An incremental method of finding multivariate splits for decision trees. *Machine Learning*, *Proceedings of the Seventh International conference on Machine Learning*. Austin, Texas: Morgan Kaufmann.

Van Genderen, J. L., and Lock, B. F. (1977) Testing land use map accuracy. *Photogrammetric Engineering and Remote Sensing*, **43**, 1135-1137.

Vapnik, W. N., **and Chervonenkis, A. Y. (1971)** On the uniform convergence of relative frequencies of events to their probabilities. *Theory of Probability and its Applications*. **17**, 264-280.

Vapnik, W. N., **and Chervonenkis, A. Y. (1979)** *Theory of Pattern Recognition*. Berlin: Akademia-Verlag.

Vapnik, W. N. (1982) *Estimation of dependencies based on empirical data*. Berlin: Springer-Verlag.

Vapnik, W. N., **and Chervonenkis, A. Y. (1991)** The necessary and sufficient conditions for consistency in the empirical risk minimisation method. *Pattern Recognition and Image Analysis*. **1**, 283-305.

Vapnik, V. N. (1995) *The Nature of Statistical Learning Theory*. New York: Springer-Verlag.

Vapnik, V. N. (1999) An overview of statistical learning theory. *IEEE Transactions of Neural Networks*, **10**, 988-999.

Watanabe, S. (1965) Karhunen-Loeve expansion and factor analysis, theoretical remarks and applications. *Transactions of the Fourth Prague Conference on Information Theory*, Prague, Czechoslovakia.

Wegmuller, U., and Werner, C. (1994) Analysis of interferometric land surface signatures. *Proceedings of Progress in Electromagnetic Research Symposium*, Noordwijk, July 11-15, Noordwijk, The Netherlands.

Wegmuller, U., Werner, C., Neusch, D., and Borgeoud, M. (1995) Land – surface analysis using ERS-1 SAR interferometry, *ESA Bulletin*, **81**, 30-37.

Wegmuller, U., and Werner, C. (1995) SAR interferometric signature of forests. *IEEE Transactions on Geoscience and Remote Sensing*, **33**, 1153-1161.

Wegmuller, U., and Werner, C. (1996) Land application using ERS –1/2 tandem data. *FRINGE-ESA Workshop on Application of ERS SAR Interferometry*, University of Zurich, 30 September to 2 October, http://www.geo.unizh.ch/rsl/fringe96/.

Wegmuller, U., and Werner, C. (1997) Retrieval of vegetation parameters with SAR interferometry, *IEEE Transactions on Geoscience and Remote Sensing*, **35**, 18-24.

Westin, J., and Watkins, C. (1998) *Multi-class Support Vector Machines*. Royal Holloway, University of London, U. K., Technical Report CSD-TR-98-04.

Weszka, J. S., Dyer, C. R., and Rosenfeld, A. (1976) A comparitive study of texture measures for terrain classification. *IEEE Transactions on Systems, Man, and Cybernetics*, **SMC-6**, 269-285.

Wharton, S (1987) A spectral-knowledge-based approach for urban and land-cover discrimination. *IEEE Transactions of Geoscience and Remote Sensing*, **25**, 272-282.

Wilkinson, G. G. (1997) Open questions in neurocomputing for earth observation. In *Neuro-Computation in Remote Sensing Data Analysis*, edited by I. Kanellopoulos, G. G. Wilkinson, F. Roli and J. Austin. London: Springer, 3-13.

Wilkinson, G. G. (2000) Processing and classification of satellite images. *Encyclopaedia of Analytical Chemistry*, Edited by R. A. Meyers. John Wiley and sons, 8679-8693.

Woodcock, C. E., and Strahler, A. H. (1987) The factor of scale in remote sensing. *Remote Sensing of Environment*, **21**, 311-332.

Xia, Z. G., Clarke, K., C. (1997) Approaches to scaling of geo-spatial data. *Scale in Remote Sensing and GIS,* Quattrochi, D. A., and Goodchild, M. A. (ed.), Boca Raton: CRC Press, 309-360.

You, K. C., and Fu, K. S. (1976) An approach to the design of a linear binary tree classifier. *Proceedings of the Symposium on Machine Processing of Remotely Sensed Data*. 3A-1-3A-10.

Zebker, H. A., and Goldstein, R. M. (1986) Topographic mapping from interferometric synthetic aperture radar observations. *Journal of Geophysical Research*, **91**, 4993-4999.

Zebker, H. A., and Villasenor, I. (1992) Decorrelation in interferometric radar echoes. *IEEE Transaction of Geoscience and Remote Sensing*, **30**, 950-959.

Zhang, M., and Scofield, R. A. (1994) Artificial neural network techniques for estimating heavy convective rainfall and recognising cloud mergers. *International Journal of Remote Sensing*, **15**, 3241-3261.

Zhu, G., and Blumberg, D. G., (2002) Classification using ASTER data and SVM algorithms; The case study of Beer Sheva, Israel. *Remote Sensing of Environment*, **80**, 233-240.

Zmuda, A., Slater, J., Batts, A., and Seaman, E. (1988) Mapping land cover, soil cultivation and crop establishment for nitrate sensitivity analysis using ERS InSAR data. *Retrieval of Bio- and Physical Parameters from SAR Data fo*r *Land Application Workshop*. ESTEC, The Netherlands, 21-23 October 1998, http://www.estec.esa.nl/CONFANNOUN/98c07/.

APPENDIX A

CONFUSION MATRICES FOR CHAPTER 5 (Section 5.1)

Univariate decision tree classifier with different training data

700 training pixels

Class	1	2	3	4	5	6	7	Total	User's
1	281	7	15	2	0	0	0	305	92.13
2	10	191	37	14	23	10	0	285	67.02
3	7	32	179	8	3	10	1	240	74.58
4	2	28	61	249	7	19	7	373	66.76
5	0	22	1	3	266	0	0	292	91.1
6	0	17	4	17	1	209	10	258	81.01
7	0	3	3	7	0	52	219	284	77.11
Total	300	300	300	300	300	300	237	2037	
produc	93.67	63.67	59.67	83	88.67	69.67	92.41		

Overall Accuracy = 78.25 Kappa value = 0.75

1050 training pixels

Class	1	2	3	4	5	6	7	Total	User's
1	273	8	10	4	0	0	0	295	92.54
2	21	225	11	15	30	7	1	310	72.58
3	5	24	221	32	7	13	4	306	72.22
4	1	22	47	233	10	15	3	331	70.39
5	0	4	4	0	252	5	1	266	94.74
6	0	13	3	10	1	228	21	276	82.61
7	0	4	4	6	0	32	207	253	81.82
Total	300	300	300	300	300	300	237	2037	
produc	91	75	73.67	77.67	84	76	87.34		

Overall accuracy =80.46 Kappa value = 0.772

1400 training pixels

Class	1	2	3	4	5	6	7	Total	User's
1	282	8	4	2	0	0	0	296	95.27
2	12	236	22	24	34	6	0	334	70.66
3	4	15	233	21	8	10	2	293	79.52
4	2	17	29	233	3	10	4	298	78.19
5	0	5	1	2	254	0	0	262	96.95
6	0	19	9	11	1	237	27	304	77.96
7	0	0	2	7	0	37	204	250	81.6
Total	300	300	300	300	300	300	237	2037	
produc	94	78.67	77.67	77.67	84.67	79	86.08		

Overall accuracy = 82.43 kappa value = 0.795

1750 training pixels

Class	1	2	3	4	5	6	7	Total	User's
1	277	5	5	2	0	0	0	289	95.85
2	13	217	11	11	28	12	1	293	74.06
3	6	26	240	26	5	15	2	320	75
4	4	18	31	242	3	7	5	310	78.06
5	0	15	0	2	263	0	0	280	93.93
6	0	18	10	7	1	251	21	308	81.49
7	0	1	3	10	0	15	208	237	87.76
Total	300	300	300	300	300	300	237	2037	
produc	92.33	72.33	80	80.67	87.67	83.67	87.76		

Overall accuracy = 83.36 Kappa value = 0.806

2100 training pixels

Class	1	2	3	4	5	6	7	Total	User's
1	287	6	13	7	1	0	0	314	91.4
2	8	224	14	7	32	5	1	291	76.98
3	3	21	234	18	2	12	3	293	79.86
4	2	20	26	239	2	7	3	299	79.93
5	0	16	1	2	262	0	0	281	93.24
6	0	11	9	16	1	262	24	323	81.11
7	0	2	3	11	0	14	206	236	87.29
Total	300	300	300	300	300	300	237	2037	
produc	95.67	74.67	78	79.67	87.33	87.33	86.92		

Overall accuracy = 84.14 Kappa value = 0.815

2400 training pixels

Class	1	2	3	4	5	6	7	Total	User's
1	272	6	7	2	0	0	0	287	94.77
2	20	221	19	14	20	16	0	310	71.29
3	3	17	228	17	3	12	3	283	80.57
4	5	18	31	245	4	5	1	309	79.29
5	0	20	1	3	270	0	0	294	100
6	0	17	10	13	3	257	30	330	77.88
7	0	1	4	6	0	10	203	224	90.63
Total	300	300	300	300	300	300	237	1696	
produc	90.67	73.67	76	81.67	90	85.67	67.67		

Overall accuracy = 83.26 Kappa value = 0.805

2700 training pixels (without boosting)

Class	1	2	3	4	5	6	7	Total	User's
1	277	10	2	2	2	0	0	293	94.54
2	14	219	13	10	20	12	2	290	75.52
3	6	23	242	16	1	11	5	304	79.61
4	3	12	33	253	5	7	3	316	80.06
5	0	20	0	2	269	1	0	292	92.12
6	0	15	8	13	3	255	26	320	79.69
7	0	1	2	4	0	14	201	222	90.54
Total	300	300	300	300	300	300	237	2037	
produc	92.33	73	80.67	84.33	89.67	85	84.81		

Overall accuracy = 84.24   Kappa value = 0.816

2700 training pixels (with boosting)

Class	1	2	3	4	5	6	7	Total	User's
1	289	4	2	3	0	0	0	298	96.98
2	6	243	13	6	17	14	1	300	81
3	4	15	248	7	2	7	4	287	86.41
4	1	10	27	267	4	3	3	315	84.76
5	0	14	1	2	274	1	0	292	93.84
6	0	12	7	11	3	264	21	318	83.02
7	0	2	2	4	0	11	208	227	91.63
Total	300	300	300	300	300	300	237	2037	
Produc	96.33	81	82.67	89	91.33	88	87.76		

Overall accuracy = 88.46   kappa value = 0.865

ETM+ and internal texture derived from PAN

Class	1	2	3	4	5	6	7	Total	User's
1	282	7	8	0	0	0	0	297	94.95
2	6	221	14	16	25	14	1	297	74.41
3	8	19	245	17	1	9	3	302	81.13
4	3	25	20	248	2	5	9	312	79.49
5	1	11	2	6	272	2	0	294	92.52
6	0	17	9	13	0	250	25	314	79.62
7	0	0	2	0	0	20	197	219	89.95
Total	300	300	300	300	300	300	235	2035	
produc	94	73.67	81.67	82.67	90.67	83.33	83.83		

Overall accuracy = 84.3   Kappa value = 0.816

ETM+ with PAN and internal texture of PAN

Class	1	2	3	4	5	6	7	Total	User's
1	277	9	2	2	0	0	0	290	95.52
2	8	236	11	16	23	2	1	297	79.46
3	9	9	248	21	2	12	5	306	81.05
4	4	12	27	247	5	7	3	305	80.98
5	2	27	1	2	268	2	0	302	88.74
6	0	7	9	9	1	258	28	312	82.69
7	0	0	2	3	1	19	197	222	88.74
Total	300	300	300	300	300	300	234	2034	
Produc	92.33	78.67	82.67	82.33	89.33	86	84.19		

Overall accuracy = 85.10 Kappa value = 0.826

ETM+ with PAN and internal texture+three GLCM features of PAN

class	1	2	3	4	5	6	7	Total	User's
1	291	10	2	0	0	0	0	303	96.04
2	5	235	15	16	16	4	0	291	80.76
3	3	21	246	26	4	4	6	310	79.35
4	1	19	28	243	8	5	5	309	78.64
5	0	9	0	2	269	0	0	280	96.07
6	0	6	8	12	3	261	18	308	84.74
7	0	0	1	1	0	26	214	242	88.43
Total	300	300	300	300	300	300	243	2043	
Produc	97	78.33	82	81	89.67	87	88.07		

Overall accuracy = 86.1 Kappa value = 0.838

ETM+,PAN and internal texture+3GLCM features of PAN (boosted)

Class	1	2	3	4	5	6	7	Total	User's
1	292	7	1	2	0	0	0	302	96.69
2	5	252	8	12	14	1	3	295	85.42
3	3	21	269	15	6	6	4	324	83.02
4	0	8	16	254	4	4	6	292	86.99
5	0	8	0	2	273	1	0	284	96.13
6	0	4	5	14	3	272	11	309	88.03
7	0	0	1	1	0	16	219	237	92.41
Total	300	300	300	300	300	300	243	2043	
produc	97.33	84	89.67	84.67	91	90.67	90.12		

Overall accuracy = 89.6 Kappa value = 0.879

Maximum likelihood classifier results

ETM+ data

class	1	2	3	4	5	6	7	Total	User's
1	288	5	1	0	0	0	0	294	98
2	2	235	10	8	16	2	0	273	86.1
3	7	19	246	34	3	9	3	321	76.6
4	3	6	31	212	4	3	5	264	80.3
5	0	13	0	1	277	0	0	291	95.2
6	0	21	8	15	0	209	7	260	80.4
7	0	1	4	30	0	77	222	334	66.5
Total	300	300	300	300	300	300	237	2037	
Produ	. 96.0	78.3	82	70.7	92.3	69.7	93.7		

Overall accuracy = 82.9 Kappa Value = 0.801

ETM+ with internal texture of PAN

Class	1	2	3	4	5	6	7	Total	Users
1	283	8	0	1	0	0	0	292	96.9
2	6	234	4	12	24	4	0	284	82.4
3	8	10	249	30	2	12	2	313	79.6
4	1	13	27	226	1	8	3	279	81
5	0	10	2	2	273	0	0	287	95.1
6	2	25	14	18	0	204	7	270	75.6
7	0	0	4	11	0	72	223	310	71.9
Total	300	300	300	300	300	300	235	2035	
Produ.	94.3	78	83	75.3	91	68	94.9		

Overall accuracy = 83.1 Kappa value = 0.803

ETM+ with PAN and internal texture of PAN

Class	1	2	3	4	5	6	7	Total	Users
1	279	7	0	1	0	0	0	287	97.2
2	9	241	12	18	19	3	0	302	79.8
3	6	10	232	25	1	8	1	283	82
4	6	5	41	232	1	4	13	302	76.8
5	0	22	1	1	276	0	0	300	92
6	0	15	14	15	3	215	14	276	77.9
7	0	0	0	8	0	70	206	284	72.5
Total	300	300	300	300	300	300	234	2034	
Produ.	93	80.3	77.3	77.3	92	71.7	88		

Overall accuracy = 82.6 Kappa value = 0.798

ETM+ with PAN and internal texture+3 GLCM features of PAN

Class	1	2	3	4	5	6	7	Total	Users
1	292	6	1	0	0	0	0	299	97.7
2	5	256	8	24	21	8	0	322	79.5
3	1	11	237	10	7	8	0	274	86.5
4	0	5	43	250	1	2	1	302	82.8
5	0	12	0	0	269	0	0	281	95.7
6	2	10	4	8	2	197	11	234	84.2
7	0	0	7	8	0	85	231	331	69.8
Total	300	300	300	300	300	300	243	2043	
Produ.	97.3	85.3	79	83.3	89.7	65.7	95.1		

Overall accuracy = 84.8 Kappa value = 0.823

Neural network classifier results

ETM+ data

Class	1	2	3	4	5	6	7	Total	Users
1	288	3	3	1	0	0	0	295	97.6
2	2	242	8	0	12	5	1	270	89.6
3	2	16	258	22	2	10	5	315	81.9
4	3	4	12	229	5	2	1	256	89.5
5	0	7	0	1	272	0	0	280	97.1
6	0	10	1	5	1	256	26	299	85.6
7	0	0	0	0	0	1	188	189	99.5
Uncla.	5	18	18	42	8	26	16	133	7
Total	300	300	300	300	300	300	237	2037	
Produ.	96	80.7	86	76.3	90.7	85.3	79.3		

Overall accuracy = 85.1 Kappa value = 0.829

ETM+ and internal texture of PAN

Class	1	2	3	4	5	6	7	Total	Users
1	277	3	1	1	0	0	0	282	98.2
2	8	251	7	4	27	0	1	298	84.2
3	4	16	262	14	1	12	1	310	84.5
4	1	8	14	250	1	4	5	283	88.3
5	0	2	0	2	266	0	0	270	98.5
6	0	4	2	5	0	245	25	281	87.2
7	0	0	0	0	0	6	186	192	96.9
Uncla.	10	16	14	24	5	33	17	119	6.2
Total	300	300	300	300	300	300	235	2035	
Produ.	92.3	83.7	87.3	83.3	88.7	81.7	79.1		

Overall accuracy = 85.4 Kappa value = 0.832

ETM+with PAN and internal texture of PAN

Class	1	2	3	4	5	6	7	Total	Users
1	285	9	1	4	0	0	0	299	95.3
2	0	238	3	2	16	0	0	259	91.9
3	5	5	231	10	1	5	0	257	89.9
4	2	4	31	259	0	7	4	307	84.4
5	0	10	0	0	269	0	0	279	96.4
6	0	6	3	1	3	261	24	298	87.6
7	0	0	1	0	0	6	199	206	96.6
Uncla.	8	28	30	24	11	21	7	129	6.8
Total	300	300	300	300	300	300	234	2034	
produc	95	79.3	77	86.3	89.7	87	85		

Overall accuracy = 85.6 Kappa value = 0.836

ETM+ with PAN and internal texture+3 GLCM features of PAN

Class	1	2	3	4	5	6	7	Total	Users
1	287	5	1	0	0	0	0	293	98
2	7	271	8	9	20	0	1	316	85.8
3	2	3	257	13	3	7	1	286	89.9
4	1	6	8	247	0	3	4	269	91.8
5	0	3	0	0	270	1	0	274	98.5
6	0	3	4	2	2	251	14	276	90.9
7	0	0	0	0	0	14	208	222	93.7
Uncla.	3	9	22	29	5	24	15	107	5.5
Total	300	300	300	300	300	300	243	2043	
Produ.	95.7	90.3	85.7	82.3	90	83.7	85.6		

Overall accuracy = 87.7 Kappa value = 0.858

Multivariate decision tree (QUEST) classifier with different training data

700 training pixels

Class	1	2	3	4	5	6	7	Total	Users
1	270	6	16	0	0	0	0	292	92.47
2	11	216	28	28	32	13	4	332	65.06
3	3	23	223	44	3	12	7	315	70.79
4	15	18	17	196	5	6	3	260	75.38
5	0	6	0	0	251	1	0	258	97.29
6	1	29	13	11	9	238	25	326	73.01
7	0	2	3	21	0	30	198	254	77.95
Total	300	300	300	300	300	300	237	2037	
Produ.	90	72	74.33	65.33	83.67	79.33	66		

Overall accuracy = 78.15

1050 training pixels

Class	1	2	3	4	5	6	7	Total	Users
1	273	8	11	2	1	0	0	295	92.54
2	17	238	26	19	31	22	3	356	66.85
3	3	20	222	31	4	8	2	290	76.55
4	7	10	33	210	2	18	9	289	72.66
5	0	7	0	9	255	0	0	271	94.1
6	0	17	6	8	7	238	27	303	78.55
7	0	0	2	21	0	14	196	233	84.12
Total	300	300	300	300	300	300	237	2037	
Produ.	91	79.33	74	70	85	79.33	82.7		

Overall accuracy = 80.12

1400 training pixels

Class	1	2	3	4	5	6	7	Total	Users
1	278	6	8	2	1	0	0	295	94.24
2	13	214	16	11	22	8	1	285	75.09
3	4	22	214	25	4	8	0	277	77.26
4	5	24	42	230	8	9	2	320	71.88
5	0	5	0	0	263	0	0	268	98.13
6	0	29	20	25	2	254	23	353	71.95
7	0	0	0	7	0	21	211	239	88.28
Total	300	300	300	300	300	300	237	2037	
Produ.	92.67	71.33	71.33	76.67	87.67	84.67	89.03		

Overall accuracy = 81.69

1750 training pixels

Class	1	2	3	4	5	6	7	Total	Users
1	287	6	7	2	2	0	0	304	94.41
2	3	232	21	13	20	9	2	300	77.33
3	4	16	219	30	4	11	1	285	76.84
4	6	24	34	225	11	6	3	309	72.82
5	0	5	0	2	260	0	0	267	97.38
6	0	17	17	11	3	251	20	319	78.68
7	0	0	2	17	0	23	211	253	83.4
Total	300	300	300	300	300	300	237	2037	
Produ.	95.67	77.33	73	75	86.67	83.67	89.03		

Overall accuracy =82.72

2100 training pixels

Class	1	2	3	4	5	6	7	Total	Users
1	281	6	7	0	2	0	0	296	94.93
2	10	223	21	16	20	6	1	297	75.08
3	2	14	209	16	4	13	0	258	81.01
4	7	24	52	246	7	14	11	361	68.14
5	0	12	0	1	263	6	0	282	93.26
6	0	21	10	12	4	245	29	321	76.32
7	0	0	1	9	0	16	196	222	88.29
Total	300	300	300	300	300	300	237	2037	
Produ.	93.67	74.33	69.67	82	87.67	81.67	82.7		

Overall accuracy = 81.64

2400 training pixels

Class	1	2	3	4	5	6	7	Total	Users
1	285	9	9	1	4	0	0	308	92.53
2	7	232	21	7	17	9	1	294	78.91
3	2	7	210	16	2	4	0	241	87.14
4	6	21	42	239	10	8	4	330	72.42
5	0	5	0	0	256	0	0	261	98.08
6	0	24	7	9	11	252	23	326	77.3
7	0	2	11	28	0	27	209	277	75.45
Total	300	300	300	300	300	300	237	2037	
Produ.	95	77.33	70	79.67	85.33	84	88.19		

Overall accuracy = 82.62

2700 training pixels

Class	1	2	3	4	5	6	7	Total	Users
1	286	5	3	2	1	0	0	297	96.3
2	5	245	19	8	28	7	2	314	78.03
3	4	16	234	36	6	4	3	303	77.23
4	5	10	32	232	9	12	2	302	76.82
5	0	4	0	0	245	0	0	249	98.39
6	0	20	10	15	11	254	17	327	77.68
7	0	0	2	7	0	23	213	245	86.94
Total	300	300	300	300	300	300	237	2037	
Produ.	95.33	81.67	78	77.33	81.67	84.67	89.87		

Overall accuracy = 83.9

APPENDIX B

CONFUSION MATRICES FOR CHAPTER 5 (Section 5.2)

"one against one" multi-class method using Royal Holloway and AT&T SVM software

700 training pixels

Class	1	2	3	4	5	6	7	Total	Users
1	285	10	3	3	0	0	0	301	94.68
2	10	246	17	7	25	11	0	316	77.85
3	2	24	212	3	2	9	2	254	83.46
4	2	7	57	269	2	14	7	358	75.14
5	1	6	0	1	270	0	0	278	97.12
6	0	7	10	7	1	221	16	262	84.35
7	0	0	1	10	0	45	212	268	79.1
Total	300	300	300	300	300	300	237	2037	
Produ.	95	82	70.67	89.67	90	73.67	89.45		

Overall accuracy =84.19 Kappa value = 0.82

1050 training pixels

Class	1	2	3	4	5	6	7	Total	Users
1	290	5	3	3	0	0	0	301	96.35
2	3	250	10	8	23	9	1	304	82.24
3	4	21	216	4	4	9	3	261	82.76
4	3	7	59	263	2	8	3	345	76.23
5	0	7	2	0	268	1	0	278	96.4
6	0	10	9	10	3	232	18	282	82.27
7	0	0	1	12	0	41	212	266	79.7
Total	300	300	300	300	300	300	237	2037	
Produ.	96.67	83.33	72	87.67	89.33	77.33	89.45		

Overall accuracy = 84.98 Kappa value = 0.825

1400 training pixels

Class	1	2	3	4	5	6	7	Total	Users
1	290	5	4	3	0	0	0	302	96.03
2	1	251	10	7	21	9	0	299	83.95
3	7	23	219	3	4	9	2	267	82.02
4	1	6	56	260	2	7	5	337	77.15
5	1	6	2	1	270	0	0	280	96.43
6	0	9	8	8	3	244	22	294	82.99
7	0	0	1	18	0	31	208	258	80.62
Total	300	300	300	300	300	300	237	2037	
Produ.	96.67	83.67	73	86.67	90	81.33	87.76		

Overall accuracy = 85.52 Kappa value = 0.831

1750 training pixels

Class	1	2	3	4	5	6	7	Total	Users
1	287	4	1	3	0	0	0	295	97.29
2	2	248	8	5	20	6	0	289	85.81
3	8	21	218	4	5	8	2	266	81.95
4	2	8	59	267	4	8	4	352	75.85
5	1	7	2	0	268	0	0	278	96.4
6	0	12	10	7	3	245	22	299	81.94
7	0	0	2	14	0	33	209	258	81.01
Total	300	300	300	300	300	300	237	2037	
Produ.	95.67	82.67	72.67	89	89.33	81.67	88.19		

Overall accuracy = 85.52 Kappa value = 0.831

2100 training pixels

Class	1	2	3	4	5	6	7	Total	Users
1	289	4	1	3	0	0	0	297	97.31
2	1	252	8	7	19	7	0	294	85.71
3	7	21	225	3	5	8	2	271	83.03
4	3	6	57	269	2	9	5	351	76.64
5	0	7	0	0	271	0	0	278	97.48
6	0	10	7	11	3	251	25	307	81.76
7	0	0	2	7	0	25	205	239	85.77
Total	300	300	300	300	300	300	237	2037	
Produ.	96.33	84	75	89.67	90.33	83.67	86.5		

Overall accuracy = 86.5 Kappa value = 0.842

2400 training pixels

Class	1	2	3	4	5	6	7	Total	Users
1	290	5	2	3	0	0	0	300	96.67
2	1	254	9	7	19	8	0	298	85.23
3	7	21	229	7	4	9	2	279	82.08
4	2	6	52	264	2	6	3	335	78.81
5	0	7	0	0	272	0	0	279	97.49
6	0	7	7	14	3	261	26	318	82.08
7	0	0	1	5	0	16	206	228	90.35
Total	300	300	300	300	300	300	237	2037	
Produ.	96.67	84.67	76.33	88	90.67	87	86.92		

Overall accuracy = 87.19 Kappa value = 0.85

2700 training pixels

Class	1	2	3	4	5	6	7	Total	Users
1	289	5	3	3	0	0	0	300	96.33
2	2	248	8	6	18	6	0	288	86.11
3	7	20	242	9	4	7	2	291	83.16
4	2	6	39	263	1	6	4	321	81.93
5	0	9	1	1	276	0	0	287	96.17
6	0	12	7	18	1	267	27	332	2.781
7	0	0	0	0	0	14	204	218	93.58
Total	300	300	300	300	300	300	237	2037	
Produ.	96.33	82.67	80.67	87.67	92	89	86.08		

Overall accuracy = 87.37 Kappa value = 0.86

"one against one" multi-class method using LIBSVM software

With 2700 training pixels

Class	1	2	3	4	5	6	7	Total	Users
1	290	5	3	3	0	0	0	301	96.35
2	2	249	9	7	21	6	1	295	84.41
3	6	20	244	10	2	7	1	290	84.14
4	2	7	37	263	1	6	5	321	81.93
5	0	8	0	1	275	0	0	284	96.83
6	0	11	7	16	1	267	27	329	81.16
7	0	0	0	0	0	14	203	217	93.55
Total	300	300	300	300	300	300	237	2037	
Produ.	96.67	83	81.33	87.67	91.67	89	85.65		

Overall accuracy = 87.92 Kappa value = 0.87

"one against rest" multi-class method

700 training pixels

Class	1	2	3	4	5	6	7	Total	Users
1	283	6	2	2	0	0	0	293	96.59
2	3	226	10	1	15	4	1	260	86.92
3	4	8	188	1	2	6	0	209	89.95
4	1	1	26	207	0	0	1	236	87.71
5	0	5	0	0	263	0	0	268	98.13
6	0	2	6	1	0	193	3	205	94.15
7	0	0	0	0	0	31	192	223	86.1
Uncla.	9	52	68	88	20	66	40	343	
Total	300	300	300	300	300	300	237	2037	
Produ.	94.33	75.33	62.67	69	87.67	64.33	81.01		

Overall accuracy = 76.19   Kappa value = 0.73

2700 training pixels

Class	1	2	3	4	5	6	7	Total	Users
1	285	3	1	2	0	0	0	291	97.94
2	2	229	10	0	14	0	0	255	89.8
3	3	11	209	3	1	7	0	234	89.32
4	2	3	19	213	0	1	4	242	88.02
5	0	7	0	0	266	0	0	273	97.44
6	0	6	4	4	0	236	21	271	87.08
7	0	0	0	0	0	10	186	196	94.9
Uncla.	8	41	57	78	19	46	26	275	
Total	300	300	300	300	300	300	237	2037	
Produ.	95	76.33	69.67	71	88.67	78.67	78.48		

Overall accuracy = 79.73   Kappa value = 0.77

APPENDIX C

CONFUSION MATRICES FOR CHAPTER 6

Confusion matrices with maximum likelihood classifier

Data set1

Class	1	2	3	4	5	6	7	Total	Users
1	265	48	10	15	147	14	17	516	51.4
2	7	155	35	34	8	2	69	310	50
3	5	25	190	66	20	0	21	327	58.1
4	1	24	45	160	10	1	9	250	64
5	17	13	6	10	80	11	3	140	57.1
6	2	24	10	13	11	272	60	392	69.4
7	3	11	4	2	24	0	121	165	73.3
Total	300	300	300	300	300	300	300	2100	
Produ.	88.3	51.7	63.3	53.3	26.7	90.7	40.3		

Overall acuuracy = 59.2 Kappa value = 0.526

Data set 2

Class	1	2	3	4	5	6	7	Total	Users
1	277	33	4	7	47	0	13	381	72.7
2	12	189	7	27	26	0	83	344	54.9
3	2	23	192	43	15	1	26	302	63.6
4	0	27	61	199	15	0	13	315	63.2
5	6	7	12	13	154	10	3	205	75.1
6	0	6	18	8	33	287	17	369	77.8
7	3	15	6	3	10	2	145	184	78.8
Total	300	300	300	300	300	300	300	2100	
Produ.	92.3	63	64	66.3	51.3	95.7	48.3		

Overall accuracy = 68.7 Kappa value = 0.635

Data set 3

Class	1	2	3	4	5	6	7	Total	Users
1	240	49	11	20	33	0	30	383	62.7
2	27	154	22	49	13	1	81	347	44.4
3	5	9	33	6	7	0	19	79	41.8
4	2	24	6	90	40	9	6	177	50.8
5	23	29	31	58	131	14	6	292	44.9
6	0	24	170	69	70	274	36	643	42.6
7	3	11	27	8	6	2	122	179	68.2
Total	300	300	300	300	300	300	300	2100	
Produ.	80	51.3	11	30	43.7	91.3	40.7		

Overall accuracy = 49.7 Kappa value = 0.413

Data set 4

Class	1	2	3	4	5	6	7	Total	Users
1	272	54	6	4	32	0	17	385	70.6
2	9	148	12	36	6	3	31	245	60.4
3	4	21	193	39	20	1	16	294	65.6
4	2	26	50	194	10	1	6	289	67.1
5	9	18	15	15	186	20	8	271	68.6
6	0	5	3	7	12	271	4	302	89.7
7	4	28	21	5	34	4	218	314	69.4
Total	300	300	300	300	300	300	300	2100	
Produ.	90.7	49.3	64.3	64.7	62	90.3	72.7		

Overall accuracy = 70.6 Kappa value = 0.657

Data set 5

Class	1	2	3	4	5	6	7	Total	Users
1	273	36	2	7	13	0	6	337	81
2	10	200	13	35	25	8	10	301	66.4
3	1	15	239	46	13	3	13	330	72.4
4	0	19	22	191	14	2	9	257	74.3
5	4	11	7	6	201	8	2	239	84.1
6	0	1	3	5	2	276	1	288	95.8
7	12	18	14	10	32	3	259	348	74.4
Total	300	300	300	300	300	300	300	2100	
Produ.	91	66.7	79.7	63.7	67	92	86.3		

Overall accuracy = 78.0 Kappa value = 0.744

Data set 6

Class	1	2	3	4	5	6	7	Total	Users
1	262	39	2	1	79	0	7	390	67.2
2	7	169	32	28	44	7	46	333	50.8
3	4	28	207	35	18	0	10	302	68.5
4	1	30	39	222	14	9	28	343	64.7
5	15	5	5	2	119	4	1	151	78.8
6	0	22	5	6	4	280	25	342	81.9
7	11	7	10	6	22	0	183	239	76.6
Total	300	300	300	300	300	300	300	2100	
Produ.	87.3	56.3	69	74	39.7	93.3	61		

Overall accuracy = 68.7 Kappa value = 0.634

Data set 7

Class	1	2	3	4	5	6	7	Total	Users
1	277	37	1	2	12	0	2	331	83.7
2	4	182	18	22	31	10	57	324	56.2
3	3	19	228	28	16	1	11	306	74.5
4	1	40	34	236	17	7	16	351	67.2
5	11	9	8	2	213	10	2	255	83.5
6	0	7	3	0	1	272	0	283	96.1
7	4	6	8	10	10	0	212	250	84.8
Total	300	300	300	300	300	300	300	2100	
Produ.	92.3	60.7	76	78.7	71	90.7	70.7		

Overall accuracy = 77.1 Kappa value = 0.733

Confusion matrix using neural network classifier

Data set 1

Class	1	2	3	4	5	6	7	Total	Users
1	217	21	3	6	56	3	10	316	68.7
2	0	147	1	6	1	0	25	180	81.7
3	0	8	165	15	1	1	14	204	80.9
4	1	14	38	190	7	3	3	256	74.2
5	13	11	5	9	120	2	1	161	74.5
6	0	5	3	3	3	262	0	276	94.9
7	0	11	4	4	4	0	175	198	88.4
U	69	83	81	67	108	29	72	509	32
Total	300	300	300	300	300	300	300	2100	
Produc	72.3	49	55	63.3	40	87.3	58.3		

Overall accuracy = 60.8 Kappa value = 0.572

Data set 2

Class	1	2	3	4	5	6	7	Total	Users
1	243	20	1	0	2	0	2	268	90.7
2	7	171	5	13	5	0	16	217	78.8
3	0	0	188	24	2	1	11	226	83.2
4	0	13	28	188	3	2	3	237	79.3
5	4	14	9	20	240	3	7	297	80.8
6	0	9	3	2	2	288	4	308	93.5
7	0	9	1	2	0	1	145	158	91.8
U	46	64	65	51	46	5	112	389	22.7
Total	300	300	300	300	300	300	300	2100	
Produ.	81	57	62.7	62.7	80	96	48.3		

Overall accuracy = 69.7 Kappa value = 0.664

Data set 3

Class	1	2	3	4	5	6	7	Total	Users
1	160	14	5	8	14	0	18	219	73.1
2	9	123	2	31	0	0	31	196	62.8
3	0	3	79	1	0	3	10	96	82.3
4	0	3	2	45	8	2	0	60	75
5	19	29	27	50	130	28	3	286	45.5
6	0	0	1	0	0	0	0	1	0
7	0	3	21	2	0	0	104	130	80
U	112	125	163	163	148	267	134	1112	112.6
Total	300	300	300	300	300	300	300	2100	
Produ.	53.3	41	26.3	15	43.3	0	34.7		

Overall accuracy = 30.5 Kappa value = 0.279

Data set 4

Class	1	2	3	4	5	6	7	Total	Users
1	253	20	2	5	1	0	3	284	89.1
2	10	166	5	12	2	0	11	206	80.6
3	0	10	192	14	3	0	15	234	82.1
4	1	18	30	189	3	1	10	252	75
5	9	19	16	11	256	0	12	323	79.3
6	0	1	2	4	0	292	4	303	96.4
7	0	4	5	3	7	0	199	218	91.3
U	27	62	48	62	28	7	46	280	15.4
Total	300	300	300	300	300	300	300	2100	
Produ.	84.3	55.3	64	63	85.3	97.3	66.3		

Overall accuracy = 73.7 kappa value = 0.705

Data set 5

Class	1	2	3	4	5	6	7	Total	Users
1	266	19	3	7	1	0	2	298	89.3
2	10	201	7	13	5	0	2	238	84.5
3	0	6	207	14	3	1	8	239	86.6
4	1	5	21	197	5	1	2	232	84.9
5	1	10	5	6	244	1	3	270	90.4
6	0	8	1	0	1	292	2	304	96.1
7	0	7	6	6	1	0	255	275	92.7
U	22	44	50	57	40	5	26	244	13.1
Total	300	300	300	300	300	300	300	2100	
Produ.	88.7	67	69	65.7	81.3	97.3	85		

Overall accuracy = 79.1 Kappa value = 0.765

Data set 6

Class	1	2	3	4	5	6	7	Total	Users
1	193	3	0	0	9	0	0	205	94.1
2	11	190	2	5	9	4	4	225	84.4
3	2	7	235	14	4	11	20	293	80.2
4	0	20	16	224	3	2	12	277	80.9
5	37	7	0	0	222	5	3	274	81
6	0	4	0	4	0	249	0	257	96.9
7	0	3	1	6	1	0	222	233	95.3
U	57	66	46	47	52	29	39	336	19
Total	300	300	300	300	300	300	300	2100	
Produ.	64.3	63.3	78.3	74.7	74	83	74		

Overall accuracy = 73.1 Kappa value = 0.701

Data set 7

Class	1	2	3	4	5	6	7	Total	Users
1	255	7	0	1	0	0	1	264	96.6
2	13	208	5	12	1	1	2	242	86
3	1	14	254	27	1	2	17	316	80.4
4	0	23	12	216	3	1	3	258	83.7
5	3	4	3	7	285	9	1	312	91.3
6	0	3	0	1	0	272	0	276	98.6
7	0	3	6	9	0	0	250	268	93.3
U	28	38	20	27	10	15	26	164	8.5
Total	300	300	300	300	300	300	300	2100	
Produ.	85	69.3	84.7	72	95	90.7	83.3		

Overall accuracy = 82.9 Kappa value = 0.805

Confusion matrices using Decision tree classifier

Data set 1

class	1	2	3	4	5	6	7	Total	Users
1	225	23	7	7	43	3	11	319	71
2	24	178	11	17	14	1	27	272	65.4
3	6	22	191	45	9	6	19	298	64.1
4	3	18	55	191	19	2	12	300	63.7
5	35	18	12	24	197	7	12	305	64.6
6	2	12	5	4	3	275	8	309	89
7	5	29	19	12	15	6	211	297	71
Total	300	300	300	300	300	300	300	2100	
Produc	75	59.3	63.67	63.67	65.67	91.67	70.33		

Overall accuracy = 69.9 Kappa value = 0.649

Data set 2

class	1	2	3	4	5	6	7	Total	Users
1	253	19	2	4	1	0	5	284	89.1
2	29	204	11	31	19	2	20	316	64.6
3	5	20	216	45	5	8	21	320	67.5
4	3	20	50	187	17	3	7	287	65.2
5	8	17	6	23	252	1	4	311	81
6	1	1	5	2	1	284	5	299	95
7	1	19	10	8	5	2	238	283	84.1
Total	300	300	300	300	300	300	300	2100	
Produc	84.3	68	72	62.3	84	94.7	0.793		

Overall accuracy = 77.8 Kappa value = 0.741

Data set 3

Class	1	2	3	4	5	6	7	Total	users
1	182	30	6	16	17	0	17	268	67.91
2	51	165	16	48	38	9	61	388	42.53
3	7	21	175	43	37	124	49	456	38.38
4	20	28	30	113	48	51	17	307	36.81
5	30	41	29	56	141	25	12	334	42.22
6	1	2	23	18	15	80	4	143	55.94
7	9	13	21	6	4	11	140	204	68.63
Total	300	300	300	300	300	300	300	2100	
Produc	60.67	55	58.33	37.67	47	26.67	46.67		

Overall accuracy = 47.43 Kappa value = 0.388

Data set 4

Class	1	2	3	4	5	6	7	Total	User's
1	265	18	4	7	2	0	9	305	86.89
2	24	201	16	32	11	3	13	300	67
3	2	10	202	43	8	8	23	296	68.24
4	0	28	38	198	10	2	5	281	70.46
5	9	18	16	8	254	5	9	319	79.62
6	0	3	4	1	3	280	5	296	94.59
7	0	22	20	11	12	2	236	303	77.89
Total	300	300	300	300	300	300	300	2100	
Produc	88.33	67	67.33	66	84.67	93.33	78.67		

Overall accuracy = 77.9 Kappa value = 0.742

Data set 5

class	1	2	3	4	5	6	7	Total	User's
1	269	21	5	5	5	0	2	307	87.62
2	18	196	21	38	16	4	14	307	63.84
3	1	20	209	29	5	3	10	277	75.45
4	4	31	37	207	11	1	7	298	69.46
5	6	23	10	10	255	6	3	313	81.47
6	1	3	5	3	3	285	1	301	94.68
7	1	6	13	8	5	1	263	297	88.55
Total	300	300	300	300	300	300	300	2100	
Produc	89.67	65.33	69.67	69	85	95	87.67		

Overall accuracy = 80.20 Kappa value = 0.769

Data set 6

class	1	2	3	4	5	6	7	total	Users
1	244	16	6	5	17	1	3	292	83.56
2	17	206	21	26	14	6	18	308	66.88
3	5	20	214	42	6	5	12	304	70.39
4	5	24	38	213	5	2	12	299	71.24
5	21	13	4	7	249	5	10	309	80.58
6	1	7	3	4	4	281	2	302	93.05
7	7	14	14	3	5	0	243	286	84.97
Total	300	300	300	300	300	300	300	2100	
Produc	81.33	68.67	71.33	71	83	93.67	81		

Overall acuuracy=78.57 Kappa value = 0.75

Data set 7

Class	1	2	3	4	5	6	7	Total	Users
1	255	13	2	3	4	0	4	281	90.75
2	33	220	22	22	7	5	22	331	66.47
3	5	19	234	27	11	5	21	322	72.67
4	2	21	20	233	2	4	2	284	82.04
5	4	14	8	10	272	8	2	318	85.53
6	0	6	2	2	2	277	4	293	94.54
7	1	7	12	3	2	1	245	271	90.41
Total	300	300	300	300	300	300	300	2100	
Produc	85	73.33	78	77.67	90.67	92.33	81.67		

Overall accuracy = 82.7 Kappa value = 0.797

APPENDIX D

CONFUSION MATRICES FOR "MNF" BASED FEATURE EXTRACTION (CHAPTER 7)

With maximum likelihood classifier

Class	1	2	3	4	5	6	7	8	Total	Users
1	0	0	0	0	0	0	0	0	0	0
2	0	0	0	0	0	0	0	0	0	0
3	0	15	369	9	4	2	5	57	461	80
4	0	0	1	372	36	12	51	19	491	75.8
5	16	41	8	5	319	20	20	5	434	73.5
6	0	32	1	1	15	356	31	3	439	81.1
7	0	0	3	6	16	10	240	16	291	82.5
8	384	312	18	7	10	0	53	300	1084	27.7
Total	400	400	400	400	400	400	400	400	3200	
Produ.	0	0	92.2	93	79.8	89	60	75		

Overall accuracy = 61.1 Kappa value = 0.556

With neural network classifier

Class	1	2	3	4	5	6	7	8	Total	Users
1	399	1	0	0	0	0	0	2	402	99.3
2	0	386	0	0	2	2	0	6	396	97.5
3	0	0	370	10	3	1	4	34	422	87.7
4	0	0	1	355	23	6	15	2	402	88.3
5	0	1	1	14	331	18	4	7	376	88
6	0	0	1	0	15	355	19	1	391	90.8
7	0	0	3	7	11	10	319	39	389	82
8	0	0	15	4	3	2	20	272	316	86.1
U	1	12	9	10	12	6	19	37	106	3.4
Total	400	400	400	400	400	400	400	400	3200	
Produ.	99.8	96.5	92.5	88.8	82.8	88.8	79.8	68		

Overall accuracy = 87.10 Kappa value = 0.854

With decision tree classifier

Class	1	2	3	4	5	6	7	8	Total	Users
1	399	0	0	0	0	0	0	2	401	99.5
2	0	390	0	1	1	2	0	8	402	97.01
3	0	0	381	5	7	1	6	42	442	86.2
4	0	0	1	376	31	6	21	2	437	86.04
5	0	4	2	7	314	22	2	11	362	86.74
6	0	3	1	1	14	352	17	2	390	90.26
7	0	0	3	6	23	14	332	43	421	78.86
8	1	3	12	4	10	3	22	290	345	84.06
Total	400	400	400	400	400	400	400	400	3200	
Produc	99.75	97.5	95.25	94	78.5	88	83	72.5		

Overall accuracy = 88.56 Kappa value = 0.869

with SVMs

Class	1	2	3	4	5	6	7	8	Total	Users
1	498	0	0	1	0	0	0	6	505	96.8
2	0	495	0	1	1	5	0	4	506	97.8
3	0	1	447	1	7	1	5	46	508	88
4	1	0	20	448	25	2	16	10	522	85.8
5	0	0	1	16	411	16	10	22	476	86.3
6	0	1	3	12	31	447	16	5	515	86.8
7	0	0	4	18	18	28	393	19	480	81.9
8	1	3	25	3	7	1	60	388	488	79.5
Total	500	500	500	500	500	500	500	500		
Produc	99.6	99	89.4	89.6	82.2	89.4	78.6	77.6		

Overall accuracy = 88.2 Kappa vlaue = 0.865

APPENDIX E

CONFUSION MATRICES FOR DECISION TREE BASED FEATURE EXTRACTION (CHAPTER 7)

With maximum likelihood classifier

Class	1	2	3	4	5	6	7	8	Total	Users
1	499	0	0	0	0	0	0	0	499	100
2	0	500	0	0	0	0	0	0	500	100
3	0	0	483	12	1	0	5	34	535	90.3
4	0	0	4	462	7	3	5	3	484	95.5
5	0	0	1	13	463	10	6	19	512	90.4
6	0	0	0	10	27	480	22	2	541	88.7
7	0	0	3	0	2	6	257	3	271	94.8
8	1	0	9	3	0	1	5	439	458	95.9
Total	500	500	500	500	500	500	300	500	3800	
Produ.	99.8	100	96.6	92.4	92.6	96	85.7	87.8		

Overall accuracy = 94.3 Kappa value = 0.935

With neural network classifier

Class	1	2	3	4	5	6	7	8	Total	Users
1	500	0	0	0	0	0	0	0	500	100
2	0	500	1	0	0	0	0	0	501	99.8
3	0	0	475	7	0	0	3	39	524	90.6
4	0	0	2	474	2	2	1	4	485	97.7
5	0	0	0	3	463	4	0	12	482	96.1
6	0	0	0	7	9	459	9	7	491	93.5
7	0	0	1	4	0	20	258	6	289	89.3
8	0	0	16	4	3	0	4	372	399	93.2
U	0	0	5	1	23	15	25	60	129	3.5
Total	500	500	500	500	500	500	300	500	3800	
Produ.	100	100	95	94.8	92.6	91.8	86	74.4		

Overall accuracy = 92.1 Kappa value = 0.911

with decision tree classifier

Class	1	2	3	4	5	6	7	8	Total	Users
1	500	0	0	0	0	0	0	0	500	100
2	0	500	2	0	0	0	0	0	502	99.6
3	0	0	430	4	11	2	5	71	523	82.22
4	0	0	10	455	10	3	3	14	495	91.92
5	0	0	2	6	409	7	12	27	463	88.34
6	0	0	4	12	26	449	21	16	528	85.04
7	0	0	3	10	18	33	243	30	337	72.11
8	0	0	49	13	26	6	16	342	452	75.66
Total	500	500	500	500	500	500	300	500	3800	
Produc	100	100	86	91	81.8	89.8	81	68.4		

Overall accuracy = 87.6 Kappa value =0.858

with SVMs

Class	1	2	3	4	5	6	7	8	Total	Users
1	500	0	0	0	0	0	0	0	500	100
2	0	500	2	0	0	0	0	0	502	99.6
3	0	0	458	4	1	0	3	34	500	91.6
4	0	0	4	481	5	1	3	3	497	96.8
5	0	0	0	3	481	9	0	3	496	97
6	0	0	0	6	8	471	6	6	497	94.8
7	0	0	6	4	2	19	287	11	329	87.2
8	0	0	30	2	3	0	1	443	479	92.5
Total	500	500	500	500	500	500	300	500		
Produc	100	100	91.6	96.2	96.2	94.2	95.7	88.6		

Overall accuracy = 95.3 Kappa value = 0.946

APPENDIX F

CONFUSION MATRICES FOR ETM+ SPAIN DATA (CHAPTER 7)

With maximum likelihood classifier

Class	1	2	3	4	5	6	Total	Users
1	147	0	0	0	0	0	147	100
2	0	0	0	0	0	0	0	0
3	0	0	163	5	1	2	171	95.3
4	0	0	13	207	12	6	238	87
5	0	6	4	12	108	0	130	83.1
6	3	40	9	7	8	42	109	38.5
Total	150	46	189	231	129	50	795	
Produ.	98	0	86.2	89.6	83.7	84		

Overall accuracy = 83.9 Kappa value = 0.797

With neural network classifier

Class	1	2	3	4	5	6	Total	Users
1	148	0	0	0	0	0	148	100
2	0	46	0	0	0	0	46	100
3	1	0	174	10	2	6	193	90.2
4	0	0	3	196	8	1	208	94.2
5	0	0	4	10	107	1	122	87.7
6	0	0	4	7	6	40	57	70.2
U	1	0	4	8	6	2	21	2.7
Total	150	46	189	231	129	50	795	
Produ.	98.7	100	92.1	84.8	82.9	80		

Overall accuracy = 89.4 Kappa value = 0.869

With decision tree classifier

Class	1	2	3	4	5	6	Total	Users
1	147	0	0	0	0	0	147	100
2	0	46	0	0	0	0	46	100
3	0	0	161	23	1	4	189	85.19
4	0	0	11	168	11	2	192	87.5
5	0	0	4	23	109	2	138	78.99
6	3	0	13	17	8	42	83	50.6
Total	150	46	189	231	129	50	795	
Produc	98	100	85.19	72.73	84.5	84		

Overall accuracy = 84.65 Kappa value = 0.808

with SVMs

Class	1	2	3	4	5	6	Total	Users
1	148	0	0	0	0	0	148	100
2	0	46	0	0	0	0	46	100
3	0	0	170	12	3	2	187	90.9
4	0	0	9	205	10	2	226	90.7
5	0	0	6	7	109	0	122	89.3
6	2	0	4	7	7	46	66	69.7
Total	150	46	189	231	129	50	795	
Produ.	98.7	100	89.9	88.7	84.5	92		

Overall accuracy = 91.1 Kappa value = 0.887